

University of Warwick institutional repository: <http://go.warwick.ac.uk/wrap>

A Thesis Submitted for the Degree of PhD at the University of Warwick

<http://go.warwick.ac.uk/wrap/58582>

This thesis is made available online and is protected by original copyright.

Please scroll down to view the document itself.

Please refer to the repository record for this item for information to help you to cite it. Our policy information is available from the repository home page.

Cyclometalation: 2,6-Diphenylpyridine Complexes of Platinum

By G W V CAVE



A thesis submitted for the part requirement for the degree of
Doctor of Philosophy

Presented to
The University of Warwick
Department of Chemistry

October 1999

**PAGE
NUMBERING
AS
ORIGINAL**

Table of Contents.

Table of Contents.....	ii
Table of illustrations.....	v
Acknowledgements.....	vii
Acknowledgements.....	vii
Declaration.....	viii
Summary.....	ix
Abbreviations.....	x
Chapter 1: Introduction to liquid crystals.....	1
Section 1.1. Introduction.....	1
Section 1.2. Lyotropic Mesogens.....	2
Section 1.3. Thermotropic mesogens.....	4
1.3.1: Calamitic mesophases.....	6
1.3.2: Discotic mesophases.....	9
Section 1.4. Polymeric Mesogens.....	11
Section 1.5. Metallomesogens.....	13
1.5.1: Calamitic metallomesogens.....	14
1.5.2: Columnar metallomesogens.....	17
1.5.3: Polymeric metallomesogens.....	21
Section 1.6. Future prospects for liquid crystal technology.....	22
Section 1.7. References.....	24
Chapter 2: Cyclometalation.....	27
Section 2.1. Introduction.....	27
Section 2.2. Cyclometalation mechanisms.....	27
2.2.1: Oxidative Addition.....	28
2.2.2: Electrophilic Substitution.....	29
2.2.3: Multicentred Pathway.....	29
Section 2.3. Effective molarity, M_{eff}	29
Section 2.4. A comparative study.....	30
2.4.1: Rules for <i>ortho</i> -palladation of aromatic amines.....	30
2.4.2: <i>Exo</i> versus <i>endo</i> palladocycles.....	33
2.4.3: Di-cyclometalations.....	35
2.4.4: Tridentate complexes.....	35
2.4.5: Nucleophilic displacement.....	39
2.4.6: C-X Bond activation (X = C or Si).....	40
Section 2.5. Conclusion.....	41
Section 2.6. References.....	42
Chapter 3: Results and discussion.....	45
Section 3.1. Introduction.....	45
Section 3.2. Ligand synthesis.....	45
3.2.1: Synthesis of 2,6-bis-(alkoxyaryl)pyridines.....	46
3.2.2: Synthesis of triazines.....	47
3.2.3: Synthesis of 4'-(4-alkoxyphenyl)-2',6'-diphenylpyridine.....	49
3.2.4: Synthesis of stilbazoles.....	50
Section 3.3. Mono-cycloplatination.....	51
3.3.1: Introduction.....	51
3.3.2: Synthesis of C ^N mono-cycloplatinated chloride bridged dimers.....	52
3.3.3: Mono-cycloplatination of the triazine ligand.....	56
3.3.4: Cycloplatination of 2-phenylpyridine.....	57
3.3.5: Conclusion.....	60
Section 3.4. Cleaving the chloride bridge.....	60
3.4.1: Introduction.....	60
3.4.2: Addition of trimethylphosphine to mono-metalated dimers.....	61
3.4.3: Addition of DMSO to mono-metalated dimers.....	62
3.4.4: Addition of carbon monoxide to mono-metalated dimers.....	64
3.4.5: Conclusion.....	66

Section 3.5. Di-cycloplatination.....	67
3.5.1: Introduction.....	67
3.5.2: Di-cycloplatinated 2,6-bis(4'-alkoxyphenyl)pyridines.....	68
3.5.3: C-H activation induced by water.....	72
3.5.4: Molecular structures of CO complexes.....	75
3.5.5: Cycloplatination mechanism.....	77
Section 3.6. Theoretical Studies.....	80
Section 3.7. Ligand substitution.....	84
3.7.1: Introduction.....	84
3.7.2: C ^N C Platinum PMe ₃ complexes.....	84
3.7.3: C ^N C Platinum stilbazole complexes.....	85
3.7.4: Thermal behaviours.....	86
3.7.5: Conclusion.....	87
Section 3.8. Platinum carbene complex.....	88
3.8.1: Synthesis of 2,6-bis(2',4'-dihexyloxyphenyl)pyridine platinum dichloride dimer.....	88
Section 3.9. References.....	92
Chapter 4: Experimental.....	96
Section 4.0. General considerations.....	96
Section 4.1. Preparation and characterisation of 2,6-bis-(4-hexyloxyphenyl)pyridine.....	96
4.1.1: Preparation of 4-hexyloxychlorobenzene.....	96
4.1.2: Preparation of 3-Hexyloxyphenyl magnesium chloride.....	97
Section 4.2. Preparation and characterisation of 2,6-bis-(2,4-dialkoxyphenyl)pyridines.....	99
4.2.1: Preparation of 2,6-bis-(2,4-dihexyloxyphenyl)pyridine.....	99
Section 4.3. Preparation and characterisation of 2,4,6-tris-(4-alkoxyphenyl)-[1,3,5]triazine.....	101
Section 4.4. Preparation and characterisation of 4-(4-alkoxyphenyl)-2,6-diphenylpyridine.....	102
4.4.1: Preparation of 4-octyloxybenzaldehyde.....	102
4.4.2: Preparation of 1-(2-phenyl)-3-[4-octyloxyphenyl]propen-1-one.....	103
4.4.3: Preparation of 4-(4-octyloxyphenyl)-2,6-diphenylpyridine.....	104
Section 4.5. Preparation and characterisation of 4-octyloxystilbazole.....	105
4.5.1: Preparation of 4-octyloxyiodobenzene.....	105
4.5.2: Preparation of 4-octyloxystilbazole.....	106
Section 4.6. Preparation and characterisation of [(2,6-diphenylpyridine)Pt-Cl] ₂	107
Section 4.7. Preparation and characterisation of [{2,6-bis(4-alkoxyphenyl)pyridine}Pt-Cl] ₂	109
4.7.1: Preparation of [{2,6-bis(4-hexyloxyphenyl)pyridine}Pt-Cl] ₂	109
Section 4.8. Preparation and characterisation of [{4-(4-octyloxyphenyl)-2,6-diphenylpyridine}Pt-Cl] ₂	110
Section 4.9. Preparation and characterisation of [{2,4,6-tris-(4-alkoxyphenyl)-[1,3,5]triazine}Pt-Cl] ₂	112
Section 4.10. Preparation and characterisation of Pt(phpy)(Hphpy)Cl.....	113
Section 4.11. Preparation and characterisation of Pt ^{IV} (phpy) ₂ Cl ₂	114
Section 4.12. Preparation and characterisation of [2,6-bis(4-hexyloxyphenyl)pyridine]Pt-Cl(PMe ₃) ₂	115
Section 4.13. Preparation and characterisation of (2,6-diphenylpyridine)Pt(DMSO)Cl.....	117
Section 4.14. Preparation and characterisation of [2,6-bis-(4-alkoxyphenyl)pyridine]-Pt(DMSO)Cl.....	117
Section 4.15. Preparation and characterisation of [4(4octyloxyphenyl)2,6diphenylpyridine]Pt(DMSO)Cl.....	119
Section 4.16. Preparation and characterisation of (2,6-diphenylpyridine)Pt(CO)Cl.....	120
4.16.1: Complex (36).....	120
4.16.2: Complex (38).....	121
Section 4.17. Preparation and characterisation of [4-(4-Octyloxy-phenyl)-2,6-diphpy]Pt(Cl)(CO).....	121
4.17.1: Complex (37).....	121
4.17.2: Complex (39).....	123
Section 4.18. Preparation and characterisation of {2,4,6-tris-(4-alkoxyphenyl)-[1,3,5]triazine}Pt-(CO)Cl.....	124
Section 4.19. Preparation and characterisation of C ^N C [2,6-bis(4-alkoxyphenyl)pyridine]Pt-CO.....	125
4.19.1: Preparation of C ^N C [2,6-bis(4-hexyloxyphenyl)pyridine]Pt-CO.....	125
Section 4.20. Preparation and characterisation of C ^N C [2,6-bis(4-alkoxyphenyl)pyridine]Pt-DMSO.....	126
4.20.1: Preparation of C ^N C [2,6-bis(4-hexyloxyphenyl)pyridine]Pt-DMSO.....	126
Section 4.21. Preparation and characterisation of C ^N C [2,6-diphenylpyridine]Pt-DMSO.....	127
Section 4.22. Preparation and characterisation of [4-(4-octyloxyphenyl)-2,6-diphenylpyridine]Pt-DMSO.....	128
Section 4.23. Preparation and characterisation of C ^N C [2,6-diphenylpyridine]Pt-CO.....	130
Section 4.24. Preparation and characterisation of [4-(4-octyloxyphenyl)-2,6-diphenylpyridine]Pt-CO.....	131
Section 4.25. Preparation and characterisation of C ^N C [2,6-diphenylpyridine]Pt-PMe ₃ , (49).....	133

Section 4.26: Preparation and characterisation of C ^N C [2,6-diphenylpyridine]Pt-(4-octyloxystilbazole).	134
Section 4.27. Preparation and characterisation of C ^N C [4-(4-octyloxyphenyl)-2,6-diphenylpyridine]Pt-(4-octaloxystilbazole).	135
Section 4.28. Preparation and characterisation of [{2,6-bis(2,4-dihexyloxyphenyl)pyridine}PtCl ₂] ₂	136
Appendix 1.....	A1:CXXXVIII
X-Ray crystallographic details for (5d).....	A1:CXL
X-Ray crystallographic details for (24).....	A1:CXLIII
X-Ray crystallographic details for (28).....	A1:CXLVIII
X-Ray crystallographic details for (29).....	A1:CLI
X-Ray crystallographic details for (40).....	A1:CLIV
X-Ray crystallographic details for (44).....	A1:CLVII
X-Ray crystallographic details for (46).....	A1:CLXII
X-Ray crystallographic details for (47).....	A1:CLXVI
X-Ray crystallographic details for (53).....	A1:CLXXI
Appendix 2.....	A2:I
Photographic plates of mesogenic optical textures.	A2:I
Appendix 3.....	A3:I
Refereed Publications.	A3:I

Table of Illustrations.

Figure 1.1:	Cholesteryl benzoate.....	1
Figure 1.2:	Liquid crystal classification.....	2
Figure 1.3:	Formation of a lyotropic mesophase.....	3
Figure 1.4:	Schematic representation of a thermotropic mesogen.....	4
Figure 1.5:	Schematic representation of nematic phase.....	6
Figure 1.6:	The diffuse layer structure of the smectic A phase.....	7
Figure 1.7:	Schematic representation of the hexagonal packing in a smectic B phase.....	7
Figure 1.8:	Tilt direction of the smectic F phase.....	8
Figure 1.9:	Tilt direction of the smectic I phase.....	8
Figure 1.10:	Thermal stability of thermotropic mesophases.....	8
Figure 1.11:	Helical twisting of director in cholesteric phase.....	9
Figure 1.12:	Nematic discotic phase.....	10
Figure 1.13:	Columnar hexagonal phases.....	10
Figure 1.14:	Tilted hexagonal columnar phases.....	11
Figure 1.15:	The proposed structure of a columnar nematic phase.....	11
Figure 1.16:	Discotic and calamitic main chain polymeric mesogens.....	12
Figure 1.17:	Calamitic side chain polymeric mesogen.....	12
Figure 1.18:	The first organometallic liquid crystal: Mercury(II) bis-4(4'-alkoxy)benzylidene.....	13
Figure 1.19:	Giroud and Muller-Westerhoff's nickel dithiolenes.....	13
Figure 1.20:	Matth��te and Billard's monosubstituted ester ferrocene complexes.....	14
Figure 1.21:	1,1' Disubstituted ferrocenes.....	15
Figure 1.22:	Platinum/Palladium(II) cyanobiphenyls.....	15
Figure 1.23:	Alkene substituted platinum stilbazole complexes.....	16
Figure 1.24:	Dimeric ortho-palladated Schiff's base.....	16
Figure 1.25:	Amino acid chelated cyclopalladated metallomesogens.....	17
Figure 1.26:	Octahedral rhodium(III) metallomesogen.....	17
Figure 1.27:	Copper(II) discotic metallomesogens.....	18
Figure 1.28:	Octahedral Chromium(III) columnar metallomesogen.....	19
Figure 1.29:	Helical self-assembling <i>trans</i> chiral β -diketone columnar metallomesogen complexes.....	19
Figure 1.30:	Columnar metallomesogen porphyrins.....	20
Figure 1.31:	Phthalocyaninatoxoxtitanium columnar liquid crystals.....	20
Figure 1.32:	Tetranuclear cyclopalladated columnar liquid crystals.....	21
Figure 1.33:	Mesogenic cobalt cyclopentadienylide cyclobutadiene acetylene co-polymer.....	22
Figure 1.34:	Calamitic side chain metallomesogen.....	22
Figure 2.1:	Basic mechanism for the formation of metallacycles.....	27
Figure 2.2:	Basic mechanism for the intermolecular activation of C-H bonds.....	28
Figure 2.3:	Oxidative addition mechanism, followed by reductive elimination.....	28
Figure 2.4:	Electrophilic substitution mechanism.....	29
Figure 2.5:	Multicentered pathway mechanism.....	29
Figure 2.6:	Periodic Table.....	30
Figure 2.7:	Formation of five-membered cyclopalladated metallacycle.....	31
Figure 2.8:	The first six-membered cyclometalated ring system.....	31
Figure 2.9:	Reaction of Li_2PdCl_4 with primary, secondary and tertiary amines.....	32
Figure 2.10:	Proposed mechanism for cyclopalladation.....	33
Figure 2.11:	Bonding modes for <i>exo</i> and <i>endo</i> palladocycles.....	34
Table 2.1:	Order of stability of final products for cyclopalladation in acetic acid.....	34
Figure 2.12:	Cyclopalladation of bis(<i>N</i> -benzylidene)-1,4-phenylenediamine.....	35
Figure 2.13:	The first di-cyclometalated complexes.....	35
Figure 2.14:	First $\text{N}^{\wedge}\text{N}^{\wedge}\text{C}$ tridentate complex.....	36
Figure 2.15:	Cyclometalated $\text{N}^{\wedge}\text{N}^{\wedge}\text{C}$ bipyridine complexes.....	36
Figure 2.16:	Possible binding modes for (3-dimethylaminomethylbenzyl)dimethylamine.....	37
Figure 2.17:	Divergent behaviour of Pd(II) and Pt(II) in the metalation of 1,3-di(2-pyridyl)benzene.....	38
Figure 2.18:	New $\text{P}^{\wedge}\text{C}^{\wedge}\text{P}$ complexes.....	39
Figure 2.19:	Cyclometalation <i>via</i> a nucleophilic displacement of a halide.....	39

Figure 2.20:	“Square planar” platinum(II) complexes showing helical chirality.	40
Figure 2.21:	Cyclometalation via C _{aryl} -R bond activation.	40
Figure 2.22:	Examples of double cyclometalated rings.	40
Figure 3.2.1:	Synthetic route to 2,6-bis-(alkoxyaryl)pyridines.	46
Figure 3.2.2:	Molecular structure of (5d).	47
Figure 3.2.3:	Synthetic route to 2,4,6-tris-(4-hexyloxyphenyl)-[1,3,5]triazine.	47
Figure 3.2.4:	Synthetic route to 4'-(4-octyloxyphenyl)-2',6'-diphenylpyridine.	49
Figure 3.2.5:	N [^] N [^] C and N [^] N [^] N Kröhnke ligands.	49
Figure 3.2.6:	Synthetic route to 4'-octyloxystilbazole.	50
Figure 3.2.7:	Mesogenic behaviour of 4'-octyloxystilbazole.	51
Figure 3.3.1:	Synthetic route to chloride bridged dimers.	52
Figure 3.3.2:	Molecular structure of (24).	53
Figure 3.3.3:	N [^] C (2-Phenylpyridine) ₂	54
Figure 3.3.4:	C [^] N [(MeOC ₆ H ₃ CH ₂ NMe ₂)Pt(py)Cl]	55
Figure 3.3.5:	Synthetic route to the triazine chloride bridged dimer.	56
Figure 3.3.6:	Synthetic route to N [^] C (2-phenylpyridine) ₂ Pt ^{IV} Cl ₂	57
Figure 3.3.7:	Molecular structure of (28).	58
Figure 3.3.8:	Molecular structure of (29).	59
Figure 3.3.9:	The formation of the <i>trans</i> Pt(IV) -enantiomeric isomer complex.	60
Figure 3.4.1:	Cleaving the chloride bridge with PMe ₃	61
Figure 3.4.2:	Cleaving the chloride bridge with DMSO.	62
Figure 3.4.3:	Synthetic route to mono-cyclometalated platinum carbon monoxide complexes.	65
Figure 3.4.4:	<i>trans</i> Ligand addition.	67
Figure 3.5.1:	Synthetic route to di-cycloplatinated 2,6-bis(4'-alkoxyphenyl)pyridines	68
Figure 3.5.2:	Molecular structure of (40).	70
Figure 3.5.3:	Mono-cyclometalated to di-cyclometalated C [^] N [^] C tridentate platinum DMSO complexes	72
Figure 3.5.4:	Molecular structure of (44).	73
Figure 3.5.5:	Mono-cyclometalated to di-cyclometalated C [^] N [^] C tridentate platinum CO complexes.	74
Figure 3.5.6:	Molecular structure of (46).	75
Figure 3.5.7:	Molecular structure of (47).	76
Figure 3.5.8:	Molecular structure of (47) showing two complexes in the unit cell.	77
Figure 3.5.9:	Di-cyclometalated 2-phenylpyridine.	79
Figure 3.6.1:	The optimised structure of (46).	81
Table 3.6.1:	Selected bond lengths (Å) in the structure of (46).	82
Figure 3.6.2:	The optimised structure of (36).	83
Figure 3.6.3:	The optimised structure of (38).	83
Figure 3.7.1:	Synthetic route to (49) and (50).	84
Figure 3.7.2:	Synthetic route to (51) and (52).	85
Table 3.7.1:	Thermal comparison of platinum 2,6-diphenylpyridine complexes.	86
Figure 3.8.1:	Synthetic route to platinum carbene complex.	88
Figure 3.8.2:	The carbene (53) and the zwitterions (54) as possible formal structures.	89
Figure 3.8.3:	Molecular structure of (53).	90

Acknowledgements.

I would like to acknowledge the assistance of the following, over the past three years:

Dr Jonathan Rourke for his advice, help and use of his research facilities;

Dr Donocadh Lydon for his help and advice in the laboratory;

Dr Robert Deeth for the computational work;

Dr William Errington and Dr Nathaniel Alcock for solving the X-ray crystallographic structures;

Warwick Analytical Services;

Johnson-Matthey for the loan of precious metal salts;

EPSRC for my studentship.

Declaration.

I hereby declare that this thesis is my own work and that to the best of my knowledge and belief, it contains neither material previously published or written by another person, nor material which has been accepted for the award of any other degree or diploma of a university or institute of higher education, except where due acknowledgement is made in the text. Some of the material contained within this thesis has been accepted for academic publication with the following references:

G W V Cave, A J Hallett, W Errington and J P Rourke, "Inter- versus intramolecular C-H activation: the synthesis and characterisation of a novel platinum complex"; *Angewandte Chemie*, 1998, **110**, 3466-3468; *Angewandte Chemie International Edition*, 1998, **37**, 3270-3272.

G W V Cave, N W Alcock and J P Rourke, "High yield synthesis of a di-cyclometalated C^NC tridentate platinum complex"; *Organometallics*, 1999, **18**, 1801-1803.

G W V Cave (BSc., MSc.).

Summary.

This thesis describes the synthesis and characterisation of novel cycloplatinated 2,6-diphenylpyridine complexes and an interesting platinum carbene complex formed by an unusual intermolecular C-H activation.

2,6-Diphenylpyridine, 2,6-bis(4'-alkoxyphenyl)pyridines, 4-(4-octyloxyphenyl)-2,6-diphenylpyridine and 2,4,6-tris-(4-alkoxyphenyl)-[1,3,5]triazine have all been mono-cycloplatinated to form chloride bridged dimers. These dimers have been cleaved with various ligands including trimethylphosphine, dimethylsulfoxide and carbon monoxide.

The synthesis and characterisation of the cyclometalated products of 2-phenylpyridine, and subsequent oxidation to a platinum(IV) complex has been described.

A novel high yield synthetic route to the di-cycloplatination of C^NC type ligands involving a C-H activation induced by water has also been reported. The synthesis of di-cycloplatinated 2,6-diphenylpyridine, 2,6-bis(4'-alkoxyphenyl)pyridines and 4-(4'-octyloxyphenyl)-2,6-diphenylpyridine ligands has been recorded.

The lability of the dimethylsulfoxide ligand used in the di-cyclometalation reaction is demonstrated by its substitution with trimethylphosphine, carbon monoxide and the stilbazole ligand.

Thermal analyses of all the ligands and cyclometalated products have been recorded. The mesogenic behaviour of four materials has been described and discussed.

This report also includes a synthetic route to a platinum carbene dimer formed from a 2,6-bis(2',4'-alkoxyphenyl)pyridine ligand.

Abbreviations.

Å	Angstrom ($1 \text{ Å} = 1 \times 10^{-10} \text{ m}$)
Ac	Acyl
CI	Chemical ionisation
Cp	η^5 -Cyclopentadienyl
d	Doublet
DMF	Dimethylformamide
DMSO	Dimethylsulfoxide
DSC	Differential scanning calorimetry
EI	Electron impact
FAB	Fast atom bombardment
FT	Fourier transform
h	Hours
I	Isotropic liquid
ICP	Inductively coupled plasma
IR	Infra-red
J	coupling constant (Hz)
K	Crystal
LCD	Liquid crystal display
M	Metal
m	Multiplet
MALDI	Matrix assisted LASER desorption ionisation
Me	Methyl

min	Minute
Mp.	Melting point
MS	Mass spectrometry
N	Nematic phase
nOe	Nuclear Overhauser effect
NMR	Nuclear magnetic resonance
ph	Phenyl
ppm	Parts per million
py	Pyridine
R	Hydride, alkyl or aryl substituent
s	Singlet
TGA	Thermal gravitational analysis
TOF	Time of flight
t	Triplet
	Stretching band frequency (cm^{-1})
δ	Chemical shift (ppm)

Chapter 1: Introduction to liquid crystals.

Section 1.1. Introduction

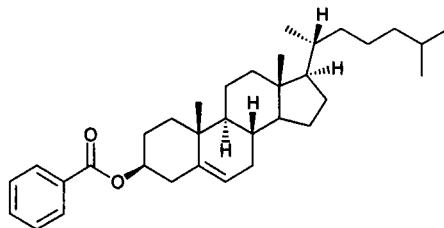


Figure 1.1: Cholesteryl benzoate.

A whole new field of chemistry and physics developed in Prague, 1888, to the words, “turbid fluid”.¹ These were the words of Friedrich Reinitzer, when he first observed what we now refer to as liquid crystals. He found that when he heated a pure sample of cholesteryl benzoate, the crystal solid melted at 145 °C, but not into a normal liquid, and that when he heated it further this new phase subsequently cleared into the normal liquid at 179 °C.

Liquid crystals were not invented in a laboratory, but have been around since the first signs of life. The cell membrane has been known for years to contain a phospholipid bilayer, however, it was not until this century that they were realised to be liquid crystalline. Scientists now produce liquid crystals with a wide range of applications, varying from colour changing charity red noses, portable television screens, to more recently, memory storage systems for computer data. It is therefore not difficult to see how liquid crystals have produced a multi-billion dollar industry, with demands on scientists to search for materials, with new properties and applications.

One definition² of a liquid crystal is a thermodynamically stable state of matter, which exists between the crystal and the isotropic liquid. This fourth state of matter does not possess the positional molecular order that a crystal lattice exhibits. However, the molecules do align with a certain degree of orientational order. Perhaps, therefore, a better term for

liquid crystal is *mesogen* (taken from the Greek mesosmorphe, meaning between two states or forms); the phenomenon then would be *mesomorphism*, and *mesophase* would describe the state of matter. It was Friedel who proposed this nomenclature, in 1922.³

The highly ordered structures of solids dictates their anisotropic physical properties, brought about by the regular position and orientation of the molecules, within the crystal lattice. In the liquid crystal phase the exact position and orientation of the molecules is lost.

Mesogens can be divided into essentially two classes, namely *thermotropics*⁴ and *lyotropics*.⁵

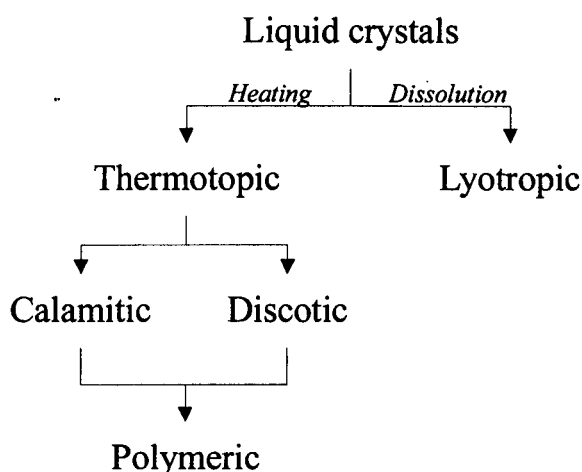


Figure 1.2: Liquid crystal classification.

Section 1.2. Lyotropic Mesogens

Lyotropic mesophases are formed when a solute exceeds a particular concentration. This behaviour is not observed with every concentrated solution; the solute molecules must be of a certain type. An understanding of the processes that are involved in this mesomorphism is essential when predicting which materials will form lyotropic mesophases.

Micelle formation is the key to understanding lyotropic mesomorphism. The molecules, which are responsible for the formation of micelles, are of a specific type; they

must contain a long hydrophobic alkyl chain (tail), as well as a hydrophilic head. One example of such a group is the phospholipids. When the solvent is in large excess the molecules are free to move about individually. In this instance the solution is termed as an isotropic solution. As the concentration is increased, the molecules group together to form spheres with their hydrophobic tails toward the centre (when the solvent is aqueous in nature). The hydrophilic head will be orientated to the centre if the solvent is organic. These spheres are referred to as micelles. The concentration at which micelles are first formed from the isotropic solution is known as the *critical micelle concentration* (CMC). The micelles are able to develop into disc or rod like shapes when the concentration is further increased. These micelles then align next to one another; to form a partly ordered structure called a lyotropic mesophase. Further increase in concentration would lead to the formation of the solid phase.

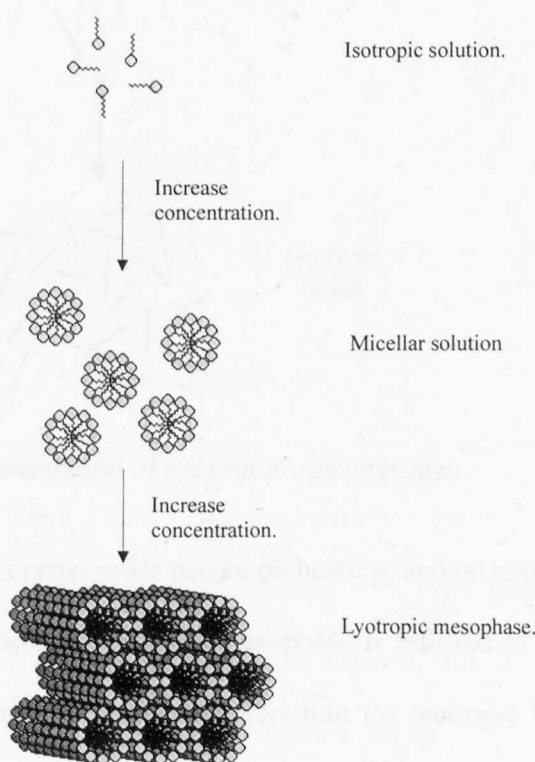


Figure 1.3: Formation of a lyotropic mesophase.

Section 1.3. Thermotropic mesogens.

As the name implies, thermotropic mesogens have temperature dependent properties. In general, when a solid thermotropic material is heated from its solid phase it melts into a liquid crystal. On further heating the mesogenic texture clears into the normal (isotropic) liquid. These thermal properties are reversible on cooling.

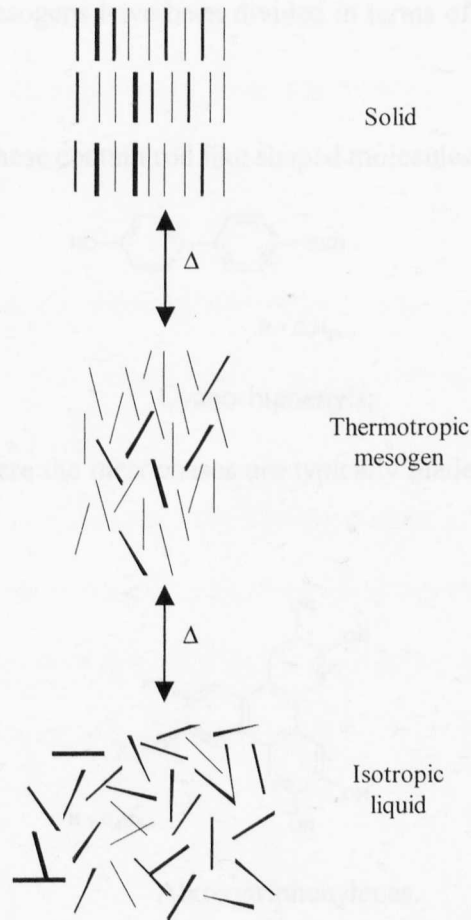


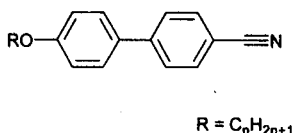
Figure 1.4: Schematic representation of a thermotropic mesogen.

If the disruption of the crystal order occurs on heating, and on cooling of the isotropic liquid a mesogenic state is observed, then the mesophase is referred to as an *enantiotropic* phase. The temperature at which the material enters into the isotropic liquid is termed the *clearing point*. It is possible that a crystal may go straight to the isotropic liquid from the

crystal without showing any mesogenic behaviour, but when it is super-cooled below its melting point, before recrystallisation can occur, a mesophase forms. Such a mesophase is referred to as a *monotropic* phase. The mesophase will then transform back into the crystal with further cooling, or with time. Therefore, unlike the enantiotropic phases formed on heating (or cooling), the monotropic phase is not thermodynamically stable.

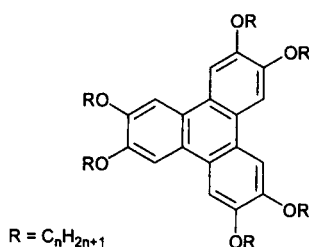
Thermotropic mesogens have been divided in terms of their shape, into two different types, namely:

Calamitic - These contain rod like shaped molecules, *e.g.*



Cyano-biphenyls;

Discotic - Here the mesophases are typically made up of disk shaped molecules, *e.g.*



Alkoxytriphenylenes.

Both types of thermotropic mesogens have a rigid core, are electronically anisotropic and have one or more long flexible side chains. The long alkyl chains help the molecules to remain in an ordered fashion whilst in the mesophase. The rigid cores of the molecules enable them to maintain a certain extent of crystal packing order. It is a combination of these two properties which causes the mesogenic behaviour of molecules.

1.3.1: Calamitic mesophases.

Cyano-biphenyls are a prime example of calamitic mesogens. The classic rod shape of this class of mesogen consists of two parts. The shape of the molecule is controlled by a rigid core structure, usually consisting of a series of *para* substituted aromatic rings. In order for the molecules to retain their orientational order, one or more long n-alkyl chains are added parallel to the linear core. This allows the molecules within a calamitic mesophase to arrange themselves in such a way as to form arrays about their long axis. Calamitic liquid crystals can exhibit several mesophases, and when they do they are described as *polymorphic*.

A vector known as the *director*, \mathbf{n} is defined as the net orientation of the molecules within the phase.² In the liquid phase there is a lack of correlation between the positional and orientational ordering (see *Figure .4*).

The *nematic phase*, N, has the simplest structure of all the mesophases, having only orientation order. If a nematic phase is to be observed it will therefore appear first on cooling the isotropic liquid. The director is established as the mean orientation of the molecules, with respect to their longest axis (see *Figure .5*).

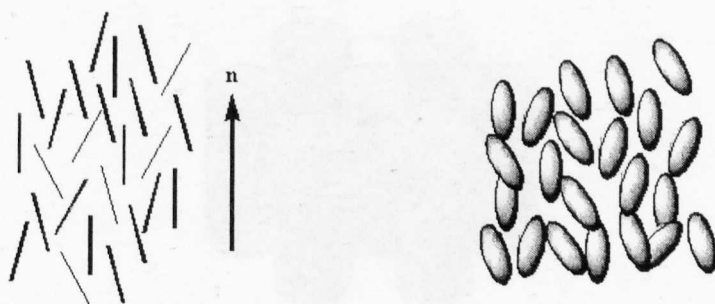


Figure 1.5: Schematic representation of nematic phase.

Smectic phases contain the same sort of orientational order as the nematic phase, as well as a layered structure. Smectic phases can also be fluid, and diffusion between the layers is dynamic. Unlike the nematic phase the smectic phases are further subdivided into several sub phases, varying in order. The smectic A phase, S_A (Figure 1.6) is the least ordered and therefore, if present follows all the other smectic phases on heating.

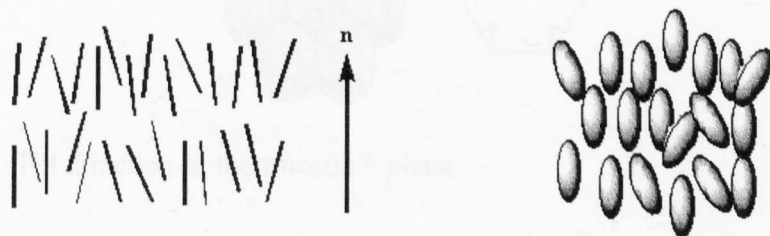


Figure 1.6: The diffuse layer structure of the smectic A phase.

X-ray diffraction studies⁶ of the smectic B phase show that the molecules are arranged in a layered, close packed hexagonal array, with their long axes running perpendicular to the hexagonal face, as shown in Figure 1.7. The individual molecules are observed to rotate freely about their long axes. This close packing of the individual molecules leads to a more highly ordered system than in the smectic A phase.

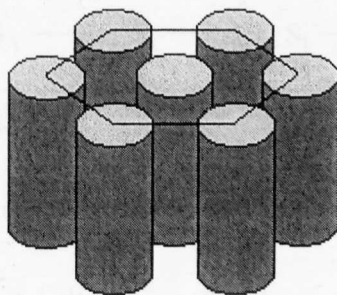


Figure 1.7: Schematic representation of the hexagonal packing in a smectic B phase.

There are also tilted analogues of some of the smectic phases. For example the smectic F and I mesophases (Figure .8 and .9) are analogues of the smectic B, whilst the smectic C is the tilted analogue of the smectic A.

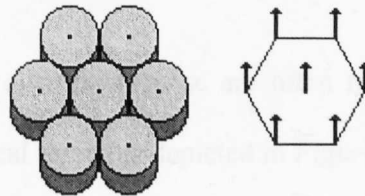


Figure 1.8: Tilt direction of the smectic F phase.

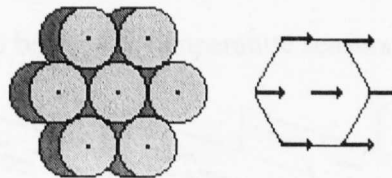


Figure 1.9: Tilt direction of the smectic I phase.

The thermal stability order of several calamitic mesophases exhibited by a hypothetical mesogen are shown in Figure . 0.

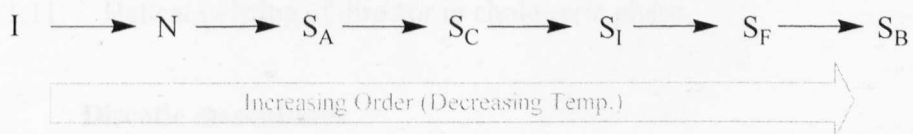


Figure 1.10: Thermal stability of thermotropic mesophases.

Chiral modifications of the tilted smectic phases can be obtained by resolving a racemic mixture of a chiral mesogenic material or by the addition of a chiral dopant to the mesophase. The director of each of these layers is helical with its principal axis

perpendicular to the smectic layer. The helix can be unravelled by applying an external field or by surface stabilisation within a very thin cell. Such cells often exhibit bistable switching, on reversing the polarity of an electric field. This can then result in the display of electro-optical effects.⁷ Chiral phases are represented by an asterisk, for example a chiral smectic C phase can be written as SmC^* .

Chiral nematic phases also exist, these are often referred to as cholesteric phases. Here the director twists in helical array (as depicted in Figure 1.11). The pitch length is often small enough to allow an interaction with the visible region of the electromagnetic spectrum, thus enabling the phase to display iridescence. As the pitch length varies with temperature an observable colour change in the liquid crystal phases is observed. It is this property that enables these liquid crystals to be used as temperature sensors.⁸

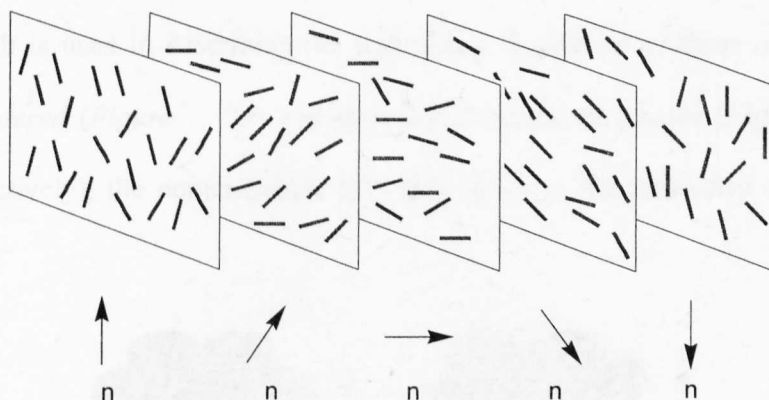


Figure 1.11: Helical twisting of director in cholesteric phase.

1.3.2: Discotic mesophases.

Chandrasekhar first reported discotic mesophases in 1977.⁹ The molecules within a discotic mesophase are arranged in such a way as to form arrays along their short axes. As in the case of the calamitic mesogens, discotic liquid crystals are also polymorphic. The least ordered discotic phase, *nematic discotic phase*, N_D , shows only orientational order and is

therefore very fluid. A schematic representation of a nematic discotic phase is shown in Figure . 2.

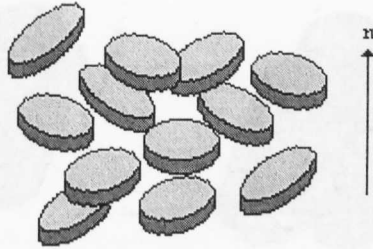


Figure 1.12: Nematic discotic phase.

When the molecules become packed closer together, particularly in side-by-side arrangements, the order of the discotic phase increases in comparison to the nematic discotic phase. It is the symmetry of the side-to-side arrangements, as well as the stacking in columns, which is used in describing the mesophase. Examples of these *columnar* phases include the *ordered* (Figure . 3a) and *disordered hexagonal phases* (Figure . 3b) (D_{ho} and D_{hd} respectively), the nomenclature of which refers to the symmetry of the columnar packing.

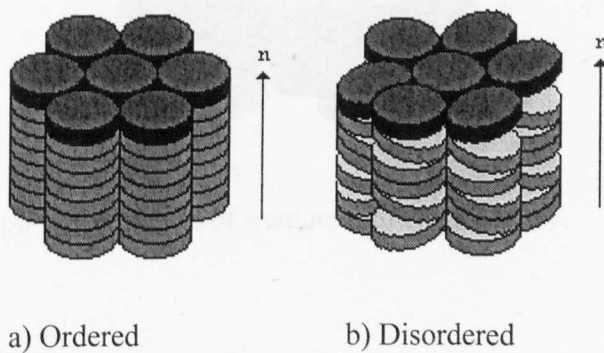


Figure 1.13: Columnar hexagonal phases.

Since their discovery, several discotic mesogenic phases have been reported. However, there still remains some discrepancy in the nomenclature of these phases. It should

be noted that there have been several reports¹⁰ of tilted columnar phases, both ordered and disordered, such as the tilted hexagonal phase D_{hot} , D_{hdt} (Figure . 4).

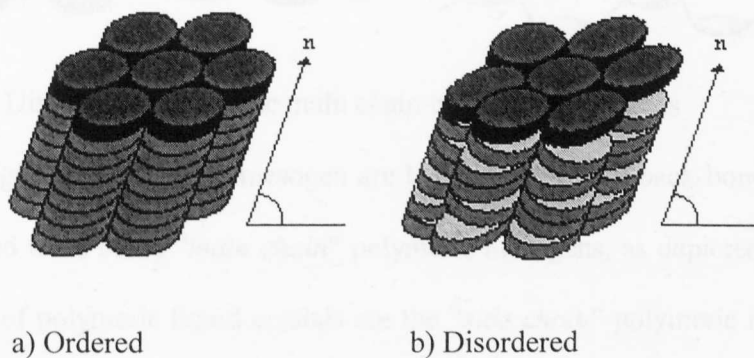


Figure 1.14: Tilted hexagonal columnar phases.

The most recently reported columnar phase is the columnar nematic phase; discovered by Ringsdorf *et al.*, in 1991.¹¹ A postulated schematic structure of Ringsdorf's columnar nematic phase is depicted below (Figure . 5).

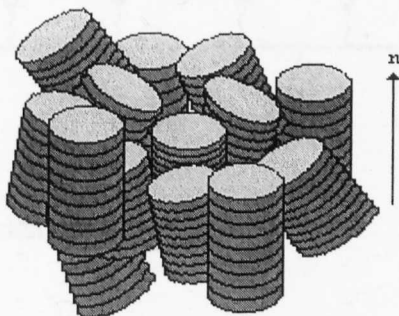


Figure 1.15: The proposed structure of a columnar nematic phase.

Section 1.4. Polymeric Mesogens

A third group of liquid crystals are the polymeric mesogens, these have rigid cores (discotic or calamitic) joined together by long alkyl chains (Figure . 6).

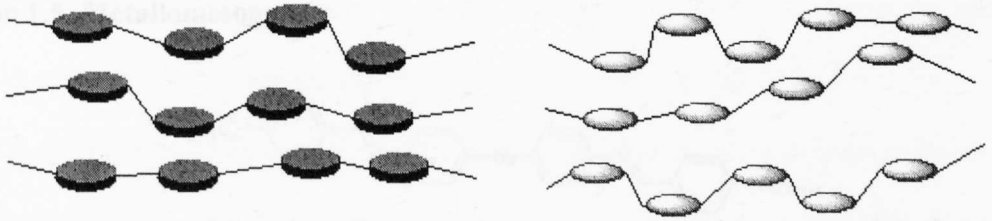


Figure 1.16: Discotic and calamitic main chain polymeric mesogens.

If the rigid sections of the mesogen are located within the back-bone of the polymer they are referred to as being “*main chain*” polymeric mesogens, as depicted in Figure . 6. A second type of polymeric liquid crystals are the “*side chain*” polymeric mesogens. These have mesogenic groups pendant to the polymeric back-bone, as represented in Figure . 7.

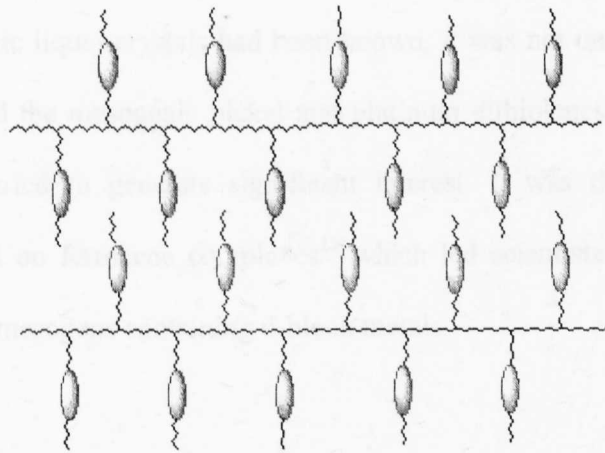


Figure 1.17: Calamitic side chain polymeric mesogen.

Section 1.5. Metallomesogens.

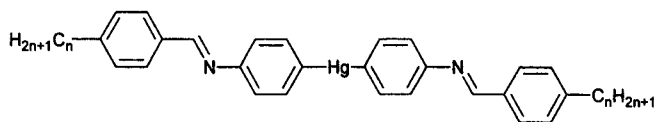


Figure 1.18: The first organometallic liquid crystal: Mercury(II) bis-4(4'-alkoxy)benzylidene.

It was not until 1910 that Vorländer¹² reported the first observed metal containing thermotropic liquid crystals (or *metallomesogens*), in the form of alkali metal carboxylates, $\text{Me}(\text{CH}_2)_n\text{COONa}$. He also noted in 1923 that diarylmercurials formed smectic phases.¹³ Up until then only organic liquid crystals had been known, it was not until Giroud and Muller-Westerhoff¹⁴ reported the mesogenic nickel and platinum dithiolenes in 1977 that work on metallomesogens started to generate significant interest. It was this work and that by Matthête and Billard on ferrocene complexes¹⁵ which led scientists all over the world to synthesise and study mesogens containing d-block metals.

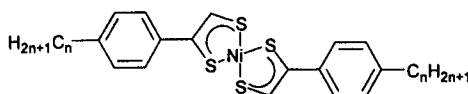


Figure 1.19: Giroud and Muller-Westerhoff's nickel dithiolenes.

The potential advantages of metallomesogens over organic mesogens are numerous:

- a) Organic liquid crystals are often naturally colourless products. Colouring is achieved by the incorporation of dyes, or with filters that slow down the transitions between phases. However, if a transition metal mesogen is used then highly coloured products can be produced without the use of dyes. These colours are brought about by charge

transfer and/or d-d transitions in the visible spectrum. Thus by varying the metal and its oxidation state colour of the liquid crystal can be changed.

- b) The polarisability of the mesogen and the overall anisotropy of the polarisability can be increased with respect to organic molecules by incorporating a metal with either a high or low electron density. This could decrease the response times of future LCD units.
- c) The use of metals in mesogens also leads to a greater selection of possible geometries, over simple organic compounds for example by the use of octahedral complexes.
- d) Mesogenic complexes containing paramagnetic metal centres may be used to produce “fast switching” in optical devices.

The structural criteria of a metallomesogen is that it must contain a metal bound to one or more ligands, with a highly anisotropic shape. The remainder of this chapter reviews some of the important research in the areas of calamitic, columnar and polymeric metallomesogens.

1.5.1: Calamitic metallomesogens.

The ability to build liquid crystals from ferrocene units was a breakthrough for metallomesogen research. Malthête and Billard noted the high thermal stabilities and solubilities for their original ferrocene liquid crystals.¹⁵

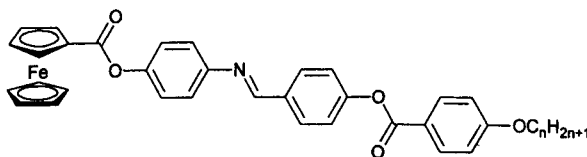


Figure 1.20: Matthête and Billard's monosubstituted ester ferrocene complexes.

Following this result, many research groups turned their attention to the ferrocene moiety as a potential metallomesogen building block.^{16,17} This led to the development of 1,1'

disubstituted ferrocenes. The linearity of these complexes is somewhat discontinuous due to the freedom of rotation about the ferrocene core. This causes a disturbance in the mesophase, resulting in interesting phase behaviour being observed.¹⁸

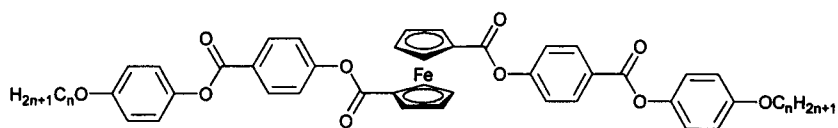


Figure 1.21: 1,1' Disubstituted ferrocenes.

The versatility of ferrocene as a mesogenic core has enabled workers to make many novel metallomesogens with diverse thermal behaviours.^{19,20} Examples include 1,3-disubstituted and 1,1',3-trisubstituted ferrocene cores.

Platinum and palladium have dominated the field of metallomesogen research over the last decade. The reason for this is their ability to form complexes with highly anisotropic shapes, arising from the square planar geometries of the metal (in its +2 oxidation state). Examples of palladium and platinum coordinating to a ligand to produce a metallomesogen are numerous.^{21,22} The *trans* addition of cyanobiphenyls to platinum or palladium demonstrates the simplicity of assembling such a mesogenic system.

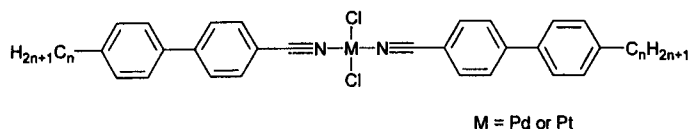


Figure 1.22: Platinum/Palladium(II) cyanobiphenyls.

The phase behaviour of such complexes can often be altered dramatically by subtly altering the ligand environment. Mesogenic platinum *trans*-distilbazole complexes show mesophases above 200 °C. However, by substituting one of the stilbazole ligands with an alkene with long alkyl chain attached, mesophases can be observed at much lower temperatures (<60 °C).²³

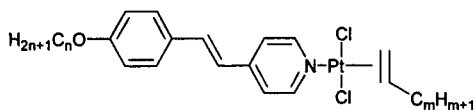


Figure 1.23: Alkene substituted platinum stilbazole complexes.

Anisotropic platinum and palladium metallacycles formed by cyclometalation are convenient building blocks for ortho-metallated metallomesogens. Preliminary work in this field concentrated on the planar geometries of the dimeric bridged species.²⁴ There are many examples of bridging groups able to maintain this “open book” geometry.²⁵ However, acetates and halogens are by far the most common. Examples of chiral *cis* and *trans* isomers of such complexes exist.²⁵

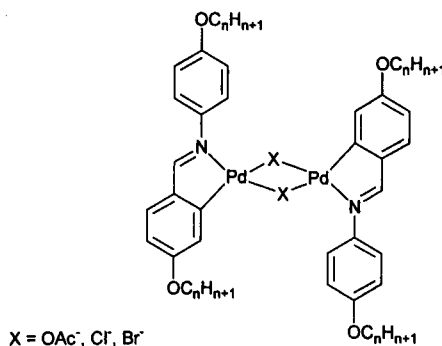


Figure 1.24: Dimeric ortho-palladated Schiff's base complexes.

More recent work reports the effect of cleaving the dimer with groups such as β -diketones and cyclopentadiene.^{26,27} These modifications produce low melting point metallomesogens exhibiting a wider range of mesophases than their dimeric precursors. Several chiral modifications of this type of complex have been reported over the last few years. There are two relatively simple ways of synthesising these analogues, the first of which is to add a chiral group to one of the terminal alkyl chains.²⁸ A second more novel approach is the addition of an amino acid directly to the metal. Enantiomerically pure compounds of this type can be obtained by first cleaving the dimer with a β -diketone, followed

by a regiospecific substitution by the amino acid, yielding only the compound with nitrogen *trans* to nitrogen.²⁹

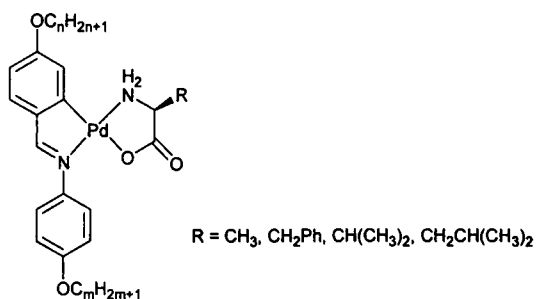


Figure 1.25: Amino acid chelated cyclopalladated metallomesogens.

Attention has turned recently to utilising the many coordination geometries available to metals. To this end several octahedral liquid crystal complexes have been reported.^{30,31} One such example is that of an octahedral rhodium(III) metallomesogen, reported in 1995.³² In order to overcome the disruption in the molecular packing, brought about by the octahedral geometry, a large liquid crystal ligand was used. Another point to note about this complex is that this is the first metallomesogen to be reported with a metal-hydride bond.

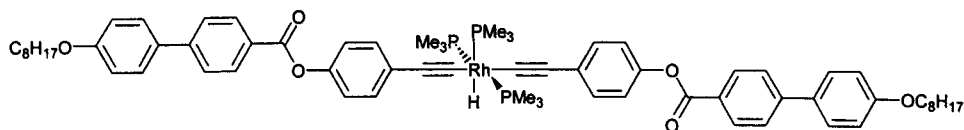


Figure 1.26: Octahedral rhodium(III) metallomesogen.

1.5.2: Columnar metallomesogens.

Traditionally, columnar liquid crystal research has concentrated on the using molecular units that are naturally disk-like and are able to self organise into columnar structures. However, modern techniques often use non-discotic or sub-discotic molecular fragments, which coordinate to each other to form supramolecular columnar structures. The

aim of such investigations is not only to produce self-organising systems, but to build new materials which can exhibit properties such as ferroelectricity,³³ helical superstructure³⁴ and photoconductivity.³⁵ Such properties can be directly attributed to the presence of a metal within the material.

Although organic columnar liquid crystalline materials have frequently been reported since the late seventies⁹ relatively few examples of columnar metallomesogens appeared in the literature until the mid eighties.³⁶ The first paramagnetic columnar metallomesogens achieved a disk-like structure by coordinating copper to two β -diketone groups (*Figure .27*). These complexes showed very ordered columnar phases at relatively low temperatures.³⁷ Numerous analogues of these complexes have been synthesised by varying the substituents on the phenyl groups, many with novel thermal behaviour.

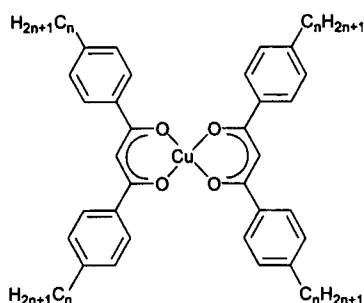


Figure 1.27: Copper(II) discotic metallomesogens.

When a similar β -diketone ligand was treated with chromium(III) the expected distorted octahedral complex was formed (*Figure .28*). Despite the non-discotic geometry of the complex, it exhibited a columnar mesophases at room temperature. On further heating a second columnar phase was observed before clearing into the isotropic liquid.³⁸

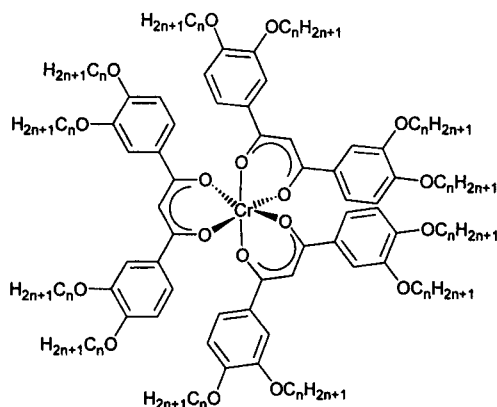


Figure 1.28: Octahedral Chromium(III) columnar metallomesogen.

β -Diketones have also been used to synthesise chiral columnar mesogens. Barberá *et al.* have prepared oxovanadium(IV), copper(II) and palladium(II) β -diketonate complexes with eight chiral centres (Figure 1.29).³⁹ X-Ray studies of these complexes show that the intracolumnar metal-metal distances in the palladium complexes are quite short, relative to those observed in the copper and vanadium compounds. The columnar stacking order within the palladium materials extend over a large range in comparison to the paramagnetic complexes. This indicates that the palladium mesophases are more ordered. This is reiterated by the fact that the palladium materials are very viscous. All the complexes are observed to undergo ferroelectric switching.

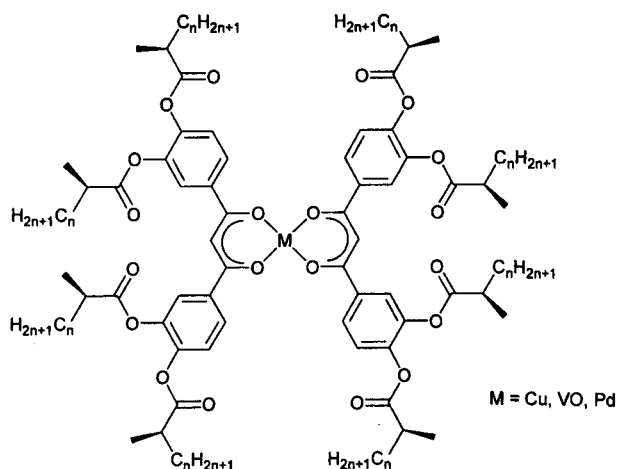


Figure 1.29: Helical self-assembling *trans* chiral β -diketone columnar metallomesogens.

A second class of columnar metallomesogen ligands are the porphyrins. Once a metal is coordinated to the centre of a porphyrin the core of the complex becomes discotic in nature. To this end a series of octaethanolporphyrin derivatives have been prepared by Bard *et al.* in which single columnar phases were observed.⁴⁰ By varying the metal and the alkyl chains the thermal properties and stabilities of such complexes have been utilised for applications ranging from readily processed paints to solubilised dyes.

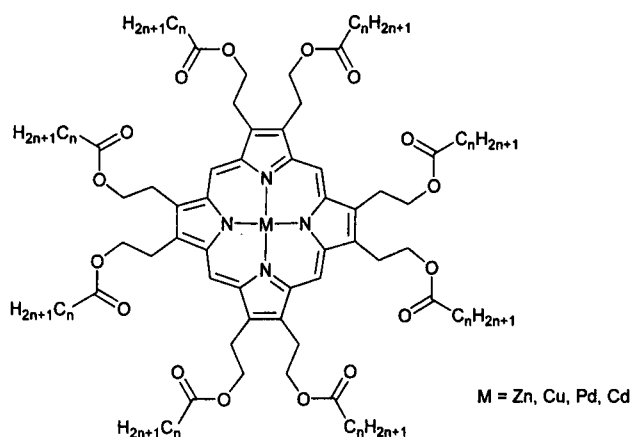


Figure 1.30: Columnar metallomesogen porphyrins.

Shimizu *et al.* observed, by DSC analysis, previously unrecognised mesophases formed when phthalocyaninatooxotitanium was heated. Two mesophases were subsequently identified by X-ray diffraction techniques.⁴¹ This was the first reported oxotitanium discotic metallomesogen.

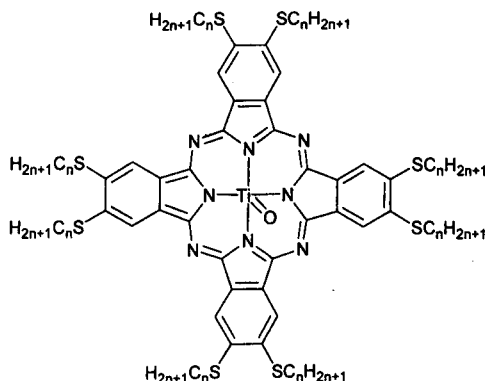


Figure 1.31: Phthalocyaninatooxotitanium columnar liquid crystals.

Various examples of cyclometalated columnar liquid crystals also exist. The most common of these are cyclopalladated Schiff's bases complexes. One such series of mesogens arise from the cyclopalladation of bis(N-benzlidene)-1,4-phenylenediamines with aliphatic peripheral chains (*Figure 1.32*). Four palladium atoms are contained in each molecule, an important factor which contributes to their physical properties, many of which are yet to be understood.⁴² One common factor of this series is that the mesophases do not show any long range order between the positions of the flat cores, thus, they are disordered in nature.

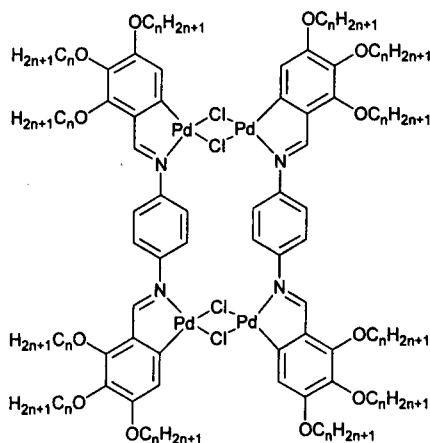


Figure 1.32: Tetranuclear cyclopalladated columnar liquid crystals.

1.5.3: Polymeric metallomesogens.

By combining metallomesogens with polymeric units, new materials have been formed with a large range of applications.⁴³ Examples of main chain and side chain polymeric metallomesogens are given below.

Figure 1.33 shows a typical main chain metallomesogenic polymer. As with normal calamitic and columnar metallomesogens polymeric mesophases can be identified from their optical textures. This cobalt complex shows a calamitic nematic phase, identified by its optical schlieren texture (*Appendix 2*). Unlike the mesophases displayed by the complexes described above, it does not clear into the isotropic liquid but instead starts to decompose on

further heating. The disruption in the packing of this polymer comes from the lateral alkyl chains as well as the cobalt cyclopentadienyl group. The rigidity of the polymeric backbone maintains the overall orientational order of the packing enabling the formation of a nematic phase.

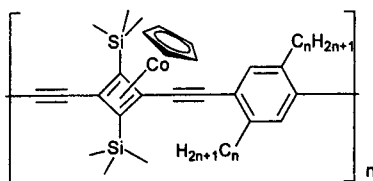


Figure 1.33: Mesogenic cobalt cyclopentadienylide cyclobutadiene acetylene co-polymer.

The ferrocene building block has been utilised in polymeric metallomesogens, *Figure 1.34* shows one such side chain polymeric complex. This material is of particular interest due to the close proximity of the iron atoms to each other and its possible electronic properties.⁴⁴

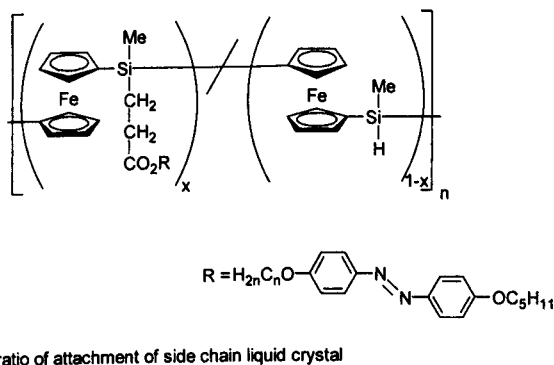


Figure 1.34: Calamitic side chain metallomesogen.

Section 1.6. Future prospects for liquid crystal technology.

The electronics industry has utilised the properties of liquid crystals for many years. The most commercially important application for liquid crystals is in display devices. The advantages of the LCD over the cathode-ray tube are numerous. However, despite the fact that modern LCD units are inexpensive, reliable and have low power consumption, cathode-ray screens still dominate the video industry. The primary reason for this is the fact that LCD

units are unable to provide competitive frame refresh rates. Needless to say, modern research is concentrating on developing liquid crystalline materials that have the potential to switch on a microsecond time scale.

The ability of chiral liquid crystals to change colour with changes in temperature, and thus generate an optical signal has aroused great interest. One application of this which is being explored is the storage of large amounts of information within a small area.

To conclude, the dynamic ordering behaviour and properties characteristic of mesogenic materials has been, and will continue to be, utilised as a truly versatile medium.⁴⁵

Section 1.7. References.

- ¹ F Reinitzer, *Montash. Chem.*, 1888, **9**, 421.
- ² D W Bruce and D O'Hare, "Inorganic Materials"; Chapter 8; John Wiley and Son; Chichester, 1992; 407.
- ³ G Friedel, *Annl. Phys.*, 1922, **18**, 273.
- ⁴ G Vertogen and W H d Jeu, "Thermotropic Liquid Crystals: Fundamentals"; Springer; Berlin, 1988.
- ⁵ G J D Tiddy, *Phys. Rev.*, 1980, **57c**, 1.
- ⁶ Z Luz, R C Hewitt and S Meiboom, *J. Chem. Phys.*, 1974, **61**, 1758.
- ⁷ A Fukuda, *J. Mater. Chem.*, 1994, **4**, 997.
- ⁸ D Lacey in "An Introduction to Molecular Electronics"; 1st edn.; M C Petty, M R Bryce and D Bloor Eds.; Edward Arnold: London, 1995; pp 184.
- ⁹ S Chandrasekhar, *Paramana*, 1977, **9**, 471.
- ¹⁰ B Xu and T M Swager, *J. Chem. Soc., Dalton Trans.*, 1996, 3913.
- ¹¹ H Bengs, O Karthaus, H Ringsdorf, C Baerhr, Mebert and J H Wendorff, *Liq. Cryst.*, 1991, **10**, 161.
- ¹² D Vorländer, *Ber. Dtsch. Chem. Ges.*, 1910, **43**, 3120.
- ¹³ D Vorländer, *Z. Phys. Chem.*, 1923, **105**, 211.
- ¹⁴ A M Giroud and U T M Iler-Westerhoff, *Mol. Cryst., Liq. Cryst.*, 1977, **41**, 11.
- ¹⁵ J Malthête and J Billard, *Mol. Cryst., Liq. Cryst.*, 1976, **34**, 117.
- ¹⁶ J Bhatt, B M Fung, K M Nicholas and C-D Poon, *J. Chem. Soc., Chem. Commun.*, 1988, 1439.
- ¹⁷ R Deschenaux and J-L Marendaz, *J. Chem. Soc., Chem. Commun.*, 1991, 909.
- ¹⁸ R Deschenaux, J-L Marendaz and J Santiago, *Helv. Chim. Acta*, 1993, **76**, 865.

- 19 R Deschenaux, J-L Marendaz, J Santiago and J W Goodby, *Helv. Chim. Acta*, 1995, **78**, 1215.
- 20 R Deschenaux, I Kosztics and B Nicolet, *J. Mater. Chem.*, 1995, **5**, 2291.
- 21 J P Rourke, F P Fanizzi, N J S Salt, D W Bruce, D A Dunmur and P M Maitlis, *J. Chem. Soc., Chem. Commun.*, 1990, 229.
- 22 M Lee, Y Yoo, M Choi and H Chang, *J. Mater. Chem.*, 1998, **8**, 277.
- 23 J P Rourke, F P Fanizzi, D W Bruce, D A Dunmur and P M Maitlis, *J. Chem. Soc., Dalton Trans.*, 1992, 3009.
- 24 J Barberá, P Espinet, E Lalinde, M Marcos and J L Serrano, *Liq. Cryst.*, 1987, **2**, 833.
- 25 J Buey, G A Díez, P Espinet, S García-Granda and E Pérez-Carreño, *Eur. J. Inorg. Chem.*, 1988, 1235.
- 26 G W V Cave, D P Lydon and J P Rourke, *J. Organomet. Chem.*, 1998, **555**, 81.
- 27 D P Lydon, G W V Cave and J P Rourke, *J. Mater. Chem.*, 1997, **7**, 403.
- 28 M J Baena, J Barberá, P Espinet, A Ezcurra, M B Ros and J L Serrano, *J. Am. Chem. Soc.*, 1994, **116**, 1899.
- 29 R Navarro, J Garía, E P Urriolabeitia, C Cateviela and M D Diaz-de-Villegas, *J. Organomet. Chem.*, 1995, **490**, 35.
- 30 D W Bruce and X-H Liu, *J. Chem. Soc., Chem. Commun.*, 1994, 729.
- 31 S Morrone, G Harrison and D W Bruce, *Adv. Mat.*, 1995, **7**, 665.
- 32 J P Rourke, D W Bruce and T B Marder, *J. Chem. Soc., Dalton Trans.*, 1995, 317.
- 33 B Xu and T M Swager, *J. Am. Chem. Soc.*, 1993, **115**, 1159.
- 34 A El-Ghayoury, L Douce, A Skoulios and R Ziessel, *Angew. Chem., Int. Ed. Engl.*, 1998, **37**, 2205.
- 35 J Santiago, T Sugino and Y Shimizu, *Chem. Lett.*, 1998, 661.

- ³⁶ B A Gregg, M A Fox and A J Bard, *J. Chem. Soc., Chem. Commun.*, 1987, 1134.
- ³⁷ A M Giroud-Godquin and P Maitlis, *Angew. Chem., Int. Ed. Engl.*, 1991, **30**, 375.
- ³⁸ H Zheng and T Swager, *J. Am. Chem. Soc.*, 1994, **116**, 761.
- ³⁹ J Barberá, A Elduque, R Giménez, L A Oro and J L Serrano, *Angew. Chem., Int. Ed. Engl.*, 1996, **35**, 2832.
- ⁴⁰ B A Gregg, M A Fox and A J Bard, *J. Am. Chem. Soc.*, 1989, **111**, 3024.
- ⁴¹ J Santiago, T Sugino and Y Shimizu, *Chem. Lett.*, 1998, 661.
- ⁴² B Heinrich, K Praefche and D Guillon, *J. Mater. Chem.*, 1997, **7**, 1363.
- ⁴³ L Oriol and J L Serrano, *Adv. Mat.*, 1995, **7**, 348.
- ⁴⁴ X Liu, D W Bruce and I Manners, *J. Chem. Soc., Chem. Commun.*, 1997, 289.
- ⁴⁵ G W Gray, *Proc. R. Soc. London A*, 1985, **402**, 1.

Chapter 2: Cyclometalation.

Section 2.1. Introduction.

"Sir: An unusual reaction has been found between aromatic azo compounds and potassium tetrachloroplatinate(II) or palladium(II) dichloride."

A C Cope.¹

These words published in 1965 opened the doors to a new and exciting field of chemistry, namely *cyclometalation*. Metallacycle complexes have since found applications in organic synthesis,² enantiomeric excess determination,³ as carcinostatic agents⁴ and novel metallomesogens.⁵

Section 2.2. Cyclometalation mechanisms.

Fundamentally, cyclometalation reactions can be defined as the formation of a cyclic ring containing a carbon metal bond, *via* an intramolecular mechanism. *Figure 2.* summarises the reaction process. Initially, the metal **M** coordinates to the donor atom **Y** of the ligand. The metal then forms a bond to the ligand at a carbon **C** thus evolving a leaving hydrogen atom **H**. (Note, neither the nature nor the final environment of the leaving atom **H** has not been defined at this point.)

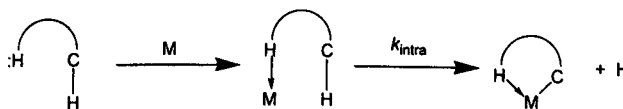


Figure 2.1: Basic mechanism for the formation of metallacycles.

This review deals only with cyclometalation reactions, however Chapter 3 of this report refers to a closely related mechanism, namely the intermolecular activation of C-H bonds. A basic mechanistic approach to this process is represented in *Figure 2.2*.

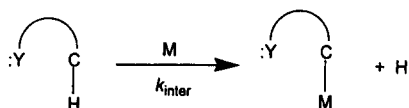


Figure 2.2: Basic mechanism for the intermolecular activation of C-H bonds.

There are thought to be essentially three basic mechanisms for the C-H bond activation during the formation of the metallacycle:^{6,7,8,9}

2.2.1: Oxidative Addition.

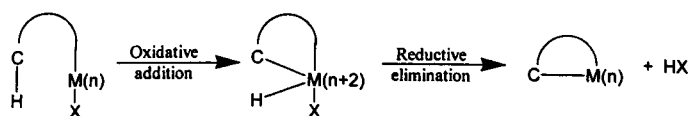


Figure 2.3: Oxidative addition mechanism, followed by reductive elimination.

In order for an oxidative addition to occur the metal **M** can be considered as a nucleophilic centre. During this mechanism the C-H fragment formally receives two electrons from **M**. This increases the formal oxidation state of the **M** by two. The C-H bond is then cleaved forming a metallacycle, with the hydride transferred to the coordination sphere of **M**.¹⁰

The absence of the hydride in the coordination sphere of the metal does not necessarily rule out an oxidative addition mechanism.¹¹ If there is a suitable ligand **X** available, a subsequent reductive elimination reaction can occur, allowing the metal to return to its original oxidation state.

These reactions can be made more favourable by an increase in electron density at the metal.¹² This can be achieved by the addition of electron donating groups to the metal or to the ligand system.

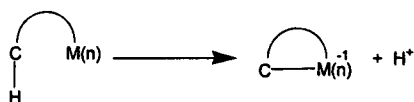
2.2.2: Electrophilic Substitution.

Figure 2.4: Electrophilic substitution mechanism.

During the mechanism for the formation of a metallacycle *via* an electrophilic substitution, the metal forms a bond with the carbon by cleaving the C-H bond. The oxidation state of the metal does not change and no metal hydrides are formed.¹³ Instead, the hydrogen dissociates as a proton. These reactions are therefore assisted by the addition of free or coordinated base, which “mops-up” the leaving proton.¹⁴

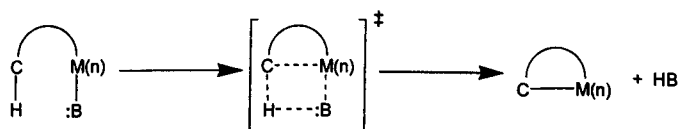
2.2.3: Multicentred Pathway.

Figure 2.5: Multicentered pathway mechanism.

In contrast to the electrophilic substitution reactions, the multicentered pathway mechanism uses alkyl, acetate, benzyl or phenyl groups coordinated to the metal as a base B (Figure 2.5). In order for a multicentered reaction to occur, the reactive species must contain an empty acceptor molecular orbital, to stabilise the σ -bond electron pair in the transition state.⁹

Section 2.3. Effective molarity, M_{eff} .

A key term that is useful to understand when discussing cyclometalation reactions/mechanisms is effective molarity, M_{eff} . The effective molarity has been defined as

the ratio of the rate constants of intra and intermolecular C-H activation, as defined in Figures 2. and 2.2.¹⁵ In practice this is a measure of the effective concentration of C-H bonds in the near vicinity of the metal, once initially coordinated to the ligand. These values can be predicted and are measured in mol dm^{-3} .¹⁶ If $M_{\text{eff}} < 10$ then both intra and intermolecular C-H activation can be expected. When $M_{\text{eff}} > 10$ only cyclometalation will occur.

Section 2.4. A comparative study.

		H		He																	
Li	Be											B	C	N	O	F	Ne				
Na	Mg											Al	Si	P	S	Cl	Ar				
K	Ca	Sc	Ti	V	Cr	Mn	Fe	Co	Ni	Cu	Zn	Ga	Ge	As	Se	Br	Kr				
Rb	Sr	Y	Zr	Nb	Mo	Tc	Ru	Rh	Pd	Ag	Cd	In	Sn	Sb	Te	I	Xe				
Cs	Ba		Hf	Ta	W	Re	Os	Ir	Pt	Au	Hg	Tl	Pb	Bi	Po	At	Rn				
Fr	Ra																				
La	Ce	Pr	Nd	Pm	Sm	Eu	Gd	Tb	Dy	Ho	Er	Tm	Yb	Lu							
Ac	Th	Pa	U	Np	Pu	Am	Cm	Bk	Cf	Es	Fm	Md	No	Lr							

Figure 2.6: Periodic Table (elements carrying out cyclometalation are in red).

A number of metals known to exhibit cyclometalation are shown in Figure 2.6. This report will centre around complexes of platinum and palladium, with a few key examples of other relevant work.

2.4.1: Rules for *ortho*-palladation of aromatic amines.

Following Cope's preliminary investigations into the cyclometalation of azobenzene, Friedrich and Cope performed numerous experiments with primary, secondary and tertiary benzylamines under cyclopalladation conditions.¹⁷ They found that all the systems they studied followed three basic rules:

Rule 1 – Palladium electrophilically attacks the phenyl ring.

The palladium ion acts as an electrophile by accepting electron density from the phenyl ring, during the formation of a covalent Pd-C bond. When an electron withdrawing group is attached to the aromatic ring Pd-C bond formation is unfavourable. In order to overcome this problem electron donating groups may be attached to the phenyl ring.¹⁸

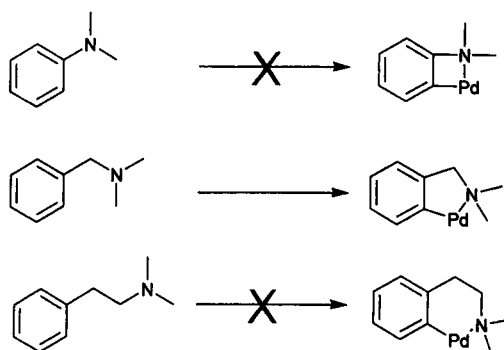
Rule 2 – The cyclometalated ring must be five-membered.

Figure 2.7: Formation of five-membered cyclopalladated metallacycle.

Up until 1977 there were no exceptions to this rule. However, Cameron *et al.* found that when sodium tetrachloropalladate was treated with an *N*-arylamidine, under standard cyclometalation conditions, a six membered metallacycle was formed.¹⁹ Since then several other six membered cyclometalated rings have been synthesised.²⁰

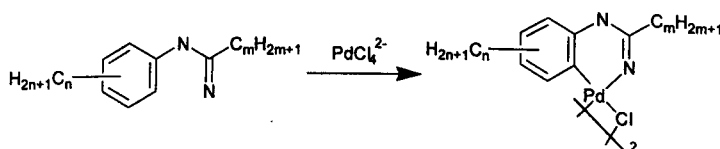


Figure 2.8: The first six-membered cyclometalated ring system.

Rule 3 – The Nitrogen atom must be tertiary.

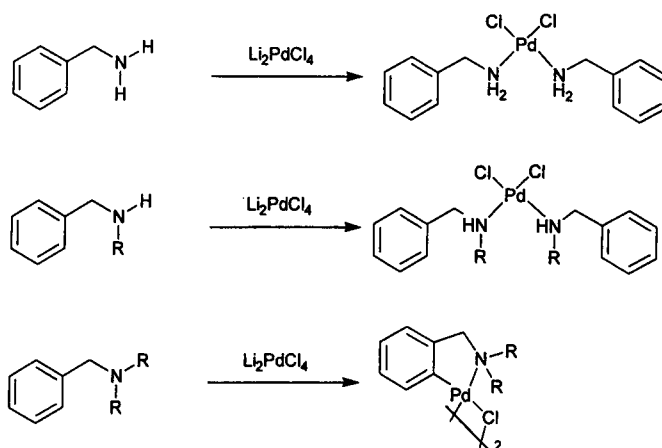


Figure 2.9: Reaction of Li_2PdCl_4 with primary, secondary and tertiary amines.

Cope *et al.* found that only tertiary amines were able to cyclometalate under standard conditions.¹⁷ He hypothesised that both primary and secondary amines form stronger bonds to the metal ion due to there being less steric hindrance around the nitrogen atom than in tertiary amines. This strong bond means more electron donation towards the metal ion, hence satisfying the affinity of palladium for electron density. The stabilised ion has less demand for electrons and so does not perform electrophilic attack on the ring resulting in no Pd-C bond formation.

Work by Avshu *et al.* in 1983 with *trans*-diiodobis(cyanobenzene)palladium(II) and primary amines afforded the cyclometalated iodide bridged dimers.²¹ This encouraged other organometallic chemists investigating this area further. It was found that primary amines could be introduced to form their respective metallacycles by first making the coordination product (as shown in Figure 2.9) and then adding two equivalents of AgClO_4 .²² It was also found that adding an electron donating group such as OMe to the cyclometalating phenyl ring of a primary amine allowed the formation of an acetato bridged dimer metallacycle.²³ The metal ion salt used in this reaction was palladium acetate. It is thought that the acetate

acts as a better base than the halide and thus promotes C-H bond activation.

There are two steps involved in the cyclometalation process using palladium acetate. The first of these is the coordination of the imine to the palladium acetate. This step is considered to be the fast step in the reaction and is not detectable. The second, rate limiting step involves the C-H bond activation. Kinetic studies in acetic acid have probed the transition state.²⁴ On the basis of thermal activation parameters and activation volumes it has been concluded that the transition state must be highly ordered. Supporting information for this comes from X-ray crystallography.²⁰

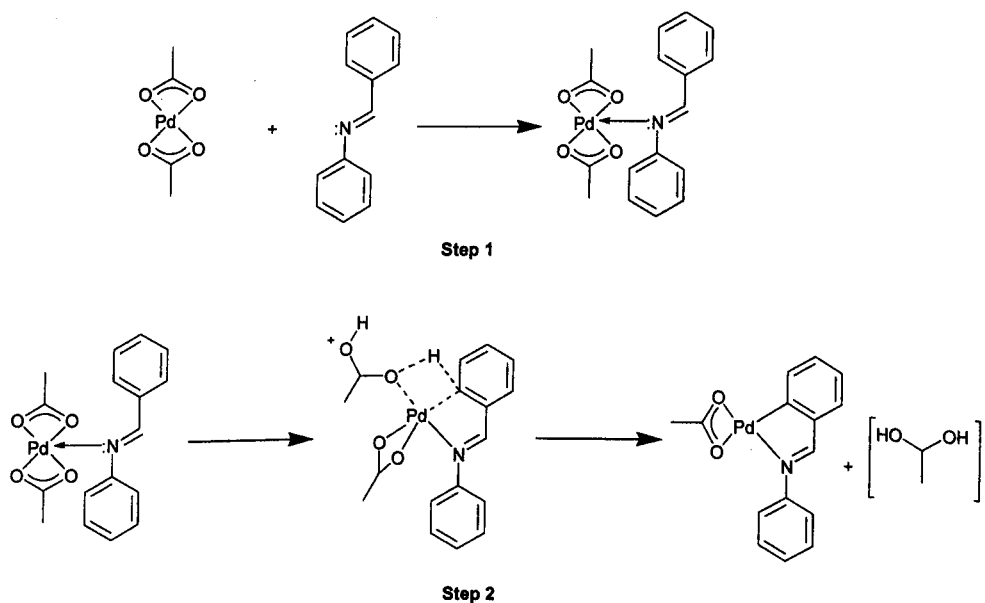


Figure 2.10: Proposed mechanism for cyclopalladation.

2.4.2: *Exo* versus *endo* palladocycles.

Azobenzenes, benzyldienes and *N,N*-dimethyl benzylamine ligands have been used extensively in cyclopalladation due to their ability to donate a lone pair of electrons from a nitrogen atom and subsequently bring about intramolecular C-H activation. In compliance with Cope's second rule, a five membered *endo* metallacycle is the most favoured. However, examples of *exo* metallacycles occur in the literature, where activation of an aliphatic C-H

bond leads to a more unusual metallacycle.²⁵

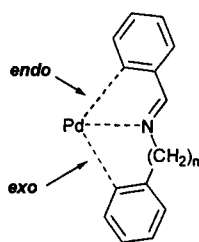


Figure 2.11: Bonding modes for *exo* and *endo* palladacycles.

The following table ranks the stability order of the final products of a given cyclometalation reaction in acetic acid.

Rank	Ring size	Nature of activated C-H bond	Class of palladacycle
1	5	Aromatic	<i>endo</i>
2	6	Aliphatic	<i>endo</i>
3	5	Aromatic	<i>exo</i>
4	5	Aliphatic	<i>exo</i>
5	4	Aromatic / Aliphatic	<i>endo / exo</i>

Table 2.1: Order of stability of final products for cyclopalladation in acetic acid.

The selectivity of the cyclopalladation reaction towards the formation of a five membered *endo* metallacycle is evident when bis(*N*-benzylidene)-1,4-phenylenediamine is treated with palladium acetate. Palladium may dicyclopalladate to the central phenyl ring, or it may monocyclopalladate the two phenyl rings furthest from the imine groups, or both the central phenyl ring and one of the terminal ones. The product distribution shows that the *endo* form of the metallacycle is favoured.²⁶ No cyclopalladation was observed at the central

phenyl ring as this would have required the formation of a four membered *exo* metallacycle.

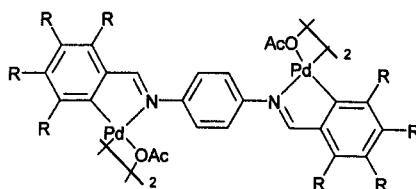


Figure 2.12: Cyclopalladation of bis(*N*-benzylidene)-1,4-phenylenediamine.

2.4.3: Di-cyclometalations.

As early as 1971 chemists started to look at cyclometalation of two metals at the same phenyl ring.²⁷ *N,N,N',N'*-Tetraethyl-*p*-xylene- α,α' -diamine was treated with a tetrachloropalladate salt under normal cyclometalation conditions. The reaction yielded two compounds, namely the *cis* and *trans* chloride bridged products of di-metallation. Following this result, many chemists have applied similar methods to produce many novel complexes with interesting properties.^{28,29} Preliminary mechanistic studies into how this second cyclometalation occurs have recently been reported, but will not be discussed here.³⁰

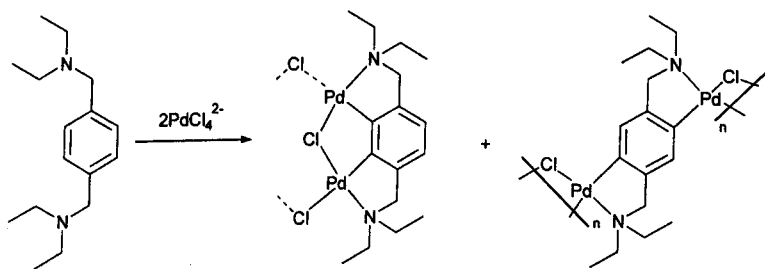


Figure 2.13: The first di-cyclometalated complexes.

2.4.4: Tridentate ligand complexes.

By using two nitrogen donor atoms to coordinate to the same metal researchers attempted to increase the M_{eff} and thus increase the rate of cyclometalation. However, when

dibenzylamine was treated with sodium tetrachloropalladate only the N[^]N coordinated products were observed. The N[^]N[^]C cyclometalated product was produced in high yield following the addition of sodium acetate.³¹ These findings inspired organometallic chemists to synthesis other potentially tridentate prolignands.

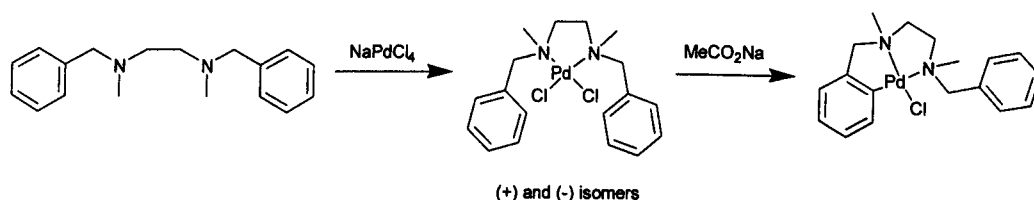


Figure 2.14: First N[^]N[^]C tridentate complex.

2.4.4.1: Cyclometalated N[^]N[^]C complexes.

The next step in investigating the effects of tridentate ligands in cyclometalation was the addition of an extra carbon atom between the two nitrogens atoms. This enabled the formation of a more flexible six membered N[^]N intermediate. Under the same reaction conditions as for the initial coordination in *Figure 2. 4*, the metal cyclometalated in the absence of sodium acetate.³²

Current work with N[^]N[^]C ligands includes the use of two pyridine rings as the ligand donors (*Figure 2. 5*).²⁹ In an attempt to synthesise chemiluminescent metallomesogens, Neve *et al.* synthesised functionalised N[^]N[^]C bipyridine type ligands and treated them with platinum and palladium salts.^{33,34} Although the reaction proceeded in high yield, no mesogenic behaviour was observed.

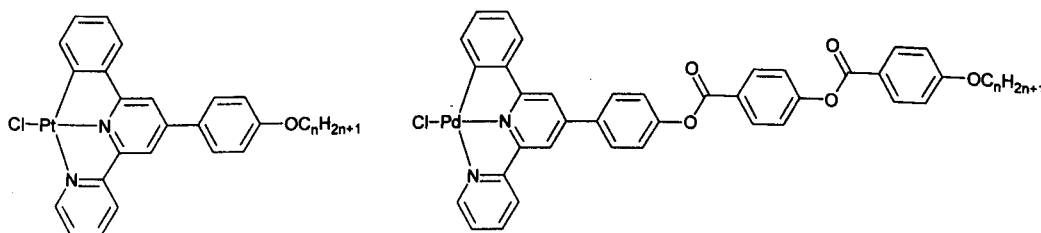


Figure 2.15: Cyclometalated N[^]N[^]C bipyridine complexes.

2.4.4.1: Cyclometalated N[^]C[^]N complexes.

Much of today's research into cyclometalated tridentate complexes involves the use of N[^]C[^]N proligands.³⁵ When *N,N,N',N'*-Tetramethy-*m*-xylene- α,α' -diamine is treated with palladium or platinum salts there are three possible cyclometalation pathways:

- The metal may coordinate to the two donor atoms and subsequently cyclometalate to the central carbon of the phenyl ring, thus forming two cyclometalated rings (*Figure 2. 6a*).
- The metal may coordinate to one of the nitrogen atoms and then cyclometalate to the phenyl carbon *para* to the second amine group, forming one cyclometalated ring (*Figure 2. 6b*).
- The central phenyl ring can become di-metalated by two metals each coordinated to different nitrogen atoms and cyclometalating *meta* to each other on the phenyl ring (*Figure 2. 6c*).

The products of these reactions are dependent on the metal, metal source, temperature and solvent system in which the cyclometalated product was formed.^{35,36,37,38}

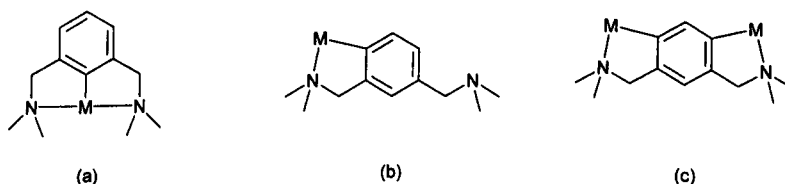


Figure 2.16: Possible binding modes for (3-dimethylaminomethylbenzyl)dimethylamine.

A recent paper describes the effects of cyclometalation of 1,3-bis(2-pyridyl)benzene with platinum and palladium.³⁹ When palladium acetate was used as a metal source, a double metalation takes place on the aryl ring, giving rise to a dimeric open book complex. However, when lithium tetrachloropalladate was used only the coordination complex was isolated. In contrast potassium tetrachloroplatinate afforded the formation of a N[^]C[^]N

tridentate cyclometalated product. The dramatic differences in the cyclometalated products are illustrated in *Figure 2. 7*.

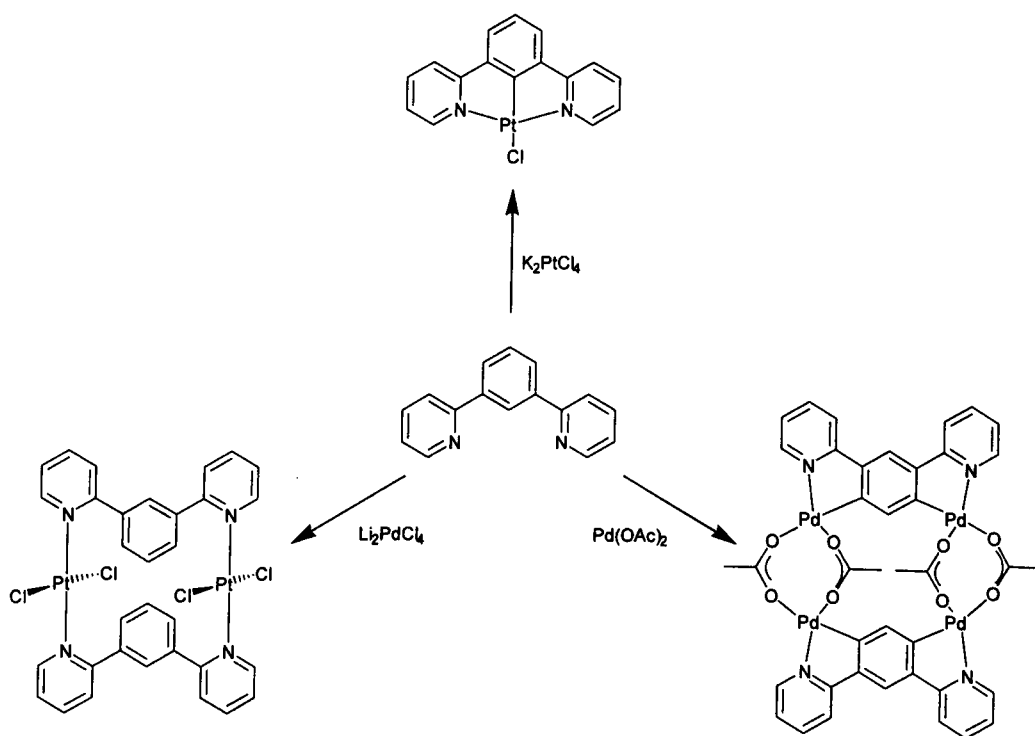
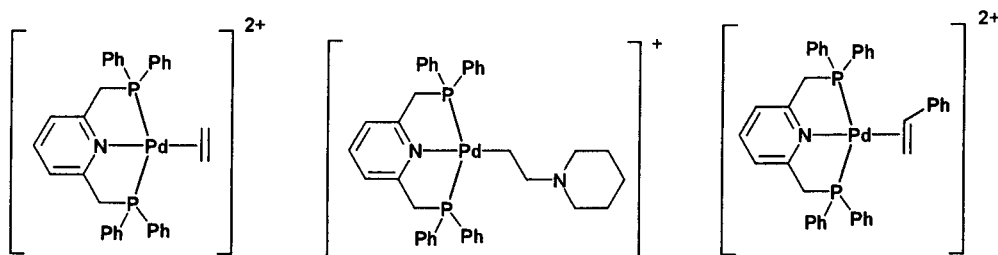


Figure 2.17: Divergent behaviour of Pd(II) and Pt(II) in the metalation of 1,3-di(2-pyridyl)benzene.

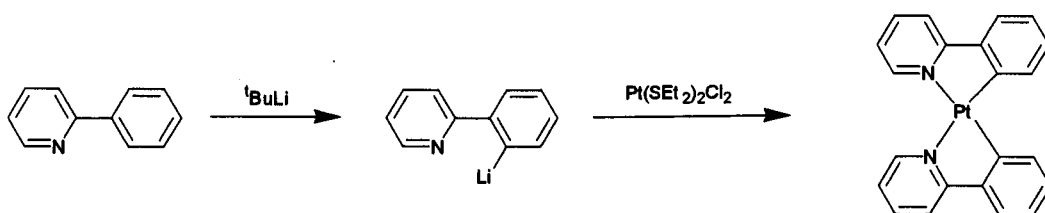
2.4.4.3: Cyclometalated P[^]C[^]P complexes.

The last decade has seen a number of cyclometalated complexes containing phosphorus as a donor atom.^{40,41} Tridentate ligand analogues of those described above have been cyclometalated with various metals.⁴² As with the tridentate N[^]C[^]N complexes the fourth coordination site is often occupied by a chloride ion. Recently Hahn *et al.*⁴³ have published several synthetic routes to complexes with more labile substituents, thus enabling a variety of new uses, such as metallomesogens.

Figure 2.18: New P[^]C[^]P complexes.

Sulphur electron pair donor groups have also been used in tridentate ligands.⁴⁴

2.4.5: Nucleophilic displacement.

Figure 2.19: Cyclometalation *via* a nucleophilic displacement of a halide.

Another approach to cyclometalation is to displace a halide at the metal by a carbanion. Von Zelewsky *et al.* have utilised this method to synthesise square planar platinum(II) complexes, *Figure 2.20*.⁴⁰ Some of these complexes show helical chirality due to the steric constraints of the ligands, *Figure 2.21*.^{45,46} This approach of using the ligand to attack the metal has proved to be very successful for C[^]N ligands such as 2-phenylpyridine but less so for C[^]N[^]C ligands.⁴⁷ Research into dilithiation of the 2,6-diphenylpyridine ligand in an attempt to form a C[^]N[^]C di-cyclometalated core have so far only produced very low yields (<5%) due to the poorly regioselective nature of the second lithiation.⁴⁸

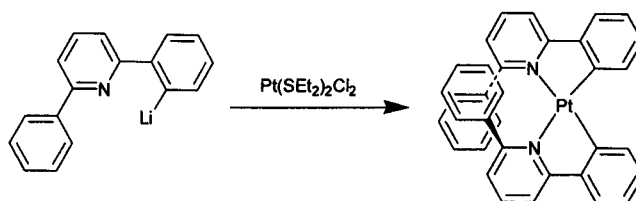


Figure 2.20: “Square planar” platinum(II) complexes showing helical chirality.

2.4.6: C-X Bond activation (X = C or Si).

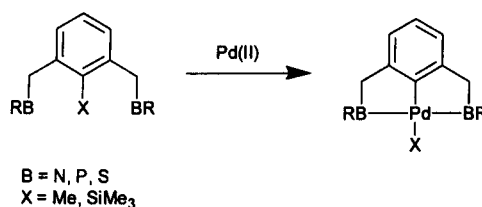


Figure 2.21: Cyclometalation via $\text{C}_{\text{aryl}}\text{-R}$ bond activation.

Van Koten *et al.* have synthesised a series of unusual tridentate cyclometalated complexes formed by novel C-C and C-Si bond activations.⁴⁹ The metal is thought to first co-ordinate to the two donor atoms and then cleave the C-X bond *via* an insertion mechanism.⁵⁰ Such insertion cyclometalations have enabled the formation of di-metalated phenyl rings, as illustrated in Figure 2.2.⁵¹ Two different metals can be used to cyclometalate to the same ring system using such insertion reactions.⁴⁶

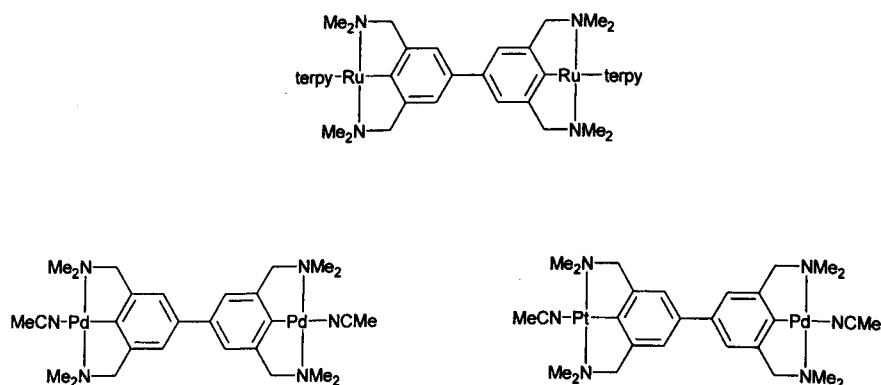


Figure 2.22: Examples of double cyclometalated rings.

Section 2.5. Conclusion.

Cyclometalation chemistry has grown tremendously over the last thirty-five years. This research has helped develop a wide variety of new and mild reaction pathways to novel organometallic products. The cyclometalated systems have been shown to be very robust, enabling the formation of secondary coordinations to other groups under milder conditions than previous possible. There are many possible applications for such complexes.^{44,45}

Section 2.6. References.

- 1 A C Cope and R W Siekman, *J. Am. Chem. Soc.*, 1965, **87**, 3272.
- 2 A D Ryabov, *Synthesis*, 1985, 233.
- 3 M Pabel, A C Wills and S B Wild, *Angew. Chem., Int. Ed. Engl.*, 1994, **33**, 1835.
- 4 R Navarro, J Garcia, E P Urriolabeitie, C Cativiela and M D Diaz-de-Villegas, *J. Organomet. Chem.*, 1995, **490**, 35.
- 5 G W V Cave, D P Lydon and J P Rourke, *J. Organomet. Chem.*, 1998, **55**, 81.
- 6 A E Shilov and A A Shteinman, *Coord. Chem. Rev.*, 1977, **24**, 97.
- 7 R Crabtree, *Chem. Rev.*, 1985, **85**, 245.
- 8 M L Deem, *Coord. Chem. Rev.*, 1986, **74**, 101.
- 9 H Rabaa, J -Y Saillard and R Hoffmann, *J. Am. Chem. Soc.*, 1986, **108**, 4327.
- 10 H Rabaa, J Y Saillard and R Hoffmann, *J. Am. Chem. Soc.*, 1988, **110**, 1449.
- 11 R Crabtree, *Chem. Rev.*, 1985, **85**, 245.
- 12 J Halpern, *Inorg. Chim. Acta*, 1985, **100**, 41.
- 13 J K Jawad, R J Puddephatt and M A Stalteri, *Inorg. Chem.*, 1982, **21**, 332.
- 14 J K Jawad and R Puddephatt, *J. Chem. Soc., Chem. Commun.*, 1977, 892.
- 15 A D Ryabov, *Chem. Rev.*, 1990, **90**, 403.
- 16 A D Jones and F J Feher, *J. Am. Chem. Soc.*, 1985, **107**, 620.
- 17 A C Cope and E C Fridrich, *J. Am. Chem. Soc.*, 1968, **90**, 909.
- 18 D P Lydon, G W V Cave and J P Rourke, *J. Chem. Soc., Chem. Commun.*, 1997, 1741.
- 19 N D Cameron and M Kilner, *J Chem. Soc., Chem. Commun.*, 1975, 687.
- 20 K Hiraki, Y Fuchita and K Takachi, *Inorg. Chem.*, 1981, **20**, 4316.
- 21 A Avshu, R D O'Sullivan and A W Parkins, *J. Chem. Soc., Dalton Trans.*, 1983,

1619.

- 22 J Vincente, I Saura-Llamas and P G Jones, *J. Chem. Soc., Dalton Trans.*, 1993, 3619.
- 23 M I Bruce, *Angew. Chem., Int. Ed. Engl.*, 1977, **16**, 73.
- 24 M Gómez, J Gayoso, M T Pereira and M Martínéz, *J. Chem. Soc., Dalton Trans.*, 1998, 37.
- 25 S Chakladar, P Paul, K Venkatsubramanian and K Nag, *J. Chem. Soc., Dalton Trans.*, 1991, 2669.
- 26 J M Vila, M Gayoso, M T Pereira, M C Rodriguez, J M Ortigueira and M T Pett, *J. Organomet. Chem.*, 1992, **426**, 267.
- 27 S Trofimenko, *J. Am. Chem. Soc.*, 1971, **93**, 1808.
- 28 D P Lydon and J P Rourke, *Abs. Pap. Am. Chem. Soc.*, 1998, **215**, 470-INOR.
- 29 S Chakladar, P Paul, A K Mukherjee, S K Dutta, K K Nanda, D Podder and K Nag, *J. Chem. Soc., Dalton Trans.*, 1992, 3119.
- 30 P Steenwinkel, R A Gossage, T Maunula, D M Grove and G v Kotten, *Chem. Eur. J.*, 1998, **4**, 763.
- 31 M F Clerici, B Show and B Weeks, *J. Chem. Soc., Dalton Trans.*, 1973, 516.
- 32 G Minghetti, M A Ginellu, G Chelucci and S Gladiali, *J. Organomet. Chem.*, 1986, **307**, 107.
- 33 F Neve, O Francescangeli and S Campagna, *Liquid Cryst.*, 1998, **24**, 673.
- 34 F Neve, A Crispini and S Campagna, *Inorg. Chem.*, 1997, **36**, 6150.
- 35 R A Gossage, A D Ryabov, A L Spek, D J Stufens, J A M v Beek, R v Eldik and G v Kotten, *J. Am. Chem. Soc.*, 1999, **121**, 2488.
- 36 M Schmülling, D M Grove, G v Kotten, R v Eldik, N Veldman and A L Spek,

Organometallics, 1996, **15**, 1384.

37 C M Hartshort and P J Steel, *Organometallics*, 1998, **17**, 3487.

38 P Steenwinkel, R A Gossage and G v Kotten, *Chem. Eur. J.*, 1998, **4**, 759.

39 D J Cárdenas, A M Echavarren and M C R d Arellano, *Organometallics*, 1999, **18**, 3337.

40 M A Bennett, H Jin and A C Willis, *J. Organomet. Chem.*, 1993, **451**, 249.

41 A Weisman, M Gozin, H-B Kraatz and D Milstein, *Inorg. Chem.*, 1996, **35**, 1792.

42 C J Moulton and B L Shaw, *J. Chem. Soc., Dalton Trans.*, 1976, 1020.

43 C Hahn, A Vitagliano, F Giordano and R Taube, *Organomet.*, 1998, **17**, 2060.

44 J Dupont, N Beydoun and M Pfeffer, *J. Chem. Soc., Dalton Trans.*, 1989, 1715.

45 C Deushel-Cornioley, H Stoeckli-Evans and A v Zelewsky, *J. Chem. Soc., Chem. Commun.*, 1990, 121.

46 L Chassot and A v Zelewsky, *Helv. Chim. Acta*, 1986, **69**, 1855.

47 M Gianini, A v Zelewsky and H Stoeckli-Evans, *Inorg. Chem.*, 1997, **36**, 6094.

48 C Cornioley-Deuschel, T Ward and A v Zelewsky, *Helv. Chim. Acta*, 1988, **71**, 130.

49 P Steenwinkel, R A Gossage and G v Kotten, *Chem. Eur. J.*, 1998, **5**, 759.

50 P Steenwinkel, R A Gossage, T Maunula, D M Grove and G v Kotten, *Chem Eur. J.* 1998, **5**, 763.

51 P Steenwinkel, S L James, D M Grove, H Kooijman, A L Spek and G v Kotten, *Organometallics*, 1997, **16**, 513.

Chapter 3: Results and discussion.

Section 3.1. Introduction.

Cyclometalation, a recent paper begins, “has been so well refined that a new but standard report in this area seems rather ordinary”.¹ Cyclometalation might well have been both widely studied,^{2,3} and widely used,^{4,5} but it is still generating much interest.⁶

Some researchers have returned to the area of double cyclometalation of the same aromatic ring,^{7,8} as pioneered by Trofimenko^{9,10} more than 25 years ago. Another area of research has been the synthesis of tridentate cyclometalated species formed when two coordinating groups hold a C-H bond close to the metal and this bond is activated.¹¹ Such N[^]C[^]N[^],^{11,12} P[^]C[^]P[^]^{13,14} and S[^]C[^]S[^] donor sets¹⁵ are well known. Some groups have used two ligating groups to induce a C-C¹⁶ or C-Si activation.¹⁷ In addition, the use of a chelating N[^]N donor set to yield N[^]N[^]C tridentate cyclometalated species has been reported.¹⁸ Double cyclometalation reactions to give complexes with tridentate C[^]N[^]C or C[^]P[^]C donor sets are relatively rare.^{19,20}

This chapter describes the synthesis and cycloplatination of a range of phenylpyridine ligands. The synthesis of a novel platinum carbene *via* an unusual C-H activation reaction is also discussed.

Section 3.2. Ligand synthesis.

This section reports the synthesis and characterisation of several potential C[^]N[^]C donor type ligands.

[§] The abbreviation N[^]C[^]N refers to a tridentate ligand bonding through two N donors and one C donor, with the ligand connectivity being N linked to C linked to N. Thus N[^]N[^]C also represents a tridentate ligand bonding through two N donors and one C donor, but this time the ligand connectivity is N linked to N linked to C.

3.2.1: Synthesis of 2,6-bis-(alkoxyaryl)pyridines, (5).

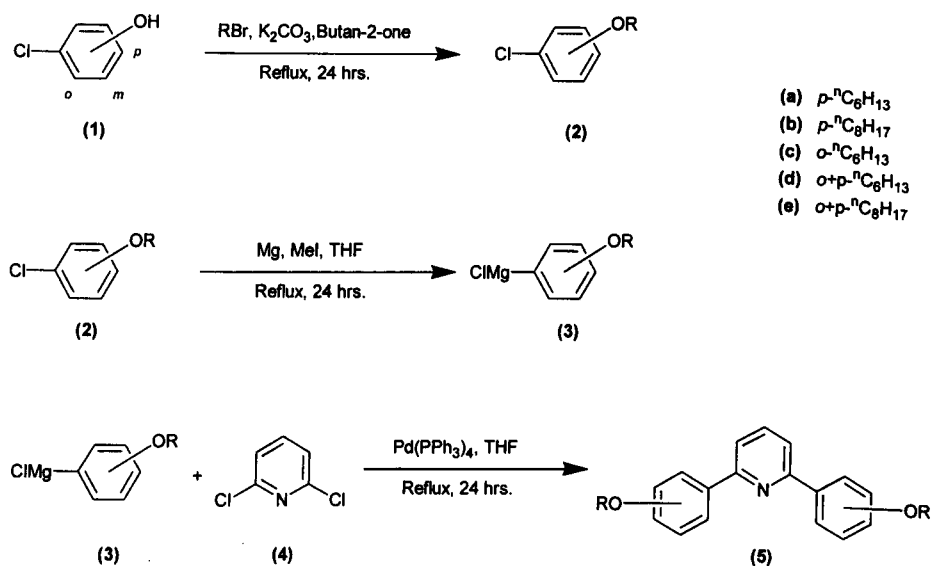


Figure 3.2.1: Synthetic route to 2,6-bis-(alkoxyaryl)pyridines, (5).

A series of 2,6-bis-(alkoxyaryl)pyridines, (5) were synthesised in > 80 % yield by palladium catalysed cross-coupling of Grignard reagent (3) and a dihalopyridine (4).²¹ The colourless products were purified by recrystallisation from ethyl acetate, except (5c) which was distilled, and were characterised by NMR spectroscopy and microanalysis.

The ^1H NMR spectra of these compounds were as expected. The H atoms *meta* to the nitrogen on the pyridine ring appear as simple doublets, thus confirming that the pyridine nucleus is symmetrically substituted. The aryl resonances of (5a) and (5b) show typical AA'XX' splitting patterns. In the cases of (5d) and (5e) the ^1H signals arising from the two aryl rings also show characteristic splitting patterns. The two alkoxy chains on the aryl rings of (5d) and (5e) have similar chemical shifts, suggesting no significant differences on the NMR chemical shift time scale.

Needle-like crystals of (5d) suitable for X-ray analysis were grown by slow evaporation of a solution of the compound in acetonitrile. No non-bonded inter or intramolecular interactions were observed.

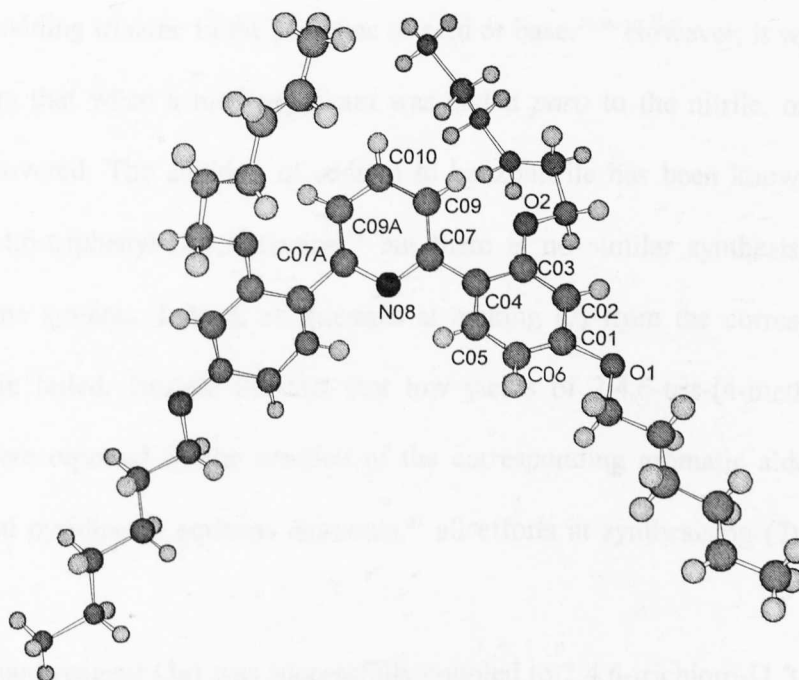


Figure 3.2.2: Molecular structure of **(5d)** (data in *Appendix*).

3.2.2: Synthesis of triazines, (7).

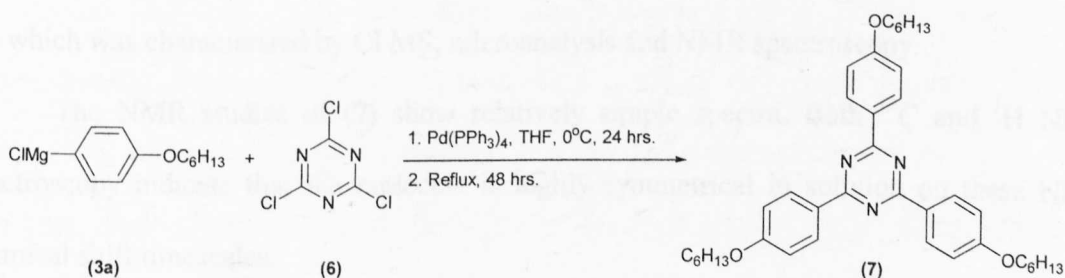


Figure 3.2.3: Synthetic route to 2,4,6-tris-(4-hexyloxyphenyl)-[1,3,5]triazine.

Synthetic routes to triazines have been studied for several years.²³ However, very few *para* substituted triphenyl-1,3,5-triazine complexes have been isolated.^{22,23}

Although near quantitative yields of 2,4,6-tris-(4-methylphenyl)-[1,3,5]triazine can be achieved by polymerisation of aromatic nitriles under extreme reaction conditions up to 50000 atm and 500 °C,^{24,25} relatively low yields (< 14 %) of the same complexes were reported²⁶ using bench top techniques. Aromatic nitriles have been reported to trimerize to

form the corresponding triazine in the presence of acid or base.^{27,28} However, it was noted by the same workers that when a methoxy chain was added *para* to the nitrile, only starting material was recovered. The addition of sodium to benzonitrile has been known for some time to form 2,4,6-triphenyl-[1,3,5]triazine,²⁹ but there is no similar synthesis of alkoxy substituted triazine systems. Indeed, all attempts at making (7) from the corresponding 4-alkoxybenzonitrile failed. Despite the fact that low yields of 2,4,6-tris-(4-methylphenyl)-[1,3,5]triazine were reported by the reaction of the corresponding aromatic aldehyde with Fremy's salt³⁰ and pyridine in aqueous ammonia,²⁷ all efforts at synthesising (7) using this method failed.

The Grignard reagent (3a) was successfully coupled to 2,4,6-trichloro-[1,3,5]triazine, (6) in the presence of tetrakis(triphenylphosphine)palladium(0). Due to the thermal instability of (6) an ice bath was used during the gradual addition of (3a). Filtration through activated charcoal and recrystallisation from hexane and ethyl acetate gave the pure product (7) which was characterised by CI MS, microanalysis and NMR spectroscopy.

The NMR studies of (7) show relatively simple spectra. Both ¹³C and ¹H NMR spectroscopy indicate that the molecule is highly symmetrical in solution on these NMR chemical shift timescales.

This is the first reported *p*-alkoxyphenyltriazine. The relatively mild reaction conditions and yield (>40%), make this method a relatively efficient synthesis of this class of compound.

3.2.3: Synthesis of 4'-(4-alkoxyphenyl)-2',6'-diphenylpyridine, (13).

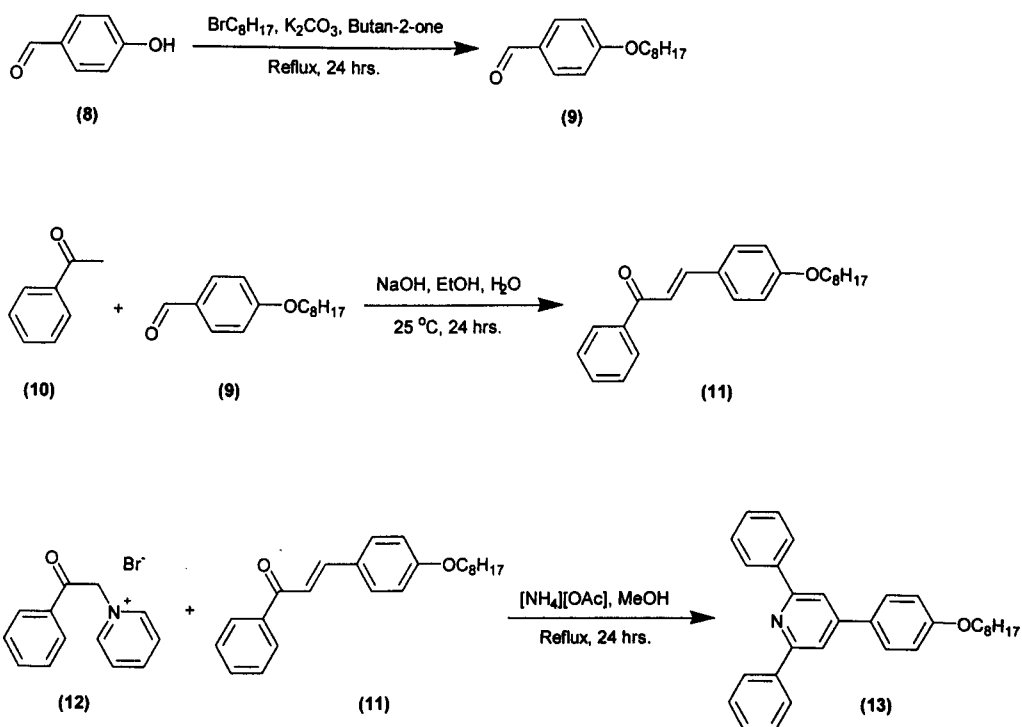
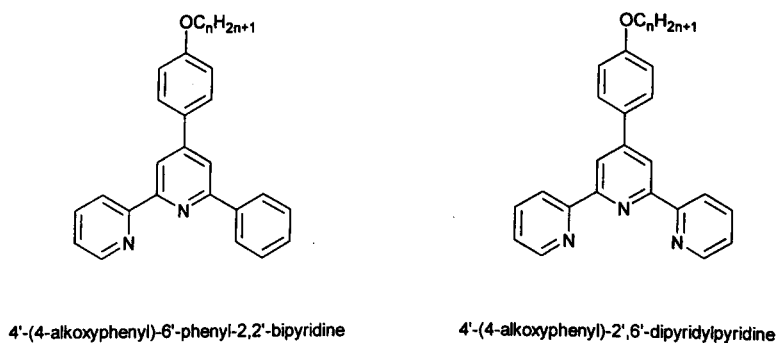


Figure 3.2.4: Synthetic route to 4'-(4-octyloxyphenyl)-2',6'-diphenylpyridine, (13).

The synthesis of 4'-(4-alkoxyphenyl)-6'-phenyl-2,2'-bipyridine and 4'-(4-alkoxyphenyl)-2,6-diphenylpyridine ligands *via* a Kröhnke type route (Figure 3.2.4) has been widely studied.³¹ The cyclometalation of such the bipyridinyl $\text{C}^{\wedge}\text{N}^{\wedge}\text{N}$ type ligand has also been investigated.³² However, the di-cyclometalation of the $\text{C}^{\wedge}\text{N}^{\wedge}\text{C}$ analogue has not been reported.

Figure 3.2.5: $\text{N}^{\wedge}\text{N}^{\wedge}\text{C}$ and $\text{N}^{\wedge}\text{N}^{\wedge}\text{N}$ Kröhnke ligands.

The product (9) of the alkylation of 4-hydroxybenzaldehyde (8) was treated with acetophenone (10) under basic conditions, to give the ketone (11) in > 80 % yield. This product was treated with the commercially-available pyridinium salt (12) in the presence of ammonia. The product (13) separated from the reaction mixture as a colourless oil and solidified on standing at room temperature (80 % yield). The solid (13) was characterised by microanalysis and NMR spectroscopy.

The NMR spectra of (13) are as expected.

3.2.4: Synthesis of stilbazoles, (17).

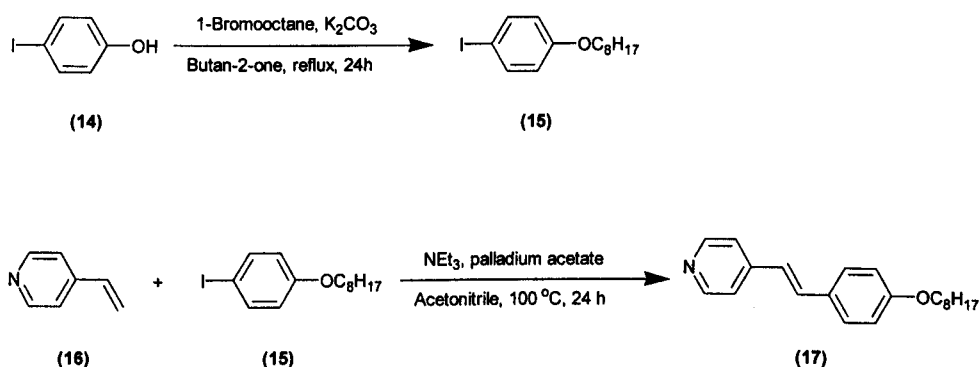


Figure 3.2.6: Synthetic route to 4'-octyloxystilbazole, (17).

The mesogenic behaviour of stilbazoles has been known for some time.³³ The long alkyl chains and the rigid linear aromatic cores enable them to produce calamitic mesophases both on their own and in conjunction with a coordinated metal.³⁴

The synthesis of 4'-octyloxystilbazole (17) was achieved *via* a published route³⁴ and the material was characterised by microanalysis and NMR spectroscopy. The thermal behaviour of this ligand was examined using hot-stage polarised optical microscopy. The mesophases were identified on the basis of their optical textures.



Figure 3.2.7: Mesogenic behaviour of 4'-octyloxystilbazole, (17).

Complex (17) melted from its crystalline form into the mosaic texture of a smectic E phase (*Appendix 2*) at 75.2 °C. On further heating the smectic E phase changed into the paramorphic focal-conic texture of a smectic B phase (*Appendix 2*) at 85.2 °C. At 88.9 °C the smectic B phase cleared into the isotropic liquid with no signs of decomposition. All phases were reproducible on cooling.

Section 3.3. Mono-cycloplatination.

3.3.1: Introduction.

The molecular structure of (5d) shows that the system is non-planar. The NMR spectra show that the two aryl rings are able to rotate freely on the NMR chemical shift time scale in solution about the bond to the pyridine ring. In order to develop a planar mesogenic core, at least one of these groups must be co-planar with the pyridine ring.³⁵ By forming a five-membered cyclometalated ring such a geometry can be achieved. This section outlines a high yield synthesis of such mono-cyclometalated dimers *via* an adaptation of a published route.³⁶

3.3.2: Synthesis of C^N mono-cycloplatinated chloride bridged dimers, (19), (20), (21) and (24).

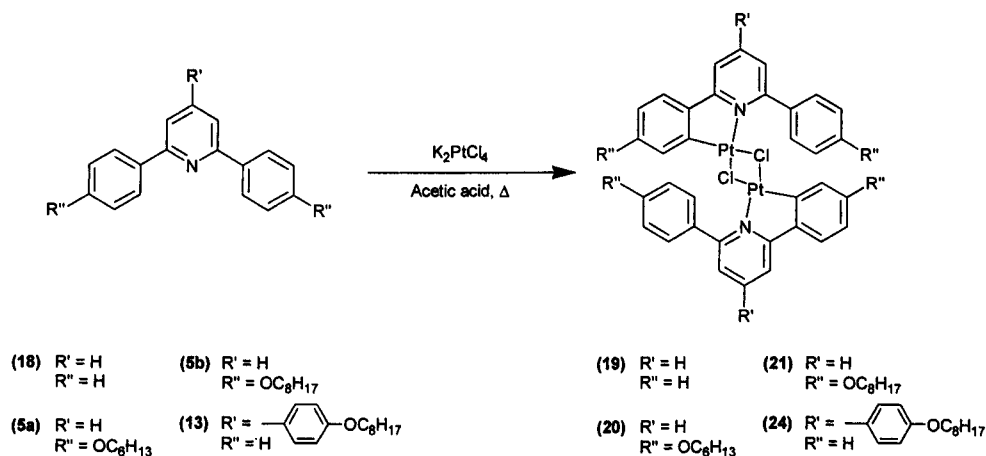


Figure 3.3.1: Synthetic route to chloride bridged dimers, (19), (20), (21) and (24).

A series of C^N mono-cycloplatinated chloride bridged dimers, (19), (20), (21) and (24) were synthesised from the respective pyridines, (18), (5a), (5b) and (13). An equimolar quantity of pro-ligand and potassium tetrachloroplatinate were mixed together in glacial acetic acid. The reaction was stirred at temperatures of 60 to 120 °C until the red K_2PtCl_4 crystalline salt was no longer visible (2 to 3 days). The solvent was removed in *vacuo*. Traces of potassium tetrachloroplatinate and ligand were removed by washing with water and hexane respectively, yielding the product as an amorphous yellow powder. In the case of pyridine (18) a very insoluble yellow precipitate of the product (19) was formed.

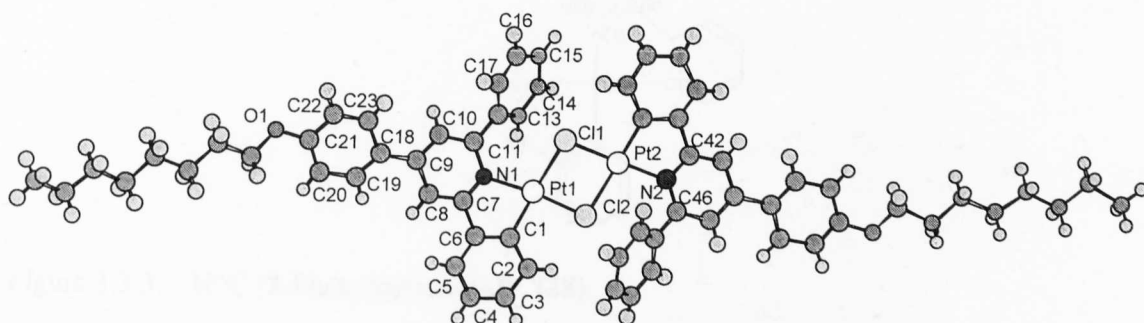


Figure 3.3.2: Molecular structure of **(24)** (data in *Appendix*).

Orange crystals of **(24)** suitable for X-ray analysis were formed by slow evaporation of a solution in chloroform. The X-ray data from **(24)** (see *Appendix*) and the mass spectra of the other mono-cyclometalated complexes described below show that such systems exist as dimers bridged by two chlorine atoms. The structure of **(24)** thus has a central core consisting of a Pt_2Cl_2 rectangle, with Cl-Pt-Cl angles of $81.2(2)$ and $80.9(2)^\circ$ and Pt-Cl-Pt angles of $99.1(2)$ and $98.2(2)^\circ$. The geometry about the platinum centres is essentially square planar, with a slightly larger bond angle of $104.4(5)$ for N1-Pt1-Cl1 caused by the close proximity of the Cl1 to the uncyclometalated phenyl ring and the *trans* influence of the Cl1 atom. The formation of the cyclometalated 5-membered ring system holds the phenyl and pyridine rings together in an essentially planar arrangement (angle between least squares planes *ca.* 8.7°). The angles between the planes of the uncyclometalated rings and the pyridyl ring are *ca.* 51.4° (for the phenyl ring ortho to the nitrogen) and 19.9° (for the phenyl ring *para* to the nitrogen). The fact that the former angle is the greatest is presumably a result of steric factors.

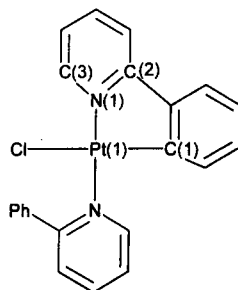


Figure 3.3.3: $N^C(2\text{-Phenylpyridine})_2\text{Pt}$, (**28**).

It should also be noted that the cyclometalated rings *ortho* to the nitrogen of the dimer are *trans* to each other. The bond distance N1-C7 of 1.26(3) Å is relatively short by comparison to the N08-C06 length of 1.349(3) Å in (**5d**). The angles at the pyridine N atom are 113.2(17)° (Pt1-N1-C7), 111.9(16)° (Pt2-N2-C42), 119(2)° (Pt1-N1-C11) and 121(2)° (Pt2-N2-C46), these are comparable to those observed by Ford *et al.* for $N^C(2\text{-phenylpyridine})_2\text{Pt}$ (**28**) (Figure 3.3.3) where the distances and angles are reported as follows: 2011(6) (Pt1-N1), 1975(8)Å (Pt1-C1), 81.6(3)° (N1-Pt1-C1), with the angles at the N atom being 115.2(2) (Pt1-N1-C2), 119.6(3) (C3-N1-C2) and 125.1(2)° (Pt1-N1-C3).⁴¹ Further distortion of the pyridine ring is evident in the unmetalated ring. The N1-C11 the bond length 1.41(3) Å is significantly larger than N1-C7 bond distance of 1.26(3) Å. The Pt1-C11 distance of 2.460(7) is significantly longer than the Pt1-C12 distance of 2.339(7) Å. This difference in bond lengths is to be expected on the basis of the *trans* influence. For example, in the isomers A and B of $C^N[(\text{MeOC}_6\text{H}_3\text{CH}_2\text{NMe}_2)\text{Pt}(\text{py})\text{Cl}]$ a Pt-Cl distance of 2.408(5) Å is seen in the isomer B, compared to one of 2.300(1) Å in the isomer A.³⁷ There are no significant intermolecular interactions in the structure of (**28**), all other bond lengths and angles are as expected.

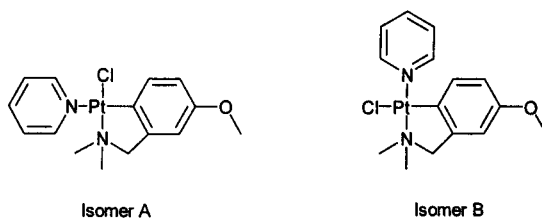


Figure 3.3.4: $C^N [(MeOC_6H_3CH_2NMe_2)Pt(py)Cl]$

Further evidence of cyclplatination can be seen in both the 1H and ^{13}C NMR spectra of these complexes. Several of the above dimers show ^{195}Pt satellites on the signals arising from the cyclometalated phenyl ring. The 1H resonances of the pyridine protons *meta* to the nitrogen are seen to be doublets of doublets in **(19)**, **(20)** and **(21)** and as two doublets in **(24)** and must therefore be inequivalent. The ^{13}C and 1H resonances corresponding to the uncyclometalated phenyl ring *ortho* to the nitrogen show that it is able to freely rotate about the C-C bond in solution on these chemical shift timescales.

Complex **(19)** is an air and water stable yellow powder which decomposes without melting at 320-370 °C (TGA analysis shows this decomposition process to be complete, leaving only Pt metal). In an attempt to prepare a sample of **(19)** for ICP analysis it was refluxed in *aqua regia* overnight without any signs of decomposition. By comparison **(20)**, **(21)** and **(24)** are all soluble in chloroform and melt at moderate temperatures.

In the FAB mass spectra molecular ions were detected for complexes **(20)**, **(21)** and **(24)**. Due to the insolubility of **(19)**, a FAB mass spectrum could not be readily obtained. Instead, a solution of **(19)** in DMF was added directly to a MALDI TOF slide in the absence of a matrix. By gradually increasing the power to the LASER a peak corresponding to the molecular ion of **(19)** was observed.

3.3.3: Mono-cycloplatination of the triazine ligand.

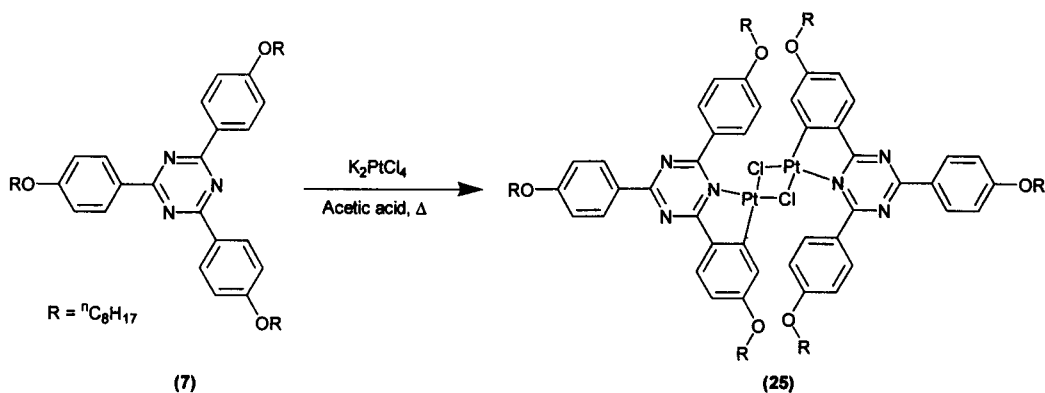


Figure 3.3.5: Synthetic route to the triazine chloride bridged dimer, (25).

The multi-dentate triazine ligand (7) was added in excess to a suspension of potassium tetrachloroplatinate in glacial acetic acid. The reaction was stirred until there were no visible traces of the platinum starting material (about 3 days). The solvent was concentrated and the yellow product (25) precipitated. The product was isolated by suction filtration and washed with water and hexane to remove traces of starting materials and platinum(0) black. The pure product, (25) was characterised by MALDI TOF MS, microanalysis and NMR techniques.

Complex (25) is stable to air and water, and melts at 201 °C into the isotropic liquid without any signs of decomposition.

The ^1H NMR spectrum of (25) shows 7 aromatic resonances in comparison to the 2 observed in the ligand (7). The splitting pattern due to the cyclometalated ring is comparable to that observed for (20) and (21). Platinum satellites ($^3J = 27.3$ Hz) were observed for the cyclometalated phenyl ring H atom *ortho* to the platinum. In the mass spectrum, the presence of a peak at m/z 1847 corresponding to the molecular ion of (25) indicates that it is in the dimeric form as illustrated in Figure 3.3.5.

When (7) was treated with an equimolar quantity of the platinum salt several products formed besides (25). Preliminary MS experiments indicate the possibility of the presence of a complex in which a second platinum is attached to (7) forming a chlorine bridged trimer. This complex was not isolated from the crude reaction mixture.

There are no published results referring to the cyclometalation of any triazine type ligands. Attempts at coordination of copper to 2,4,6-tris(2-pyrimidyl)- and 2,4,6-tris(2-pyridyl)-1,3,5-triazines resulted in hydrolysis to form the bis(aryl)carboximidato chelate.^{38,39} The use of platinum and (7) to form (25) is therefore a key result in this area of triazine chemistry.

3.3.4: Cycloplatination of 2-phenylpyridine.

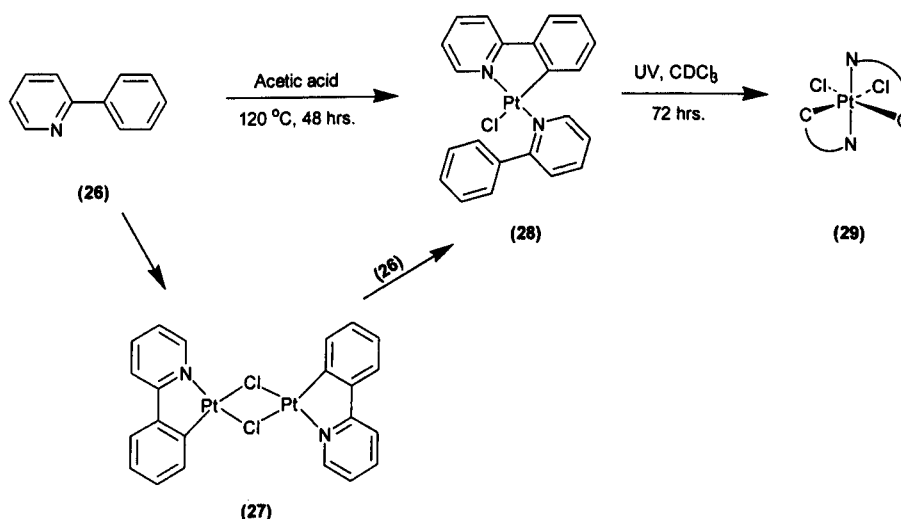


Figure 3.3.6: Synthetic route to $N^C(2\text{-phenylpyridine})_2Pt^{IV}Cl_2$, (29) via a chloride bridged dimer, (27).

2-Phenylpyridine, (26) was treated with potassium tetrachloroplatinate in glacial acetic acid. When the platinum salt was no longer visible (2 to 3 days) the acid was removed under reduced pressure. The resulting yellow powder was recrystallised from ethyl acetate in

good yield (> 86 %). The yellow crystalline product, **(28)** was analysed by X-ray diffraction, microanalysis and NMR spectroscopy.

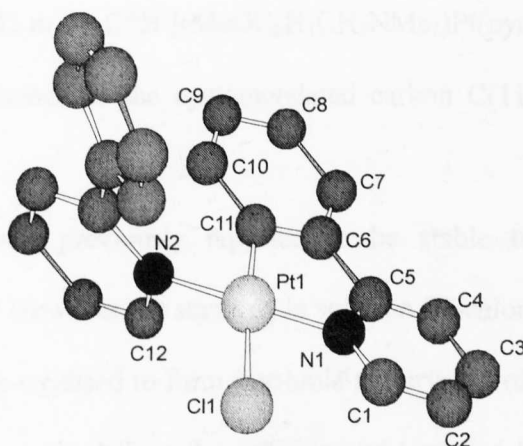


Figure 3.3.7: Molecular structure of **(28)** (data in *Appendix*).

The synthesis of **(28)** has been previously reported, in low yield (<10 %), as an intermediate in the formation of $\text{Bu}_4\text{N}[(2\text{-phenylpyridine})\text{PtCl}_2]$, by direct addition of $(\text{Bu}_4\text{N})_2\text{PtCl}_4$ to four equivalents of **(26)** in dichloromethane.⁴⁰

Attempts to isolate the chlorine-bridged dimer **(27)** during this reaction failed. Complex **(27)** can be synthesised by reacting **(26)** with $(\text{Bu}_4\text{N})_2\text{PtCl}_4$ in methanol or ethanol. The dimer **(27)** can then be cleaved by **(26)** to produce **(28)** by heating in chloroform, in quantitative yield.

The ^1H NMR spectrum of **(28)** shows three distinctive sets of ^{195}Pt satellites corresponding to the H atoms resonances *ortho* to platinum. The two pyridine H atom resonances are downfield of the cyclometalated resonance and the platinum coupling is reduced from $^3J_{(\text{Pt-H})} = 23 \text{ Hz}$ to $^3J_{(\text{Pt-H})} = 19 \text{ Hz}$. It was possible to differentiate the two pyridine rings from each other using a nOe experiment. The ^1H resonances of the uncyclometalated phenyl ring indicate free rotation in solution on these chemical shift timescales.

The molecular structure of **(28)** has been previously reported.⁴¹ The nitrogen atoms are mutually *trans* and the Pt(1)-Cl(1) bond is long [2.4082(8) Å] compared to the Pt-Cl bond length [2.300(1) Å] in *cis* C^N [(MeOC₆H₃CH₂NMe₂)Pt(pyr)Cl].³⁸ This is a reflection of the strong *trans* influence of the cyclometalated carbon C(11) of the *ortho*-metalated ligand.³⁸

Complex **(28)** was previously reported to be stable to air as well as being photochemically stable.⁴¹ However, on standing in solution (D-chloroform) in the presence of ultraviolet light, **(28)** was oxidised to form insoluble red crystals of a platinum(IV) complex **(29)**. The crystals were removed from the solution and analysed by X-ray crystallography, microanalysis and MALDI TOF MS.

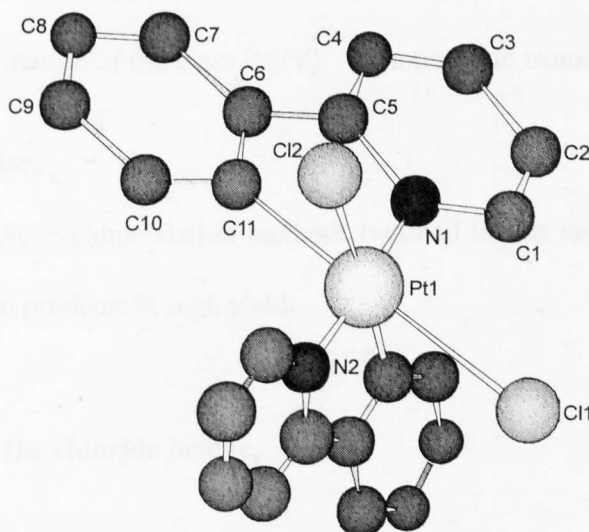


Figure 3.3.8: Molecular structure of **(29)** (data in *Appendix*).

The X-ray crystal data of **(29)** is unexceptional for an octahedral platinum(IV) complex.⁴² The *trans* influence from both the cyclometalated carbons is evident by considering the bond lengths of Pt1-Cl2 and Pt-Cl1 of 2.4383(14) and 2.443(2) Å respectively.^{41,42} There is no significant difference in bond lengths or angles of the

phenylpyridine ligands in the platinum(IV) complex (29) and those observed for the platinum(II) complex (28).

The formation of platinum(IV) complexes from compounds similar to (28) is not unknown. The complex *cis*-bis(2-phenylpyridine)platinum(II) (48) is stable in most organic solvents,⁴⁴ but when exposed to visible light (sunlight or a 250 W halogen lamp) a photochemical addition occurs, resulting in *cis* and *trans* platinum(IV) complexes (Figure 3.3.9).⁴³

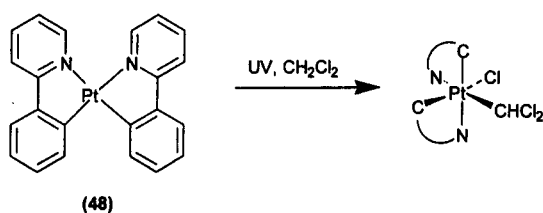


Figure 3.3.9: The formation of the *trans* Pt(IV) -enantiomeric isomer complex from (48).

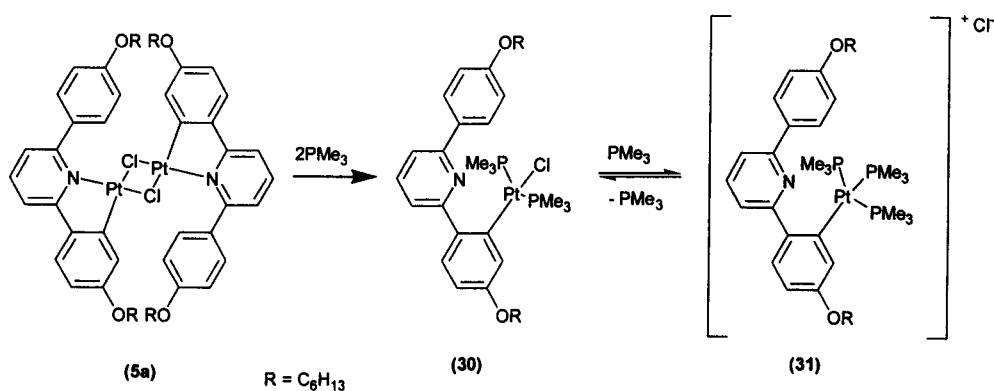
3.3.5: Conclusion.

To conclude, the cyclometalation methods outlined in this section provide a simple route to relatively clean products in high yield.

Section 3.4. Cleaving the chloride bridge.

3.4.1: Introduction.

Functionalisation of the materials described in the previous section was undertaken to investigate their thermal stabilities and other behaviour. One such area open to investigation was the possibility of cleaving the chloride bridge with a neutral ligand, to form a monomeric species. Several examples of such reactions are detailed in this section. A possible mechanism of the reaction is also discussed.

3.4.2: Addition of trimethylphosphine to mono-metalated dimers.Figure 3.4.1: Cleaving the chloride bridge with PMe₃.

Phosphines have been used as donor ligands for many years.⁴⁴ Due to the complex splitting patterns in the aromatic region of the NMR spectra of the 2,6-diphenylpyridine type ligands (5) and their complexes, it was decided to opt for trimethylphosphine instead of the more commonly used triphenylphosphine to avoid further complication.

An excess of trimethylphosphine was added to a solution of (5a) in deuterated chloroform, under an inert atmosphere. An immediate decolourisation of the yellow solution was observed. Both the ¹H and ³¹P NMR spectra at this time indicated the formation of (31). The ³¹P NMR spectrum of (31) showed a doublet at -23.0 ppm (integrating to 2P) coupling through to a triplet at -33.1 ppm, with an integration of 1P. Both signals showed platinum satellites, the doublet had a coupling constant consistent with phosphorus *trans* to phosphorus (¹J_(Pt-P) = 1861 Hz) and the triplet exhibited a coupling constant consistent with a phosphorus *trans* to carbon (¹J_(Pt-P) = 2759 Hz).⁴⁶

Evaporation of the solution and drying in *vacuo* led to the loss of one PMe₃ group. Spectroscopically the integration of the phosphine ligand in the ¹H NMR spectrum reduced from 27 to 18H, and the ³¹P NMR spectrum showed a singlet at -14.46 ppm with ¹⁹⁵Pt

satellites ($^1J_{\text{Pt-P}} = 2834 \text{ Hz}$), indicating the formation of complex (30). The mono-phosphine substituted analogue of (5a) was not isolated.

3.4.3: Addition of DMSO to mono-metalated dimers.

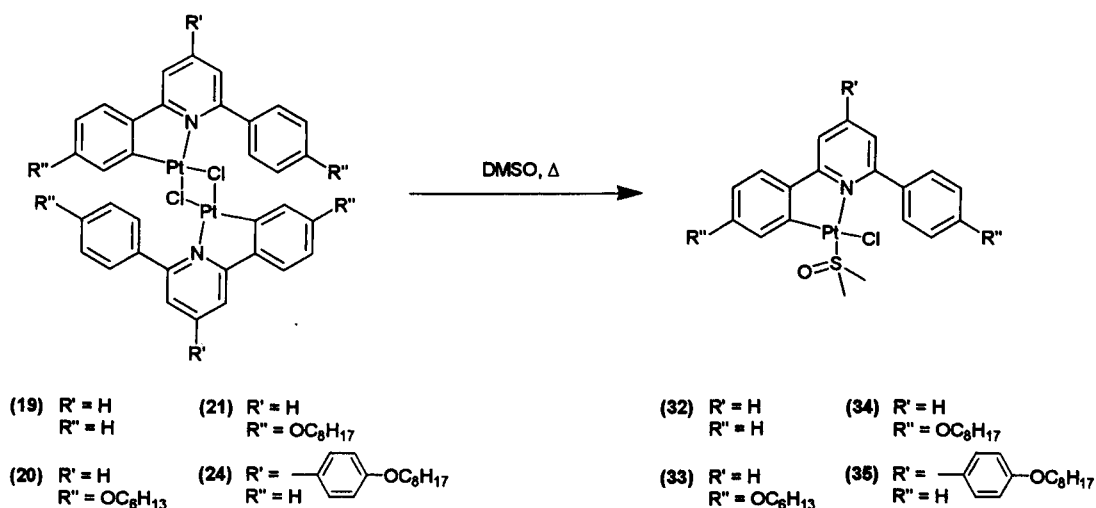


Figure 3.4.2: Cleaving the chloride bridge with DMSO.

Solution NMR spectroscopic data on (33), (34) and (35) were obtained after dissolving the corresponding mono-metalated dimers (20), (21) and (24), respectively, in warm deuterated chloroform and adding one equivalent of dry DMSO. The ^1H NMR spectra show similar splitting patterns to those observed before the addition of the DMSO. All the appropriate couplings, corresponding to the expected compounds (33), (34) and (35) are clearly seen. One crucial difference between these spectra and those obtained for the starting materials (20), (21) and (24) is the clear presence of a DMSO co-ordinated to platinum (^{195}Pt satellites on the signal, $^3J_{\text{Pt-H}} = 23 \text{ Hz}$) suggesting that the chloride bridged dimers (20), (21) and (24) have been split.

An isomer consistent with the formulation of (32), (33), (34) and (35) is depicted in Figure 3.4.2, a second isomer with the Cl atom *trans* and the S atom *cis* with respect to the N atom is also mechanistically feasible. However, all NMR spectra showed only one isomer. It

is assumed, on the basis of theoretical studies and chemical reactivities (see later) that the isomer with DMSO *trans* to the N atom was the single compound formed.

The cleavage of (20), (21) and (24) by DMSO to give (33), (34) and (35), respectively, is relatively slow at room temperature (1 h) compared to the reaction with PMe_3 (instantaneous). The application of moderate heat reduced reaction times (< 10 min at *ca.* 60 °C). Using such conditions a definite colour change from an intense yellow solution to a paler yellow colour can be observed more readily.

Unlike complexes (20), (21) and (24) which are soluble in most common organic solvents, (19) is only soluble in DMF and reacts with wet DMSO to form a di-cyclometalated species (44) (described later). Therefore, in order to obtain definitive solution NMR spectroscopic characterisation results of (32) two separate experiments were carried out. In the first of these (19) was added to dry deuterated DMSO with a minimum of heat to assist dissolution. The ^1H NMR spectrum of (32) shows twelve proton resonances with the characteristic splitting pattern similar to that of (19) in deuterated DMF. However, a peak corresponding to the 0.5 % ^1H -DMSO was noted at its relative intensity. Further, complex (19) was treated with a minimum DMSO and dissolved in deuterated chloroform the ^1H NMR spectrum indicated traces of the di-cyclometalated complex (44) and a singlet (integrating to 6H) with ^{195}Pt satellites ($^3J_{(\text{Pt-H})} = 23$ Hz) appearing up-field (by 0.3 ppm) from the DMSO singlet found in (44). The ^{195}Pt coupling constants for the phenyl ring H atoms observed in (44) ($^3J_{(\text{Pt-H})} = 27$ Hz) are also different to those in (32) ($^3J_{(\text{Pt-H})} = 24$ Hz). The mass spectrum of (32) was obtained by analysing a solution of (19) in a minimum of dry DMSO using a MALDI-TOF mass spectrometer (in the absence of an additional matrix). The spectrum showed a peak at m/z 502, corresponding to the molecular ion of (32).

The ^{13}C NMR spectra of (32), (33), (34), and (35) were complicated by the presence of peaks arising from their respective di-cyclometalated analogues (see later) which were formed over the long acquisition times required.

3.4.4: Addition of carbon monoxide to mono-metalated dimers.

When a dimethylformamide solution of (19) was exposed to carbon monoxide gas the colour of the solution changed rapidly (< 5 s) to a much paler yellow. The ^1H NMR spectrum changed significantly from that of (19), while maintaining the same number of H atom signals with similar coupling patterns. The presence of a strong band in the IR spectrum at 2088 cm^{-1} is consistent with the formation of compound (36). Compound (36) underwent isomerisation to complex (38) as evidenced in particular by ^1H NMR spectroscopy, where ^1H signals move by up to 0.8 ppm. This isomerisation is less obvious by IR, where a difference of only 6 cm^{-1} between the two isomers was observed.

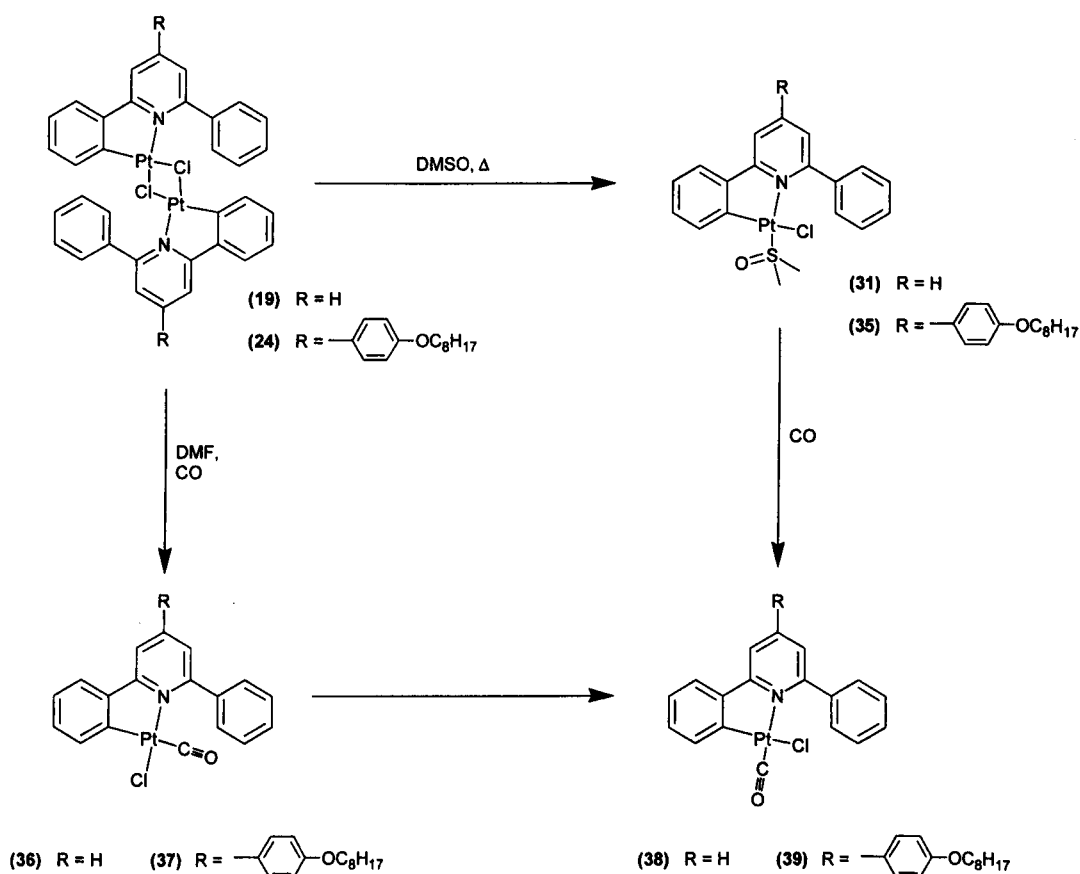


Figure 3.4.3: Synthetic route to mono-cyclometalated platinum carbon monoxide complexes, (38) and (39).

The addition of carbon monoxide gas to a solution of (31) in deuterated DMSO, resulted in the rapid formation of (38), within 2 minutes only peaks corresponding to (38) were seen by ^1H NMR spectroscopy, indicating 100 % conversion. Similar behaviour was seen in the reaction of (24) in deuterated chloroform to give (37). The isomerisation of (37) to (39) was clearly seen by ^1H NMR spectroscopy (half way by about 3 hours and complete in less than 16 hours, 100 % conversion).

The isomerisation of (37) to (39), and that of (36) to (38), occurred after the solutions had been flushed with nitrogen to remove any excess CO. Together with the independence of the isomerisation rate upon concentration, and the observation of isomerisation in

deuterated dichloromethane (*i.e.* no hydrochloric acid present) at a similar rate to that observed in deuterated chloroform (potential contamination with trace of hydrochloric acid present), an associative ligand exchange type of reaction being responsible for the isomerisation, can therefore be ruled out. This leaves a dissociative mechanism as the likely route. Addition of four equivalents of tetrabutylammonium chloride to a solution of (37) effectively suppressed the isomerisation to (39). Therefore, the reaction most likely proceeds *via* a chloride dissociation mechanism.

3.4.5: Conclusion.

Conventional arguments based on *trans* effects would suggest that each of the compounds (31), (35), (36), (37), (38) and (39) should form with the ligand coming in *trans* to the carbon bound to the platinum, and *cis* to the nitrogen.³⁸ This is observed when mild conditions of a CO atmosphere with a room temperature solution of the chloride bridged dimers (19) and (24) to form (36) and (37). Quite how large this *trans* effect is in cyclometalated complexes has been the subject of some debate recently, and will not be discussed further here.^{45,46,47} However, it is apparent from our modelling studies (see later) that these isomers (36) and (38) (the kinetic products) with the CO *cis* to the nitrogen are unfavourable with respect to those with the chloride *cis* to the nitrogen (37) and (39) (the thermodynamic products). Thus it would be expected that (36) and (37) isomerise to (38) and (39). When DMSO is used as the ligand, it might be expected that the energy difference between the isomers of (31) and (35) would be even greater than in the analogous CO complexes. Thus, the fact that the isomers of the DMSO *cis* to the nitrogen are not observed, could be due to the very unfavourable thermodynamics of this isomer with respect to the other.

Since the DMSO would be less strongly bound than the CO a dissociative isomerisation mechanism is more feasible. Alternatively, the steric constraints posed by the non-cyclometalated phenyl ring could render bridge cleavage *trans* to the C energetically unfavourable. In any event, once the geometry in (31) and (35) is established with the chloride *cis* to the nitrogen, displacement of DMSO with CO gas gives compounds (38) and (39) exclusively.

Similar compounds to (38) have been reported.⁴¹ When the cyclometalated phenyl pyridine compound (27) is treated with phenylpyridine, or CO, the only complexes isolated have the new ligand *trans* to the nitrogen (Figure 3.4.4) as evidenced by the molecular structure of (28) and its CO analogue.⁴¹

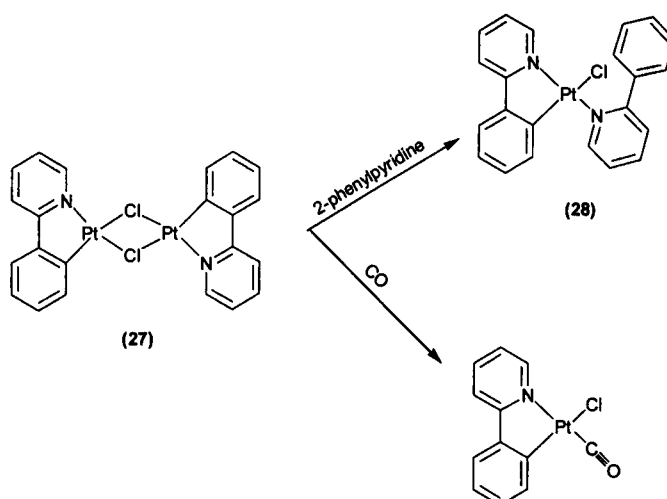


Figure 3.4.4: *Trans* ligand addition to (27).

Section 3.5. Di-cycloplatinatation.

3.5.1: Introduction.

Constraining the pyridine and the two phenyl rings of a 2,6-diphenylpyridine ligand system so as to introduce planarity of the core is of much interest and importance in the design of metallomesogens.³⁶ One possible approach to this is to hold the three groups

together using a metal.³³ Very few examples of a metal cyclometalating twice to a ligand exist. This section details two methods of di-cycloplatinating a series of 2,6-diphenylpyridine type ligands, producing a series of C^NC tridentate platinum complexes in high yield. The first method adopts a “classical” approach to cyclometalation.⁴ However, the second approach is a novel and is shown to be produce in high yield *via* a relatively simple procedure. Theoretical studies of the later method are also discussed.

3.5.2: Di-cycloplatinated 2,6-bis(4'-alkoxyphenyl)pyridines, (41) and (42).

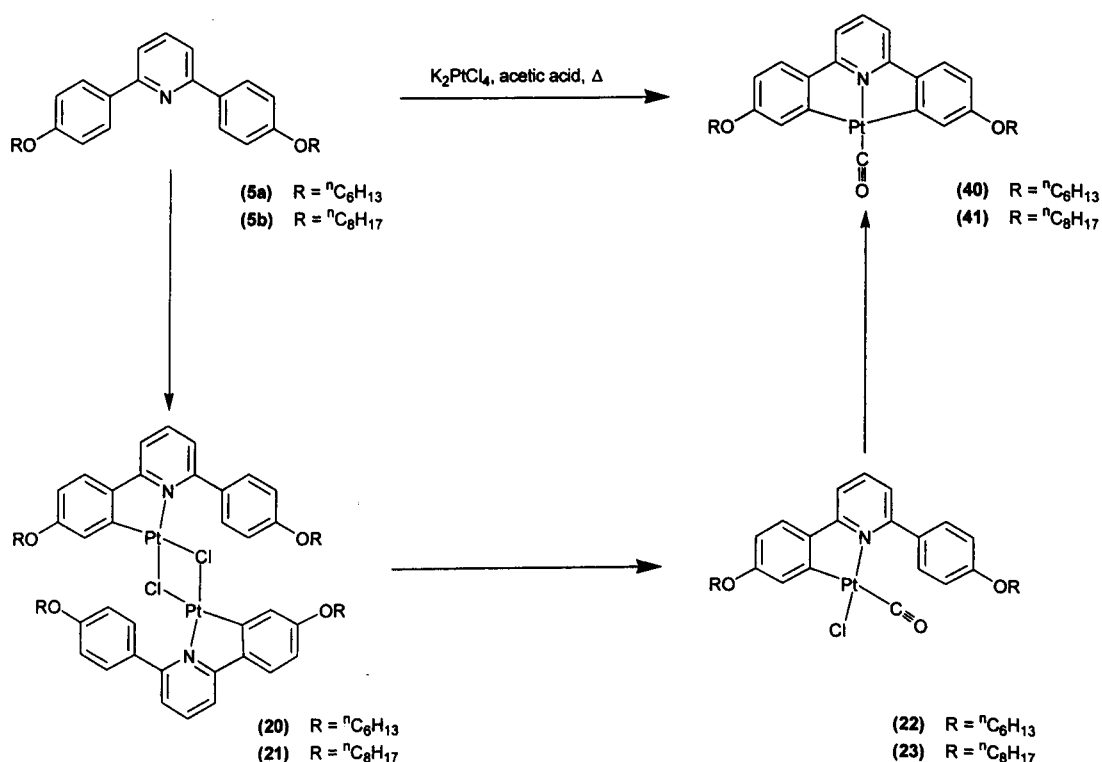


Figure 3.5.1: Synthetic route to di-cycloplatinated 2,6-bis(4'-alkoxyphenyl)pyridines, (40) and (41).

The cycloplatination of (5a) and (5b) with potassium tetrachloroplatinate(II) under mild conditions has been discussed earlier. When more forcing conditions of increased

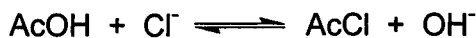
temperatures and reaction times are used, novel di-cycloplatinated 2,6-bis(4'-alkoxyphenyl)pyridines, (40) and (41) can be isolated. Under such conditions complexes (40) and (41) are the only major products and were purified by column chromatography. The carbonyl complexes (40) and (41) were analysed by microanalysis, IR and NMR spectroscopies. The molecular structure of (40) was determined by X-ray crystallography.

In order to ascertain an intermediate in the di-cyclometalation mechanism an aliquot was removed from the reaction mixture after 6 h. The solvent was removed under *vacuo* and the sample was analysed by ^1H and ^{13}C NMR spectroscopy. The mono-cyclometalated chloride bridged dimers (20) and (21) were confirmed as intermediates in the formation of (40) and (41). FT IR studies throughout the reaction (monitoring the $\nu(\text{C}\equiv\text{O})$ stretching band) showed the initial formation of (22) and (23). These bands slowly decreased in intensity over time. Bands at 2042 cm^{-1} due to (40) and (41) were observed to increase in intensity at the same rate.

The ^1H NMR spectra of (40) and (41) both show five signals in the aromatic region integrating 9H, with splitting patterns consistent with the formulation of (40) and (41). The ^{13}C NMR indicates the presence of a carbonyl at 207.0 ppm.

Complex (40) is remarkably stable, melting (in air) at $120\text{ }^\circ\text{C}$ with no sign of decomposition until $310\text{ }^\circ\text{C}$. The structure of this compound is unusual, though not unprecedented, in that the metal has cyclometalated to the same ligand twice.¹⁹ In addition to a report of a platinum complex of 2,6-diphenylpyridine, there are only three such structurally characterised species. The first reported example being a platinum phosphine complex and the other examples being palladium species metalated to a pyridine with pendant β -dicarbonyls.^{19,20}

114



Even though this equilibrium will lie on the side of acid and chloride ion, there will be a small quantity of acyl chloride, and the decarbonylation of an acyl chloride to generate a carbonyl complex and an alkyl halide has been known for some time.⁴⁸ Indeed, it even has some synthetic use.⁴⁹ When the carbonyl labelled form of the acetic acid under an inert atmosphere was treated using the same conditions as outlined in *Figure 3.5*, the reaction proceeded as normal. However, there was no evidence for the incorporation ¹³C into the complex.

It is possible that the CO ligand was generated from an impurity found in the acetic acid and until studies using the methyl ¹³C labelled form of the acetic acid have been preformed, further deliberation on the source of the CO is speculation. It is interesting to note that when the reaction is carried out in anhydrous propionic acid only starting materials were found. This is probably due to the fact that acetic acid is able to self ionise to produce the acetate ion whereas with propionic acid this process is less favourable.

Complexes **(40)** and **(41)** were made in moderate yields (*ca.* 35 %) by reacting potassium tetrachloroplatinate(II) with the pyridine **(5a)** and **(5b)** in an acetic acid solution. By contrast, other workers have had to use a ligand doubly deprotonated with a strong base, and then reacted that compound with a metal source.¹⁹ Such methods are not only low yielding (<5 %) but are very limited when it comes to ligand substituents.¹⁹

3.5.3: C-H activation induced by water.

3.5.3.1: Di-cyclometalated C^NC tridentate platinum DMSO complexes, (42), (43), (44) and (45).

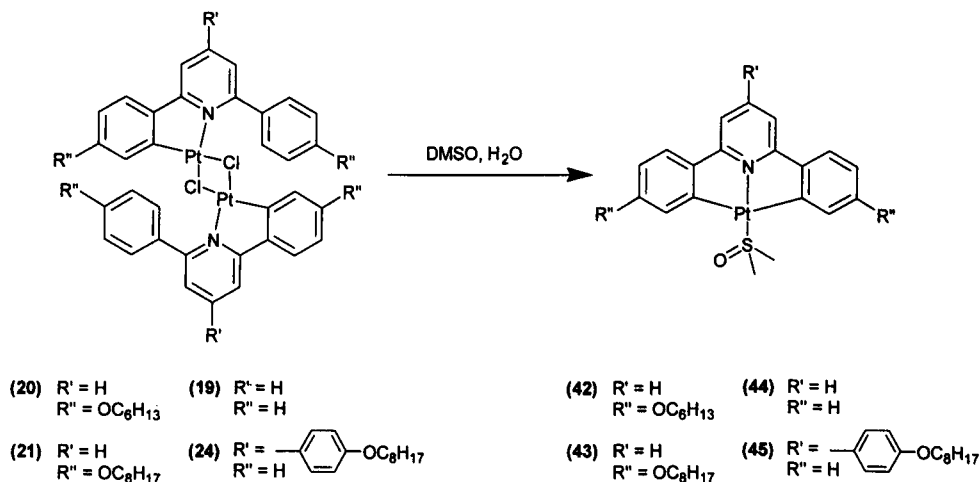


Figure 3.5.3: Mono-cyclometalated to di-cyclometalated C^NC tridentate platinum DMSO complexes, (42), (43), (44) and (45).

The previously prepared mono-cycloplatinated chloride bridged dimers (19), (20), (21) and (24) were added to warm DMSO and stirred until they dissolved. The solution turned yellow and all traces of solid disappeared. Distilled water was added to the solution. The resulting yellow precipitate was washed with water and hexane, affording a near quantitative yield of the pure di-cyclometalated C^NC tridentate platinum DMSO complexes (42), (43), (44) and (45) which were analysed by NMR spectroscopy, MS and elemental analysis. Crystals suitable for X-ray analysis of (44) were obtained by layering the DMSO solution with water.

The NMR spectrum of (44) is quite different to that of (24). The ¹H NMR spectrum of (44) shows six signals in the aromatic region of the spectrum integrating to 11H, indicating the equivalence of the two aryl rings on the chemical shift time scale. The ¹H NMR resonance corresponding to the H atom *ortho* to the platinated C atom on the phenyl

ring shows a splitting pattern complete with a $^3J_{\text{Pt-H}}$ coupling. In **(24)** the H atoms *meta* to the nitrogen atom of the pyridine ring are a single doublet coupling to the H atom nucleus *para* to the N atom, indicating equivalence on the NMR chemical shift time scale. In **(24)** the H atoms *meta* to the nitrogen atom are inequivalent on the chemical shift timescale, coupling through to each other. The DMSO H atom signals are downfield of “free” DMSO at 3.68 ppm (in CDCl_3) and have ^{195}Pt satellites (27 Hz).

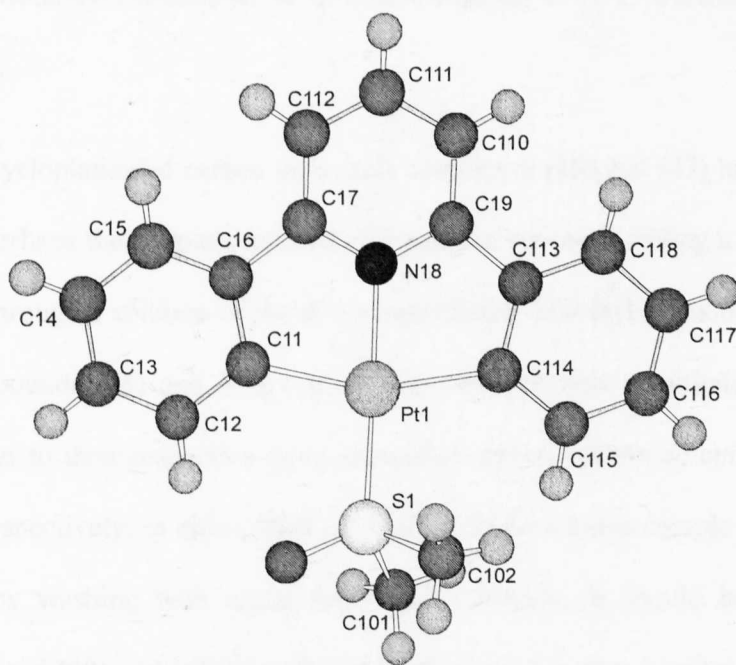


Figure 3.5.4: Molecular structure of **(44)** (data in *Appendix*).

The molecular structure of **(44)** is unexceptional (*Figure 3.5.4*): the three independent molecules in the asymmetric unit were essentially indistinguishable. The S atom of the DMSO ligand is displaced out of the diphenylpyridine-platinum plane, with N-Pt-S angles of $170.9(2) - 173.8(2)^\circ$. This is presumably a consequence of steric effects. All other bond lengths and angles are unexceptional.

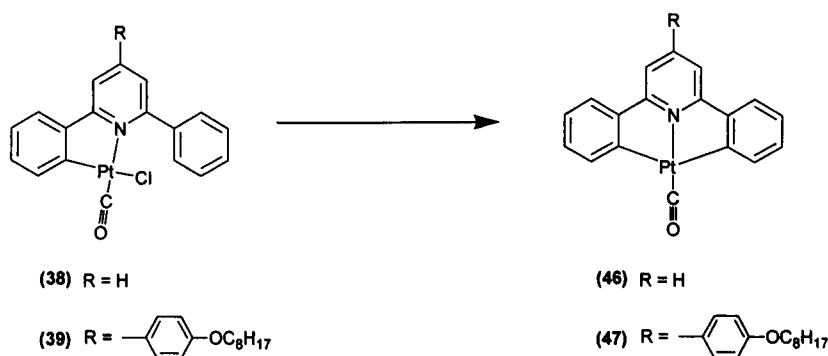
3.5.3.2: Di-cyclometalated C^NC tridentate platinum CO complexes, (46) and (47).

Figure 3.5.5: Mono-cyclometalated to di-cyclometalated C^NC tridentate platinum CO complexes.

The di-cycloplatinated carbon monoxide complexes (46) and (47) have been made in several ways. Perhaps the simplest method of formation was by bubbling a stream of carbon monoxide gas through a solution of the di-cycloplatinated dimethylsulfoxide complexes (44) and (45). Compounds (46) and (47) can also be made in near quantitative yields by the addition of water to their respective mono-metallated carbon monoxide compounds, namely (38) and (39) respectively, in either DMF or DMSO. In both cases complexes (46) and (47) were purified by washing with water followed by hexane. It should be noted that the previously prepared (40) and (41) can also be made using the above techniques. Complexes (46) and (47) were analysed by elemental analysis, IR and NMR spectroscopy. Molecular structures of (46) and (47) have also been determined by X-ray analysis (*Appendix*).

3.5.4: Molecular structures of CO complexes (46) and (47).

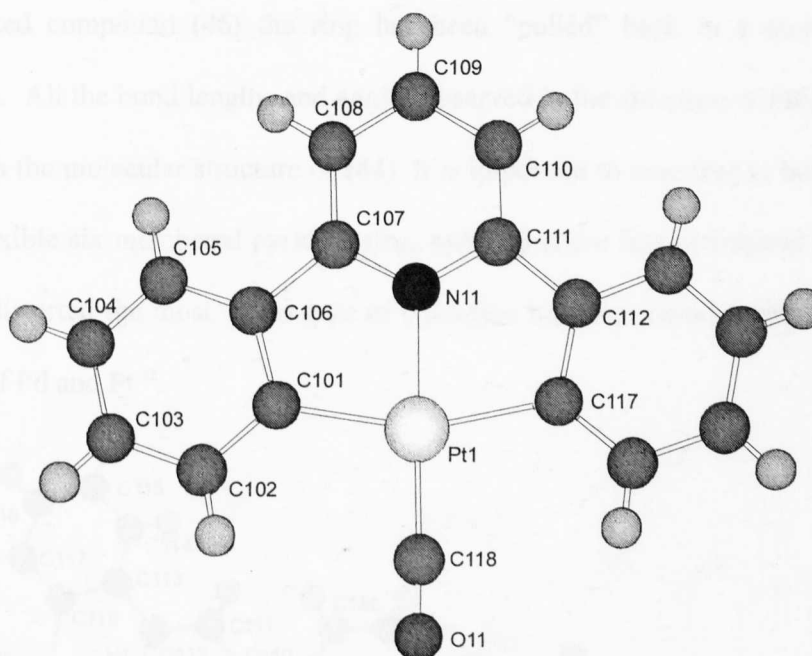


Figure 3.5.6: Molecular structure of **(46)** (data in *Appendix*).

The crystalline complex **(46)** contains two essentially identical molecules in the asymmetric unit. The molecules are essentially planar, with RMS deviations of 0.0368 and 0.0499 Å. In the crystal structure, the molecular planes are inclined at only 1.87(8)°. There were no significant differences between the chemically equivalent bond lengths and angles within the molecules. The two five-membered cyclometalated rings, fused along the Pt-N bond, had similar bond lengths to those observed in the mono-cyclometalated compounds **(24)** and **(28)**. The Pt-N distances are 2.027(7) and 2.003(7) Å and the Pt-C distances were between 2.057(9) and 2.084(10) Å. The N-Pt-C angles [80.2(3), 80.0(3), 80.0(3) and 80.1(3)°] were also similar to those observed in the mono-cyclometalated compounds. A significant difference was observed in the angles at the pyridine N atom: Pt-N11-C111 [117.6(6)°], Pt-N11-C106 [117.9(6)°], and C111-N11-C107 [124.0(8)°]. In the mono-cyclometalated compounds **(24)** and **(28)** the pyridine ring was distorted by the

cyclometalation with the pyridine being “pulled over” by the five-membered ring, in the di-cyclometalated compound (**46**) the ring has been “pulled” back to a more symmetrical arrangement. All the bond lengths and angles observed in the structure of (**46**) are similar to those seen in the molecular structure of (**44**). It is important to note that in both cases it was the more flexible six membered pyridine ring, rather than the five membered metalated ring which was distorted the most. This type of distortion has been noted previously in $N^{\wedge}N^{\wedge}C$ complexes of Pd and Pt.⁵²

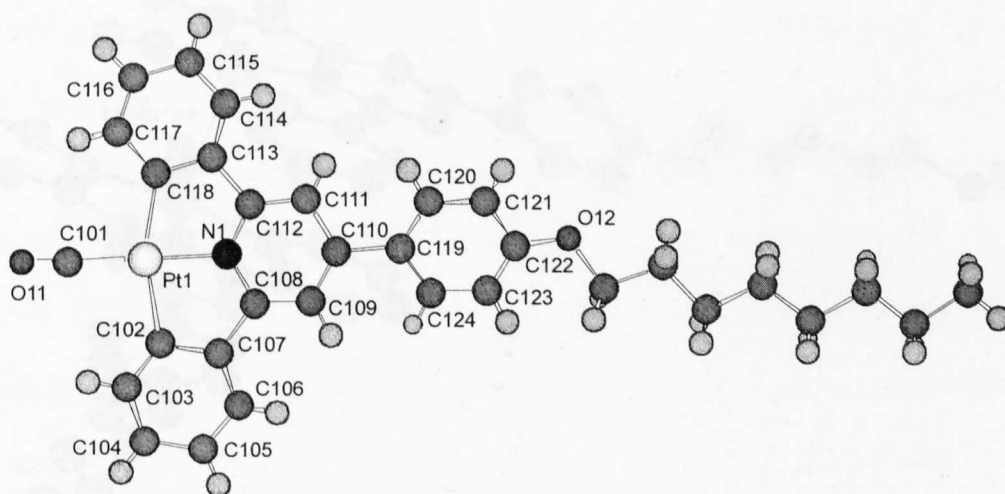


Figure 3.5.7: Molecular structure of (**47**) (data in *Appendix*).

The unit cell of structure of (**47**) contains two essentially identical molecules in the asymmetric unit. The cycloplatinated core of these molecules are essentially planar, with RMS deviations of 0.0409 and 0.0546 Å and are inclined at 5.71(33)° to each other. There were no significant differences between the chemically equivalent bond lengths and angles in each molecule. All the bond lengths and angles observed in the structure of (**47**) are comparable to those observed in the molecular structures of (**46**) and (**40**). The uncyclometalated phenyl ring *para* to the nitrogen has typical bond lengths and angles for an aromatic system and is essentially planar. Predictably, this disubstituted phenyl ring is twisted out of plane about the C110-C119 axis by 12.7°. The key difference to the other di-

cyclometalated complexes described in this section is the relatively short distance between the two platinum centres contained within the asymmetric unit [$3.2322(11)$ Å], as shown in *Figure 3.5.8*. This is comparable to the Pt-Pt bond [$3.28(1)$ Å] observed in the dimeric units of $N^{\wedge}N^{\wedge}C$ [(6-phenyl-2,2'-bipyridine)PtCl].⁵⁰ The Pt-Pt vector is inclined at an angle of *ca.* 87.2° to the stacked aromatic ligands with an inter-planar angle within the dimer of 5.7° . The two CO ligands are twisted by *ca.* 110.6° to each other about the Pt-Pt bond.

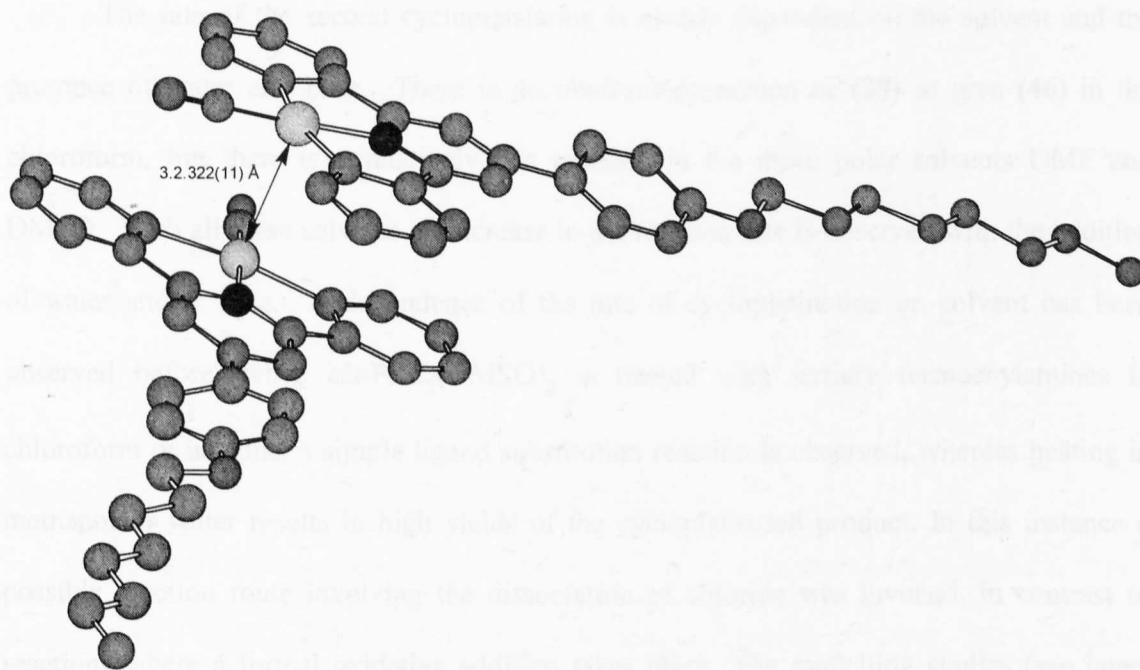


Figure 3.5.8: Molecular structure of **(47)** showing two complexes in the unit cell (data in *Appendix*).

3.5.5: Cycloplatination mechanism.

The reaction of **(38)** to give **(46)** in DMSO is complete within *ca.* 3 h at room temperature, but the rate is increased dramatically by the addition of base. If solid Na_2CO_3 is added, the reaction is complete in less than 15 min. The reaction of **(36)** in DMF gives **(46)** on a similar timescale (*ca.* 3 h); again the addition of base increased the rate of reaction. Since **(36)** isomerises to **(46)** it is impossible to conclusively determine whether it is **(36)** or

(38) which reacts to form (46). The isomerisation reaction of (37) to (39) was much faster than the reaction of (39) to give (47) in deuterated chloroform, which appeared to be very slow (no observable reaction after one week). The addition of base to pure (37) resulted in a comparable rate of formation of (47) to that when a mixture of the two isomers was treated in the same way. This suggests that it is indeed the isomers (38) and (39) which react on to give (46) and (47) respectively.

The rate of the second cyclometalation is clearly dependant on the solvent and the presence of water and base. There is no observable reaction of (38) to give (46) in the chloroform, but there is a relatively fast reaction in the more polar solvents DMF and DMSO. With all these solvents an increase in the reaction rate is observed with the addition of water and/or base. A dependence of the rate of cycloplatination on solvent has been observed before: when *cis*-PtCl₂(DMSO)₂ is treated with tertiary ferrocenylamines in chloroform or acetone, a simple ligand substitution reaction is observed, whereas heating in methanol or water results in high yields of the cycloplatinated product. In this instance a possible reaction route involving the dissociation of chloride was invoked, in contrast to reactions where a formal oxidative addition takes place. The modelling studies (see later) indicate that a possible driving force for the cycloplatination is the elimination of HCl, which must then be subsequently ionised. This need for the HCl to be ionised fits with the experimentally observed reaction rates, and in particular the dependence on the presence of water.

The rate of reaction of (31) to (44) was significantly slower than the rate of reaction of (38) to (46) under identical conditions (including using the same batch of DMSO as solvent): the first reaction took 5 days to go to completion, whereas the second one took 14 h. Such a variation provides evidence to suggest that the second cyclometalation proceeds

via an electrophilic attack by the platinum. It is to be expected that the CO ligand acts as a much better acceptor than DMSO, giving rise to a decrease in electron density on the platinum. The dissociation of chloride prior to an electrophilic type mechanism has been postulated and would seem to be likely in this case, given the analogous dependence of reaction rate on solvent.² The addition of AgBF_4 to a solution of (39) in acetone under conditions that have been used to induce cyclometalations resulted in the rapid formation of (47) in high yield. This provides further evidence for chloride dissociation and for the elimination of HCl being the driving force for the reaction.

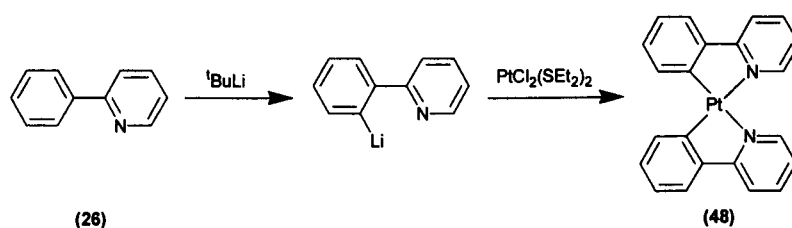


Figure 3.5.9: Di-cyclometalated 2-phenylpyridine, (48).

The fact that the second cyclometalation requires different conditions than the first is evident, unlike in other examples of di-cyclometalation. Whether the second cyclometalation proceeds *via* a mechanistically different reaction route is less clear. The first cyclometalation goes in high yield in acetic acid under conditions that parallel those reported before. In the case of (26), prolonged reaction times under these conditions do not result in a second cyclometalation, even when two equivalents of (26) were used. One might have expected to make (48) *via* (28). The only reported conditions for the synthesis of compounds such as (48) entail the use of two equivalents of lithiated phenyl pyridine (*Figure 3.5.9*), and whilst this method has been used successfully with a variety of pyridine derivatives, it only resulted in very poor yields of (46) from (19) (due to the non-regiospecific nature of the second lithiation).¹⁹ Thus it appears that the different reaction conditions that are need for the first

and second cyclometalations in the synthesis of compounds such as (44) cannot be attributed to steric crowding or unfavourable distortions within the C[^]N[^]C platinum moiety: they must either be due to the changed properties of the metal affecting the rate of reaction substantially or, the changed nature of the metal requiring a mechanistically different reaction route.

Since the first cyclometalation will not proceed under the conditions required for the second one this would suggest that the two cyclometalations have different mechanisms. Despite evidence here that the second cyclometalation arises through electrophilic attack by platinum, the mechanism of the first cyclometalation is unknown and thus it cannot be said for certain that the two metalations take place *via* mechanistically different routes. Previous examples of double cyclometalation have required similar conditions for both cyclometalations.⁵¹

Section 3.6. Theoretical Studies.

Density functional theoretical (DFT) calculations on compounds (36), (38) and (46) were performed,[†] in order to arrive at relative ground state energies. A series of unconstrained geometry optimisations was carried out for (46) (where an X-ray crystal structure was available) to determine the optimal combination of Pt frozen core size and functional. Both Pt[4f] and Pt[5p] were considered in conjunction with the Becke/Perdew (BP) gradient corrected functional or the Local Density Approximation (LDA). Scalar relativistic corrections were included throughout.

[†] All theoretical calculations were performed by Dr R J Deeth at the University of Warwick, UK.

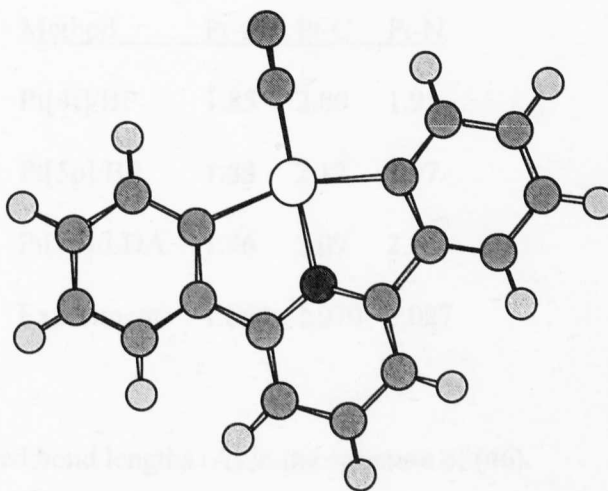


Figure 3.6.1: The optimised structure of **(46)**.

Selected optimised Pt-ligand distances for **(46)** are listed in *Table 3.6*. . The effect of the frozen core and functional on the Pt-CO distance is minimal but there are significant variations in the calculated Pt-C and Pt-N distances. With the ADF program, the best combination is the simple LDA and the larger Pt frozen core. This result parallels Deeth's⁵² previous findings inasmuch as the LDA-optimised metal-ligand distances are in better agreement with experiment than those obtained from a gradient-corrected functional. However, it is also demonstrated that the LDA gives poorer energies.⁵³ Thus, the optimal theoretical methodology for the present systems is to optimise the structure at the LDA/Pt[5p] level and to compute the total binding energy at this geometry using the BP functional.

Method	Pt-CO	Pt-C	Pt-N
Pt[4f]/BP	1.85	2.00	1.95
Pt[5p]/BP	1.88	2.12	2.07
Pt[5p]/LDA	1.86	2.09	2.04
Experiment	1.864	2.070	2.027

Table 3.6.1: Selected bond lengths (Å) in the structure of (46).

The optimised structures of (36) and (38) are shown in *Figure 3.6.2* and *Figure 3.6.3* respectively. In both cases, the uncoordinated phenyl ring is not perpendicular to the coordination plane. The steric interactions between this group and the ligand directed towards it cause the phenyl ring to rotate and the Pt coordination geometry to distort away from strict planarity. The calculated binding energies show that (38) is 16 kJmol⁻¹ lower in energy than (36). This energy difference allows us to rationalise (36) as the kinetic product and (38) as the thermodynamic product in *Figure 3.4.3*, and is in agreement with the experimentally observed isomerisation of (36) to (38). It is expected that the energy difference between (36) and (38) will be similar in magnitude, and hence would expect that (37) is the kinetic product and (39) the thermodynamic product in *Figure 3.4.3*.

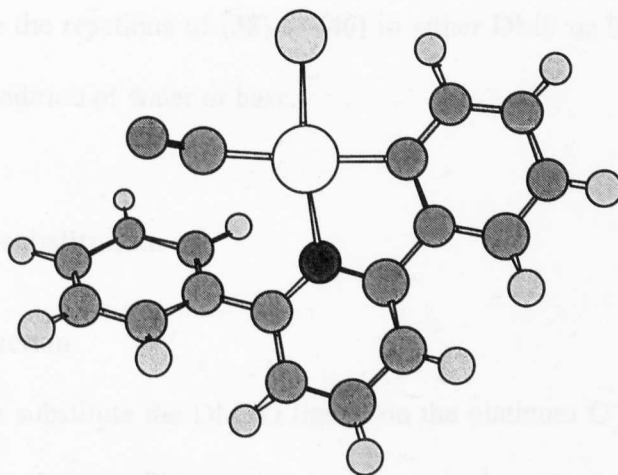


Figure 3.6.2: The optimised structure of (36).

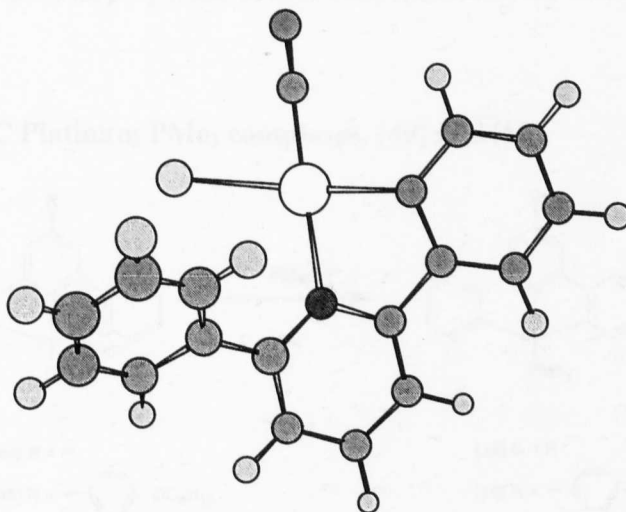


Figure 3.6.3: The optimised structure of (38).

The same calculations indicate that (46) is 68 kJmol^{-1} higher in energy than (38), implying that the reactions in Figure 3.4.1 are endothermic. However, it must be noted that the calculations assume that the other product of the reaction (HCl) is free and not solvated or ionised. The ionisation of HCl in water is known to be exothermic to the tune of 74.8 kJmol^{-1} , with the neutralisation of the liberated proton generating a further 55.8 kJmol^{-1} . These quantities of energy are more than sufficient to drive the reaction. Experimentally, complex (39) does not react on to form (47) in deuterated chloroform unless water and/or

base is present. Also the reactions of (38) to (46) in either DMF or DMSO are accelerated dramatically by the addition of water or base.

Section 3.7. Ligand substitution.

3.7.1: Introduction.

The ability to substitute the DMSO ligand on the platinum C[^]N[^]C complexes with CO has been mentioned above. This section demonstrates the potential of these compounds to form new complexes. The properties of four such molecules are discussed here.

3.7.2: C[^]N[^]C Platinum PMe₃ complexes, (49) and (50).

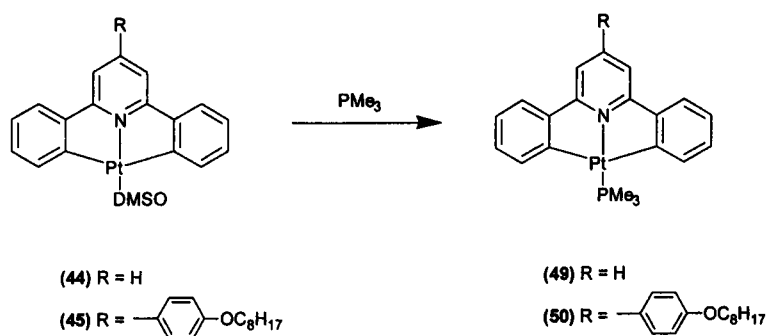


Figure 3.7.1: Synthetic route to (49) and (50).

Trimethylphosphine was added to a stirred solution of (44)/(45) in chloroform, under an inert atmosphere. An instant decolourisation to a lighter yellow was observed. The solvent was removed by evaporation and the amorphous yellow product washed with acetone to remove traces of DMSO. Complexes (49) and (50) were analysed by microanalysis and NMR spectroscopy.

The ¹H NMR spectrum of (49) and (50) show a similar splitting patterns to (44) and (45). The main difference was the absence of the coordinated DMSO peak and the presence of a doublet (²J_(P-H) = 1.8 Hz) with platinum satellites (²J_(Pt-H) = 64.5 Hz), indicating the

substitution of PMe_3 for DMSO. Further evidence for the ligand exchange was observed in the ^{31}P NMR spectrum which showed one single singlet at -20.98 ppm with ^{195}Pt coupling constants consistent with a $^1J_{(\text{Pt-P})}$ interaction (1606 Hz).

3.7.3: C[^]N[^]C Platinum stilbazole complexes, (51) and (52).

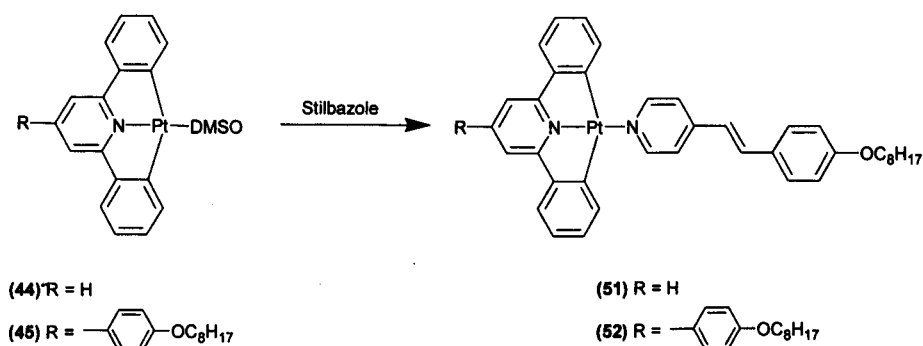


Figure 3.7.2: Synthetic route to (51) and (52).

One equivalent of 4-alkyloxystilbazole was added to a stirred solution of (44)/(45) in chloroform. Light was excluded from the reaction in order to prevent the stilbazole isomerising about the alkene bond to the *cis* form. The reaction was warmed until the reaction was complete (*ca.* 2 h). The solvent was removed and the amorphous yellow product washed with diethyl ether to remove traces of DMSO. Complexes (51) and (52) were analysed by microanalysis and NMR spectroscopy.

The ^1H NMR spectra of both (51) and (52) show similar splitting patterns to those observed for (44) and (45). Clear evidence for the coordination of the stilbazole to the platinum can be seen from the presence of ^{195}Pt coupling to the H atoms *ortho* to the N atom of the stilbazole [43.5 and 48.0 Hz for (51) and (52) respectively]. The same H atom was shifted downfield by *ca.* 1.41 ppm with respect to the uncoordinated stilbazole signal.

Once isolated and removed from solution complexes (51) and (52) were stable to air and light. Complex (51) melted without decomposition into an isotropic liquid at 77.8°C .

However, complex **(52)** melted from a crystalline form into a schleiren nematic phase (identified by its optical texture *Appendix 2*) at 198 °C. On further heating the material cleared into an isotropic liquid at 230 °C. The nematic phase was reproduced on cooling the isotropic liquid.

3.7.4: Thermal behaviours.

Complex	2,6-diphenylpyridine	4'-(4-alkoxyphenyl)-2',6'-diphenylpyridine
Ligand	(18) Mp. 75°C	(13) Mp. 56 °C
Dimer	(19) 370 °C (decomp)	(24) Mp. 270 °C
DMSO	(44) Mp. 143 °C	(45) Smectic phases 117 - 185 °C
CO	(46) Mp. 210 °C	(47) Smectic phases 74 - 203 °C
PMe ₃	(49) Mp. 130 °C	
Stilbazole	(51) Mp. 78 °C	(52) Nematic phase from 198 - 230 °C

Table 3.7.1: Thermal comparison of 2,6-diphenylpyridine and 4'-(4-alkoxyphenyl)-2',6'-diphenylpyridine complexes.

The cyclometalated dimeric complexes **(19)** and **(24)** show much increased melting points compared to the ligands **(18)** and **(13)** (*Table 3.7.*), as to be expected. In fact, complex **(19)** decomposed before melting at 370 °C. By comparison complex **(24)** melts 100 °C below this, due to the addition of the third *para* substituted phenyl ring with attendant alkoxy chain attached to the pyridine ring, thus disrupting the crystal packing. Once these chloride bridges have been cleaved and the smaller dicyclometalated species formed there is a significant reduction in melting points, due to the decrease in size of the complex.

The CO complexes (46) and (47) show the highest melting points of all the di-cyclometalated materials as the CO ligand is co-planar with the cyclometalated diphenylpyridine core. This is emphasised by the crystal structure of (46) which consists of essentially planar molecules, thus allowing very efficient packing. Both the PMe_3 and DMSO complexes (49), (44) and (45) have a tetrahedrally co-ordinated ligating group attached to the platinum, thus disturbing the crystal packing. Interestingly, all the di-cyclometalated 4'-(4-alkoxyphenyl)-2',6'-diphenylpyridine complexes show mesogenic behaviour, due to the extended cores of the molecules. The CO complex (47) which is known to be a dimer with Pt-Pt interactions in the crystal phase, exhibits a re-entrant mesophase at 199 °C, where, presumably the dimer breaks into the monomeric form. Therefore both species exhibit liquid crystalline properties. None of the simple diphenylpyridine complexes exhibit mesogenic behaviour; even the stilbazole derivative (51) melts into the isotropic liquid at 78 °C. By comparison the 4'-(4-alkoxyphenyl)-2',6'-diphenylpyridine stilbazole complex (52) shows a nematic phase between 198 and 230 °C. Thus, the extension to the linearity of the mesogenic core provided by the additional phenyl ring (with alkoxy chain) on the pyridine plays a vital role in the thermal behaviour of these materials.

3.7.5: Conclusion.

The stability of the di-cycloplatinated cores and the simple reaction conditions used to substitute the co-ordinating ligand enables the facile synthesis of a diverse series of complexes. Although this thesis only reports the use of 2,6-diphenylpyridine complexes as calamitic metallomesogens, it would be trivial to extend the work on triazines to produce multiple cyclometalated complexes that exhibit both calamitic and discotic phases. Additionally, the use of other metals (in particular palladium) could easily be used to

broaden this work. Another potential avenue of research would be the use of two or even three different metals in the cyclometalation of triazines.

Section 3.8. Platinum carbene complex.

3.8.1: Synthesis and characterisation of 2,6-bis(2',4'-dihexyloxyphenyl)pyridine platinum dichloride dimer, (53).

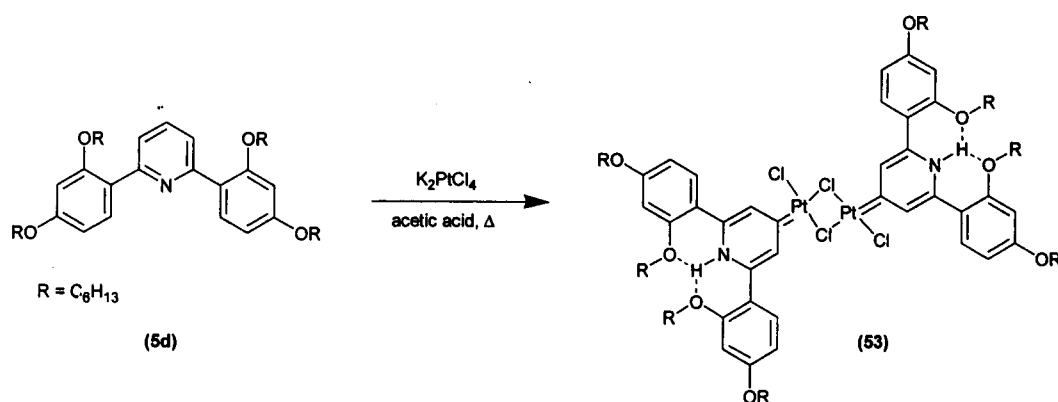


Figure 3.8.1: Synthetic route to platinum carbene complex, (53).

Pyridine (5d) was added to a suspension of potassium tetrachloroplatinate in glacial acetic acid. The mixture was stirred at 70 °C for 60 h by which time all traces of the platinum starting material had visibly disappeared. The solvent was removed under reduced pressure and the product (53) was washed with water, dissolved in chloroform, filtered, washed with hexane and crystallised from acetone. Complex (53) was isolated in reasonable yield and analysed by NMR spectroscopy and single crystal X-ray diffraction.

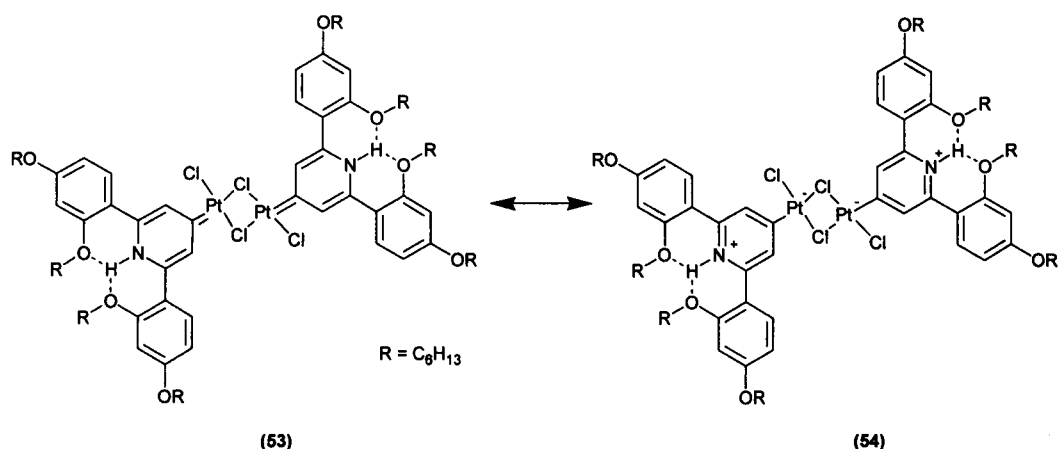


Figure 3.8.2: The carbene **(53)** and the zwitterions **(54)** as possible formal structures.

The molecular structure of **(53)** shows a number of interesting features (*Figure 3.8.3*). There is a crystallographically imposed centre of symmetry mid-way between the two platinum atoms, with the result that Pt1, Pt1', Cl1 and Cl1' from a plane. The chlorine atoms Cl2 and Cl2' are displaced by 0.082(4) Å from this plane. The plane of the N atom containing ring is at an angle of 38.62(24)° to the plane defined by the Pt₂Cl₂ rectangle.

Two extremes for the bonding of this organic fragment to the Pt atom centres are illustrated in *Figure 3.8.2*. The Pt1-C9 bond length of 1.951(9) Å is very similar to the 1.959(8) and 1.942(8) Å observed for the Pt(0) carbene derived from 1,3-dimesitylimidazol-2-ylidene⁵⁴ and the value of 1.973(11) Å observed for the cationic Pt(IV) carbene complex [PtCl₂{C(NHMe)(NHC₆H₄Cl)}(PEt₃)₂]-ClO₄.⁵⁵ It is however, significantly shorter than the single Pt-C bond length of 2.062(6) Å observed in the non-carbene cycloplatinated species [PtCl(ᵀBu₂PCMe₂CH₂)]₂.⁵⁶ A C-Pt bond length of 1.82(6) Å has been reported for the platinum carbene [PtCl(ᵀBuCH₂COⁱPr)]₂,⁵⁷ although there is a relatively large ESD associated with this measurement. The non-carbene Pt-aryl bond length [2.047(3) Å] observed in the molecular structure of [Pt(PPh₂CH₂CH₂PPh₂)(MeC₆H₃NHCNHC₆H₄Me)] is also significantly longer than that observed in the title complex.⁵⁸ Thus, the short C9-Pt1 bond

length would seem to suggest a carbene structure, *i.e.* **(53)** (Figure 3.8.2). Further evidence for this resonance form being the major contributor to the structure comes from ^{13}C NMR spectroscopy, with the carbene C atom resonance 324.3 ppm. The π back-bonding from the Pt atom to the the C atom is characteristic of a Fisher type carbene.⁵⁹

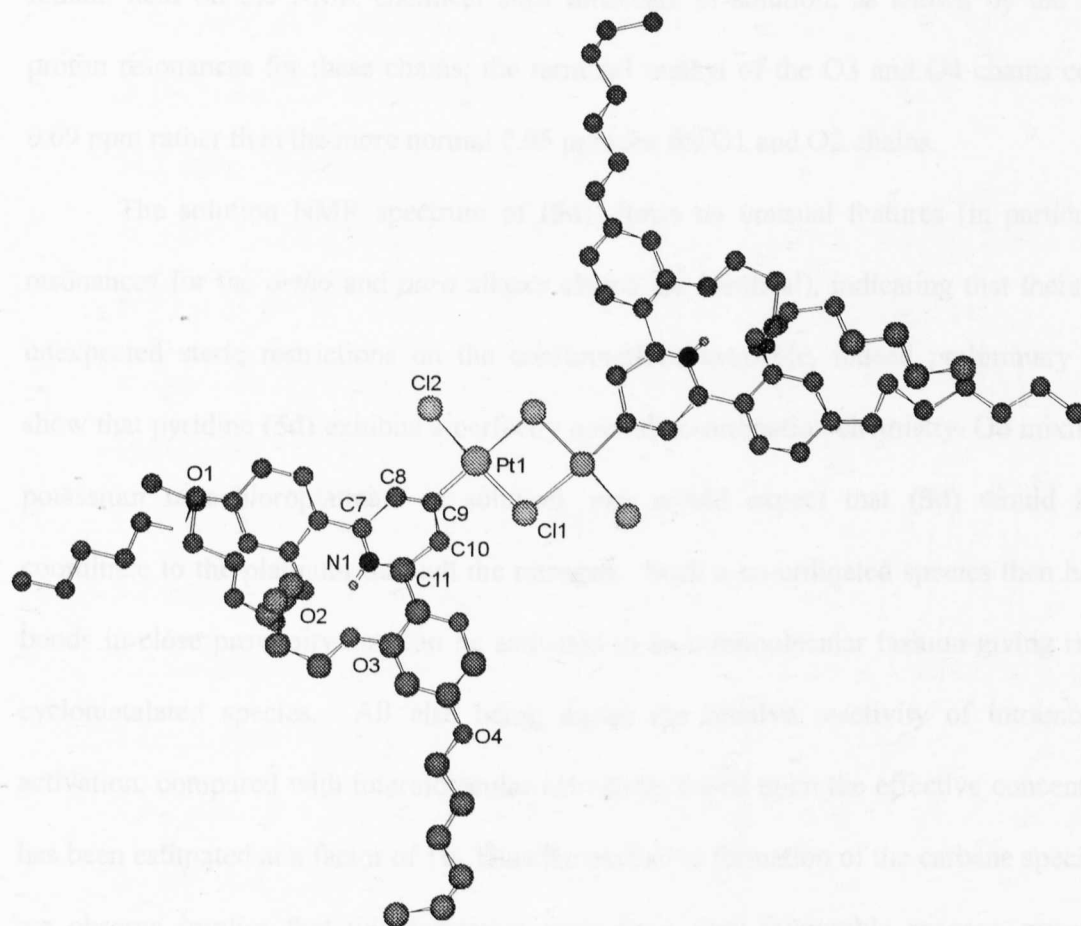


Figure 3.8.3: Molecular structure of **(53)** (data in *Appendix I*).

The H atom attached to the N atom was inserted at a calculated position. The O3-N1 and the O2-N1 distances are 2.622(9) and 2.720(8) Å respectively. These distances are substantially shorter than the sum of the Van der Waals radii of O and N (3.07 Å), thus confirm the H-bonding interaction. The O2-O3 distance, at 3.742(9) Å, is longer than the sum of the Van der Waals radii indicating no particular O-O interaction. One of the effects

of this hydrogen bonding is to twist both of the phenyl rings to angles of $34.63(29)^\circ$ and $32.79(36)^\circ$ with respect to the ring containing the N atom. In the solution, ^1H NMR spectra show that this H atom is very deshielded, with a chemical shift of 12.77 ppm. The positions of the two alkoxy chains that H-bond to this proton are “locked” in the solid state, and remain held on the NMR chemical shift timescale in solution, as shown by the unusual proton resonances for these chains; the terminal methyl of the O3 and O4 chains comes at 0.69 ppm rather than the more normal 0.95 ppm for the O1 and O2 chains.

The solution NMR spectrum of (**5d**) shows no unusual features (in particular the resonances for the *ortho* and *para* alkoxy chains are identical), indicating that there are no unexpected steric restrictions on the conformations available, indeed preliminary studies show that pyridine (**5d**) exhibits a perfectly normal co-ordination chemistry. On mixing with potassium tetrachloroplatinate in solution, one would expect that (**5d**) would initially coordinate to the platinum through the nitrogen. Such a co-ordinated species then has C-H bonds in close proximity that can be activated in an intramolecular fashion-giving rise to a cyclometalated species. All else being equal, the relative reactivity of intramolecular activation, compared with intermolecular activation, based upon the effective concentration, has been estimated at a factor of 10. Thus the exclusive formation of the carbene species that we observe implies that this formation must be a very favourable process, presumably assisted by the stabilisation offered by the hydrogen bonded proton.

Section 3.9. References.

- ¹ A D Ryabov, I M Panyashkina, V A Polyakov, J A K Howard, L G Kuz'mina, M S Datt and C Sacht, *Organometallics* 1998, **17**, 3615.
- ² A D Ryabov, *Chem. Rev.*, 1990, **90**, 403.
- ³ P Steenwinkel, R A Gossage and G van Koten, *Chem. Eur. J.*, 1998, **4**, 759.
- ⁴ A D Ryabov, *Synthesis*, 1985, 233.
- ⁵ M Pfeffer, *Pure Appl. Chem.*, 1992, **64**, 335.
- ⁶ K G Gaw, A M Z Slawin and M B Smith, *Organometallics*, 1999, **18**, 3255.
- ⁷ D P Lydon and J P Rourke, *J. Chem. Soc., Chem. Commun.* 1997, 1741.
- ⁸ S Chakladar, P Paul, K Venkatsubramanian and K Nag, *J. Chem. Soc., Dalton Trans.*, 1991, 2669.
- ⁹ S Trofimenko, *J. Am. Chem. Soc.*, 1971, **93**, 1808.
- ¹⁰ S Trofimenko, *Inorg. Chem.*, 1973, **12**, 1215.
- ¹¹ J Terheijden, G van Koten, F Muller, D M Grove, K Vrieze, E Nielsen and C H Stam, *J. Organomet. Chem.* 1986, **315**, 401.
- ¹² R A Gossage, A D Ryabov, A L Spek, D J Stufkens, J A M v Beek, R van Eldik and G van Koten, *J. Am. Chem. Soc.* 1999, **121**, 2488.
- ¹³ C J Moulton and B L Shaw, *J. Chem. Soc., Dalton Trans.* 1976, 1020.
- ¹⁴ A Weisman, M Gozin, H -B Kraatz and D Milstein, *Inorg. Chem.* 1996, **35**, 1792.
- ¹⁵ J Dupont, N Beydon, and M Pfeffer, *J. Chem. Soc., Dalton Trans.* 1989, 1715.
- ¹⁶ R Rybtchinski, A Vigalok, Y Ben-David and D Milstein, *J. Am. Chem. Soc.*, 1996, **118**, 12406.
- ¹⁷ P Steenwinkel, R A Gossage, T Maunula, D M Grove and G v Koten, *Chem. Eur. J.*, 1998, **4**, 763.

- 18 E C Constable, R P G Henney, R A Leese and D A Tocher, *J. Chem. Soc., Chem. Commun.* 1990, 513.
- 19 A J Canty, N J Minchin, B W Skelton and A M White, *J. Chem. Soc. Dalton Trans.*, 1985, **107**, 2891.
- 20 C Cornioley-Deuschel, T Ward and A v Zelewsky, *Helv. Chim. Acta*, 1988, **71**, 130.
- 21 J March, "*Advanced Organic Chemistry*"; Wiley and sons; Chichester, 1992, p 624.
- 22 I S Bengelsdorf, *J. Am. Chem. Soc.*, 1958, **80**, 1442.
- 23 S Yanagida, M Yokoe, I Katagiri, M Ohoka and S Komori, *Bull. Chim. Soc. Jap.*, 1973, **46**, 306.
- 24 I S Bengelsdorf, *J. Am. Chem. Soc.*, 1958, **80**, 1442.
- 25 J E Mahan and S D Turk (Phillips Petroleum C.), 1952, US patent 2598811.
- 26 A Llobera, J M Saa and A Peralta, *Synthesis*, 1984, 95.
- 27 S Yanagida, M Yokoe, I Katagiri, M Ohoka and S Komori, *Bull. Chem. Soc. Jap.*, 1973, **46**, 306.
- 28 J H Forstberg, V T Spaziano, S P Klump and K M Sanders, *J. Heterocyclic Chem.*, 1988, **25**, 767.
- 29 J J Ritter and R D Anderson, *J. Am. Chem. Soc.*, 1958, **24**, 208.
- 30 W Moser and R A Howie, *J. Chem. Soc. Inorg. Phys.*, 1968, 3039.
- 31 F Kröhnke, *Synthesis*, 1976, 1.
- 32 F Neve, A Crispin and S Campagna, *Inorg. Chem.*, 1997, **36**, 6150.
- 33 D W Bruce, D A Aunmur, E Laline, P M Matilis and P Styring, *Liq. Cryst.*, 1988, **3**, 285.
- 34 J P Rourke, D W Bruce and Y B Marder, *J. Chem. Soc., Dalton Trans.*, 1995, 317.
- 35 D W Bruce in "*Inorganic Materials*"; D W Bruce and D O'Hare Eds.; Wiley:

Chichester, 1992.

- 36 R M Ceder and J Sales, *J. Organomet. Chem.*, 1985, **294**, 389.
- 37 A D Ryabov, L G Kuz'mina, V A Polyakov, G M Kazankov, E S Ryabova, M Pfeffer and R v Eldik, *J. Chem. Soc., Dalton Trans.*, 1995, 999.
- 38 E I Lerner and S J Lippard, *J. Am. Chem. Soc.*, 1976, **98**, 5397.
- 39 A Cantarero, J M Amigó, J Faus, T Debaerdemaeker and M Julve, *J. Chem. Soc., Dalton Trans.*, 1988 2033.
- 40 M M Mdleleni, J S Bridgewater, R J Watts and P C Ford, *Inorg. Chem.*, 1995, **34**, 2334.
- 41 M E Curriolito, A Panuzi and F Ruffo, *Organometallics*, 1999, **18**, 3482.
- 42 C R Baar, G S Hill, J J Vittal and R J Puddephatt, *Organometallics*, 1999, **18**, 32.
- 43 L Chassot and A von Zelewsky, *Helv. Chim. Acta.*, 1986, **69**, 1855.
- 44 M A Bennett, H Jin and A C Willis, *J. Organomet. Chem.*, 1993, **451**, 249.
- 45 M Schmülling, A D Ryabov and R v Eldik, *J. Chem. Soc., Dalton Trans.* 1996, 1742.
- 46 L I Elding and R Romeo, *J. Chem. Soc., Dalton Trans.* 1996, 1741.
- 47 O F Wendt, A Oskarsson, J G Leipoldt and L I Elding, *Inorg. Chem.* 1997, **36**, 4514.
- 48 M C Baird, J T Mague, J A Osborn and G Wilkinson, *J. Chem. Soc. (A)*, 1967, 1347.
- 49 J Tsuji and K Ohno, *J. Am. Chem. Soc.*, 1966, **88**, 3452.
- 50 E C Constable, R P G Henney, T A Leese and D A Tocher, *J. Chem. Soc., Chem. Commun.*, 1990, 513.
- 51 M-C Lagunas, R A Gossage, A L Spek and G v Koten, *Organometallics*, 1998, **17**, 731.
- 52 M R Bray, R J Deeth, V J Paget and P D Sheen, *Int. J. Quant. Chem.*, 1997, **61**, 85.
- 53 R J Deeth and H D B Jenkins, *J. Phys. Chem.*, 1997, **101**, 4793.

- ⁵⁴ A J Arduengo, S F Gamper, J C Calabrese and F Davidson, *J. Am. Chem. Soc.* 1994, **116**, 4391.
- ⁵⁵ R Walker and K W Muir, *J. Chem. Soc., Dalton Trans.* 1975, 272.
- ⁵⁶ A B Goel, S Goel and D Vanderveer, *Inorg. Chim. Acta*, 1981, **54**, L267.
- ⁵⁷ Y T Struchkov, G G Aleksandrov, V B Pukhnarevich, S P Sushchinskaya and M G Voronkov, *J. Organomet. Chem.* 1979, **172**, 269.
- ⁵⁸ D F Christian, D A Clark, D H Farrar and N C Payne, *Can. J. Chem.*, 1978, **56**, 2516.
- ⁵⁹ R H Crabtree, "The Organometallic Chemistry Of The Transition Metals"; Wiley and sons; Chichester, 1994, p 270.

Chapter 4: Experimental.

Section 4.0. General considerations.

All chemicals were used as supplied, unless noted otherwise. ^1H and ^{13}C NMR spectra were obtained on Bruker AC250, AC400, DPX300 or DPX400 spectrometers, and were referenced to external TMS, assignments being made with the use of decoupling, the DEPT, COSY and GOESY pulse sequences. ^{31}P NMR spectra were obtained on Bruker DPX300 and AC400 spectrometers, and are referenced to 85 % H_3PO_4 . An Olympus BH2 microscope equipped with a Linkam HFS 91 heating stage and a TMS90 controller was used for thermal analysis, at a heating rate of $10\text{ }^\circ\text{C min}^{-1}$. Dr W Errington and Dr N W Alcock performed the single crystal X-ray diffraction structures at the University of Warwick using a Siemens SMART system equipped with a CCD detector. Warwick Analytical Service performed all elemental analyses and mass spectrometry.

Section 4.1. Preparation and characterisation of 2,6-bis-(4-hexyloxyphenyl)pyridine, (5a).

A series of 2,6-bis-(alkoxyphenyl)pyridine ligands (5a), (5b) and (5c) were synthesised using the same procedure. A detailed synthetic route to (5a) is given below, as an example.

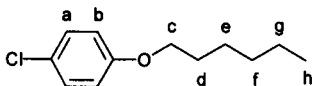
4.1.1: Preparation of 4-hexyloxychlorobenzene, (2a).

4-Chlorophenol (5.00 g, 3.89×10^{-2} mol), 1-bromohexane (7.71 g, 4.67×10^{-2} mol) and potassium carbonate (10.75 g, 7.78×10^{-2} mol) were heated to reflux in butan-2-one (250 cm^3 , 24 h.). The reaction mixture was filtered and the solvent was removed from the filtrate. The residue was dissolved in diethyl ether (100 cm^3), washed with water ($2 \times 50\text{ cm}^3$) and dried

(magnesium sulfate). The solvent was removed and the 4-hexyloxychlorobenzene purified by vacuum fractional distillation (120 °C, 1 mm Hg).

Yield: 7.63 g (3.59×10^{-2} mol), 92 %.

NMR Data (CDCl_3 , 250.13 MHz):



δ_{H} :	7.19	2H, AA'XX', H_a
	6.84	2H, AA'XX', H_b
	3.93	2H, t, $^3J = 7.2$ Hz, H_c
	1.79	2H, m, H_d
	1.35	6H, m, H_{e-g}
	0.90	3H, t, $^3J = 7.2$ Hz, H_h

4.1.2: Preparation of 3-Hexyloxyphenyl magnesium chloride, (3a).

Freshly prepared magnesium turnings (6.16 g, 0.254 mol) were dried under an inert atmosphere (70 °C, 24 h.). Dry THF (50 cm^3) was added to the magnesium and the solution was heated to reflux. A catalytic quantity of methyl iodide (1.5 g, 1.06 mmol) was added to the stirred solution. 3-Hexyloxychlorobenzene (50.0 g, 0.254 mol) was added dropwise to the reaction mixture. The reaction was refluxed under an inert atmosphere until all the magnesium disappeared (24 h.). The grey slurry was transferred to a graduated airtight ampoule, diluted with THF (made up to 100 cm^3) and stored (-20 °C) until required.

Yield: 48.8 g (0.206 mol), 81 %.

Preparation of 2,6-bis-(4-hexyloxyphenyl)pyridine, (5a).

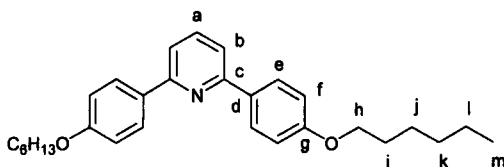
A freshly prepared solution of 3-hexyloxyphenyl magnesium chloride in THF (48.0 mmol, 22.9 cm^3 , 2.06 mol dm^{-3}) was slowly added to a solution of 2,6-dichloropyridine

(2.96 g, 20.0 mmol) and tetrakis(triphenylphosphine)palladium (0.45 g, 0.50 mmol) in THF (25 cm³). The solution was heated to reflux under an inert atmosphere (48 h.). Water (20 cm³) and hydrochloric acid (5 cm³, 2 mol dm⁻³) were added to destroy excess Grignard and the mixture was neutralised (NaOH_(aq)). The organic phase was collected, dried (magnesium sulfate) and the solvent was removed under vacuum. The product was recrystallised from ethyl acetate. The expected product 2,6-bis(4-hexyloxyphenyl)pyridine crystallised out as white needle like crystals.

Yield: 10.2 g (19.0 mmol), 95 %.

Analytical data for (**5a**):

NMR Data (CDCl₃, 250.13 MHz):



δ_{H} :	8.07	4H, AA'XX', H _e
	7.72	1H, t, ³ J = 7.6 Hz, H _a
	7.77	2H, d, ³ J = 7.6 Hz, H _b
	6.99	4H, AA'XX', H _f
	4.02	4H, ³ J = 7.0 Hz, H _h
	1.81	4H, m, H _i
	1.40	12H, m, H _{j-l}
	0.92	6H, ³ J = 7.0 Hz, H _m

δ_{C} :	159.9 (C _g)	156.2 (C _a)	137.2 (C _c)	131.8 (C _d)	128.1 (C _e)
	117.0 (C _b)	114.4 (C _f)	68.0 (C _h)	31.5 (C _i)	29.1 (C _j)
	25.6 (C _k)	22.5 (C _l)	15.6 (C _m)		

Elemental analysis:

2,6-bis-(4-hexyloxyphenyl)pyridine, (**5a**)

Found (expected) C 80.2 (80.7), H 8.4 (8.6), N 3.4 (3.3).

2,6-bis-(4-octyloxyphenyl)pyridine, (**5b**)

Found (expected) C 81.2 (81.3), H 9.3 (9.3), N 2.8 (2.8).

2,6-bis-(2-hexyloxyphenyl)pyridine, (**5c**)

Found (expected) C 80.5 (80.7), H 8.3 (8.6), N 3.3 (3.3).

Section 4.2. Preparation and characterisation of 2,6-bis-(2,4-dialkoxyphenyl)pyridines, (5d) and (5e).

Both (**5d**) and (**5e**) were synthesised and analysed using the same techniques. A detailed synthetic route to (**5d**) is described bellow.

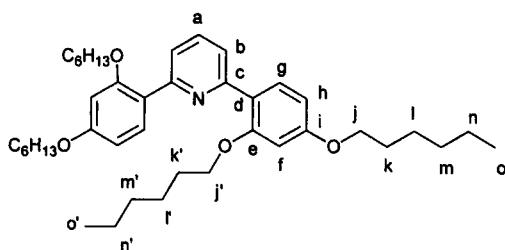
4.2.1: Preparation of 2,6-bis-(2,4-dihexyloxyphenyl)pyridine, (5d).

2,4-Dihexyloxychlorobenzene (15.0 g, 48.0 mmol) was added dropwise to a stirred solution of magnesium (1.22 g, 50.0 mmol) and methyl iodide (0.30 g, 2.11 mmol) in THF (25 cm³) under an inert atmosphere. The resulting Grignard was transferred *via* a cannula to a stirred solution of 2,6-dichloropyridine (2.96 g, 20.0 mmol) and tetrakis(triphenylphosphine)palladium (0.45 g, 0.50 mmol) in THF (25 cm³). The reaction mixture was then heated to reflux (24 h) under an inert atmosphere. Excess Grignard was destroyed with water (20 cm³) and hydrochloric acid (5 cm³, 2 M). The mixture was neutralised (NaOH_(aq)) and extracted with diethyl ether (2 × 200 cm³). The ether extract was dried (magnesium sulfate), the solvent removed under vacuum and the product crystallised out as white needle-like crystals.

Yield: 12.0 g (19.0 mmol), 95 %.

Analytical data for **(5d)**:

NMR Data (CDCl₃, 250.13 MHz):



δ_{H} :	7.96	2H, d, $^3J = 8.5$ Hz, H _g
	7.75	2H, d, $^3J = 7.3$ Hz, H _b
	7.60	1H, t, $^3J = 7.3$ Hz, H _a
	6.59	2H, dd, $^3J = 8.5$, $^4J = 2.1$ Hz, H _h
	6.53	2H, d, $^4J = 2.1$ Hz, H _f
	3.99	8H, t, $^3J = 6.7$ Hz, H _j & H _{j'}
	1.79	8H, m, H _k & H _{k'}
	1.48	24H, m, H _{l-n} & H _{l'-n'}
	0.89	12H, m, H _o & H _{o'}

δ_{C} :	160.5 (C _g)	157.7 (C _i)	154.7 (C _e)	134.8 (C _a)	132.1 (C _e)
	131.5 (C _d)	121.9 (C _b)	105.6 (C _f)	100.0 (C _h)	68.2 (C _j)
	31.4 (C _k)	29.1 (C _l)	25.7 (C _m)	22.5 (C _n)	13.9 (C _o)

Elemental analysis:

2,6-bis-(2,4-dihexyloxyphenyl)pyridine, **(5d)**

Found (expected) C 76.8 (77.9), H 9.6 (9.7), N 2.4 (2.2).

2,6-bis-(2,4-dioctyloxyphenyl)pyridine, **(5e)**

Found (expected) C 79.5 (79.1), H 10.6 (10.4), N 2.1 (1.9).

X-ray crystal data for **(5d)** in *Appendix* .

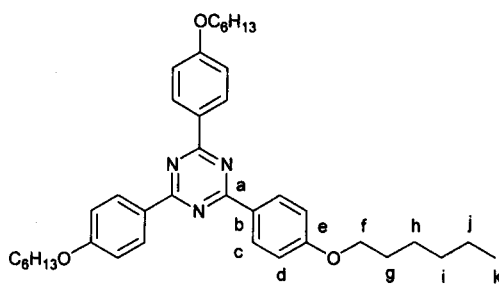
Section 4.3. Preparation and characterisation of 2,4,6-tris-(4-alkoxyphenyl)-[1,3,5]triazine, (7).

A pre-prepared solution of 3-hexyloxyphenyl magnesium chloride in THF (97.1 cm³, 2.06 M, 0.2 mol) was added dropwise to a cold (0 °C) solution of 2,4,6-trichloro-[1,3,5]triazine (9.22 g, 5.0 × 10⁻² mol) and tetrakis(triphenylphosphine)palladium (0.54 g, 0.6 mmol) in THF (50 cm³) under an inert atmosphere. An ice bath was used to control the exothermic reaction during addition of the Grignard. The solution stirred at room temperature (24 h) and then heated to reflux (48 h). Water (20 cm³) followed by hydrochloric acid (5 cm³, 2 M) were gradually added to the reaction flask to destroy excess Grignard. The mixture was neutralised (NaOH_(aq)) and the organic phase was collected, dried (magnesium sulfate) and the solvent removed. The oily product was recrystallised from hexane, to give brown crystals, which were dissolved in chloroform (25 cm³) and decolourised using activated charcoal. The solvent was removed and the pure product recrystallised from ethyl acetate as white needle like crystals.

Yield: 12.9 g (12.2 mmol), 42 %.

Mp.: 95.1 °C

NMR Data (CDCl₃, 250.13 MHz):



δ_H : 8.68 6H, AA'XX', H_c

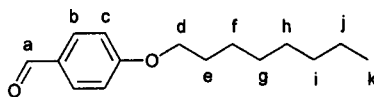
7.03 6H, AA'XX', H_d4.06 6H, t, ³J = 6.71 Hz, H_f1.83 6H, m, H_g1.40 18H, m, H_{h-j}0.92 9H, t, ³J = 7.0 Hz, H_k δ_C : 171.0 (C_a) 163.1 (C_e) 131.0 (C_c) 129.3 (C_b) 114.7 (C_d)68.6 (C_f) 32.0 (C_g) 29.6 (C_j) 26.1 (C_h) 23.0 (C_i)14.4 (C_k)

Elemental analysis: Found (expected): C 76.6 (76.8), H 8.4 (8.4), N 6.5 (6.9).

Section 4.4. Preparation and characterisation of 4-(4-alkoxyphenyl)-2,6-diphenylpyridine, (13).**4.4.1: Preparation of 4-octyloxybenzaldehyde, (9).**

4-Hydroxybenzaldehyde (20.0 g, 0.160 mol) was added to a solution containing 1-bromooctane (32.8 g, 0.170 mol) and potassium carbonate (23.5 g, 0.170 mol) in acetone (300 cm³). The reaction was stirred and heated to reflux (24 h), cooled to room temperature and filtered. The filtrate was collected and the solvent removed. The product was isolated by vacuum distillation (150 °C, 1 mmHg), to yield a colourless liquid.

Yield: 35.2 g (0.150 mol), 91 %.

NMR Data (CDCl₃, 250.13 MHz): δ_H : 9.82 1H, s, H_a7.78 2H, AA'XX', H_b6.94 2H, AA'XX', H_c

3.99 2H, $^3J = 6.7$ Hz, H_d

1.77 2H, m, H_e

1.35 10H, m, $H_{f,j}$

0.85 3H, $^3J = 7.2$ Hz, H_d

4.4.2: Preparation of 1-(2-phenyl)-3-[4-octyloxyphenyl]propen-1-one, (11).

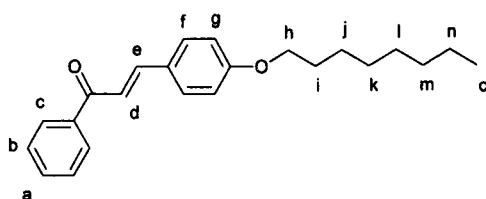
A solution of acetophenone (5.13 g, 42.7 mmol) in ethanol (50 cm³) was added dropwise (1 hr) to a stirred emulsion of 4-octyloxybenzaldehyde (10.0 g, 42.7 mmol) and NaOH (2.8 g, 70.0 mmol) in ethanol/water (200 cm³, 3:1, v/v). After stirring at room temperature (24 h.), the resulting yellow solid was filtered off, washed with cold diethyl ether (2 × 10 cm³) and dried under *vacuo*.

Yield: 14.3 g (42.7 mmol), 100 %.

Mp.: 79 °C.

FT-IR: $\nu_{(C=O)}$ 1661 cm⁻¹ (KBr disk)

NMR Data (CDCl₃, 300.13 MHz):



δ_H : 7.99 2H, dd, $^3J = 7.9$, $^4J = 1.8$ Hz, H_c

7.77 1H, d, $^3J = 15.6$ Hz, H_d

7.58 2H, AA'XX', H_f

7.50 3H, m, H_a & H_b

7.40 1H, d, $^3J = 15.6$ Hz, H_e

6.91 2H, AA'XX', H_g

3.99 2H, t, ³J = 6.5 Hz, H_h

1.79 2H, m, H_i

1.37 10H, m, H_{j-n}

0.87 3H, t, ³J = 7.0 Hz, H_o

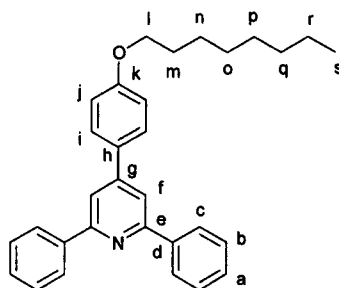
4.4.3: Preparation of 4-(4-octyloxyphenyl)-2,6-diphenylpyridine, (13).

N-(2-Oxo-2-phenylethyl)pyridinium bromide (2.06 g, 7.39 mmol), 1-(2-phenyl)-3-[4-octyloxyphenyl]propen-1-one (2.50 g, 7.39 mmol) and ammonium acetate (5.00 g, 64.0 mmol) were mixed together in methanol (50 cm³), producing an orange solution. The reaction mixture was stirred (24 h) under reflux. The dark green solution was allowed to cool to room temperature, when a colourless oil separated on standing. The solvent was decanted off and the oil washed with methanol (1 × 10 cm³), yielding the pure product, which solidified on standing.

Yield: 2.58 g (5.93 mmol), 80 %.

Mp.: 55.7 °C

NMR Data (CDCl₃, 300.13 MHz):



δ_H : 8.20 4H, dd, $^3J = 8.5$, $^4J = 1.8$ Hz, H_c

7.86 2H, s, H_f

7.70 2H, AA'XX', H_i

7.50 6H, m, H_a & H_b

7.04 2H, AA'XX', H_j

4.03 2H, t, $^3J = 6.4$ Hz, H_l

1.83 2H, m, H_m

1.41 10H, m, H_{n-r}

0.91 3H, t, $^3J = 6.7$ Hz, H_s

δ_C : 160.5 (C_k) 157.8 (C_e) 150.1 (C_g) 140.1 (C_h) 131.4 (C_d)

129.4 (C_a) 129.1 (C_b) 128.7 (C_i) 127.6 (C_c) 117.0 (C_f)

115.5 (C_j) 68.4 (C_l) 32.3 (C_q) 29.8 (C_m) 29.7 (C_o)

26.7 (C_p) 26.5 (C_n) 23.1 (C_r) 14.6 (C_s)

Elemental analysis: Found (expected) C 85.5 (85.5), H 7.7 (7.6), N 3.0 (3.2).

Section 4.5. Preparation and characterisation of 4-octyloxystilbazole, (17).

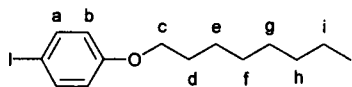
4.5.1: Preparation of 4-octyloxyiodobenzene, (15).

A stirred solution containing 4-iodophenol (20.0 g, 0.091 mol), 1-bromooctane (19.3 g, 0.10 mol) and potassium carbonate (18.9 g, 0.14 mol) in butan-2-one (200 cm³) was heated to reflux (24 h). The reaction mixture was cooled to room temperature and the potassium carbonate was filtered off. The solvent was then removed from the filtrate. The resulting orange oil was solvated with diethyl ether (50 cm³), washed with water (10 cm³) and dried (magnesium sulfate). The ether was removed to yield the crude product as a pale

yellow oil, which was purified by vacuum distillation (170 °C, 1 mm Hg), to give a colourless oil.

Yield: 23.6 g (71.0 mmol), 78%.

NMR Data (CDCl₃, 300.13 MHz):



δ_{H} :	7.53	2H, AA'XX', H _a
	6.66	2H, AA'XX', H _b
	3.90	2H, t, $^3J = 6.4$ Hz, H _c
	1.79	2H, m, H _d
	1.39	10H, m, H _{e-i}
	0.88	3H, $^3J = 7.0$ Hz, H _j

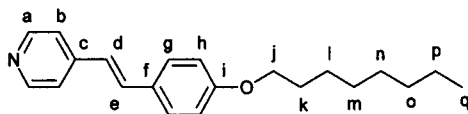
4.5.2: Preparation of 4-octyloxystilbazole, (17).

4-Vinylpyridine (5.29 g, 5.00×10^{-2} mol), 4-octyloxyiodobenzene (15.0 g, 4.51×10^{-2} mol), triethylamine (4.57 g, 4.51×10^{-2} mol) and a catalytic quantity of palladium acetate (103 mg, 4.50×10^{-4} mol) were dissolved in a stirred solution of acetonitrile (20 cm³) in an air tight ampoule, under an inert atmosphere. The reaction vessel was heated (100 °C, 24 h) and allowed to cool to room temperature, forming a yellow solid. This was then dissolved in dichloromethane (100 cm³) and washed with water (20 cm³). After drying (magnesium sulfate), the solvent was removed to leave a pale yellow powder. The crude product was extracted with hexane (250 cm³) using a Soxhlet apparatus (2 h). The hexane was removed and the product recrystallised from acetone, to yield the pure product as white crystals.

Yield: 12.32 g (3.97×10^{-2} mol), 88%.

Phase behaviour (°C): $K \xrightarrow{75} S_E \xrightarrow{85} S_B \xrightarrow{99} I$

NMR Data (CDCl₃, 300.13 MHz):



δ_H :	8.46	2H, AA'XX', H_a
	7.39	2H, AA'XX', H_g
	7.25	2H, AA'XX', H_b
	7.17	1H, $^3J = 15.9$ Hz, H_e
	6.85	2H, AA'XX', H_h
	6.69	1H, $^3J = 15.9$ Hz, H_d
	3.90	2H, $^3J = 6.9$ Hz, H_j
	1.71	2H, m, H_k
	1.28	10H, m, H_{l-p}
	0.85	3H, t, $^3J = 7.0$ Hz, H_q

δ_C :	169.7 (C_i)	150.1 (C_a)	145.0 (C_c)	132.7 (C_e)	128.6 (C_f)
	128.3 (C_g)	123.6 (C_b)	120.5 (C_d)	114.8 (C_h)	68.1 (C_j)
	22-32 (C_l, C_k)		14.0 (C_m)		

Elemental analysis: Found (expected) C 79.9 (81.5), H 8.5 (8.5), N 4.1 (4.5).

Section 4.6. Preparation and characterisation of [(2,6-diphenylpyridine)Pt-Cl]₂, (19).

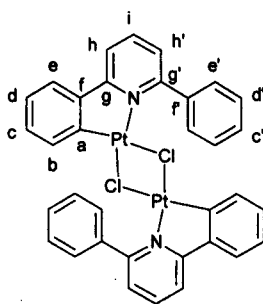
Potassium tetrachloroplatinate (374 mg, 0.900 mmol) was added to a solution of 2,6-diphenylpyridine (233 mg, 1.00 mmol) in glacial acetic acid (250 cm³). The reaction was stirred (80 °C) until the red platinum salt was no longer visible (3 days). The reaction

mixture was filtered yielding the product as an insoluble yellow powder, which was washed with water (5 cm³), acetone (30 cm³) and ether (15 cm³).

Yield: 407 mg (98 %, 0.442 mmol).

Decomposition without melting at 320-370 °C

NMR Data (D7-DMF, 400.03 MHz):



δ_{H} :	8.22	2H, t, $^3J = 7.8$ Hz, H_i
	8.10	2H, dd, $^3J = 7.6$, $^4J = 1.1$ Hz, H_h
	7.95	4H, m, $\text{H}_{e'}$
	7.86	2H, dd, $^3J = 7.8$, $^4J = 1.2$, H_b
	7.71	2H, dd, $^3J = 7.8$, $^4J = 1.2$ Hz, H_e
	7.56	6H, m, $\text{H}_{c'}$ & $\text{H}_{d'}$
	7.54	2H, dd, $^3J = 7.6$, $^4J = 1.1$ Hz, $\text{H}_{h'}$
	7.11	2H, dt, $^3J = 7.3$, $^4J = 1.2$ Hz, H_d
	7.05	4H, dt, $^3J = 7.3$, $^4J = 1.2$ Hz, H_c

MS (MALDI TOF): 922 (M^+); Negative ion: peaks at m/z 35 and 37 indicate Cl^- .

Elemental analysis: Found (expected) C 43.7 (44.3), H 2.6 (2.6), N 3.0 (3.0).

Section 4.7. Preparation and characterisation of [{2,6-bis(4-alkoxyphenyl)pyridine}Pt-Cl]₂, (20) and (21).

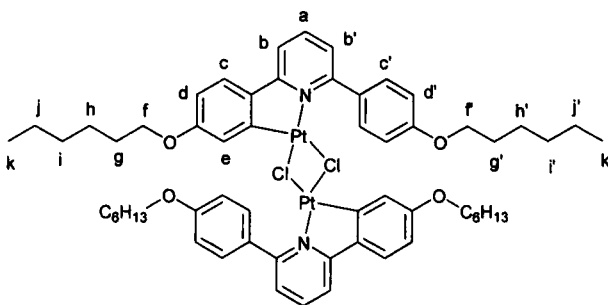
Complexes (20) and (21) were prepared and characterised in the same way. A detailed synthetic route to (20) is give below.

4.7.1: Preparation of [{2,6-bis(4-hexyloxyphenyl)pyridine}Pt-Cl]₂, (20).

2,6-Bis(4-hexyloxyphenyl)pyridine (103 mg, 0.239 mmol) was added to a solution of potassium tetrachloroplatinate(II) (99 mg, 0.239 mmol) in acetic acid (400 cm³). The mixture was stirred (80 °C for 48 h). The solvent was removed and the product washed with water (20 cm³). The yellow product was dissolved in chloroform (3 cm³), filtered, washed (hexane, 5 cm³) and recrystallised from ethyl acetate.

Yield: 100 mg (0.075 mmol), 63 %.

NMR Data (CDCl₃, 250.13 MHz):



δ_{H} :	7.71	4H, AA'XX', H _c
	7.70	2H, t, ³ J = 7.6 Hz, H _a
	7.36	2H, dd, ³ J = 7.6, ⁴ J = 1.2 Hz, H _b
	7.21	2H, d, ³ J = 8.5 Hz, H _c
	7.03	2H, dd, ³ J = 7.6, ⁴ J = 1.2 Hz, H _{b'}
	6.91	4H, AA'XX', H _{d'}
	6.60	2H, dd, ³ J = 8.5, ⁴ J = 2.3 Hz, H _d

6.46	2H, d, $^4J = 2.3$ Hz, H_e
3.97	4H, t, $^3J = 6.7$ Hz, H_f
3.86	4H, t, $^3J = 6.7$ Hz, H_f
1.79	8H, m, H_g & $H_{g'}$
1.44	24H, m, H_{h-j} & $H_{h'-j'}$
0.95	6H, t, $^3J = 7.0$ Hz, H_k
0.91	6, t, $^3J = 7.0$ Hz, $H_{k'}$

Mass spec (CI): m/z 1322 (calculated for M^+)

Elemental analysis:

[{2,6-bis(4-hexyloxyphenyl)pyridine}Pt-Cl]₂, (20)

Found (expected) C 52.6 (52.7), H 5.5 (5.5), N 2.2 (2.1).

[{2,6-bis(4-octyloxyphenyl)pyridine}Pt-Cl]₂, (21)

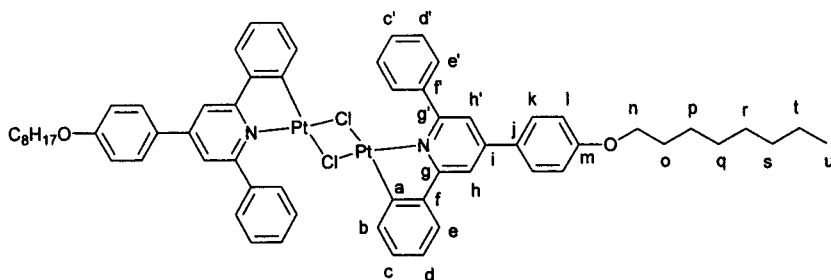
Found (expected) C 55.7 (55.3), H 5.9 (6.2), N 2.1 (2.0).

Section 4.8. Preparation and characterisation of [{4-(4-octyloxyphenyl)-2,6-diphenylpyridine}Pt-Cl]₂, (24).

A suspension of potassium tetrachloroplatinate(II) (100.85 mg, 0.243 mmol) and 4-(4-octyloxyphenyl)-2,6-diphenylpyridine (100 mg, 0.243 mmol) in glacial acetic acid (250 cm³) was stirred under reflux until the red crystals disappeared (3 days). The solvent was removed from the yellow solution. The residue was washed with water (5 cm³), cold acetone (15 cm³) and cold hexane (20 cm³). The yellow product was dried under *vacuo*.

Yield: 155.8 mg (0.117 mmol), 96 %.

Mp.: 270 °C.

NMR Data (CDCl₃, 400.03 MHz):

δ_{H} :	7.85	4H, m, $\text{H}_{\text{e}'}$
	7.72	2H, d, $^4\text{J} = 2.4 \text{ Hz}$, H_{h}
	7.65	4H, AA'XX', H_{k}
	7.51	6H, m, $\text{H}_{\text{d}'}$ & $\text{H}_{\text{c}'}$
	7.41	2H, dd, $^3\text{J} = 7.6$, $^4\text{J} = 1.2 \text{ Hz}$, H_{e}
	7.35	2H, d, $^4\text{J} = 2.4 \text{ Hz}$, $\text{H}_{\text{h}'}$
	7.06	2H, dt, $^3\text{J} = 7.6$, $^4\text{J} = 1.2 \text{ Hz}$, H_{d}
	7.00	6H, m, H_{l} & H_{c}
	6.93	2H, dd, $^3\text{J} = 7.6$, $^4\text{J} = 1.2$, $^3\text{J}_{(\text{Pt-H})} = 35.3 \text{ Hz}$, H_{b}
	4.03	4H, t, $^3\text{J} = 6.4 \text{ Hz}$, H_{n}
	1.80	4H, m, H_{o}
	1.51	20H, m, $\text{H}_{\text{p-t}}$
	0.91	6H, t, $^3\text{J} = 7.0 \text{ Hz}$, H_{u}

δ_{C} :	178.1 (C_{a})	162.1 (C_{m})	161.3 (C_{g} & $\text{C}_{\text{g}'}$)	150.0 (C_{i})
	145.0 (C_{f})	139.9 ($\text{C}_{\text{f}'}$)	132.4 (C_{b})	130.2 ($\text{C}_{\text{c}'}$)
	130.0 ($\text{C}_{\text{d}'}$)	129.2 (C_{j})	128.9 (C_{d})	128.7 (C_{k} & $\text{C}_{\text{e}'}$)
	124.2 (C_{e})	124.0 (C_{c})	121.3 ($\text{C}_{\text{h}'}$)	115.7 (C_{l})
	113.9 (C_{h})	68.7 (C_{n})	32.2 (C_{s})	32.0 (C_{o})

29.8 (C_q) 29.6 (C_r) 26.4 (C_p) 23.1 (C_t)
14.5 (C_u)

Elemental analysis: Found (expected) C 55.6 (56.0), H 5.2 (4.9), N 2.0 (2.1).

X-ray crystal data in *Appendix* .

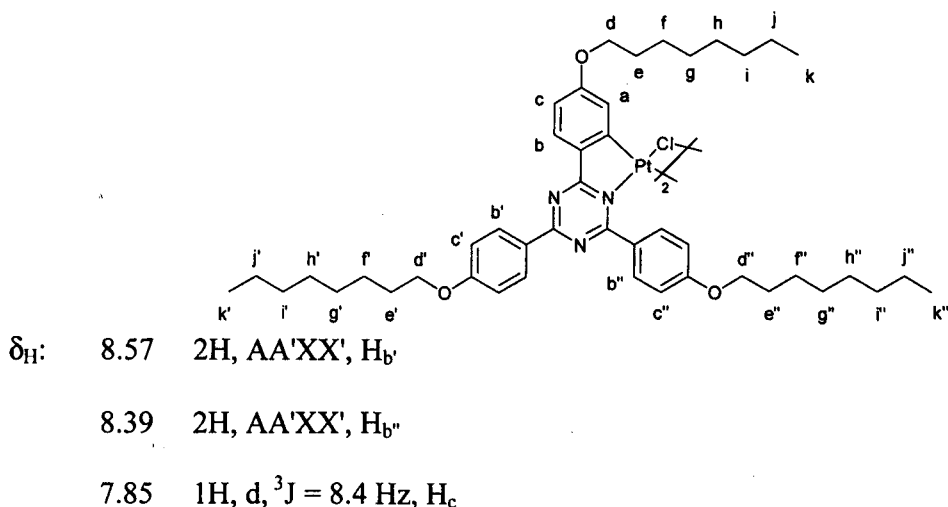
Section 4.9. Preparation and characterisation of [{2,4,6-tris-(4-alkoxyphenyl)-[1,3,5]triazine}Pt-Cl]₂, (25).

A suspension of potassium tetrachloroplatinate (25.0 mg, 0.06 mmol) and 2,4,6-tris-(4-alkoxyphenyl)-[1,3,5]triazine (55.6 mg, 0.09 mmol) in glacial acetic acid (300 cm³) was heated (60 °C). The reaction was stirred until all traces of the platinum salt disappeared (about 4 days). The solvent was reduced until the yellow product precipitated out from the solution (about 10 cm³). The reaction mixture was cooled (0 °C, 12 hours) and the product filtered off from the bulk solution. The amorphous yellow powder was washed with water (5 cm³) and hexane (10 cm³) to remove traces of starting materials.

Yield: 51.2 mg (2.77 × 10⁻² mmol). 92 %.

Mp.: 201 °C

NMR Data (CDCl₃, 300.16 MHz):



6.97	4H, m, H _{c'} & H _{c''}
6.67	1H, dd, ³ J = 8.4, ⁴ J = 2.1 Hz, H _b
6.45	1H, d, ⁴ J = 2.1, ³ J _(Pt-H) = 27.3 Hz, H _a
4.05	2H, t, ³ J = 6.3 Hz, H _{d'}
3.92	2H, t, ³ J = 7.2 Hz, H _{d''}
3.85	2H, t, ³ J = 7.5 Hz, H _d
1.80	6H, m, H _e , H _{e'} & H _{e''}
1.43	30H, m, H _{f-j} , H _{f'-j'} & H _{f''-j''}
0.93	9H, m, H _k , H _{k'} & H _{k''}

MS MALDI TOF: m/z 1847 (M⁺)

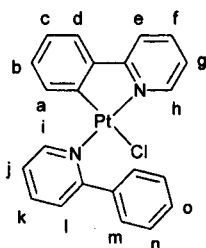
Elemental analysis: Found (expected) C 57.9 (58.5), H 6.6 (6.8), N 4.0 (4.6).

Section 4.10. Preparation and characterisation of Pt(phpy)(Hphpy)Cl, (28).

2-Phenyl-pyridine (140 mg, 0.902 mmol) was added to a stirred suspension of potassium tetrachloroplatinate (170 mg, 0.41 mmol) in glacial acetic acid (250 cm³). The reaction mixture was heated (120 °C) until the platinum salt was no longer visible (48 h). The solvents were removed under vacuum to yield the crude product as a yellow powder, which was purified by recrystallisation from ethyl acetate.

Yield: 190 mg (0.352 mmol), 86%.

NMR Data (CDCl₃, 250.13 MHz):



δ_{H} :	9.54	1H, d, $^3J = 5.5$, $^3J_{(\text{Pt-H})} = 19.0$ Hz, H_h
	9.18	1H, d, $^3J = 5.5$, $^3J_{(\text{Pt-H})} = 19.0$ Hz, H_i
	8.07	2H, dd, $^3J = 21.3$, $^4J = 7.3$ Hz, H_m
	7.91	1H, m, H_k
	7.68	1H, m, H_c
	7.61	1H, m, H_l
	7.45	1H, m, H_d
	7.34	1H, m, H_o
	7.29	5H, m, H_e , H_j & H_n
	7.02	1H, m, H_b
	6.95	1H, m, H_f
	6.85	1H, m, H_g
	6.15	1H, d, $^3J = 7.3$, $^3J_{(\text{Pt-H})} = 23.0$ Hz, H_a

Elemental analysis: Found (expected) C 48.8 (48.9), H 3.2 (3.2), N 4.9 (5.2).

X-ray crystal data in *Appendix* .

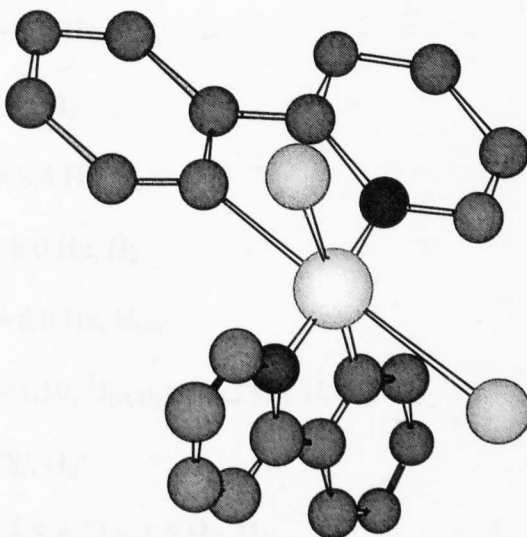
Section 4.11. Preparation and characterisation of $\text{Pt}^{\text{IV}}(\text{phpy})_2\text{Cl}_2$, (29).

A solution of $\text{Pt}(\text{phpy})(\text{Hphpy})\text{Cl}$ (95 mg, 0.175 mmol) in chloroform (1 cm^3) was irradiated with UV/vis light (from a tungsten lamp), until the insoluble product formed (3 days). The solvent was removed and the red crystals washed with hexane (5 cm^3).

Yield: 77.7 mg (0.135 mmol), 77 %.

MS (MALDI TOF): m/z 574 (M^+)

Elemental analysis: Found (expected) C 46.5 (46.0), H 3.0 (2.8), N 4.5 (4.9).



Molecular structure of **(29)**, showing the nitrogens *trans* to each other and the chlorines *cis* to each other (data in *Appendix*).

No solution data were available on this complex due to its insolubility.

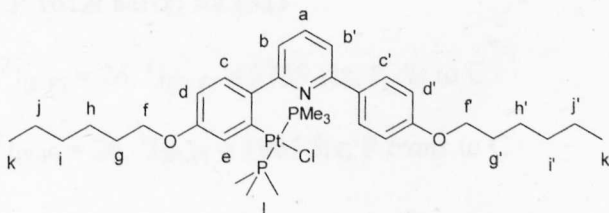
Section 4.12. Preparation and characterisation of [2,6-bis(4-hexyloxyphenyl)pyridine]

Pt-Cl(PMe₃)₂, (30) and (31).

Trimethylphosphine (excess) was added drop wise to a stirred solution of complex **(20)** (50 mg, 3.78×10^{-2} mmol) in THF (1 cm³), until an opaque white solution appeared from the original yellow, to form complex **(31)**. Unreacted trimethylphosphine and solvent were removed using high vacuum, and filtering through a silica plug then purified the product **(30)**.

Yield: 60.3 mg (7.42×10^{-2} mmol). 98 %,

NMR Data (CDCl₃, ¹H 250.13 MHz, ³¹P 161.9 MHz):



$\delta_{\text{H}}:$	8.31	1H, d, $^3J = 8.0$ Hz, $\text{H}_{\text{b/b'}}$
	8.19	2H, AA'XX', $\text{H}_{\text{c'}}$
	7.75	1H, d, $^3J = 8.4$ Hz, H_{c}
	7.70	1H, t, $^3J = 8.0$ Hz, H_{a}
	7.49	1H, d, $^3J = 8.0$ Hz, $\text{H}_{\text{b/b'}}$
	7.31	1H, d, $^4J = 1.50$, $^3J_{(\text{Pt-H})} = 36.3$ Hz, H_{e}
	6.99	2H, AA'XX', $\text{H}_{\text{d'}}$
	6.61	1H, dd, $^3J = 8.4$, $^4J = 1.5$ Hz, H_{d}
	4.01	2H, t, $^3J = 5.3$ Hz, $\text{H}_{\text{f/f'}}$
	3.95	2H, t, $^3J = 6.7$ Hz, $\text{H}_{\text{f/f'}}$
	1.79	4H, m, H_{g} & $\text{H}_{\text{g'}}$
	1.57	2H, m, $\text{H}_{\text{h/h'}}$
	1.47	2H, m, $\text{H}_{\text{h/h'}}$
	1.35	4H, m, H_{i} & $\text{H}_{\text{i'}}$
	1.25	18H, m, H_{l}
	1.14	8H, m, H_{j} & $\text{H}_{\text{j'}}$
	0.89	6H, m, H_{k} & $\text{H}_{\text{k'}}$

$\delta_{\text{P}}:$ -14.46, s, $^1J_{(\text{Pt-P})} = 2834$ Hz

Elemental analysis: Found (expected) C 51.6 (51.7), H 6.5 (6.7), N 1.7 (1.7).

NMR Data (CDCl_3 , ^{31}P 161.9 MHz) for (31)

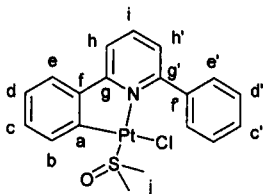
$\delta_{\text{P}}:$	-23.0	1P, d, $^2J_{(\text{P-P})} = 26$, $^1J_{(\text{Pt-P})} = 2759$ Hz, P <i>cis</i> to C
	-33.1	2P, t, $^2J_{(\text{P-P})} = 26$, $^1J_{(\text{Pt-P})} = 1861$ Hz, P <i>trans</i> to C

Section 4.13. Preparation and characterisation of (2,6-diphenylpyridine)Pt(DMSO)Cl, (32).

[2,6-Diphenylpyridine-Pt-Cl]₂ (**19**) (25.0 mg, 0.027 mmol) was dissolved in hot DMSO (1 cm³). The compound was not isolated.

Yield: 100 %

NMR Data (D6-DMSO, 400.03 MHz):



δ_{H} :	8.20	3H, m, H_b , H_h & H_i
	7.96	2H, m, H_e
	7.84	1H, dd, $^3J = 9.0$, $^4J = 1.4$ Hz, H_e
	7.72	1H, dd, $^3J = 6.2$, $^4J = 2.8$ Hz, $H_{h'}$
	7.48	3H, m, $H_{c'}$ & $H_{d'}$
	7.23	1H, dt, $^3J = 9.0$, $^4J = 1.4$ Hz, H_d
	7.14	1H, dt, $^3J = 9.0$, $^4J = 1.4$ Hz, H_c
	3.38*	6H, s, $^3J_{(\text{Pt-H})} = 24.0$ Hz, H_j

(* from a D7-DMF solution.)

Section 4.14. Preparation and characterisation of [2,6-bis-(4-alkoxyphenyl)pyridine]-Pt(DMSO)Cl, (33) and (35).

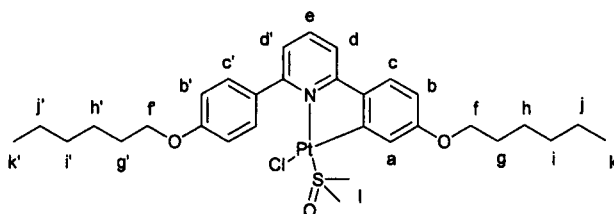
Complexes (**33**) and (**34**) were synthesised using the same techniques. A detailed synthesis of (**33**) is detailed below.

4.14.1: Preparation of 2,6-bis-(4-hexyloxyphenyl)pyridine]-Pt(DMSO)Cl, (**33**).

Complex (**20**) (100 mg, 0.076 mmol) was dissolved in hot dry DMSO (1 cm³). The product was not isolated.

Yield: 100 %.

NMR Data (CDCl₃, 300.13 MHz):



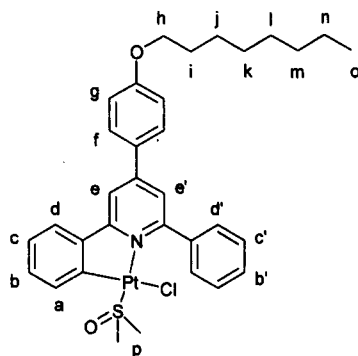
δ_{H} :	7.93	1H, d, $^4J = 2.9$ Hz, H _a
	7.87	2H, AA'XX', H _{c'}
	7.80	1H, t, $^3J = 7.8$ Hz, H _e
	7.55	1H, dd, $^3J = 7.8$, $^4J = 1.4$ Hz, H _{d'}
	7.48	2H, d, $^3J = 7.8$ Hz, H _c
	7.30	1H, dd, $^3J = 7.8$, $^4J = 2.9$ Hz, H _d
	6.95	2H, AA'XX', H _{b'}
	6.75	1H, dd, $^3J = 7.8$, $^4J = 1.4$ Hz, H _b
	4.01	4H, m, H _f & H _{f'}
	3.44	6H, s, $^3J_{(\text{Pt-H})} = 17$ Hz, H _l
	1.78	4H, m, H _g & H _{g'}
	1.40	12H, m, H _{h-j} & H _{h'-j'}
	1.92	6H, m, H _k & H _{k'}

Section 4.15. Preparation and characterisation of [4-(4-octyloxyphenyl)-2,6-diphenylpyridine]-Pt(DMSO)Cl, (35).

Complex (24) (100 mg, 0.075 mmol) was dissolved in hot dry DMSO (1 cm³). Or DMSO (12 mg, 0.15 mmol) was added to a solution of (24) (100 mg, 0.075 mmol) in CDCl₃ (0.5 cm³). The product was not isolated.

Yield: 100 %.

NMR Data (D6-DMSO, 300.13 MHz):



δ_{H} :	8.42	1H, d, $^4J = 2.6$ Hz, H _e
	8.13	6H, m, H _b , H _{c'} , H _d & H _f
	7.90	1H, d, $^4J = 2.6$ Hz, H _{e'}
	7.58*	1H, dd, $^3J = 8.2$, $^4J = 1.5$, $^3J_{(\text{Pt-H})} = 33.7$ Hz, H _a
	7.47	2H, m, H _{d'}
	7.18	4H, m, H _{b'} , H _c & H _g
	4.07	2H, t, $^3J = 7.5$ Hz, H _h
	3.44	6H, s, $^3J_{(\text{Pt-H})} = 23.0$ Hz, H _p
	1.75	2H, m, H _i
	1.37	10H, m, H _{j-n}
	0.86	3H, t, $^3J = 7.5$ Hz, H _o

(* from CDCl₃)

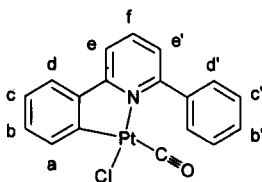
Section 4.16. Preparation and characterisation of (2,6-diphenylpyridine)Pt(CO)Cl, (36) and (38).

4.16.1: Complex (36).

Carbon monoxide gas was bubbled through a solution of the (2,6-diphenylpyridine-Pt-Cl)₂ (**19**) (25 mg, 0.027 mmol) in DMF (1 cm³). An instantaneous colour change from yellow to colourless was observed. The compound was not isolated.

Yield: 100 %.

NMR Data (D7-DMF, 400.03 MHz):



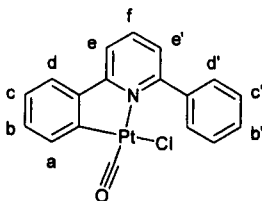
δ_{H} :	8.38	1H, t, $^3J = 7.4$ Hz, H_f
	8.33	1H, dd, $^3J = 7.4$, $^4J = 2.0$ Hz, $H_{e/e'}$
	8.02	1H, dd, $^3J = 8.2$, $^4J = 1.3$ Hz, H_a
	7.96	1H, dd, $^3J = 8.2$, $^4J = 1.3$ Hz, H_d
	7.85	2H, m, $H_{d'}$
	7.72	4H, m, $H_{e/e'}$, $H_{b'}$ & $H_{c'}$
	7.38	1H, dt, $^3J = 8.2$, $^4J = 1.3$ Hz, H_b
	7.32	1H, dt, $^3J = 8.2$, $^4J = 1.3$ Hz, H_c

FT-IR: $\nu_{(\text{C}=\text{O})}$ 2087 cm⁻¹ (DMF).

4.16.2: Complex (38).

Carbon monoxide gas was bubbled through a solution of (2,6-diphy)PtCl (DMSO) (25 mg, 0.046 mmol) in DMSO (0.5 cm³). The compound was not isolated.

NMR Data (D6-DMSO, 400.03 MHz):



δ_{H} :	8.20	3H, m, H _f , H _e & H _a
	7.95	2H, m, H _{d'}
	7.84	1H, dd, $^3J = 9.0$, $^4J = 1.4$ Hz, H _d
	7.72	1H, dd, $^3J = 6.2$, $^4J = 2.8$ Hz, H _{e'}
	7.48	3H, m, H _{b'} & H _{c'}
	7.22	1H, dt, $^3J = 9.0$, $^4J = 1.4$ Hz, H _c
	7.14	1H, dt, $^3J = 9.0$, $^4J = 1.4$ Hz, H _b

MALDI TOF MS (in DMSO): m/z 898 (M^+).

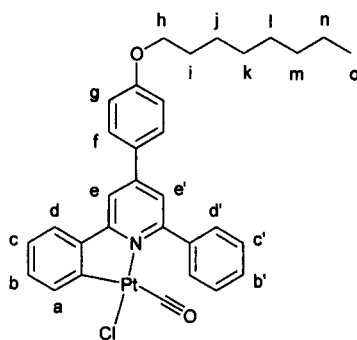
FT-IR: $\nu(\text{C}\equiv\text{O})$ 2098 cm⁻¹ (DMSO).

Section 4.17. Preparation and characterisation of [4-(4-Octyloxy-phenyl)-2,6-diphy]Pt(Cl)(CO), (37) and (39).

4.17.1: Complex (37).

Carbon monoxide gas was bubbled through a solution of complex (24) (39.0 mg, 2.93×10^{-2} mol) in chloroform (0.5 cm³). The compound was not isolated.

NMR Data (CDCl₃, 400.03 MHz):



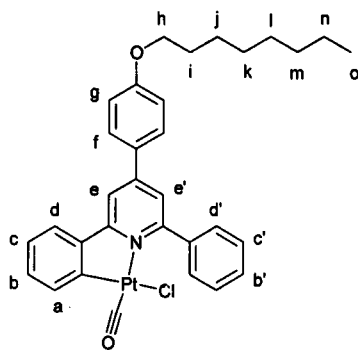
δ_{H} :	8.06	1H, dd, $^3J = 7.6$, $^4J = 1.2$, $^3J_{(\text{Pt-H})} = 34$ Hz, H_a
	7.92	1H, d, $^4J = 2.0$ Hz, $\text{H}_{e/e'}$
	7.72	2H, AA'XX', H_f
	7.68	2H, m, $\text{H}_{d'}$
	7.60	1H, dd, $^3J = 7.6$, $^4J = 1.4$ Hz, H_d
	7.55	3H, m, $\text{H}_{c'}$ & $\text{H}_{b'}$
	7.48	1H, d, $^4J = 2.0$ Hz, $\text{H}_{e/e'}$
	7.26	1H, dt, $^3J = 7.6$, $^4J = 1.4$ Hz, H_b
	7.19	1H, dt, $^3J = 9.0$, $^4J = 1.4$ Hz, H_c
	7.03	2H, AA'XX', H_g
	4.01	2H, t, $^3J = 6.4$ Hz, H_h
	1.80	2H, m, H_i
	1.51	10H, m, H_{j-n}
	0.91	3H, t, $^3J = 7.0$ Hz, H_o

FT-IR: $\nu_{(\text{C}=\text{O})}$ 2097 cm^{-1} (CDCl_3).

4.17.2: Complex (39).

Carbon monoxide gas was bubbled through a solution of [4-(4-octyloxy-phenyl)-2,6-diphenyl]Pt(DMSO)Cl (0.15 mmol) in chloroform (0.5 cm³). The compound was not isolated.

NMR Data (CDCl₃, 400.03 MHz):



δ_{H} :	7.97	1H, d, $^4J = 2.4$ Hz, $H_{e/e'}$
	7.78	2H, m, $H_{d'}$
	7.75	1H, dd, $^3J = 8.0$, $^4J = 1.4$, H_a
	7.74	2H, AA'XX', H_f
	7.60	1H, d, $^4J = 2.4$ Hz, $H_{e/e'}$
	7.56	1H, dd, $^3J = 8.0$, $^4J = 1.4$ Hz, H_d
	7.53	3H, m, $H_{c'}$ & $H_{b'}$
	7.28	1H, dt, $^3J = 8.0$, $^4J = 1.4$ Hz, H_b
	7.17	1H, dt, $^3J = 8.0$, $^4J = 1.4$ Hz, H_c
	7.06	2H, AA'XX', H_g
	4.04	2H, t, $^3J = 6.4$ Hz, H_h
	1.80	2H, m, H_i
	1.51	10H, m, H_{j-n}
	0.91	3H, t, $^3J = 7.0$ Hz, H_o

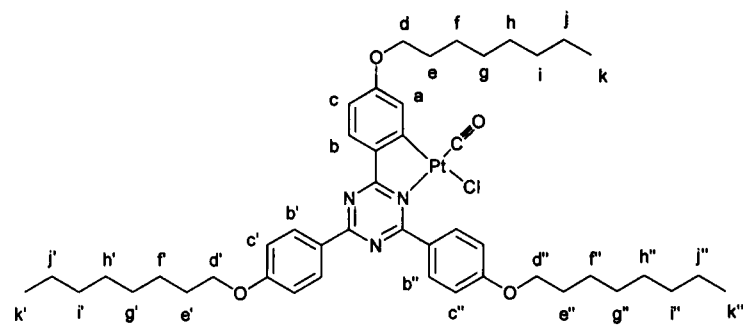
FT-IR: $\nu_{(\text{C}\equiv\text{O})}$ 2103 cm^{-1} (CDCl_3).

Section 4.18. Preparation and characterisation of {2,4,6-tris-(4-alkoxyphenyl)-[1,3,5]triazine}Pt-(CO)Cl.

Carbon monoxide gas was bubbled through a solution of complex (45) (51.2 mg, 2.77×10^{-2} mmol) in chloroform (0.5 cm^3) until the yellow solution went pale (10 seconds). The solvent was removed to yield a pale yellow product.

Yield: 52.7 mg (5.54×10^{-2} mmol). 100 %.

NMR Data (CDCl_3 , 300.16 MHz):



$\delta_{\text{H}}:$	8.63	2H, AA'XX', $\text{H}_{\text{b'}}$
	8.25	1H, d, $^3\text{J} = 8.4$ Hz, H_{c}
	8.08	2H, AA'XX', $\text{H}_{\text{b''}}$
	7.27	2H, AA'XX', $\text{H}_{\text{c''}}$
	7.17	1H, d, $^4\text{J} = 2.4$ Hz, H_{a}
	7.04	2H, AA'XX', $\text{H}_{\text{c'}}$
	6.94	1H, dd, $^3\text{J} = 8.4$, $^4\text{J} = 2.4$ Hz, H_{b}
	4.10	6H, m, H_{d} , $\text{H}_{\text{d'}}$ & $\text{H}_{\text{d''}}$
	1.83	6H, m, H_{e} , $\text{H}_{\text{e'}}$ & $\text{H}_{\text{e''}}$
	1.41	30H, m, $\text{H}_{\text{f,j}}$, $\text{H}_{\text{f',j'}}$ & $\text{H}_{\text{f'',j''}}$
	0.92	9H, m, H_{k} , $\text{H}_{\text{k'}}$ & $\text{H}_{\text{k''}}$

FT-IR: $\nu_{(\text{C}\equiv\text{O})}$ 2104 cm^{-1} (CDCl_3).

Section 4.19. Preparation and characterisation of $\text{C}^{\wedge}\text{N}^{\wedge}\text{C}$ [2,6-bis(4-alkoxyphenyl)pyridine]Pt-CO, (40) and (41).

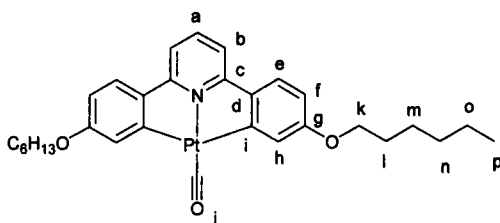
Complexes (40) and (41) were synthesised following the same procedure. A detailed synthetic route to the formation of (40) is detailed below.

4.19.1: Preparation of $\text{C}^{\wedge}\text{N}^{\wedge}\text{C}$ [2,6-bis(4-hexyloxyphenyl)pyridine]Pt-CO, (40).

2,6-Bis(4-dihexyloxyphenyl)pyridine (103.9 mg, 0.241 mmol) was added to a solution of potassium tetrachloroplatinate (100.0 mg, 0.241 mmol) in acetic acid (400 cm^3). The mixture was stirred (120 $^{\circ}\text{C}$, 120 h). The solvent was removed and the product washed with water (10 cm^3). The product was dissolved in chloroform (5 cm^3), filtered, washed with hexane (10 cm^3) and recrystallised from ethyl acetate.

Yield: 78.5 mg (0.123 mmol), 51 %.

NMR Data (CDCl_3 , 250.13 MHz):



δ_{H} :	7.50	1H, t, $^3J = 8.0$ Hz, H_a
	7.35	2H, d, $^3J = 8.8$ Hz, H_e
	7.19	2H, d, $^4J = 2.5$ Hz, $^3J_{(\text{Pt-H})} = 36$ Hz, H_h
	6.99	2H, d, $^3J = 8.0$ Hz, H_b
	6.59	2H, dd, $^3J = 8.8$ Hz, $^4J = 2.5$ Hz, H_f
	3.99	4H, t, $^3J = 6.7$ Hz, H_k
	1.84	4H, q, $^3J = 6.7$ Hz, H_l

1.38 4H, m, H_m

1.41 8H, m, H_n & H_o

0.98 6H, t, ³J = 7.0 Hz, H_p

δ_C: 207.0 (C_j) 167.9 (C_g) 162.0 (C_a) 141.6 (C_{c/d}) 141.4 (C_{c/d})
 125.9 (C_i) 124.8 (C_e) 113.7 (C_b) 110.8 (C_f) 77.2 (C_h)
 67.8 (C_k) 30.9 (C_l) 29.4 (C_m) 26.0 (C_n) 22.6 (C_o)
 14.1 (C_p)

IR Data: ν_(C=O) 2042 cm⁻¹ (KBr)

X-ray crystal data in *Appendix* .

Elemental analysis:

C[^]N[^]C [2,6-bis(4-hexyloxyphenyl)pyridine]Pt-CO, (40).

Found (expected) C 55.5 (55.2), H 5.4 (5.4), N 2.1 (2.2).

C[^]N[^]C [2,6-bis(4-octyloxyphenyl)pyridine]Pt-CO, (41).

Found (expected) C 57.5 (57.6), H 6.1 (6.1), N 2.0 (2.0).

Section 4.20. Preparation and characterisation of C[^]N[^]C [2,6-bis(4-alkoxyphenyl)pyridine]Pt-DMSO, (42) and (43).

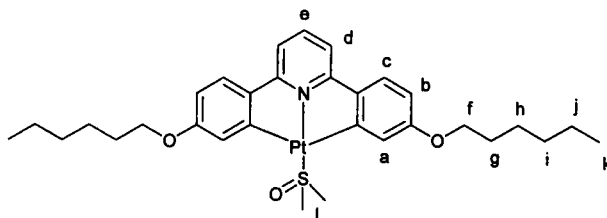
Complexes (42) and (43) were synthesised following the same procedure. A detailed synthetic route to the formation of (42) is detailed below.

4.20.1: Preparation of C[^]N[^]C [2,6-bis(4-hexyloxyphenyl)pyridine]Pt-DMSO, (42).

Distilled water (0.2 cm³) was added to a solution of (33) in D6-DMSO (1 cm³). The solution was warmed (50 °C, 10 min.). The product was not isolated.

Yield: 100 %.

NMR Data (CDCl₃, 400.03 MHz):



δ_{H} :	7.50	1H, t, $^3J = 7.8$ Hz, H_e
	7.41	2H, d, $^3J = 8.9$ Hz, H_c
	7.39	2H, d, $^4J = 2.3$ Hz, H_a
	7.08	2H, d, $^3J = 7.8$ Hz, H_d
	6.62	2H, dd, $^3J = 8.9$, $4J = 2.4$ Hz, H_b
	4.50	4H, t, $^3J = 7.0$ Hz, H_f
	3.69	6H, s, $^3J_{(\text{Pt-H})} = 26$ Hz, H_i
	1.78	4H, m, H_g
	1.40	12H, m, H_{h-j}
	0.90	6H, t, $^3J = 7.2$ Hz, H_k

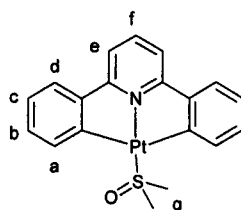
Section 4.21. Preparation and characterisation of C[^]N[^]C [2,6-diphenylpyridine]Pt-DMSO, (44).

(2,6-Diphenylpyridine-Pt-Cl)₂ (**19**) (407 mg, 0.441 mmol) was dissolved in hot DMSO (1 cm³), allowed to cool, precipitated with water (1 cm³) and heated to reflux (10 min). The solution was allowed to cool to room temperature to give a yellow crystalline product, which was isolated by filtration.

Yield: 443 mg (98 %, 0.882 mmol).

Mp. (°C): 143

NMR Data (CDCl₃, 400.03 MHz):



δ_{H} : 7.80 2H, dd, $^3J = 7.6$, $^4J = 1.2$, $^3J_{(\text{Pt-H})} = 24$ Hz, H_a

7.62 1H, t, $^3J = 7.3$ Hz, H_f

7.47 2H, dd, $^3J = 7.6$, $^4J = 1.2$ Hz, H_d

7.30 2H, d, $^3J = 7.3$ Hz, H_e

7.28 2H, dt, $^3J = 7.6$, $^4J = 1.2$ Hz, H_b

7.21 2H, dt, $^3J = 7.6$, $^4J = 1.2$ Hz, H_c

3.68 6H, t, $^3J_{(\text{Pt-H})} = 26.8$ Hz, H_g

Elemental analysis: Found (expected) C 45.0 (45.4), H 3.4 (3.4), N 2.8 (2.8).

X-ray crystal data in *Appendix* .

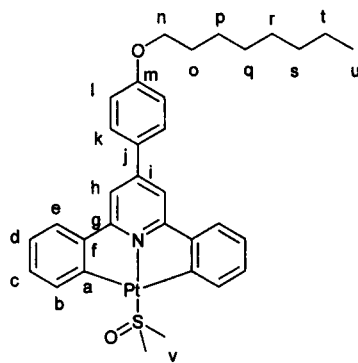
Section 4.22. Preparation and characterisation of C^NC [4-(4-octyloxyphenyl)-2,6-diphenylpyridine]Pt-DMSO, (45).

Water (1 cm³) was added to a stirred solution of the complex (24) (100 mg, 0.075 mmol), dissolved in DMSO (1 cm³). The solution was heated (100 °C, 10 min), allowed to cool to room temperature and filtered. The residue was washed with cold acetone (5 cm³) and dried under *vacuo*, to give a yellow powder.

Yield: 101.6 mg (0.148 mmol), 99 %.

Mp. (°C): K $\xrightarrow{117}$ P1 \cdot $\xrightarrow{126}$ P2 \cdot $\xrightarrow{135}$ P3 \cdot $\xrightarrow{160}$ P4 \cdot $\xrightarrow{185}$ I

(* Phases 1 to 4 were not identified, but are believed to be smectic in nature.)

NMR Data (CDCl₃, 300.13 MHz):
 $\delta_{\text{H}}:$ 7.84 2H, dd, $^3J = 7.8$, $^4J = 1.7$, $^3J_{(\text{Pt-H})} = 34.8$ Hz, H_b
7.68 2H, AA'XX', H_k7.58 2H, dd, $^3J = 7.8$, $^4J = 1.7$ Hz, H_e7.48 2H, s, H_h7.31 2H, dt, $^3J = 7.8$, $^4J = 1.7$ Hz, H_c7.15 2H, dt, $^3J = 7.8$, $^4J = 1.7$ Hz, H_d7.05 2H, AA'XX', H_l4.05 2H, t, $^3J = 7.5$ Hz, H_n3.61 6H, s, $^3J_{(\text{Pt-H})} = 26.3$ Hz, H_v1.84 2H, m, H_o1.32 10H, m, H_{p-t}0.89 3H, t, $^3J = 7.2$ Hz, H_u
 $\delta_{\text{C}}:$ 165.6 (C_g) 165.1 (C_m) 159.9 (C_a) 152.1 (C_i) 148.8 (C_f)
135.2 $^2J_{(\text{Pt-C})} = 0.6$ Hz (C_b) 129.6 $^3J_{(\text{Pt-C})} = 0.4$ Hz (C_c) 128.6 (C_j)127.4 (C_k) 123.8 (C_d) 123.3 (C_e) 114.0 (C_l) 111.6 (C_h)67.2 (C_n) 47.3 $^2J_{(\text{Pt-C})} = 1.0$ Hz (C_v) 30.8 (C_s) 28.6 (C_o)28.3 (C_q) 28.2 (C_r) 25.0 (C_p) 21.6 (C_t) 13.1 (C_u)

Elemental analysis: Found (expected) C 56.3 (56.1), H 5.5 (5.3), N 2.3 (2.0).

Section 4.23. Preparation and characterisation of C^NC [2,6-diphenylpyridine]Pt-CO, (46).

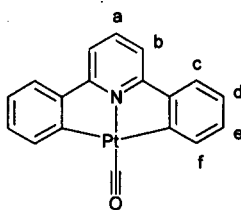
Carbon monoxide was bubbled through a solution of 2,6-diphenylpyridine-Pt-DMSO (50 mg, 0.054 mmol) in chloroform (1 cm³), until the product formed as a red precipitate.

The solution was filtered and the product was recrystallised from chloroform.

Yield: 48.9 mg (0.108 mmol), 100%.

Mp. (°C): 210

NMR Data (CDCl₃, 300.13 MHz):



δ_{H} : 7.57 2H, dd, $^3J = 7.0$, $^4J = 0.8$, $^3J_{(\text{Pt-H})} = 27.1$ Hz, H_f

7.52 1H, t, $^3J = 7.2$ Hz, H_a

7.36 2H, dd, $^3J = 7.0$, $^4J = 0.8$ Hz, H_c

7.14 6H, m, H_b, H_d & H_e

(D6-DMSO, 400.03 MHz):

δ_{H} : 7.89 1H, t, $^3J = 7.8$ Hz, H_a

7.68 2H, dd, $^3J = 7.6$, $^4J = 1.1$ Hz, H_c

7.65 2H, d, $^3J = 7.8$ Hz, H_b

7.52 2H, dd, $^3J = 7.3$, $^4J = 1.1$, $^3J_{(\text{Pt-H})} = 33.1$ Hz, H_f

7.22 2H, dd, $^3J = 7.3$, $^4J = 1.2$ Hz, H_e

7.16 2H, dd, $^3J = 7.3$, $^4J = 1.2$ Hz, H_d

(D7-DMF, 400.03 MHz):

δ_{H} : 7.99 1H, t, $^3J = 7.8$ Hz, H_a
 7.75 2H, dd, $^3J = 7.6$, $^4J = 1.1$ Hz, H_c
 7.74 2H, d, $^3J = 7.8$ Hz, H_b
 7.61 2H, dd, $^3J = 7.3$, $^4J = 1.1$, $^3J_{(\text{Pt-H})} = 33.1$ Hz, H_f
 7.28 2H, dd, $^3J = 7.3$, $^4J = 1.2$ Hz, H_e
 7.20 2H, dd, $^3J = 7.3$, $^4J = 1.2$ Hz, H_d

FAB MS (in NBA): m/z 452 (M^+).

FT-IR: $\nu_{(\text{C}=\text{O})}$ 2044 cm^{-1} (KBr), 2055 cm^{-1} (DMF), 2056 cm^{-1} (DMSO).

Elemental analysis: Found (expected) C, 47.5 (47.8); H, 2.5 (2.5); N, 3.3 (3.1).

X-ray crystal data in *Appendix* .

Section 4.24. Preparation and characterisation of $\text{C}^{\wedge}\text{N}^{\wedge}\text{C}$ [4-(4-octyloxyphenyl)-2,6-diphenylpyridine]Pt-CO, (47).

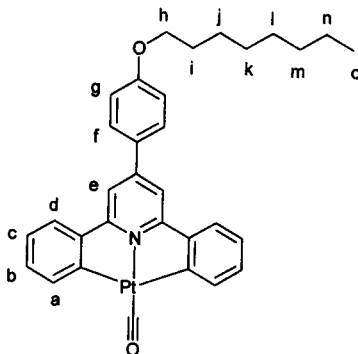
A solution of complex (45) (50 mg, 0.038 mmol) was stirred under a carbon monoxide atmosphere, resulting in an instant colour change from yellow to pale yellow and the formation of a red precipitate. The precipitate was collected and washed with cold acetone (5 cm^3).

Yield: 49.3 mg (0.075 mmol), 100 %.

Mp. ($^{\circ}\text{C}$): $\text{K} \xrightarrow{74} \text{P5}^{\bullet} \xrightarrow{135} \text{P6}^{\bullet} \xrightarrow{199} \text{P7}^{\bullet} \xrightarrow{203} \text{I}$

(* Phases 5 to 6 were not identified but thought to be smectic in nature.)

NMR Data (CDCl₃, 300.13 MHz):



δ_{H} :	7.57	2H, AA'XX', H _f
	7.50	2H, m, H _a
	7.39	2H, dd, $^3J = 7.5$, $^4J = 1.5$ Hz, H _d
	7.23	2H, s, H _e
	7.14	2H, dt, $^3J = 7.5$, $^4J = 1.5$ Hz, H _b
	7.06	2H, dt, $^3J = 7.5$, $^4J = 1.5$ Hz, H _c
	6.99	2H, AA'XX', H _g
	4.01	2H, t, $^3J = 7.0$ Hz, H _h
	1.82	2H, m, H _i
	1.34	10H, m, H _{j-n}
	0.86	3H, t, $^3J = 7.2$ Hz, H _o

Elemental analysis: Found (expected) C 57.9 (58.5), H 4.4 (4.8), N 2.6 (2.1).

X-ray crystal data in *Appendix* .

Section 4.25. Preparation and characterisation of C[^]N[^]C [2,6-diphenylpyridine]Pt-PMe₃, (49).

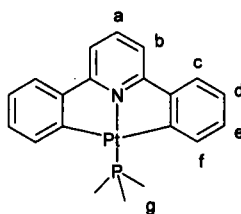
Trimethylphosphine (9 mg, 0.12 mmol) was added to a solution of [(2,6-diphy)Pt(DMSO)] (56 mg, 0.108 mmol) in chloroform (1 cm³) under an inert atmosphere.

All solvents were removed in *vacuo* to give a pale yellow product.

Yield: 54 mg (99 %, 0.107 mmol).

Mp. (°C): 130

NMR Data (CDCl₃, ¹H 250.13; ³¹P 161.9 MHz):



δ_{H} :	8.38	1H, t, $^3J = 8.5$ Hz, H _a
	8.11	2H, d, $^3J = 8.5$ Hz, H _b
	7.93	2H, dd, $^3J = 7.6$, $^4J = 1.2$ Hz, H _c
	7.80	2H, dd, $^3J = 7.6$, $^4J = 1.2$, $^3J_{(\text{Pt-H})} = 16$ Hz, H _f
	7.41	2H, td, $^3J = 7.6$, $^4J = 1.2$ Hz, H _d
	7.34	2H, td, $^3J = 7.6$, $^4J = 1.2$ Hz, H _e
	3.68	6H, d, $^2J_{(\text{P-H})} = 1.8$, $^3J_{(\text{Pt-H})} = 64.5$ Hz, H _g

δ_{P} : -20.98, s, $^1J_{(\text{Pt-P})} = 1606$ Hz

Elemental analysis: Found (expected) C 48.2 (48.0), H 4.0 (4.0), N 3.0 (2.8).

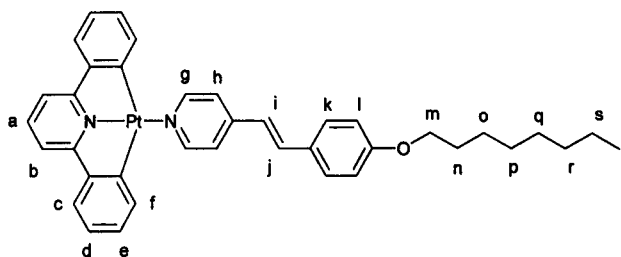
Section 4.26: Preparation and characterisation of C^NC [2,6-diphenylpyridine]Pt-(4-octyloxystilbazole), (51).

4-Octyloxystilbazole (33.0 mg, 0.119 mmol) was added to a solution of [(2,6-diphenyl)Pt(DMSO)] (56.0 mg, 0.108 mmol) in chloroform (1 cm³). The mixture was stirred (50 °C, 30 min), solvents were removed in *vacuo* and the residue washed with diethyl ether (1 cm³), to give a yellow product. Care was taken to eliminate light from the product, in order to prevent the photochemical isomerisation of the alkene bond.

Yield: 76 mg (0.108 mmol), 99 %.

Mp. (°C): 77.8

NMR Data (CDCl₃, 400.03 MHz):



¹H: 8.92 2H, AA'XX', ³J_(Pt-H) = 43.5 Hz, H_g

7.53 2H, AA'XX', H_k

7.51 1H, t, ³J = 8.0 Hz, H_a

7.46 2H, m, H_f

7.44 2H, AA'XX', H_h

7.41 1H, d, ³J = 16.6 Hz, H_i

7.23 2H, d, ³J = 8.0 Hz, H_b

7.20 2H, dt, ³J = 7.5, ⁴J = 1.3 Hz, H_d

7.05 2H, dt, ³J = 7.5, ⁴J = 1.3 Hz, H_e

7.00 2H, dd, ³J = 7.5, ⁴J = 1.3 Hz, H_c

6.93 2H, AA'XX', H_l

6.91 1H, d, $^3J = 16.6$ Hz, H_j

3.99 2H, t, $^3J = 6.5$ Hz, H_m

1.80 2H, m, H_n

1.46 2H, m, H_o

1.31 8H, m, H_{p-s}

0.89 3H, t, $^3J = 6.5$ Hz, H_t

Elemental analysis: Found (expected) C 61.0 (61.3), H 4.8 (4.9), N 4.0 (4.0).

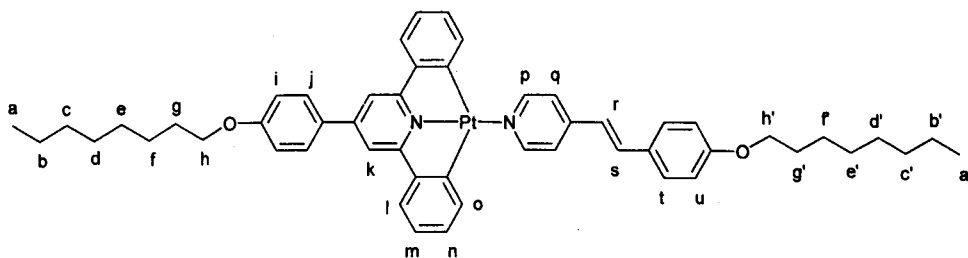
Section 4.27. Preparation and characterisation of C[^]N[^]C [4-(4-octyloxyphenyl)-2,6-diphenylpyridine]Pt-(4-octaloxystilbazole), (52).

A solution of 4-octaloxystilbazole (21.9 mg, 0.07 mmol) and complex (45) (50.0 mg, 0.07 mmol) in chloroform (1 cm³) was heated (40 °C, 20 min). Care was taken to avoid the photochemical isomerisation of the alkene bond, by elimination light from the reaction vessel. The solvent was removed and the yellow product washed with water (1 cm³) and cold acetone (2 cm³).

Yield: 63.9 mg (0.068 mmol), 97 %.

Mp. (°C): K $\xrightarrow{198}$ N $\xrightarrow{230}$ I

NMR Data (CDCl₃, 300.03 MHz):



δ_{H} : 8.94 2H, AA'XX', $^3J_{(\text{Pt-H})} = 48.0$ Hz, H_p

7.66 2H, AA'XX', H_j

- 7.54 3H, m, H_o & H_s
 7.42 6H, m, H_k, H_q & H_u
 7.21 2H, dt, ³J = 7.5, ⁴J = 1.2 Hz, H_m
 7.05 6H, m, H_i, H_l & H_n
 6.93 2H, AA'XX', H_t
 6.40 1H, d, ³J = 16.3 Hz, H_r
 3.99 4H, m, H_h & H_{h'}
 1.80 4H, m, H_g & H_{g'}
 1.39 20H, m, H_{b-f} & H_{b'-f'}
 0.89 6H, m, H_a & H_{a'}

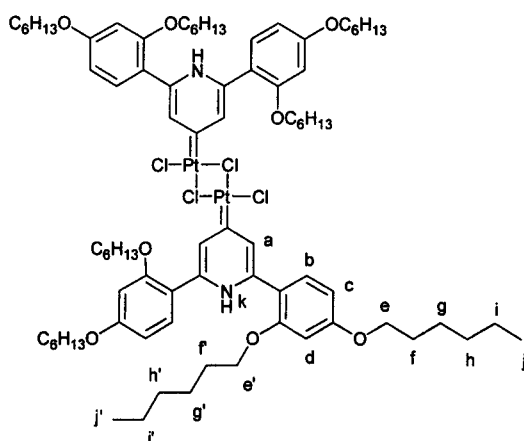
Elemental analysis: Found (expected) C 66.1 (66.6), H 6.7 (6.2), N 3.0 (3.0).

Section 4.28. Preparation and characterisation of [{2,6-bis(2,4-dihexyloxyphenyl)pyridine}PtCl₂]₂ carbene, (53).

2,6-Bis(2,4-dihexyloxyphenyl)pyridine (152.3 mg, 0.367 mmol) was added to a solution of potassium tetrachloroplatinate (231.8 mg, 0.367 mmol) in acetic acid (400 cm³). The mixture was stirred (70 °C, 72 h). The solvent was removed and the product washed with water (5 cm³). The product was dissolved in chloroform (5 cm³), filtered, washed with hexane (10 cm³) and recrystallised from acetone.

Yield: 220.9 mg (0.132 mmol), 36 %.

NMR Data (CDCl₃, 400.26 MHz):



δ_{H} :	12.77	2H, t, $^4J = 2.1$ Hz, H _k
	8.03	4H, d, $^4J = 2.1$ Hz, H _a
	7.78	4H, d, $^3J = 8.9$ Hz, H _b
	6.64	4H, dd, $^3J = 8.9$, $^4J = 2.4$ Hz, H _c
	6.52	4H, d, $^4J = 2.4$ Hz, H _d
	4.00	8H, t, $^3J = 6.4$ Hz, H _e
	3.99	8H, t, $^3J = 5.8$ Hz, H _{e'}
	1.80	8H, m, H _f
	1.58	8H, m, H _f
	1.44	8H, m, H _g
	1.34	24H, m, H _h , H _i & H _{g'}
	1.15	8H, m, H _{h'}
	0.95	20H, m, H _j & H _{j'}
	0.69	12H, m, H _{j'}

δ_{C} : 324.3 C attached to Pt.

X-ray crystal data in *Appendix* .

Appendix 1.

The X-ray crystallographic structure determinations were carried out by Dr E Errington and Dr N W Alcock at the University of Warwick. All crystals were mounted with oil onto a thin glass fibre. Data were collected at 180(2) K using a Siemens SMART CCD area-detector diffractometer, operating with Mo-*K* graphite monochromatised radiation ($\lambda = 0.71073 \text{ \AA}$). Refinement was by full matrix least-squares on F^2 for all data using SHELXL-96¹ with additional light atoms found by Fourier methods. Hydrogen atoms were added at calculated positions and refined using a riding model with freely rotating methyl groups. Anisotropic displacement parameters were used for all non-H atoms; H-atoms were given isotropic displacement parameters equal to 1.2 (or 1.5 for methyl hydrogen atoms) times the equivalent isotropic displacement parameter of the atom to which the H-atom is attached.

X-ray crystal structure data for crystals contained within this report:

- i) 2,6-bis-(2,4-dihexyloxyphenyl)pyridine, **(5d)**.
- ii) $[\text{C}^{\wedge}\text{N} \{4\text{-(4'-Octyloxyphenyl)-2,6-diphenylpyridine}\} \text{platinum(II)-chloride}]_2$, **(24)**.
- iii) $\{\text{N}^{\wedge}\text{C} (2\text{-Phenylpyridine})\} \text{platinum(II)} \{\text{N} (2\text{-phenylpyridine}) \text{chloride}\}$, **(28)**.
- iv) $\text{bis}\{\text{N}^{\wedge}\text{C} (2\text{-Phenylpyridine})\} \text{platinum(IV)dichloride}$, **(29)**.

¹ G M Sheldrick, SHELXL-96, Program for Crystal Structure Refinement; University of Göttingen, Göttingen, Germany, 1996.

- v) {C[^]N[^]C [2,6-bis(4'-Hexyloxyphenyl)pyridine]}platinum(II)-{C (carbon monoxide)}, **(40)**.
- vi) {C[^]N[^]C [2,6-bis(phenyl)pyridine]}platinum(II)-{S(dimethylsulfoxide)}, **(44)**.
- vii) {C[^]N[^]C [2,6-bis(phenyl)pyridine]}platinum(II)-{C (carbon monoxide)}, **(46)**.
- viii) {C[^]N[^]C [4-(4'-Octyloxyphenyl)-2,6-diphenylpyridine]}-platinum(II)- {C (carbon monoxide)}, **(47)**.
- ix) 2,6-bis(2,4-Dihexyloxyphenyl)pyridine platinum carbene, **(53)**.

Tables of positional parameter, bond distances, bond angles, and anisotropic parameters for the structural analysis of **(44)** are available *via* the internet at <http://pubs.acs.org> (Organometallics 1999, pages 1801-1803).

Crystallographic data (excluding structure factors) for **(53)** have been deposited with the Cambridge Crystallographic Data Centre as supplementary publication no. CCDC-101757.

X-Ray crystallographic details for (5d).

Table 1: Crystal data and structure refinement for (5d).

Empirical formula	C ₄₁ H ₆₁ NO ₄ ,
Formula weight	631.91,
Colour	Colourless blocks
Temperature	180(2) K
Wavelength	0.71073 Å
Crystal system	Monoclinic
Space group	P2/n
Unit cell dimensions	a = 11.2502(10) Å, alpha = 90 ° b = 6.9682(6) Å, beta = 93.963(2) ° c = 24.014(2) Å, gamma = 90 °
Volume, Z	1878.0(3) Å ³ , 2
Density (calculated)	1.117 Mg/m ³
Absorption coefficient	0.070 mm ⁻¹
F(000)	692
Crystal size	0.45 x 0.25 x 0.2 mm
Theta range for data collection	1.70 to 25.00 °
Limiting indices	-14 h 15, -9 k 9, -19 l 31
Reflections collected	8996
Independent reflections	3318 [R(int) = 0.0453]
Refinement method	Full-matrix least-squares on F ²
Data / restraints / parameters	3318 / 0 / 229
Goodness-of-fit on F ²	1.013
Final R indices[I > 2σ(I)]	R1 = 0.0571, wR2 = 0.1635.
R indices (all data)	R1 = 0.1268, wR2 = 0.1635
Largest diff. Peak and hole	0.211 and -0.183 eÅ ⁻³

Table 2: Bond lengths (Å) for (**5d**).

O(1)-C(01)	1.370(3)	C(010)-C(009)	1.377(3)
O(1)-C(11)	1.435(3)	C(11)-C(12)	1.510(3)
O(2)-C(03)	1.364(3)	C(12)-C(13)	1.520(3)
O(2)-C(21)	1.431(3)	C(13)-C(14)	1.517(3)
C(01)-C(06)	1.386(3)	C(14)-C(15)	1.508(3)
C(01)-C(02)	1.390(3)	C(15)-C(16)	1.518(3)
C(02)-C(03)	1.385(3)	C(21)-C(22)	1.518(4)
C(03)-C(04)	1.408(3)	C(22)-C(23)	1.457(5)
C(04)-C(05)	1.382(3)	C(23)-C24B	1.489(8)
C(04)-C(07)	1.489(3)	C(23)-C24A	1.769(12)
C(05)-C(06)	1.389(3)	C24A-C25A	1.45(2)
C(07)-N(08)	1.349(3)	C25A-C(26)	1.41(2)
C(07)-C(009)	1.392(3)	C24B-C25B	1.49(2)
N(08)-C(07)	1.349(3)	C25B-C(26)	1.603(10)
C(009)-C(010)	1.377(3)		

Table 3: Bond angles (°) for (**5d**).

C(01)-O(1)-C(11)	117.5(2)	C(07) -N(08)-C(07)	118.7(3)
C(03)-O(2)-C(21)	120.7(2)	C(010)-C(009)-C(07)	119.5(3)
O(1)-C(01)-C(06)	124.6(2)	C(009)-C(010)-C(009)	119.0(3)
O(1)-C(01)-C(02)	115.3(2)	O(1)-C(11)-C(12)	107.7(2)
C(06)-C(01)-C(02)	120.1(2)	C(11)-C(12)-C(13)	112.2(2)
C(03)-C(02)-C(01)	120.6(2)	C(14)-C(13)-C(12)	112.9(2)
O(2)-C(03)-C(02)	123.2(2)	C(15)-C(14)-C(13)	113.9(2)
O(2)-C(03)-C(04)	116.3(2)	C(14)-C(15)-C(16)	113.9(2)
C(02)-C(03)-C(04)	120.5(2)	O(2)-C(21)-C(22)	105.4(2)
C(05)-C(04)-C(03)	117.2(2)	C(23)-C(22)-C(21)	114.2(4)
C(05)-C(04)-C(07)	119.5(2)	C(22)-C(23)-C24B	127.2(6)
C(03)-C(04)-C(07)	123.3(2)	C(22)-C(23)-C24A	94.1(6)
C(04)-C(05)-C(06)	123.3(2)	C25A-C24A-C(23)	103.6(11)

C(01)-C(06)-C(05)	118.3(2)	C(26)-C25A-C24A	113.0(14)
N(08)-C(07)-C(009)	121.7(2)	C25B-C24B-C(23)	110.4(8)
N(08)-C(07)-C(04)	115.2(2)	C24B-C25B-C(26)	109.0(7)
C(009)-C(07)-C(04)	123.1(2)		

X-Ray crystallographic details for (24).

Table 1: Crystal data and structure refinement for (24).

Empirical formula	$C_{62}H_{64}Cl_2N_2O_2Pt_2$
Formula weight	1330.23
Colour	
Temperature	200(2) K
Wavelength	0.71073 Å
Crystal system	Orthorhombic
Space group	P2(1)2(1)2
Unit cell dimensions	$a = 20.8902(15)$ Å, $\alpha = 90^\circ$ $b = 34.532(2)$ Å, $\beta = 90^\circ$ $c = 7.5473(6)$ Å, $\gamma = 90^\circ$
Volume, Z	$5444.5(7)$ Å ³ , 4
Density (calculated)	1.623 Mg/m ³
Absorption coefficient	5.276 mm ⁻¹
F(000)	2624
Crystal size	0.26 x 0.04 x 0.04 mm ³
Theta range for data collection	1.53 to 23.00°
Limiting indices	-19 h 22, -37 k 37, -8 l 7
Reflections collected	23017
Independent reflections	7562 [R(int) = 0.1467]
Refinement method	Full-matrix least-squares on F ²
Data / restraints / parameters	7562 / 8 / 532
Goodness-of-fit on F ²	1.004
Final R indices[I>2σ(I)]	R1 = 0.0823, wR2 = 0.1714
R indices (all data)	R1 = 0.1432, wR2 = 0.2016
Largest diff. Peak and hole	2.768 and -2.620 e.Å ⁻³

Table 2: Bond lengths (Å) for (24).

Pt(1)-C(1)	1.98(3)	C(14)-C(15)	1.45(4)
Pt(1)-N(1)	2.078(18)	C(15)-C(16)	1.40(4)
Pt(1)-Cl(2)	2.339(7)	C(16)-C(17)	1.33(4)
Pt(1)-Cl(1)	2.460(7)	C(18)-C(19)	1.33(3)
Pt(2)-C(36)	1.96(2)	C(18)-C(23)	1.44(3)
Pt(2)-N(2)	2.07(2)	C(19)-C(20)	1.43(3)
Pt(2)-Cl(1)	2.312(6)	C(20)-C(21)	1.40(3)
Pt(2)-Cl(2)	2.468(8)	C(21)-C(22)	1.38(4)
O(1)-C(21)	1.34(3)	C(22)-C(23)	1.37(4)
O(1)-C(24)	1.44(3)	C(24)-C(25)	1.44(4)
O(2)-C(56)	1.39(3)	C(25)-C(26)	1.57(4)
O(2)-C(59)	1.42(3)	C(26)-C(27)	1.53(3)
N(1)-C(7)	1.26(3)	C(27)-C(28)	1.50(4)
N(1)-C(11)	1.41(3)	C(28)-C(29)	1.56(4)
N(2)-C(42)	1.32(3)	C(29)-C(30)	1.46(4)
N(2)-C(46)	1.35(3)	C(30)-C(31)	1.54(5)
C(1)-C(6)	1.38(3)	C(36)-C(41)	1.42(3)
C(1)-C(2)	1.40(3)	C(36)-C(37)	1.42(3)
C(2)-C(3)	1.43(4)	C(37)-C(38)	1.34(4)
C(3)-C(4)	1.40(4)	C(38)-C(39)	1.37(4)
C(4)-C(5)	1.36(4)	C(39)-C(40)	1.48(4)
C(5)-C(6)	1.37(4)	C(40)-C(41)	1.33(3)
C(6)-C(7)	1.53(3)	C(41)-C(42)	1.50(3)
C(7)-C(8)	1.37(3)	C(42)-C(43)	1.38(3)
C(8)-C(9)	1.45(3)	C(43)-C(44)	1.46(4)
C(9)-C(10)	1.33(3)	C(44)-C(45)	1.40(4)
C(9)-C(18)	1.50(3)	C(44)-C(53)	1.52(3)
C(10)-C(11)	1.36(3)	C(45)-C(46)	1.41(3)
C(11)-C(12)	1.51(4)	C(46)-C(47)	1.46(3)
C(12)-C(17)	1.37(3)	C(47)-C(48)	1.34(3)
C(12)-C(13)	1.40(4)	C(47)-C(52)	1.41(3)
C(13)-C(14)	1.40(4)	C(48)-C(49)	1.40(4)

C(49)-C(50)	1.33(4)	C(57)-C(58)	1.43(3)
C(50)-C(51)	1.38(4)	C(59)-C(60)	1.55(3)
C(51)-C(52)	1.40(4)	C(60)-C(61)	1.49(4)
C(53)-C(58)	1.34(3)	C(61)-C(62)	1.53(4)
C(53)-C(54)	1.42(3)	C(62)-C(63)	1.46(4)
C(54)-C(55)	1.42(4)	C(63)-C(64)	1.54(4)
C(55)-C(56)	1.26(3)	C(64)-C(65)	1.49(4)
C(56)-C(57)	1.41(3)	C(65)-C(66)	1.63(4)

Table 3: Bond angles (°) for (24).

C(1)-Pt(1)-N(1)	80.7(10)	C(6)-C(1)-C(2)	120(3)
C(1)-Pt(1)-Cl(2)	93.5(9)	C(6)-C(1)-Pt(1)	116(2)
N(1)-Pt(1)-Cl(2)	173.5(6)	C(2)-C(1)-Pt(1)	124(2)
C(1)-Pt(1)-Cl(1)	171.0(9)	C(1)-C(2)-C(3)	114(3)
N(1)-Pt(1)-Cl(1)	104.4(5)	C(4)-C(3)-C(2)	126(3)
Cl(2)-Pt(1)-Cl(1)	80.9(2)	C(5)-C(4)-C(3)	115(3)
C(36)-Pt(2)-N(2)	78.9(9)	C(4)-C(5)-C(6)	122(3)
C(36)-Pt(2)-Cl(1)	97.0(7)	C(5)-C(6)-C(1)	122(3)
N(2)-Pt(2)-Cl(1)	174.8(7)	C(5)-C(6)-C(7)	126(2)
C(36)-Pt(2)-Cl(2)	175.4(8)	C(1)-C(6)-C(7)	111(3)
N(2)-Pt(2)-Cl(2)	102.6(6)	N(1)-C(7)-C(8)	124(2)
Cl(1)-Pt(2)-Cl(2)	81.2(2)	N(1)-C(7)-C(6)	117(2)
Pt(1)-Cl(2)-Pt(2)	98.2(2)	C(8)-C(7)-C(6)	119(2)
Pt(2)-Cl(1)-Pt(1)	99.1(2)	C(7)-C(8)-C(9)	118(2)
C(21)-O(1)-C(24)	118(2)	C(10)-C(9)-C(8)	117(2)
C(56)-O(2)-C(59)	118(2)	C(10)-C(9)-C(18)	126(2)
C(7)-N(1)-C(11)	119(2)	C(8)-C(9)-C(18)	117(2)
C(7)-N(1)-Pt(1)	113.2(17)	C(9)-C(10)-C(11)	122(2)
C(11)-N(1)-Pt(1)	127.3(15)	C(10)-C(11)-N(1)	120(2)
C(42)-N(2)-C(46)	121(2)	C(10)-C(11)-C(12)	120(2)
C(42)-N(2)-Pt(2)	111.9(16)	N(1)-C(11)-C(12)	119(2)
C(46)-N(2)-Pt(2)	126.1(17)	C(17)-C(12)-C(13)	118(3)

C(17)-C(12)-C(11)	119(3)	N(2)-C(42)-C(43)	125(2)
C(13)-C(12)-C(11)	121(2)	N(2)-C(42)-C(41)	118(2)
C(14)-C(13)-C(12)	120(3)	C(43)-C(42)-C(41)	116(2)
C(13)-C(14)-C(15)	119(3)	C(42)-C(43)-C(44)	116(3)
C(16)-C(15)-C(14)	117(3)	C(45)-C(44)-C(43)	117(2)
C(17)-C(16)-C(15)	122(3)	C(45)-C(44)-C(53)	122(2)
C(16)-C(17)-C(12)	123(3)	C(43)-C(44)-C(53)	121(2)
C(19)-C(18)-C(23)	115(2)	C(44)-C(45)-C(46)	122(2)
C(19)-C(18)-C(9)	127(2)	N(2)-C(46)-C(45)	118(2)
C(23)-C(18)-C(9)	118(2)	N(2)-C(46)-C(47)	121(2)
C(18)-C(19)-C(20)	126(2)	C(45)-C(46)-C(47)	120(2)
C(21)-C(20)-C(19)	116(2)	C(48)-C(47)-C(52)	119(3)
O(1)-C(21)-C(22)	117(2)	C(48)-C(47)-C(46)	122(2)
O(1)-C(21)-C(20)	124(2)	C(52)-C(47)-C(46)	119(2)
C(22)-C(21)-C(20)	119(3)	C(47)-C(48)-C(49)	121(3)
C(23)-C(22)-C(21)	122(3)	C(50)-C(49)-C(48)	120(3)
C(22)-C(23)-C(18)	121(3)	C(49)-C(50)-C(51)	121(3)
O(1)-C(24)-C(25)	110(2)	C(50)-C(51)-C(52)	119(3)
C(24)-C(25)-C(26)	114(3)	C(51)-C(52)-C(47)	119(3)
C(27)-C(26)-C(25)	114(2)	C(58)-C(53)-C(54)	119(3)
C(28)-C(27)-C(26)	114(2)	C(58)-C(53)-C(44)	122(3)
C(27)-C(28)-C(29)	113(2)	C(54)-C(53)-C(44)	119(2)
C(30)-C(29)-C(28)	116(3)	C(53)-C(54)-C(55)	115(3)
C(29)-C(30)-C(31)	114(3)	C(56)-C(55)-C(54)	127(3)
C(41)-C(36)-C(37)	115(2)	C(55)-C(56)-O(2)	120(2)
C(41)-C(36)-Pt(2)	119.0(17)	C(55)-C(56)-C(57)	119(3)
C(37)-C(36)-Pt(2)	125(2)	O(2)-C(56)-C(57)	120(3)
C(38)-C(37)-C(36)	122(3)	C(56)-C(57)-C(58)	116(3)
C(37)-C(38)-C(39)	122(3)	C(53)-C(58)-C(57)	123(3)
C(38)-C(39)-C(40)	118(3)	O(2)-C(59)-C(60)	109(2)
C(41)-C(40)-C(39)	118(3)	C(61)-C(60)-C(59)	112(2)
C(40)-C(41)-C(36)	125(2)	C(60)-C(61)-C(62)	112(2)
C(40)-C(41)-C(42)	128(2)	C(63)-C(62)-C(61)	120(3)
C(36)-C(41)-C(42)	108(2)	C(62)-C(63)-C(64)	117(2)

C(65)-C(64)-C(63) 114(2)

C(64)-C(65)-C(66) 109(3)

X-Ray crystallographic details for (28).

Table 1: Crystal data and structure refinement for (28).

Empirical formula	$C_{22}H_{17}ClN_2Pt$
Formula weight	539.92
Colour	Yellow block
Temperature	180(2) K
Wavelength	0.71073 Å
Crystal system	Monoclinic
Space group	P2(1)/c
Unit cell dimensions	$a = 11.9705(5)$ Å, $\alpha = 90^\circ$ $b = 9.4874(4)$ Å, $\beta = 103.580(10)^\circ$ $c = 16.7283(6)$ Å, $\gamma = 90^\circ$
Volume, Z	1846.70(13) Å ³ , 4
Density (calculated)	1.942 Mg/m ³
Absorption coefficient	7.750 mm ⁻¹
F(000)	1032
Crystal size	0.40 x 0.20 x 0.20 mm ³
Theta range for data collection	1.75 to 26.00°
Limiting indices	-14 h 14, -10 k 11, -20 l 19
Reflections collected	9905
Independent reflections	3598 [R(int) = 0.0240]
Refinement method	Full-matrix least-squares on F ²
Data / restraints / parameters	3598 / 0 / 236
Goodness-of-fit on F ²	1.040
Final R indices[I>2σ(I)]	R1 = 0.0207, wR2 = 0.0497
R indices (all data)	R1 = 0.0235, wR2 = 0.0508
Largest diff. Peak and hole	1.250 and -1.378 e.Å ⁻³

Table 2: Bond lengths (Å) for (28).

Pt(1)-C(11)	1.996(3)	C(7)-C(8)	1.399(5)
Pt(1)-N(1)	2.018(3)	C(8)-C(9)	1.393(5)
Pt(1)-N(2)	2.031(3)	C(9)-C(10)	1.395(5)
Pt(1)-Cl(1)	2.4082(8)	C(10)-C(11)	1.389(5)
N(1)-C(1)	1.349(4)	C(12)-C(13)	1.378(5)
N(1)-C(5)	1.367(4)	C(13)-C(14)	1.381(5)
N(2)-C(12)	1.356(4)	C(14)-C(15)	1.385(5)
N(2)-C(16)	1.375(4)	C(15)-C(16)	1.394(5)
C(1)-C(2)	1.378(5)	C(16)-C(17)	1.481(4)
C(2)-C(3)	1.389(5)	C(17)-C(18)	1.395(5)
C(3)-C(4)	1.382(5)	C(17)-C(22)	1.401(5)
C(4)-C(5)	1.392(4)	C(18)-C(19)	1.394(5)
C(5)-C(6)	1.472(5)	C(19)-C(20)	1.402(6)
C(6)-C(7)	1.383(5)	C(20)-C(21)	1.376(6)
C(6)-C(11)	1.424(5)	C(21)-C(22)	1.395(5)

Table 3: Bond angles (°) for (28).

C(11)-Pt(1)-N(1)	81.48(12)	N(1)-C(1)-C(2)	121.7(3)
C(11)-Pt(1)-N(2)	93.87(12)	C(1)-C(2)-C(3)	119.4(3)
N(1)-Pt(1)-N(2)	174.07(11)	C(4)-C(3)-C(2)	119.1(3)
C(11)-Pt(1)-Cl(1)	175.65(9)	C(3)-C(4)-C(5)	119.7(3)
N(1)-Pt(1)-Cl(1)	95.44(8)	N(1)-C(5)-C(4)	120.3(3)
N(2)-Pt(1)-Cl(1)	89.00(8)	N(1)-C(5)-C(6)	113.7(3)
C(1)-N(1)-C(5)	119.6(3)	C(4)-C(5)-C(6)	125.9(3)
C(1)-N(1)-Pt(1)	125.1(2)	C(7)-C(6)-C(11)	121.9(3)
C(5)-N(1)-Pt(1)	115.2(2)	C(7)-C(6)-C(5)	123.0(3)
C(12)-N(2)-C(16)	118.4(3)	C(11)-C(6)-C(5)	114.8(3)
C(12)-N(2)-Pt(1)	116.7(2)	C(6)-C(7)-C(8)	120.0(3)
C(16)-N(2)-Pt(1)	124.8(2)	C(9)-C(8)-C(7)	118.9(3)

C(8)-C(9)-C(10)	120.9(3)	N(2)-C(16)-C(17)	119.5(3)
C(11)-C(10)-C(9)	121.5(3)	C(15)-C(16)-C(17)	120.5(3)
C(10)-C(11)-C(6)	116.9(3)	C(18)-C(17)-C(22)	119.2(3)
C(10)-C(11)-Pt(1)	129.9(3)	C(18)-C(17)-C(16)	121.3(3)
C(6)-C(11)-Pt(1)	113.2(2)	C(22)-C(17)-C(16)	119.3(3)
N(2)-C(12)-C(13)	123.0(3)	C(19)-C(18)-C(17)	120.2(3)
C(14)-C(13)-C(12)	119.1(3)	C(18)-C(19)-C(20)	120.0(4)
C(13)-C(14)-C(15)	118.7(3)	C(21)-C(20)-C(19)	119.8(4)
C(14)-C(15)-C(16)	120.7(3)	C(20)-C(21)-C(22)	120.5(4)
N(2)-C(16)-C(15)	120.0(3)	C(21)-C(22)-C(17)	120.2(4)

X-Ray crystallographic details for (29).

Table 1: Crystal data and structure refinement for (29).

Empirical formula	$C_{23}H_{17}Cl_5N_2Pt$
Formula weight	693.73
Colour	Red block
Temperature	180(2) K
Wavelength	0.71073 Å
Crystal system	Triclinic
Space group	P
Unit cell dimensions	$a = 9.5988(4)$ Å, $\alpha = 81.3380(10)^\circ$ $b = 11.0181(5)$ Å, $\beta = 79.2530(10)^\circ$ $c = 12.4407(5)$ Å, $\gamma = 64.6860(10)^\circ$
Volume, Z	1164.81(9) Å ³ , 2
Density (calculated)	1.978 Mg/m ³
Absorption coefficient	6.611 mm ⁻¹
F(000)	664
Crystal size	0.44 x 0.16 x 0.10 mm ³
Theta range for data collection	1.67 to 25.00°
Limiting indices	$-6 \leq h \leq 12$, $-1 \leq k \leq 14$, $-15 \leq l \leq 16$
Reflections collected	5894
Independent reflections	3919 [R(int) = 0.0250]
Refinement method	Full-matrix least-squares on F ²
Data / restraints / parameters	3919 / 0 / 2800
Goodness-of-fit on F ²	1.006
Final R indices[I > 2σ(I)]	R1 = 0.0317, wR2 = 0.0707
R indices (all data)	R1 = 0.0373, wR2 = 0.0727
Largest diff. Peak and hole	1.948 and -1.551 e.Å ⁻³

Table 2: Bond lengths (Å) for (29).

Pt(1)-C(11)	2.005(6)	C(8)-C(9)	1.392(11)
Pt(1)-N(2)	2.019(5)	C(9)-C(10)	1.386(9)
Pt(1)-C(22)	2.029(5)	C(10)-C(11)	1.388(8)
Pt(1)-N(1)	2.032(5)	C(12)-C(13)	1.345(9)
Pt(1)-Cl(2)	2.4383(14)	C(13)-C(14)	1.381(9)
Pt(1)-Cl(1)	2.443(2)	C(14)-C(15)	1.393(9)
N(1)-C(1)	1.346(7)	C(15)-C(16)	1.370(8)
N(1)-C(5)	1.380(8)	C(16)-C(17)	1.466(8)
N(2)-C(12)	1.369(8)	C(17)-C(22)	1.396(8)
N(2)-C(16)	1.380(7)	C(17)-C(18)	1.404(8)
C(1)-C(2)	1.380(8)	C(18)-C(19)	1.377(9)
C(2)-C(3)	1.368(9)	C(19)-C(20)	1.376(9)
C(3)-C(4)	1.384(9)	C(20)-C(21)	1.391(8)
C(4)-C(5)	1.388(8)	C(21)-C(22)	1.356(8)
C(5)-C(6)	1.452(8)	Cl(3)-C(23)	1.753(7)
C(6)-C(7)	1.408(9)	Cl(4)-C(23)	1.779(6)
C(6)-C(11)	1.408(9)	Cl(5)-C(23)	1.753(7)
C(7)-C(8)	1.380(10)		

Table 3: Bond angles (°) for (29).

C(11)-Pt(1)-N(2)	95.0(2)	N(1)-Pt(1)-Cl(2)	88.51(13)
C(11)-Pt(1)-C(22)	87.8(2)	C(11)-Pt(1)-Cl(1)	177.3(2)
N(2)-Pt(1)-C(22)	81.4(2)	N(2)-Pt(1)-Cl(1)	87.13(14)
C(11)-Pt(1)-N(1)	81.8(2)	C(22)-Pt(1)-Cl(1)	90.9(2)
N(2)-Pt(1)-N(1)	174.7(2)	N(1)-Pt(1)-Cl(1)	95.9(2)
C(22)-Pt(1)-N(1)	94.2(2)	Cl(2)-Pt(1)-Cl(1)	91.93(5)
C(11)-Pt(1)-Cl(2)	89.5(2)	C(1)-N(1)-C(5)	120.7(5)
N(2)-Pt(1)-Cl(2)	95.72(14)	C(1)-N(1)-Pt(1)	124.7(4)
C(22)-Pt(1)-Cl(2)	175.9(2)	C(5)-N(1)-Pt(1)	114.6(4)

C(12)-N(2)-C(16)	118.3(5)	C(13)-C(12)-N(2)	122.5(6)
C(12)-N(2)-Pt(1)	125.2(4)	C(12)-C(13)-C(14)	119.8(6)
C(16)-N(2)-Pt(1)	116.1(4)	C(13)-C(14)-C(15)	118.8(6)
N(1)-C(1)-C(2)	120.6(6)	C(16)-C(15)-C(14)	120.2(6)
C(3)-C(2)-C(1)	120.5(6)	C(15)-C(16)-N(2)	120.3(6)
C(2)-C(3)-C(4)	118.7(6)	C(15)-C(16)-C(17)	127.3(6)
C(3)-C(4)-C(5)	120.8(6)	N(2)-C(16)-C(17)	112.4(5)
N(1)-C(5)-C(4)	118.6(5)	C(22)-C(17)-C(18)	119.0(6)
N(1)-C(5)-C(6)	114.0(5)	C(22)-C(17)-C(16)	117.5(5)
C(4)-C(5)-C(6)	127.4(6)	C(18)-C(17)-C(16)	123.6(6)
C(7)-C(6)-C(11)	119.6(6)	C(19)-C(18)-C(17)	119.7(6)
C(7)-C(6)-C(5)	123.7(6)	C(20)-C(19)-C(18)	120.5(6)
C(11)-C(6)-C(5)	116.7(6)	C(19)-C(20)-C(21)	119.7(6)
C(8)-C(7)-C(6)	119.1(7)	C(22)-C(21)-C(20)	120.6(6)
C(7)-C(8)-C(9)	121.5(7)	C(21)-C(22)-C(17)	120.4(5)
C(10)-C(9)-C(8)	119.5(6)	C(21)-C(22)-Pt(1)	127.1(5)
C(9)-C(10)-C(11)	120.5(6)	C(17)-C(22)-Pt(1)	112.4(4)
C(10)-C(11)-C(6)	119.8(6)	Cl(5)-C(23)-Cl(3)	111.1(4)
C(10)-C(11)-Pt(1)	127.3(5)	Cl(5)-C(23)-Cl(4)	109.9(4)
C(6)-C(11)-Pt(1)	112.9(4)	Cl(3)-C(23)-Cl(4)	110.1(4)

X-Ray crystallographic details for (40).

Table 1: Crystal data and structure refinement for (40).

Empirical formula	$C_{30}H_{35}NO_3Pt$
Formula weight	652.86
Colour	Yellow prism
Temperature	180(2) K
Wavelength	0.71073 Å
Crystal system	Triclinic
Space group	P
Unit cell dimensions	$a = 10.0566(5)$ Å, $\alpha = 68.7940(10)^\circ$ $b = 11.7161(6)$ Å, $\beta = 69.2180(10)^\circ$ $c = 13.8432(8)$ Å, $\gamma = 64.7360(10)^\circ$
Volume, Z	1335.75 Å ³ , 2
Density (calculated)	1.623 Mg/m ³
Absorption coefficient	5.283 mm ⁻¹
F(000)	648
Crystal size	0.40 x 0.38 x 0.24 mm ³
Theta range for data collection	1.62 to 25.50°
Limiting indices	$-12 \leq h \leq 12$, $-12 \leq k \leq 15$, $-15 \leq l \leq 18$
Reflections collected	7048
Independent reflections	4865 [R(int) = 0.0638]
Refinement method	Full-matrix least-squares on F ²
Data / restraints / parameters	4865 / 0 / 318
Goodness-of-fit on F ²	1.004
Final R indices[I > 2σ(I)]	R1 = 0.0462, wR2 = 0.0749
R indices (all data)	R1 = 0.0354, wR2 = 0.0723
Largest diff. Peak and hole	1.948 and -1.551 e.Å ⁻³

Table 2: Bond lengths (Å) for (40).

Pt1-C18	1.827(6)	C10-C11	1.374(9)
Pt1-N1	2.007(5)	C11-C12	1.448(8)
Pt1-C17	2.055(6)	C12-C13	1.407(9)
Pt1-C1	2.070(6)	C12-C17	1.425(8)
N1-C7	1.375(7)	C13-C14	1.371(8)
N1-C11	1.381(8)	C14-C15	1.380(8)
O1-C3	1.366(8)	C15-C16	1.388(8)
O1-C101	1.428(7)	C16-C17	1.397(7)
O2-C15	1.356(7)	C101-C102	1.496(10)
O2-C201	1.441(7)	C102-C103	1.533(8)
C1-C2	1.383(9)	C103-C104	1.498(9)
C1-C6	1.437(8)	C104-C105	1.537(9)
C2-C3	1.394(8)	C105-C106	1.523(11)
C3-C4	1.403(9)	C201-C202	1.496(8)
C4-C5	1.377(9)	C202-C203	1.524(8)
C5-C6	1.371(8)	C203-C204	1.528(8)
C6-C7	1.441(9)	C204-C205	1.516(8)
C7-C8	1.386(9)	C205-C206	1.524(9)
C8-C9	1.386(10)	C18-O3	1.152(7)
C9-C10	1.407(9)		

Table 3: Bond angles (°) for (40).

C18-Pt1-N1	178.8(2)	C7-N1-Pt1	118.0(5)
C18-Pt1-C17	99.3(2)	C11-N1-Pt1	117.9(4)
N1-Pt1-C17	80.4(2)	C3-O1-C101	118.3(5)
C18-Pt1-C1	100.1(3)	C15-O2-C201	119.2(5)
N1-Pt1-C1	80.2(2)	C2-C1-C6	117.6(5)
C17-Pt1-C1	160.6(2)	C2-C1-Pt1	130.4(5)
C7-N1-C11	124.1(5)	C6-C1-Pt1	111.9(5)

C1-C2-C3	121.4(6)	C14-C13-C12	121.4(6)
O1-C3-C2	114.9(6)	C13-C14-C15	119.6(6)
O1-C3-C4	124.9(6)	O2-C15-C14	126.0(6)
C2-C3-C4	120.2(7)	O2-C15-C16	114.6(6)
C5-C4-C3	118.7(6)	C14-C15-C16	119.4(6)
C6-C5-C4	122.0(6)	C15-C16-C17	123.8(6)
C5-C6-C1	120.1(6)	C16-C17-C12	115.5(6)
C5-C6-C7	123.6(6)	C16-C17-Pt1	132.2(5)
C1-C6-C7	116.3(5)	C12-C17-Pt1	112.3(4)
N1-C7-C8	117.3(6)	O1-C101-C102	107.5(5)
N1-C7-C6	113.6(6)	C101-C102-C103	112.7(6)
C8-C7-C6	129.2(6)	C104-C103-C102	113.3(6)
C9-C8-C7	120.5(6)	C103-C104-C105	114.1(6)
C8-C9-C10	120.3(7)	C106-C105-C104	112.8(7)
C11-C10-C9	119.6(7)	O2-C201-C202	106.2(5)
C10-C11-N1	118.1(6)	C201-C202-C203	114.0(5)
C10-C11-C12	129.2(6)	C202-C203-C204	112.0(5)
N1-C11-C12	112.7(6)	C205-C204-C203	113.7(6)
C13-C12-C17	120.4(5)	C204-C205-C206	114.1(6)
C13-C12-C11	122.9(6)	O3-C18 -Pt1	179.6(5)
C17-C12-C11	116.7(6)		

X-Ray crystallographic details for (44).

Table 1: Crystal data and structure refinement for (44).

Empirical formula	$C_{38}H_{34}N_2O_2Pt_2S_2$
Formula weight	1004.97
Colour	golden-yellow prisms
Temperature	180(2) K
Wavelength	0.71073 Å
Crystal system	monoclinic
Space group	P2(1)/c
Unit cell dimensions	$a = 17.90500(10)$ Å, $\alpha = 90^\circ$ $b = 9.9528(5)$ Å, $\beta = 97.885(5)^\circ$ $c = 27.658(2)$ Å, $\gamma = 90^\circ$
Volume, Z	$4882.2(5)$ Å ³ , 6
Density (calculated)	2.051 Mg/m ³
Absorption coefficient	8.753 mm ⁻¹
F(000)	2880
Crystal size	$0.20 \times 0.06 \times 0.06$ mm ³
Theta range for data collection	1.15 to 28.62°
Limiting indices	-13 h 242, -13 k 13, -35 l 35
Reflections collected	28767
Independent reflections	11487 [R(int) = 0.0633]
Refinement method	Full-matrix least-squares on F ²
Data / restraints / parameters	11487 / 0 / 628
Goodness-of-fit on F ²	0.914
Final R indices[I > 2σ(I)]	R1 = 0.0481, wR2 = 0.0884
R indices (all data)	R1 = 0.1021, wR2 = 0.1076
Largest diff. Peak and hole	1.912 and -1.431 e.Å ⁻³

Table 2: Bond lengths (Å) for (44).

Pt1-N18	2.004(7)	S2-O2	1.474(6)
Pt1-C11	2.068(9)	S2-C201	1.766(9)
Pt1-C114	2.082(9)	S2-C202	1.777(9)
Pt1-S1	2.201(2)	C21-C22	1.399(12)
S1-O1	1.469(6)	C21-C26	1.433(12)
S1-C101	1.772(9)	C22-C23	1.389(13)
S1-C102	1.773(9)	C23-C24	1.361(13)
C11-C16	1.409(12)	C24-C25	1.365(13)
C11-C12	1.400(12)	C25-C26	1.385(12)
C12-C13	1.393(12)	C26-C27	1.465(12)
C13-C14	1.382(13)	C27-N28	1.345(11)
C14-C15	1.369(12)	C27-C212	1.374(12)
C15-C16	1.391(12)	N28-C29	1.351(10)
C16-C17	1.481(13)	C29-C210	1.373(12)
C17-N18	1.354(11)	C29-C213	1.479(12)
C17-C112	1.389(12)	C210-C211	1.364(13)
N18-C19	1.353(11)	C211-C212	1.376(14)
C19-C110	1.395(11)	C213-C218	1.399(12)
C19-C113	1.474(12)	C213-C214	1.424(12)
C110-C111	1.383(13)	C214-C215	1.378(12)
C111-C112	1.375(13)	C215-C216	1.387(12)
C113-C118	1.408(12)	C216-C217	1.374(13)
C113-C114	1.435(11)	C217-C218	1.366(13)
C114-C115	1.394(12)	Pt3-N38	2.016(7)
C115-C116	1.384(12)	Pt3-C31	2.074(9)
C116-C117	1.376(12)	Pt3-C314	2.085(9)
C117-C118	1.393(13)	Pt3-S3 2.	197(2)
Pt2-N28	2.014(7)	S3-O3	1.485(6)
Pt2-C21	2.069(9)	S3-C302	1.775(10)
Pt2-C214	2.106(9)	S3-C301	1.772(9)
Pt2-S2	2.190(2)	C31-C32	1.398(11)

C31-C36	1.430(11)	C39-C313	1.463(13)
C32-C33	1.395(13)	C310-C311	1.390(13)
C33-C34	1.384(13)	C311-C312	1.380(12)
C34-C35	1.387(12)	C313-C318	1.379(11)
C35-C36	1.403(12)	C313-C314	1.429(12)
C36-C37	1.456(11)	C314-C315	1.393(13)
C37-N38	1.358(11)	C315-C316	1.387(12)
C37-C312	1.389(12)	C316-C317	1.406(13)
N38-C39	1.340(10)	C317-C318	1.379(13)
C39-C310	1.402(12)		

Table 3: Bond angles (°) for (40).

N18-Pt1-C11	79.8(3)	N18-C17-C112	119.3(9)
N18-Pt1-C114	80.6(3)	N18-C17-C16	112.7(8)
C11-Pt1-C114	159.8(3)	C112-C17-C16	128.0(9)
N18-Pt1 S1	170.9(2)	C19-N18-C17	122.4(8)
C11-Pt1-S1	98.4(2)	C19-N18-Pt1	118.7(6)
C114-Pt1-S1	101.7(2)	C17-N18-Pt1	118.6(6)
O1-S1-C101	106.2(4)	N18-C19-C110	120.0(8)
O1-S1-C102	106.1(4)	N18-C19-C113	112.8(8)
C101-S1-C102	100.4(5)	C110-C19-C113	127.2(8)
O1-S1-Pt1	117.7(3)	C19-C110-C111	117.6(9)
C101-S1-Pt1	114.6(3)	C110-C111-C112	122.0(8)
C102-S1-Pt1	110.1(3)	C17-C112-C111	118.7(9)
C16-C11-C12	115.5(8)	C118-C113-C114	122.1(8)
C16-C11-Pt1	112.8(6)	C118-C113-C19	121.1(8)
C12-C11-Pt1	131.6(6)	C114-C113-C19	116.8(8)
C13-C12-C11	121.1(9)	C115-C114-C113	114.9(8)
C12-C13-C14	121.9(9)	C115-C114-Pt1	134.1(6)
C15-C14-C13	118.0(9)	C113-C114-Pt1	110.8(6)
C16-C15-C14	120.8(9)	C116-C115-C114	122.9(8)
C15-C16-C11	122.5(9)	C117-C116-C115	121.5(9)
C15-C16-C17	121.9(8)	C116-C117-C118	118.9(9)
C11-C16-C17	115.6(8)	C113-C118-C117	119.7(9)

N28-Pt2-C21	80.3(3)	C218-C213-C214	121.2(8)
N28-Pt2-C214	80.6(3)	C218-C213-C29	121.9(8)
C21-Pt2-C214	160.4(3)	C214-C213-C29	116.8(8)
N28-Pt2-S2	173.8(2)	C215-C214-C213	116.0(8)
C21-Pt2-S2	98.6(3)	C215-C214-Pt2	133.5(7)
C214-Pt2-S2	100.9(2)	C213-C214-Pt2	110.5(6)
O2-S2-C201	106.3(4)	C214-C215-C216	122.3(9)
O2-S2-C202	105.3(4)	C217-C216-C215	120.9(9)
C201-S2-C202	102.3(4)	C216-C217-C218	119.2(9)
O2-S2-Pt2	119.3(3)	C217-C218-C213	120.4(9)
C201-S2-Pt2	112.2(3)	N38-Pt3-C31	80.0(3)
C202-S2-Pt2	109.9(3)	N38-Pt3-C314	79.8(3)
C22-C21-C26	115.6(8)	C31-Pt3-C314	159.2(3)
C22-C21-Pt2	132.6(7)	N38-Pt3-S3	173.27(19)
C26-C21-Pt2	111.5(6)	C31-Pt3-S3	100.3(2)
C23-C22-C21	122.4(9)	C314-Pt3-S3	100.3(3)
C24-C23-C22	120.6(10)	O3-S3-C302	106.2(4)
C23-C24-C25	119.0(9)	O3-S3-C301	106.6(4)
C24-C25-C26	122.3(9)	C302-S3-C301	100.4(5)
C25-C26-C21	120.0(9)	O3-S3-Pt3	119.3(3)
C25-C26-C27	123.3(8)	C302-S3-Pt3	112.7(3)
C21-C26-C27	116.4(8)	C301-S3-Pt3	109.8(3)
N28-C27-C212	118.9(9)	C32-C31-C36	115.0(8)
N28-C27-C26	113.2(7)	C32-C31-Pt3	132.5(7)
C212-C27-C26	128.0(8)	C36-C31-Pt3	111.9(6)
C27-N28-C29	123.3(7)	C33-C32-C31	122.7(9)
C27-N28-Pt2	118.5(6)	C34-C33-C32	121.0(9)
C29-N28-Pt2	118.1(6)	C33-C34-C35	118.8(9)
N28-C29-C210	119.1(8)	C36-C35-C34	120.2(8)
N28-C29-C213	113.7(7)	C35-C36-C31	122.2(8)
C210-C29-C213	127.2(9)	C35-C36-C37	121.7(8)
C211-C210-C29	118.2(9)	C31-C36-C37	116.0(8)
C210-C211-C212	122.4(9)	N38-C37-C312	118.7(8)
C27-C212-C211	118.2(9)	N38-C37-C36	113.6(7)

C312-C37-C36	127.8(9)	C318-C313-C314	122.0(9)
C39-N38-C37	123.4(8)	C318-C313-C39	122.0(8)
C39-N38-Pt3	118.5(6)	C314-C313-C39	116.0(8)
C37-N38-Pt3	117.7(6)	C315-C314-C313	115.0(8)
N38-C39-C310	119.6(9)	C315-C314-Pt3	133.4(7)
N38-C39-C313	113.8(8)	C313-C314-Pt3	111.6(7)
C310-C39-C313	126.6(8)	C316-C315-C314	123.8(9)
C311-C310-C39	117.8(8)	C315-C316-C317	119.3(10)
C312-C311-C310	121.4(9)	C318-C317-C316	118.9(9)
C311-C312-C37	119.1(9)	C313-C318-C317	121.1(9)

X-Ray crystallographic details for (46).

Table 1: Crystal data and structure refinement for (46).

Empirical formula	$C_{18}H_{11}NOPt$
Formula weight	452.37
Colour	Orange needles
Temperature	180(2) K
Wavelength	0.71073 Å
Crystal system	orthorhombic
Space group	P2(1)2(1)2(1)
Unit cell dimensions	$a = 7.3337(6)$ Å, $\alpha = 90^\circ$ $b = 18.9464(12)$ Å, $\beta = 90^\circ$ $c = 18.9464(12)$ Å, $\gamma = 90^\circ$
Volume, Z	$2664.9(3)$ Å ³ , 8
Density (calculated)	2.255 Mg/m ³
Absorption coefficient	10.527 mm ⁻¹
F(000)	1696
Crystal size	$0.30 \times 0.12 \times 0.10$ mm ³
Theta range for data collection	1.51 to 28.54°
Limiting indices	$-9 \leq h \leq 9$, $-25 \leq k \leq 25$, $-13 \leq l \leq 25$
Reflections collected	15782
Independent reflections	6260 [$R(\text{int}) = 0.0335$]
Refinement method	Full-matrix least-squares on F^2
Data / restraints / parameters	62602 / 0 / 379
Goodness-of-fit on F^2	1.105
Final R indices [$I > 2\sigma(I)$]	$R1 = 0.0351$, $wR2 = 0.0735$
R indices (all data)	$R1 = 0.0562$, $wR2 = 0.0836$
Largest diff. Peak and hole	1.393 and -1.360 e.Å ⁻³

Table 2: Bond lengths (Å) for (46).

Pt1-C118	1.864(11)	C111-C112	1.459(13)
Pt1-N11	2.027(7)	C112-C113	1.417(11)
Pt1-C101	2.057(9)	C112-C117	1.421(12)
Pt1-C117	2.083(8)	C113-C114	1.376(13)
Pt2-C218	1.837(10)	C114-C115	1.384(14)
Pt2-N21	2.003(7)	C115-C116	1.419(13)
Pt2-C217	2.084(10)	C116-C117	1.392(12)
Pt2-C201	2.084(9)	C201-C202	1.401(13)
N11-C107	1.329(10)	C201-C206	1.418(12)
N11-C111	1.352(10)	C202-C203	1.391(13)
N21-C211	1.361(11)	C203-C204	1.382(14)
N21-C207	1.370(10)	C204-C205	1.402(13)
O11-C118	1.125(12)	C205-C206	1.394(11)
O21-C218	1.143(11)	C206-C207	1.446(13)
C101-C106	1.409(12)	C207-C208	1.419(13)
C101-C102	1.405(12)	C208-C209	1.383(13)
C102-C103	1.424(14)	C209-C210	1.359(12)
C103-C104	1.385(14)	C210-C211	1.398(12)
C104-C105	1.381(13)	C211-C212	1.453(11)
C105-C106	1.387(12)	C212-C217	1.395(12)
C106-C107	1.491(11)	C212-C213	1.415(12)
C107-C108	1.407(13)	C213-C214	1.394(13)
C108-C109	1.384(12)	C214-C215	1.384(14)
C109-C110	1.381(13)	C215-C216	1.370(14)
C110-C111	1.375(13)	C216-C217	1.402(12)

Table 3: Bond angles (°) for (46).

C118-Pt1-N11	179.4(4)	N11-Pt1-C117	80.0(3)
C118-Pt1-C101	100.4(4)	C101-Pt1-C117	160.2(4)
N11-Pt1-C101	80.2(3)	C218-Pt2-N21	179.5(4)
C118-Pt1-C117	99.4(4)	C218-Pt2-C217	99.7(4)

N21-Pt2-C217	80.0(3)	C114-C115-C116	119.3(10)
C218-Pt2-C201	100.2(4)	C117-C116-C115	121.1(9)
N21-Pt2-C201	80.1(3)	C116-C117-C112	118.2(8)
C217-Pt2-C201	160.0(4)	C116-C117-Pt1	130.6(7)
C107-N11-C111	124.0(8)	C112-C117-Pt1	111.1(6)
C107-N11-Pt1	117.6(6)	O11-C118-Pt1	178.3(10)
C111-N11-Pt1	118.3(6)	C202-C201-C206	117.9(8)
C211-N21-C207	123.5(8)	C202-C201-Pt2	130.3(7)
C211-N21-Pt2	118.5(5)	C206-C201-Pt2	111.6(7)
C207-N21-Pt2	117.9(6)	C203-C202-C201	119.5(9)
C106-C101-C102	117.3(8)	C204-C203-C202	123.6(9)
C106-C101-Pt1	113.0(6)	C203-C204-C205	117.1(9)
C102-C101-Pt1	129.7(7)	C206-C205-C204	120.9(10)
C101-C102-C103	119.7(9)	C205-C206-C201	121.0(9)
C104-C103-C102	120.9(8)	C205-C206-C207	122.3(9)
C105-C104-C103	119.6(9)	C201-C206-C207	116.7(8)
C104-C105-C106	120.0(9)	N21-C207-C208	117.7(9)
C105-C106-C101	122.4(8)	N21-C207-C206	113.6(8)
C105-C106-C107	122.6(8)	C208-C207-C206	128.7(8)
C101-C106-C107	114.9(8)	C209-C208-C207	119.0(8)
N11-C107-C108	118.5(8)	C210-C209-C208	121.2(9)
N11-C107-C106	114.2(8)	C209-C210-C211	120.4(9)
C108-C107-C106	127.3(8)	N21-C211-C210	118.1(8)
C109-C108-C107	118.6(9)	N21-C211-C212	112.1(8)
C108-C109-C110	120.6(9)	C210-C211-C212	129.8(8)
C111-C110-C109	119.3(9)	C217-C212-C213	120.1(8)
N11-C111-C110	118.9(9)	C217-C212-C211	118.2(8)
N11-C111-C112	112.9(8)	C213-C212-C211	121.7(8)
C110-C111-C112	128.2(8)	C214-C213-C212	119.8(9)
C113-C112-C117	120.3(9)	C215-C214-C213	119.3(9)
C113-C112-C111	122.1(8)	C216-C215-C214	121.1(9)
C117-C112-C111	117.6(7)	C215-C216-C217	121.0(10)
C114-C113-C112	119.7(9)	C212-C217-C216	118.6(9)
C113-C114-C115	121.3(9)	C212-C217-Pt2	111.0(6)

C216-C217-Pt2

130.3(7)

O21-C218-Pt2

178.4(9)

X-Ray crystallographic details for (47).

Table 1: Crystal data and structure refinement for (47).

Empirical formula	$C_{32}H_{31}NO_2Pt$
Formula weight	656.67
Colour	Red plate
Temperature	180(2) K
Wavelength	0.71073 Å
Crystal system	monoclinic
Space group	C2/c
Unit cell dimensions	$a = 31.9729(15)$ Å, $\alpha = 90^\circ$ $b = 19.1517(9)$ Å, $\beta = 97.977(2)^\circ$ $c = 16.9951(8)$ Å, $\gamma = 90^\circ$
Volume, Z	10306.0(8) Å ³ , 16
Density (calculated)	1.693 Mg/m ³
Absorption coefficient	5.476 mm ⁻¹
F(000)	5184
Crystal size	0.20 x 0.20 x 0.10 mm ³
Theta range for data collection	1.67 to 25.00°
Limiting indices	-37 h 29, -22 k 21, -20 l 20
Reflections collected	8341
Independent reflections	4869 [R(int) = 0.0601]
Refinement method	Full-matrix least-squares on F ²
Data / restraints / parameters	4869 / 424 / 566
Goodness-of-fit on F ²	1.118
Final R indices[I > 2σ(I)]	1971 R1 = 0.0690, wR2 = 0.1530
R indices (all data)	R1 = 0.1173, wR2 = 0.
Largest diff. Peak and hole	1.44 and -1.30 e.Å ⁻³

Table 2: Bond lengths (Å) for (47).

Pt1-C101	1.88(2)	C112-C113	1.49(3)
Pt1-N1	2.029(19)	C113-C114	1.39(3)
Pt1-C118	2.05(3)	C113-C118	1.41(3)
Pt1-C102	2.10(2)	C114-C115	1.36(3)
Pt1-Pt2	3.2322(11)	C115-C116	1.43(3)
Pt2-C201	1.83(2)	C116-C117	1.35(3)
Pt2-N2	2.000(18)	C117-C118	1.40(3)
Pt2-C218	2.05(2)	C119-C124	1.37(3)
Pt2-C202	2.07(2)	C119-C120	1.45(3)
N1-C112	1.33(3)	C120-C121	1.38(3)
N1-C108	1.35(3)	C121-C122	1.36(3)
N2-C212	1.35(3)	C122-C123	1.39(3)
N2-C208	1.39(3)	C123-C124	1.39(3)
O11-C101	1.11(3)	C125-C126	1.54(3)
O12-C122	1.33(3)	C126-C127	1.53(3)
O12-C125	1.45(3)	C127-C128	1.56(4)
O21-C201	1.14(3)	C128-C129	1.49(3)
O22-C222	1.39(3)	C129-C130	1.55(3)
O22-C225	1.45(2)	C130-C131	1.51(3)
C102-C103	1.35(3)	C131-C132	1.52(3)
C102-C107	1.45(3)	C202-C207	1.40(3)
C103-C104	1.38(3)	C202-C203	1.42(3)
C104-C105	1.44(3)	C203-C204	1.39(3)
C105-C106	1.34(3)	C204-C205	1.43(3)
C106-C107	1.37(3)	C205-C206	1.37(3)
C107-C108	1.51(3)	C206-C207	1.41(3)
C108-C109	1.36(3)	C207-C208	1.52(3)
C109-C110	1.38(3)	C208-C209	1.40(3)
C110-C111	1.43(3)	C209-C210	1.33(3)
C110-C119	1.52(3)	C210-C211	1.42(3)
C111-C112	1.38(3)	C210-C219	1.52(3)

C211-C212	1.35(3)	C221-C222	1.38(3)
C212-C213	1.51(3)	C222-C223	1.39(3)
C213-C218	1.41(3)	C223-C224	1.38(3)
C213-C214	1.48(3)	C225-C226	1.53(3)
C214-C215	1.29(3)	C226-C227	1.51(3)
C215-C216	1.41(3)	C227-C228	1.50(3)
C216-C217	1.43(3)	C228-C229	1.53(3)
C217-C218	1.43(3)	C229-C230	1.55(3)
C219-C220	1.34(4)	C230-C231	1.56(3)
C219-C224	1.42(3)	C231-C232	1.49(3)
C220-C221	1.37(4)		

Table 3: Bond angles (°) for (47).

C101-Pt1-N1	177.2(9)	C112-N1-C108	123(2)
C101-Pt1-C118	100.3(10)	C112-N1-Pt1	118.6(15)
N1-Pt1-C118	79.6(9)	C108-N1-Pt1	118.1(15)
C101-Pt1-C102	97.9(9)	C212-N2-C208	120.6(18)
N1-Pt1-C102	82.0(8)	C212-N2-Pt2	123.5(15)
C118-Pt1-C102	161.7(9)	C208-N2-Pt2	115.8(14)
C101-Pt1-Pt2	95.6(7)	C122-O12-C125	117.3(18)
N1-Pt1-Pt2	87.2(5)	C222-O22-C225	116.1(18)
C118-Pt1-Pt2	92.1(8)	O11-C101-Pt1	176(2)
C102-Pt1-Pt2	87.6(6)	C103-C102-C107	120(2)
C201-Pt2-N2	176.8(9)	C103-C102-Pt1	131.5(17)
C201-Pt2-C218	99.3(10)	C107-C102-Pt1	108.9(15)
N2-Pt2-C218	78.8(8)	C102-C103-C104	122(2)
C201-Pt2-C202	99.5(10)	C103-C104-C105	117(2)
N2-Pt2-C202	82.3(8)	C106-C105-C104	121(2)
C218-Pt2-C202	161.1(8)	C105-C106-C107	121(2)
C201-Pt2-Pt1	92.0(7)	C106-C107-C102	118.3(19)
N2-Pt2-Pt1	90.8(5)	C106-C107-C108	123.5(18)
C218-Pt2-Pt1	96.6(6)	C102-C107-C108	118.2(17)
C202-Pt2-Pt1	84.3(6)	N1-C108-C109	120(2)

Table 2: Bond lengths (Å) for (53).

Pt(1)-C(9)	1.952(7)	C(14)-C(15)	1.381(11)
Pt(1)-Cl(2)	2.281(2)	C(15)-C(16)	1.405(11)
Pt(1)-Cl(1)	2.320(2)	C(16)-C(17)	1.401(11)
Pt(1)-Cl(1)	2.449(2)	C(101)-C(102)	1.524(10)
Cl(1)-Pt(1)	2.449(2)	C(102)-C(103)	1.523(11)
N(1)-C(7)	1.353(10)	C(103)-C(104)	1.507(13)
N(1)-C(11)	1.356(10)	C(104)-C(105)	1.498(11)
O(1)-C(3)	1.365(10)	C(105)-C(106)	1.512(11)
O(1)-C(101)	1.411(11)	C(201)-C(202)	1.506(11)
O(2)-C(1)	1.358(10)	C(202)-C(203)	1.520(11)
O(2)-C(201)	1.439(10)	C(203)-C(204)	1.526(13)
O(3)-C(17)	1.360(9)	C(204)-C(205)	1.474(11)
O(3)-C(301)	1.439(9)	C(205)-C(206)	1.501(11)
O(4)-C(15)	1.338(10)	C(301)-C(302)	1.540(10)
O(4)-C(401)	1.442(10)	C(302)-C03a	1.504(12)
C(1)-C(2)	1.400(12)	C(302)-C303b	1.620(11)
C(1)-C(6)	1.406(11)	C03a-C04a	1.580(13)
C(2)-C(3)	1.377(13)	C04a-C05a	1.512(13)
C(3)-C(4)	1.381(12)	C05a-C06a	1.507(12)
C(4)-C(5)	1.396(12)	C303b-C304b	1.564(13)
C(5)-C(6)	1.384(12)	C304b-C305b	1.514(12)
C(6)-C(7)	1.498(11)	C305b-C306b	1.539(12)
C(7)-C(8)	1.358(10)	C(401)-C(402)	1.521(9)
C(8)-C(9)	1.407(10)	C(402)-C(403)	1.508(10)
C(9)-C(10)	1.398(10)	C(403)-C(404)	1.521(13)
C(10)-C(11)	1.388(10)	C(404)-C(405)	1.537(14)
C(11)-C(12)	1.471(11)	C(405)-C(406)	1.417(13)
C(12)-C(13)	1.389(11)	O(1S)-C(1S)	1.17(2)
C(12)-C(17)	1.408(10)	C(1S)-C(2S)	1.45(2)
C(13)-C(14)	1.371(11)	C(1S)-C(2S)	1.45(2)

Table 3: Bond angles (°) for (53).

C(9)-Pt(1)-Cl(2)	91.3(3)	N(1)-C(11)-C(10)	117.3(8)
C(9)-Pt(1)-Cl(1)	92.3(2)	N(1)-C(11)-C(12)	118.9(7)
Cl(2)-Pt(1)-Cl(1)	175.87(8)	C(10)-C(11)-C(12)	123.7(8)
C(9)-Pt(1)-Cl(1)	176.7(3)	C(13)-C(12)-C(17)	116.8(8)
Cl(2)-Pt(1)-Cl(1)	91.55(7)	C(13)-C(12)-C(11)	120.1(7)
Cl(1)-Pt(1)-Cl(1)	84.86(7)	C(17)-C(12)-C(11)	123.0(7)
Pt(1)-Cl(1)-Pt(1)	95.14(7)	C(14)-C(13)-C(12)	121.9(8)
C(7)-N(1)-C(11)	123.6(7)	C(13)-C(14)-C(15)	121.4(8)
C(3)-O(1)-C(101)	117.9(8)	O(4)-C(15)-C(14)	117.3(8)
C(1)-O(2)-C(201)	117.5(7)	O(4)-C(15)-C(16)	123.5(8)
C(17)-O(3)-C(301)	120.1(7)	C(14)-C(15)-C(16)	119.1(9)
C(15)-O(4)-C(401)	117.4(7)	C(17)-C(16)-C(15)	118.7(8)
O(2)-C(1)-C(2)	124.3(8)	O(3)-C(17)-C(16)	122.2(8)
O(2)-C(1)-C(6)	117.0(8)	O(3)-C(17)-C(12)	115.7(8)
C(2)-C(1)-C(6)	118.7(9)	C(16)-C(17)-C(12)	122.1(8)
C(3)-C(2)-C(1)	120.6(9)	O(1)-C(101)-C(102)	108.9(8)
O(1)-C(3)-C(2)	115.4(9)	C(103)-C(102)-C(101)	110.8(9)
O(1)-C(3)-C(4)	123.6(10)	C(104)-C(103)-C(102)	114.0(9)
C(2)-C(3)-C(4)	121.0(9)	C(105)-C(104)-C(103)	115.5(9)
C(3)-C(4)-C(5)	118.9(10)	C(104)-C(105)-C(106)	113.4(9)
C(6)-C(5)-C(4)	121.0(9)	O(2)-C(201)-C(202)	107.8(7)
C(5)-C(6)-C(1)	119.7(9)	C(201)-C(202)-C(203)	114.7(9)
C(5)-C(6)-C(7)	116.8(8)	C(202)-C(203)-C(204)	110.9(9)
C(1)-C(6)-C(7)	123.4(9)	C(205)-C(204)-C(203)	114.5(10)
N(1)-C(7)-C(8)	119.0(8)	C(204)-C(205)-C(206)	113.6(11)
N(1)-C(7)-C(6)	117.7(8)	O(3)-C(301)-C(302)	104.9(7)
C(8)-C(7)-C(6)	123.1(8)	C03a-C(302)-C(301)	127.4(11)
C(7)-C(8)-C(9)	121.6(8)	C(301)-C(302)-C303b	110.2(8)
C(10)-C(9)-C(8)	116.5(7)	C(302)-C03a-C04a	113.5(12)
C(10)-C(9)-Pt(1)	120.9(6)	C05a-C04a-C03a	113.4(13)
C(8)-C(9)-Pt(1)	122.5(6)	C06a-C05a-C04a	120(2)
C(11)-C(10)-C(9)	122.0(8)	C304b-C303b-C(302)	114.5(11)

C305b-C304b-C303b	120.1(14)	C(403)-C(404)-C(405)	124.5(14)
C304b-C305b-C306b	123.8(14)	C(406)-C(405)-C(404)	100.6(14)
O(4)-C(401)-C(402)	105.9(7)	O(1S)-C(1S)-C(2S)	122.4(9)
C(403)-C(402)-C(401)	110.9(8)	O(1S)-C(1S)-C(2S)	122.4(9)
C(402)-C(403)-C(404)	112.1(9)	C(2S)-C(1S)-C(2S)	115(2)

Appendix 2.

Photographic plates of mesogenic optical textures.

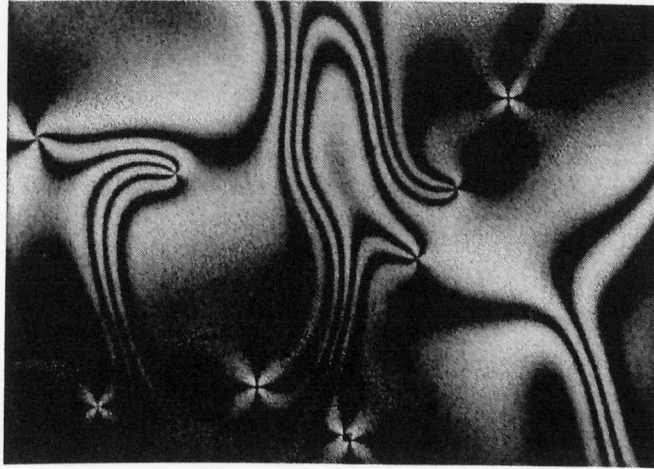


Plate 1: Schlieren texture of a nematic phase, N.

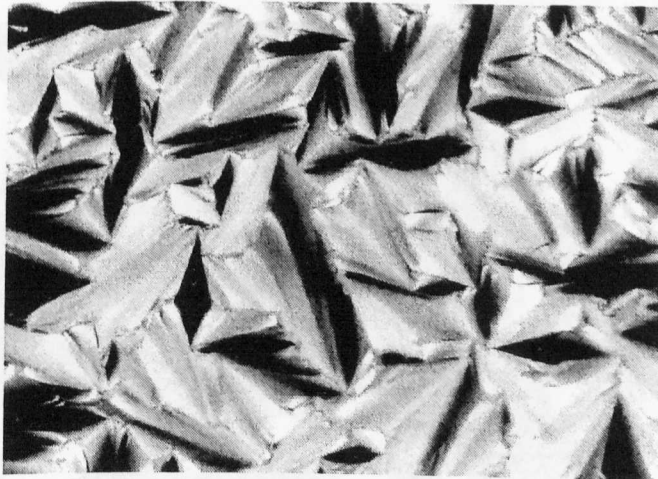


Plate 2: Focal-conic texture of a smectic A, S_A.

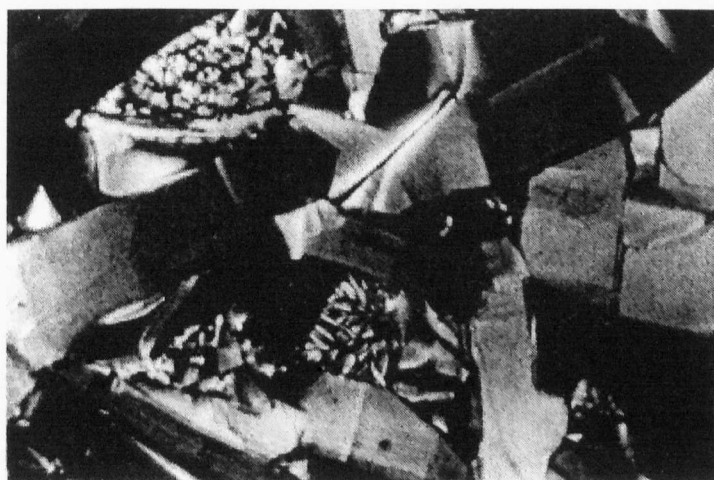


Plate 3: Paramorphotic focal-conic texture of smectic B, S_B .

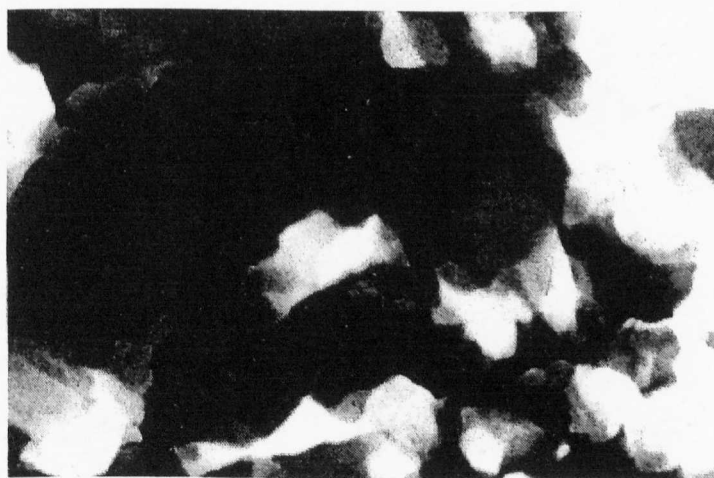


Plate 4: Mosaic texture of smectic E, S_E .

Appendix 3.

Refereed Publications.

[G1]-DB24C8 2: 84% Ausbeute; Schmp. 113–114°C (MeOH); $^1\text{H-NMR}$ (CDCl_3): δ 3.84 (8H, m), 3.93 (8H, m), 4.15 (4H, m), 4.20 (4H, m), 5.04 (4H, s), 5.26 (2H, s), 6.59 (1H, t, J 2.0 Hz), 6.67 (2H, d, J 2.0 Hz), 6.84 (1H, d, J 8.8 Hz), 6.88 (4H, m), 7.30–7.43 (10H, m), 7.55 (1H, d, J 2.0 Hz), 7.67 (1H, dd, J 2.0, 8.8 Hz); FAB-MS: m/z : 794.4 [M]; HR-FAB-MS: ber. für $\text{C}_{46}\text{H}_{50}\text{O}_{12}$ [M]: 794.3302; gef.: 794.3300; Elementaranalyse (%): ber. für $\text{C}_{46}\text{H}_{50}\text{O}_{12}$: C 69.51, H 6.34; gef.: C 69.43, H 6.31.

[G2]-DB24C8 3: 89% Ausbeute, farbloses Glas; $^1\text{H-NMR}$ (CDCl_3): δ 3.82 (8H, m), 3.91 (8H, m), 4.13–4.18 (8H, m), 4.97 (4H, s), 5.02 (8H, s), 5.25 (2H, s), 6.55 (1H, t, J 2.0 Hz), 6.56 (2H, t, J 2.0 Hz), 6.65 (2H, d, J 2.0 Hz), 6.67 (4H, d, J 2.0 Hz), 6.81 (1H, d, J 8.4 Hz), 6.84–6.90 (4H, m), 7.31–7.41 (20H, m), 7.54 (1H, d, J 2.0 Hz), 7.65 (1H, dd, J 2.0, 8.4 Hz); FAB-MS: m/z : 1218.6 [M]; HR-FAB-MS: ber. für $\text{C}_{74}\text{H}_{74}\text{O}_{16}$ [M]: 1218.4977; gef.: 1218.4943; Elementaranalyse (%): ber. für $\text{C}_{74}\text{H}_{74}\text{O}_{16}$: C 72.89, H 6.12; gef.: C 72.82; H 6.10.

[G3]-DB24C8 4: 93% Ausbeute, farbloses Glas; $^1\text{H-NMR}$ (CDCl_3): δ 3.81 (m, 8H), 3.89 (m, 8H), 4.13 (m, 8H), 4.95 (s, 12H), 5.01 (s, 16H), 5.23 (s, 2H), 6.53 (t, 2H, J 2.4 Hz), 6.56 (t, 4H, J 2.4 Hz), 6.58 (t, 1H, J 2.4 Hz), 6.66 (m, 14H), 6.80 (d, 1H, J 8.4 Hz), 6.87 (m, 4H), 7.28–7.41 (m, 40H), 7.54 (s, 1H), 7.64 (d, 2H, J 8.4 Hz); FAB-MS: m/z : 2090.9 [M Na]; HR-FAB-MS: ber. für $\text{C}_{130}\text{H}_{122}\text{O}_{24}\text{Na}$ [M Na]: 2090.8257; gef.: 2090.8227.

Eingegangen am 25. Mai 1998 [Z11898]

Stichwörter: Dendrimere • Nichtkovalente Wechselwirkungen • Pseudorotaxane • Supramolekulare Chemie

- [1] a) R. Sadamoto, N. Tomioka, T. Aida, *J. Am. Chem. Soc.* **1996**, *118*, 3978–3979; b) L. L. Miller, R. G. Duan, D. C. Tully, D. A. Tomalia, *J. Am. Chem. Soc.* **1997**, *119*, 1005–1010.
- [2] a) J. C. M. van Hest, D. A. P. Delnoye, M. W. P. L. Baars, C. Elissen-Roman, M. H. P. van Genderen, E. W. Meijer, *Chem. Eur. J.* **1996**, *2*, 1616–1626; b) G. R. Newkome, C. N. Moorefield, F. Vögtle, *Dendritic Molecules: Concepts, Synthesis, Perspectives*, VCH, Weinheim, **1996**; c) R. Kopelman, M. Shortreed, Z. Y. Shi, W. Tan, Z. Xu, J. S. Moore, A. Bar-Haim, J. Klafter, *Phys. Rev. Lett.* **1997**, *78*, 1239–1242; d) M. Kawa, J. M. J. Fréchet, *Chem. Mater.* **1998**, *10*, 286–296.
- [3] a) J. F. G. A. Jansen, E. M. M. de Brabander-van den Berg, E. W. Meijer, *Science* **1994**, *266*, 1226–1229; b) J. F. G. A. Jansen, E. W. Meijer, *J. Am. Chem. Soc.* **1995**, *117*, 4417–4417.
- [4] J. S. Moore, *Acc. Chem. Res.* **1997**, *30*, 402–413.
- [5] K. L. Wooley, C. J. Hawker, J. M. J. Fréchet, *J. Am. Chem. Soc.* **1991**, *113*, 4252–4261.
- [6] a) G. R. Newkome, Z. Yao, G. R. Baker, V. K. Gupta, P. S. Russo, M. J. Sanders, *J. Am. Chem. Soc.* **1986**, *108*, 849–850; b) D. A. Tomalia, H. Baker, J. Dewald, M. Hall, G. Kallos, S. Martin, J. Roeck, J. Ryder, P. Smith, *Macromolecules* **1986**, *19*, 2466–2468.
- [7] T. Kawaguchi, K. L. Walker, C. L. Wilkins, J. S. Moore, *J. Am. Chem. Soc.* **1995**, *117*, 2159–2165.
- [8] F. Zeng, S. C. Zimmerman, *Chem. Rev.* **1997**, *97*, 1681–1712.
- [9] Verbindung **1** wurde bereits beschrieben: P. R. Ashton, A. N. Collins, M. C. T. Fyfe, P. T. Glink, S. Menzer, J. F. Stoddart, D. J. Williams, *Angew. Chem.* **1997**, *109*, 59–62; *Angew. Chem. Int. Ed. Engl.* **1997**, *36*, 59–62.
- [10] a) P. R. Ashton, P. J. Campbell, E. J. T. Chrystal, P. T. Glink, S. Menzer, D. Philp, N. Spencer, J. F. Stoddart, P. A. Tasker, D. J. Williams, *Angew. Chem.* **1995**, *107*, 1997–2001; *Angew. Chem. Int. Ed. Engl.* **1995**, *34*, 1865–1869; b) P. R. Ashton, E. J. T. Chrystal, P. T. Glink, S. Menzer, C. Schiavo, N. Spencer, J. F. Stoddart, P. A. Tasker, A. J. P. White, D. J. Williams, *Chem. Eur. J.* **1996**, *2*, 709–728.
- [11] a) O. Mitsunobu, *Synthesis* **1981**, *1*, 1–28; b) D. L. Hughes, *Org. Prep. Proced. Int.* **1996**, *28*, 127–164.
- [12] In den $^1\text{H-NMR}$ -Spektren treten unter den Bedingungen eines auf der $^1\text{H-NMR}$ -Zeitskala langsamen Austausches Signale für den 1:1-Pseudorotaxankomplex **4(5)** und nichtkomplexiertes **4** auf. Die Assoziationskonstante für den 1:1-Komplex in Chloroform ließ sich durch Integration der Protonensignale für die komplexierte und die nichtkomplexierte Verbindung **4** nach der Beziehung K_a [**4(5)**]/
- [4][5] zu $7.9 \cdot 10^3 \text{ M}^{-1}$ (21.8°C) bestimmen. Der K_a -Wert für den 1:1-Komplex aus dem monotonen Salz **5** und DB24C8 in [D]Chloroform wurde zu $2.7 \cdot 10^4 \text{ M}^{-1}$ (25°C) bestimmt.^[10] Der kleinere Wert für die Assoziationskonstante von **4(5)** mag von der infolge der voluminösen dendritischen Substituenten geringeren Zugänglichkeit und Flexibilität der makrocyclischen Einheit in **4** herrühren.
- [13] L. J. Twyman, A. E. Beezer, J. C. Mitchell, *J. Chem. Soc. Perkin Trans.* **1994**, *4*, 407–422.
- [14] J. C. Hummelen, J. L. J. van Dongen, E. W. Meijer, *Chem. Eur. J.* **1997**, *3*, 1489–1493.
- [15] a) Z. Xu, M. Kahr, K. L. Walker, C. L. Wilkins, J. S. Moore, *J. Am. Chem. Soc.* **1994**, *116*, 4537–4550; b) J. W. Leon, J. M. J. Fréchet, *Polym. Bull. Berlin* **1995**, *35*, 449–455.
- [16] Eine Lösung von **4** ($3.0 \cdot 10^{-2} \text{ M}$) wurde 3 d mit 1/3 Moläquiv. von festem **1** gemischt. Diese Mischung wurde filtriert, und beim Einengen des Filtrats wurde ein weißer Feststoff erhalten, der durch MALDI-MS analysiert wurde.
- [17] Die auf diesem Weg festgestellte Verteilung der Komplexe deutet auf eine teilweise Dissoziation von **1(4)**, in die Untereinheiten **1(4)**₂ und **1(4)** während der Ionisierung hin. Es ist auch zu beachten, daß MALDI-MS-Detektoren in bezug auf die Molekülmasse nicht linear sind und die Signale darum auch nicht eindeutig einer Molekülmasse zugeordnet werden können. Zu Prinzip, Geräteaufbau und Anwendung der MALDI-MS siehe: F. Hillenkamp, M. Karas, R. C. Beavis, B. T. Chait, *Anal. Chem.* **1991**, *63*, 1193A–1203A. Die ESI-MS-Untersuchung ergab bislang ähnliche Resultate, wir sind allerdings derzeit dabei zu untersuchen, inwieweit man mit kleinen Spannungen am konischen Probenkopf (V_c) die Fragmentierung unterdrücken kann. In folgenden Übersichtsartikeln wird die ESI-MS-Charakterisierung von über H-Brücken gebildete Aggregate beschrieben: a) K. C. Russell, E. Leize, A. Van Dorsselaer, J.-M. Lehn, *Angew. Chem.* **1995**, *107*, 244–248; *Angew. Chem. Int. Ed. Engl.* **1995**, *34*, 209–213; b) X. Cheng, Q. Gao, R. D. Smith, E. E. Simanek, M. Mammen, G. M. Whitesides, *J. Org. Chem.* **1996**, *61*, 2204–2206.

Intermolekulare versus intramolekulare C-H-Aktivierung: Synthese und Charakterisierung eines neuartigen Carbenplatinkomplexes**

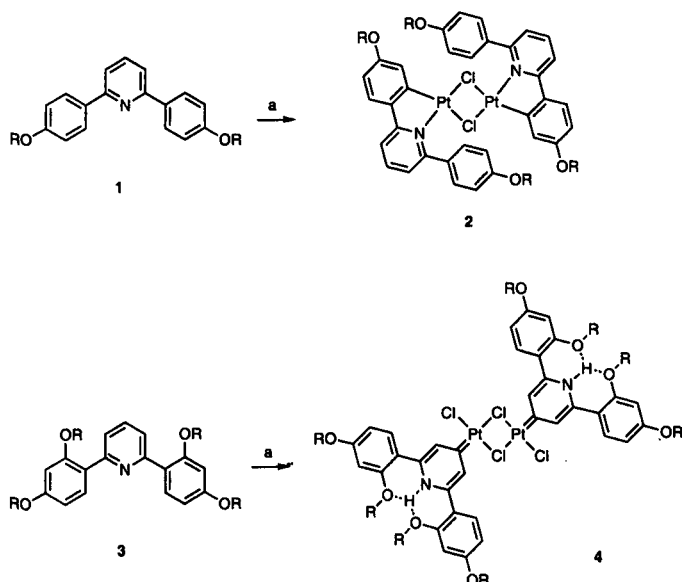
Gareth W. V. Cave, Andrew J. Hallett, William Errington und Jonathan P. Rourke*

Cyclometallierungen sind bereits häufig durchgeführt^[1, 2] und gründlich untersucht worden.^[3, 4] Typischerweise bindet die koordinierende Einheit eines Liganden ein Metallzentrum, wonach intramolekular eine C-H-Bindung aktiviert wird und daraufhin fünf- oder sechsgliedrige Chelatringe entstehen. Wir beabsichtigten, einige cycloplatinerte Verbindungen mit neuartigen mesogenen Eigenschaften zu synthetisieren. Bis jetzt haben wir einige 2,6-disubstituierte Pyridine wie **1** und **3** hergestellt und diese mit Kaliumtetrachloroplatinat unter den üblichen Bedingungen der Cycloplatinierung umgesetzt.^[5] Dabei isolierten wir ausgehend von

[*] Dr. J. P. Rourke, G. W. V. Cave, A. J. Hallett, Dr. W. Errington
Department of Chemistry, Warwick University
Coventry CV47AL (Großbritannien)
Fax: (+44) 1203-524112
E-mail: j.rourke@warwick.ac.uk

[**] Diese Arbeit wurde vom EPSRC (Großbritannien) gefördert. Der Firma Johnson Matthey danken wir für eine Spende von Platinsalzen.

1 das Cycloplatinierungsprodukt 2 in hohen Ausbeuten. Ausgehend von 3 erhielten wir allerdings ein völlig anderes Produkt: Statt der erwarteten Verbindung war das durch intermolekulare C-H-Aktivierung gebildete 4 das einzig nachweisbare Produkt (Schema 1). Es wurde in 36% Ausbeute isoliert und ^1H - sowie ^{13}C -NMR-spektroskopisch und auch kristallographisch charakterisiert.



Schema 1. Synthese der Platinchelate 2 und 4. a) $\text{K}_2[\text{PtCl}_4]$, AcOH. R $n\text{-C}_6\text{H}_{13}$.

Die Struktur von 4 im Kristall weist einige interessante Merkmale auf (Abb. 1). Zwischen den beiden Platin- und den beiden Cl1-Chloratomen, die ein planares Rechteck aufspannen, befindet sich ein Symmetriezentrum. Die beiden anderen Chloratome (Cl2) ragen aus der Ebene des Pt_2Cl_2 -Rechtecks nur um 0.082(4) Å heraus. Der Pyridinring ist um einen Winkel von 38.62(24)° gegen die Ebene des Rechtecks gedreht. In Schema 2 sind zwei Darstellungsweisen für die Bindungsart des organischen Fragments an die Platinatome gezeigt. Die Pt-C-Bindungslänge liegt mit 1.951(9) Å nahe bei denen des Pt^0 -Carbens, das aus 1,3-Dimesitylimidazol-2-yliden erhalten wurde (1.959(8) und 1.942(8) Å).^[6] Ebenso ähnelt dieser Wert dem von 1.973(11) Å, der beim kationischen Carbenplatin(IV)-Komplex $[\text{PtCl}_2[\text{C}(\text{NHMe})(\text{NHC}_6\text{H}_4\text{Cl})](\text{PEt}_3)_2]\text{ClO}_4$ ^[7] nachgewiesen wurde. Er ist aber signifikant kleiner als die Pt-C-Bindungslänge der carbenfreien cycloplatinerten Verbindung $[\text{PtCl}(\text{tBu}_2\text{PCMe}_2\text{CH}_2)]_2$ (2.062(6) Å).^[8] Auch ist die Pt-C-Bindung in 4 kürzer als die Pt^{II} -C-Bindungen in Arylplatinverbindungen (1.98–2.20 Å).^[9,10] Zwei kürzere Pt^{II} -C-Bindungen sind bekannt: Im Carbenplatin-Komplex $[\text{PtCl}(\text{tBuCH}_2\text{COiPr})]_2$ ^[11] beträgt die Pt-C-Bindungslänge 1.82(6) Å und ist angesichts der relativ großen Standardabweichung nicht signifikant kleiner als die von uns für 4

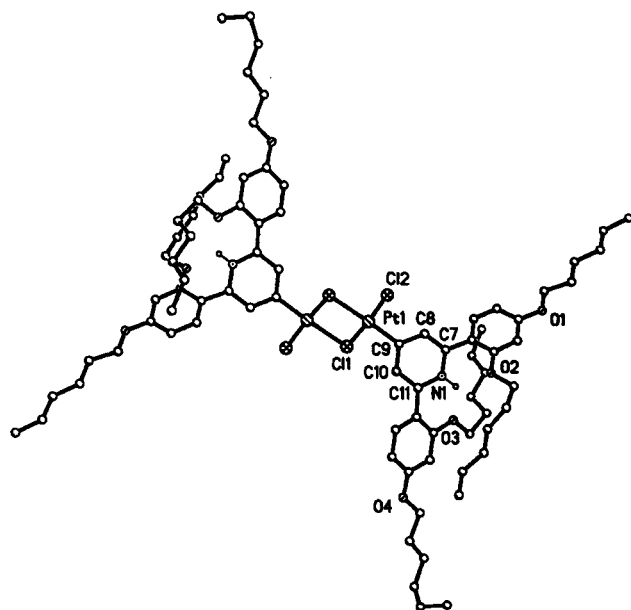
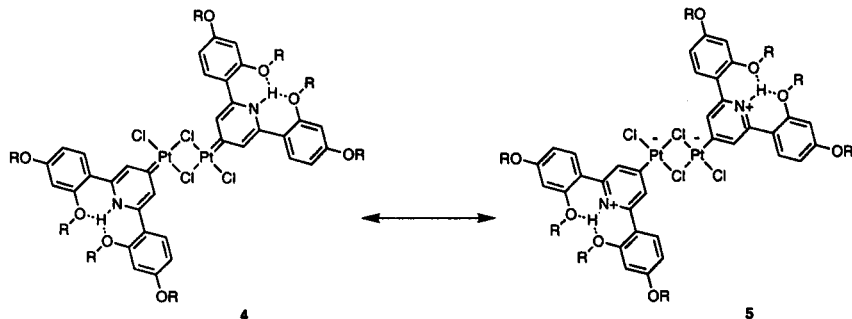


Abb. 1. Ansicht der Struktur von 4 im Kristall. Ausgewählte Bindungslängen [Å] und Winkel [°]: Pt1-C9 1.951(9), Pt1-Cl2 2.281(2), Pt1-Cl1 2.320(2), Pt1-Cl1' 2.448(2), N1-C7 1.352(10), N1-C11 1.361(10), C7-C8 1.362(10), C8-C9 1.408(10), C9-C10 1.401(10), C10-C11 1.389(10); C9-Pt1-Cl2 91.2(3), C9-Pt1-Cl1 92.4(2), Cl2-Pt1-Cl1 175.86(8), C9-Pt1-Cl1' 176.8(2), Cl2-Pt1-Cl1' 91.56(7), Cl1-Pt1-Cl1' 84.85(7), Pt1-Cl1-Pt1' 95.155(7), C7-N1-C11 123.7(7), N1-C7-C8 119.0(8), C7-C8-C9 121.5(8), C10-C9-C8 116.6(7), C10-C9-Pt1 120.7(6), C8-C9-Pt1 122.6(6), C11-C10-C9 122.0(8), N1-C11-C10 117.1(8).



Schema 2. Das Carben 4 und das Zwitterion 5 als formal mögliche Strukturen. R $n\text{-C}_6\text{H}_{13}$.

bestimmte. In einer Verbindung mit einem dreizähligen NCN-Donor, in der die Pt-C-Bindung sterisch eingeschränkt ist, hat sie einen Wert von 1.90(1) Å.^[12] Die kurze Pt-C-Bindung deutet somit auf eine Carbenstruktur hin, so daß die Struktur 4 in Schema 2 die Bindungsverhältnisse richtig wiedergibt. Weitere Belege dafür konnten dem ^{13}C -NMR-Spektrum entnommen werden, das ein typisches Carbensignal bei δ 324.3 enthält. Demnach kann die Struktur 5 ausgeschlossen werden.

Das am Stickstoffatom gebundene Proton wurde an einer berechneten Position eingeführt. Die O3-N1- und O2-N1-Abstände betragen 2.622(9) bzw. 2.720(8) Å und sind damit wesentlich kleiner als die Summe der van-der-Waals-Radien von Sauerstoff und Stickstoff (3.07 Å).^[13] Dies belegt das Vorliegen einer Wasserstoffbrückenbindung. Der O2-O3-Ab-

stand ist mit 3.742(9) Å größer als die Summe der van-der-Waals-Radien, was darauf hinweist, daß keine O-O-Wechselwirkungen vorliegen. Als Folge der Wasserstoffbrückenbindung sind die beiden Benzolringe um 34.63(29)° (der Ring, an den O1 und O2 gebunden sind) und 32.79(36)° (der Ring, an den O3 und O4 gebunden sind) gegenüber dem Pyridinring verdreht, so daß sich ein Sauerstoffatom unterhalb und eines oberhalb des N-gebundenen Protons befindet. Dem ¹H-NMR-Spektrum von **4** zufolge ist dieses Proton in Lösung stark entschirmt (δ 12.77). Die beiden über die H-Brücken an dieses Proton gebundenen OR-Ketten sind im Feststoff unbeweglich und verändern den ungewöhnlichen ¹H-NMR-Signalen der Ketten zufolge ihre Lage auch in Lösung nicht. Den endständigen Methylgruppen der Ketten entsprechen Signale bei δ 0.69 statt bei der üblichen Verschiebung von δ 0.95, bei der die Signale der Methylgruppen der anderen Ketten liegen.

Das ¹H-NMR-Spektrum von **3** weist keine ungewöhnlichen Merkmale auf; die Signale der beiden OR-Ketten sind identisch. Demzufolge unterliegen die Konformationen der Verbindung auch keinen unerwarteten sterischen Einschränkungen, und **3** verhält sich ersten Ergebnissen zufolge koordinationschemisch völlig normal.^[14] Mischt man **3** mit K₂[PtCl₄] in Lösung, würde man erwarten, daß **3** zunächst über das Stickstoffatom das Platinatom koordiniert. In einer derartigen Verbindung würden sich aktivierbare C-H-Bindungen sehr nahe beieinander befinden, so daß eine cyclo-metallierte Verbindung entstehen kann. Bei der intramolekularen Aktivierung wurde im Vergleich zur intermolekularen Aktivierung unter sonst gleichen Bedingungen eine etwa zehnfache relative Reaktivität bestimmt.^[3] Dieser hohe Unterschied wird mit der höheren effektiven Konzentration erklärt. Da ausschließlich die Carbenspezies entsteht, läuft diese Reaktion vermutlich stark bevorzugt ab, und sie wird wahrscheinlich durch das verbrückende Proton unterstützt. Bemerkenswert ist die hohe thermische Stabilität von **4**: Die Verbindung schmilzt an Luft unzersetzt bei 246 °C.

Experimentelles

2: 2,6-Bis(4-*n*-hexyloxyphenyl)pyridin **1** (103 mg, 0.239 mmol) wurde zu einer Lösung aus Kaliumtetrachloroplatinat(II) (99 mg, 0.239 mmol) und 400 mL Essigsäure gegeben. Die Mischung wurde 60 h bei 70 °C gerührt. Das Lösungsmittel wurde entfernt, das Reaktionsprodukt mit Wasser gewaschen und in Chloroform gelöst. Die Lösung wurde filtriert, der Rückstand mit Hexan gewaschen, das vereinigte Filtrat eingedunstet und das Rohprodukt aus Ethylacetat umkristallisiert: Ausbeute 100 mg (63 %, 0.075 mmol). ¹H-NMR (400 MHz, CDCl₃, 25 °C): δ 7.71 (4H, AA'XX'), 7.70 (2H, t, ³J 7.6 Hz; Pyridin), 7.36 (2H, dd, ³J 7.6, ⁴J 1.2 Hz; Pyridin), 7.21 (2H, d, ³J 8.5 Hz; cycloplatinierter Ring), 7.03 (2H, dd, ³J 7.6, ⁴J 1.2 Hz; Pyridin), 6.91 (4H, AA'XX'), 6.60 (2H, dd, ³J 8.5, ⁴J 2.3 Hz; cycloplatinierter Ring), 6.46 (2H, d, ⁴J 2.3 Hz; cycloplatinierter Ring), 3.97 (6H, t, ³J 6.7 Hz; OCH₂), 3.86 (6H, t, ³J 6.7 Hz; OCH₂), 1.79 (8H, m; CH₂), 1.44 (24H, m; CH₂), 0.95 (6H, t, ³J 7.0 Hz; CH₃), 0.91 (6H, t, ³J 7.0 Hz; CH₃); Elementaranalyse: gef. (ber.): C 52.6 (52.7), H 5.5 (5.5), N 2.2 (2.1).

4: 2,6-Bis(2,4-di-*n*-hexyloxyphenyl)pyridin **3** (159 mg, 0.260 mmol) wurde zu einer Lösung aus Kaliumtetrachloroplatinat(II) (108 mg, 0.260 mmol) und 400 mL Essigsäure gegeben. Die Lösung wurde 60 h bei 70 °C gerührt. Das Lösungsmittel wurde entfernt, das Reaktionsprodukt mit Wasser gewaschen und in Chloroform gelöst. Die Lösung wurde filtriert, der Rückstand mit Hexan nachgewaschen, das vereinigte Filtrat eingedunstet und das Rohprodukt aus Aceton umkristallisiert: Ausbeute 84 mg (36 %, 0.047 mmol).

¹H-NMR (400 MHz, CDCl₃, 25 °C): δ 12.77 (2H, t, ⁴J 2.1 Hz; NH), 8.03 (4H, d, ⁴J 2.1 Hz; Pyridin), 7.78 (4H, d, ³J 8.9 Hz), 6.64 (4H, dd, ³J 8.9, ⁴J 2.4 Hz), 6.52 (4H, d, ⁴J 2.4 Hz), 4.00 (8H, t, ³J 6.4 Hz; C4-OCH₂), 3.99 (8H, t, ³J 5.8 Hz; C2-OCH₂), 1.80 (8H, m; CH₂), 1.58 (8H, m; CH₂), 1.44 (8H, m; CH₂), 1.34 (24H, m; CH₂), 1.15 (8H, m; CH₂), 0.95 (20H, m; CH₂, CH₃ der nicht H-verbrückten Alkyloxy-Ketten), 0.69 (12H, t; CH₃ der H-verbrückten Alkyloxy-Ketten); ¹³C-NMR (100.5 MHz, CDCl₃, 25 °C): δ 324.3 (an Pt gebundenes C).

Kristallstrukturanalyse von **4**: C₈₂H₁₂₂Cl₄N₂O₈Pt₂·Me₂CO, *M*_r 1853.93, monoklin, Raumgruppe C2/c, *a* 32.261(2), *b* 15.7989(7), *c* 20.0825(9) Å, β 119.867(1)°, *V* 8876.4(7) Å³, 180(2) K; abschließende Gütefaktoren: *R*₁, *wR*₂ und *S* betragen 0.052, 0.084 bzw. 1.013 für 454 Parameter. Die Daten wurden auf einem Siemens-SMART-CCD-Diffraktometer mit Flächendetektor gemessen. Man verfeinerte mit Volle-Matrix-kleinste-Quadrate-Methoden gegen *F*² für alle Daten (SHELXL-96).^[15] Die kristallographischen Daten (ohne Strukturaktoren) der in dieser Veröffentlichung beschriebenen Struktur wurden als „supplementary publication no. CCDC-101757“ beim Cambridge Crystallographic Data Centre hinterlegt. Kopien der Daten können kostenlos bei folgender Adresse in Großbritannien angefordert werden: CCDC, 12 Union Road, Cambridge CB2 1EZ (Fax: (+44) 1223-336-033; E-mail: deposit@ccdc.cam.ac.uk).

Eingegangen am 2. Juni 1998 [Z11928]

Stichwörter: Carbenkomplexe • C-H-Aktivierung • Cyclo-metallierung • N-Liganden • Platin

- [1] A. D. Ryabov, *Synthesis* **1985**, 233–252.
- [2] M. Pfeffer, *Pure Appl. Chem.* **1992**, 64, 335–342.
- [3] A. D. Ryabov, *Chem. Rev.* **1990**, 90, 403–424.
- [4] P. Steenwinkel, R. A. Gossage, G. van Koten, *Chem. Eur. J.* **1998**, 4, 759–762.
- [5] R. M. Ceder, J. Sales, *J. Organomet. Chem.* **1985**, 294, 389–396.
- [6] A. J. Arduengo, S. F. Gamper, J. C. Calabrese, F. Davidson, *J. Am. Chem. Soc.* **1994**, 116, 4391–4394.
- [7] R. Walker, K. W. Muir, *J. Chem. Soc. Dalton Trans.* **1975**, 272–276.
- [8] A. B. Goel, S. Goel, D. Vanderveer, *Inorg. Chim. Acta* **1981**, 54, L267–L269.
- [9] L. W. Conzelman, J. D. Koola, U. Kunze, J. Strähle, *Inorg. Chim. Acta* **1984**, 89, 147–149.
- [10] L. Chassot, E. Muller, A. von Zelewsky, *Inorg. Chem.* **1984**, 23, 429–434.
- [11] Y. T. Struchkov, G. G. Aleksandrov, V. B. Pukhnarevich, S. P. Sushchinskaya, M. G. Voronkov, *J. Organomet. Chem.* **1979**, 172, 269–272.
- [12] J. Terheijden, G. van Koten, F. Muller, D. M. Grove, K. Vrieze, E. Nielsen, C. H. Stam, *J. Organomet. Chem.* **1986**, 315, 401–417.
- [13] A. Bondi, *J. Phys. Chem.* **1964**, 68, 441–445.
- [14] G. W. V. Cave, J. P. Rourke, unveröffentlichte Ergebnisse.
- [15] G. M. Sheldrick, Universität Göttingen, **1996**.

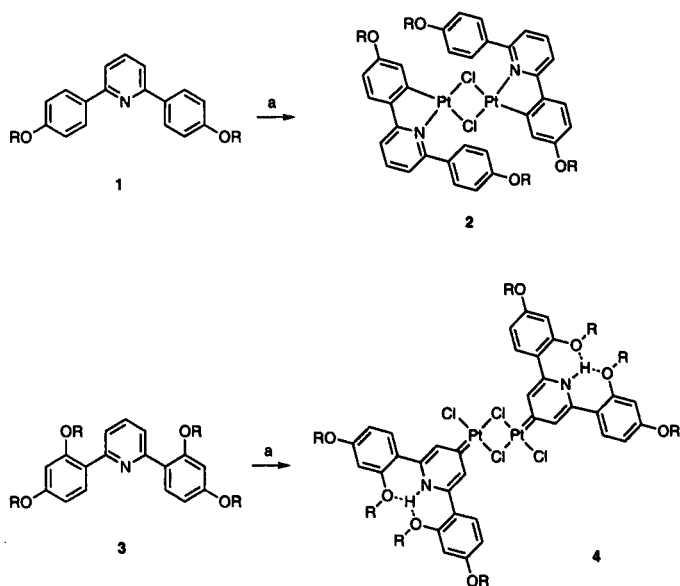
- Herdtschek, *J. Organomet. Chem.* **1997**, *548*, 73–82; d) J. Kouvetakis, J. McMurran, P. Matsunaga, M. O'Keefe, J. L. Hubbard, *Inorg. Chem.* **1997**, *36*, 1792–1797.
- [5] a) G.-C. Guo, Q.-G. Wang, G.-D. Zhou, T. C. W. Mak, *Chem. Commun.* **1998**, 339–340; b) G.-C. Guo, Q.-G. Wang, G.-D. Zhou, T. C. W. Mak, *Angew. Chem.* **1998**, *110*, 652–654; *Angew. Chem. Int. Ed.* **1998**, *37*, 630–632; c) G.-C. Guo, Q.-G. Wang, G.-D. Zhou, T. C. W. Mak, unpublished results.
- [6] G.-C. Guo, T. C. W. Mak, *Angew. Chem.* **1998**, *110*, 3296–3299; *Angew. Chem. Int. Ed.* **1998**, *37*, 3183–3186.
- [7] a) B. K. Burgess, D. J. Lowe, *Chem. Rev.* **1996**, *96*, 2983–3011; b) G. N. Schrauzer, G. W. Kiefer, P. A. Doemeny, H. Kirsh, *J. Am. Chem. Soc.* **1973**, *95*, 5582–5592.
- [8] M. A. S. Goher, F. A. Nautner, *Polyhedron*, **1995**, *14*, 1439–1446, and references therein.
- [9] a) J. I. Bryant, R. L. Brooks, *J. Chem. Phys.* **1971**, *54*, 5315–5323; b) C. D. West, *Z. Kristallogr.* **1936**, *85*, 421–425.
- [10] a) G.-D. Zhou, *Acta Sinica Peking Univ.* **1963**, *9*, 389. [In Chinese]; b) X.-L. Jin, G.-D. Zhou, N.-Z. Wu, Y.-Q. Tang, H.-C. Huang, *Acta Chemica Sinica* **1990**, *48*, 232–236. [In Chinese].
- [11] H.-J. Meyer, *Z. Anorg. Allg. Chem.* **1991**, *594*, 113–118, and references therein.
- [12] Raman spectra of solid samples were measured on a Renishaw Raman Image Microscope System 2000: NaN_3 : $\nu_s(\text{N}_3)$ 1361 cm^{-1} , $\nu_{\text{as}}(\text{N}_3)$ inactive; AgN_3 : $\nu_s(\text{N}_3)$ 1338, $\nu_{\text{as}}(\text{N}_3)$ 2070 cm^{-1} ; $\text{AgN}_3 \cdot 2\text{AgNO}_3$: $\nu_{\text{as}}(\text{N}_3)$ 2079, $\nu_s(\text{N}_3)$ 1330 cm^{-1} . The Raman spectrum of NaN_3 is consistent with $D_{\infty h}$ symmetry of the azide unit. However, the literature assignment of a linear and symmetrical structure for the azide unit in AgN_3 ^[9] is at variance with the present data, which clearly indicate a linear and asymmetrical structure in both AgN_3 and $\text{AgN}_3 \cdot 2\text{AgNO}_3$.
- [13] J. B. Howard, D. C. Rees, *Chem. Rev.* **1996**, *96*, 2965–2982.
- [14] a) I. G. Dance, *Aust. J. Chem.* **1994**, *47*, 979–990; b) I. G. Dance, *Chem. Commun.* **1998**, 523–530.
- [15] a) M. K. Chan, J. Kim, D. C. Rees, *Science (Washington)* **1993**, *260*, 792–794; b) K. K. Stavrev, M. C. Zerner, *Chem. Eur. J.* **1996**, *2*, 83–87.
- [16] N. R. Thompson in *Comprehensive Inorganic Chemistry Vol. 3* (Eds.: J. C. Bailar, H. J. Emeléus, R. Nyholm, A. F. Trotman-Dickenson), Pergamon, Oxford, **1973**, Chap. 2, Section 2.10, p. 101.

Inter- versus Intramolecular C–H Activation: Synthesis and Characterization of a Novel Platinum–Carbene Complex**

Gareth W. V. Cave, Andrew J. Hallett, William Errington, and Jonathan P. Rourke*

Cyclometalation is a reaction that has been both widely used^[1,2] and widely studied.^[3,4] Typically, the coordinating moiety within a ligand forms a bond to a metal center, and then intramolecular C–H activation takes place to yield a five- or six-membered chelate ring. In the course of our studies, we sought to synthesize a number of cycloplatinated

species that would show novel mesogenic behavior. To this end, we have prepared a number of 2,6-disubstituted pyridines, such as **1** and **3** (Scheme 1), and allowed them to react



Scheme 1. Synthesis of **2** and **4**. a) $\text{K}_2[\text{PtCl}_4]$, acetic acid. $\text{R} = n\text{-C}_6\text{H}_{13}$.

with potassium tetrachloroplatinate under normal cycloplatinated conditions.^[5] When we used pyridine **1** we isolated the expected cycloplatinated product **2**, formed by coordination of the pyridine followed by intramolecular C–H activation, in high yield. However, when we used pyridine **3** we isolated a very different product. The only product isolated (indeed, the only product observed in the crude reaction mixture) was that which forms from the intermolecular activation of a C–H bond, that is, **4**. Complex **4** was isolated in reasonable yield and analyzed by ^1H and ^{13}C NMR spectroscopy and single-crystal X-ray diffraction.

The X-ray crystal structure of **4** shows a number of interesting features (Figure 1). A crystallographically imposed center of symmetry exists between the two platinum and two chlorine atoms (Cl1) to give a flat rectangle, with the other two chlorine atoms (Cl2) only 0.082(4) Å out of this plane. The nitrogen-containing ring is at an angle of 38.62(24)° to the plane defined by the Pt_2Cl_2 rectangle. Two extremes for the bonding of this organic fragment to this rectangle are illustrated in Scheme 2. The Pt–C bond length of 1.951(9) Å is very similar to the values observed for the Pt^0 –carbene complex derived from 1,3-dimesitylimidazol-2-ylidene (1.959(8) and 1.942(8) Å).^[6] It is also similar to the length of 1.973(11) Å for the cationic Pt^{IV} –carbene complex $[\text{PtCl}_2\{\text{C}(\text{NHMe})(\text{NHC}_6\text{H}_4\text{Cl})\}(\text{PET}_3)_2]\text{ClO}_4$,^[7] and significantly shorter than that in the non-carbene cycloplatinated species $[\{\text{PtCl}(\text{tBu}_2\text{PCMe}_2\text{CH}_2)\}_2]$ (2.062(6) Å)^[8] or Pt^{II} – C_{aryl} single bond lengths of 1.98–2.02 Å in arylplatinum complexes.^[9,10] Two shorter Pt–C bonds have been reported: a bond length of 1.82(6) Å for the platinum–carbene complex $[\{\text{PtCl}(\text{tBuCH}_2\text{COiPr})\}_2]$ ^[11] (though given the relatively large estimated standard deviations associated with this measurement, this value is not significantly different from ours), and a

* Dr. J. P. Rourke, G. W. V. Cave, A. J. Hallett, Dr. W. Errington
Department of Chemistry
Warwick University
Coventry CV47AL (UK)
Fax: (+44) 1203-524-112
E-mail: j.rourke@warwick.ac.uk

** This work was supported by the Engineering and Physical Sciences Research Council (UK). We thank Johnson Matthey for the loan of platinum salts.

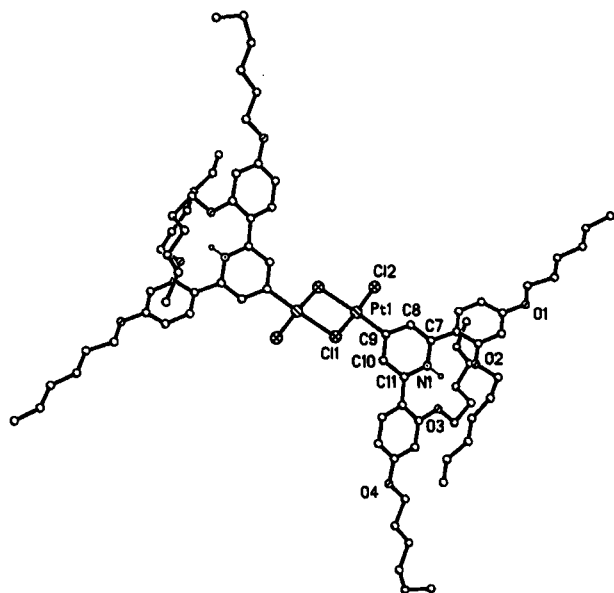
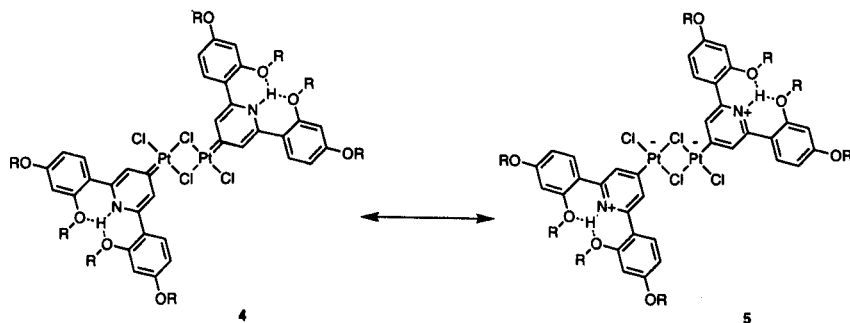


Figure 1. The crystal structure of **4**. Selected bond lengths [Å] and angles [°]: Pt1–C9 1.951(9), Pt1–Cl2 2.281(2), Pt1–Cl1 2.320(2), Pt1–Cl1' 2.448(2), N1–C7 1.352(10), N1–C11 1.361(10), C7–C8 1.362(10), C8–C9 1.408(10), C9–C10 1.401(10), C10–C11 1.389(10); C9–Pt1–Cl2 91.2(3), C9–Pt1–Cl1 92.4(2), Cl2–Pt1–Cl1 175.86(8), C9–Pt1–Cl1' 176.8(2), Cl2–Pt1–Cl1' 91.56(7), Cl1–Pt1–Cl1' 84.85(7), Pt1–Cl1–Pt1' 95.155(7), C7–N1–C11 123.7(7), N1–C7–C8 119.0(8), C7–C8–C9 121.5(8), C10–C9–C8 116.6(7), C10–C9–Pt1 120.7(6), C8–C9–Pt1 122.6(6), C11–C10–C9 122.0(8), N1–C11–C10 117.1(8).



Scheme 2. The carbene **4** and the zwitterion **5** as possible formal structures. R = *n*-C₆H₁₃.

length of 1.90(1) Å for a sterically constrained Pt—C bond in an NCN tridentate donor.^[12] Thus, the short C—Pt bond length would seem to suggest that a carbene structure—that is, **4**—is the correct representation of the structure. Further evidence for this form comes from the ¹³C NMR spectrum, where a resonance at $\delta = 324.3$ indicates a carbene, and we can discount structure **5** as a possibility.

The proton attached to the nitrogen atom was inserted at a calculated position. The O3–N1 and O2–N1 distances are 2.622(9) and 2.720(8) Å, respectively. These distances are substantially shorter than the sum of the van der Waals radii of O and N (3.07 Å)^[13] and thus confirm the presence of a hydrogen-bonding interaction. The O2–O3 distance, at 3.742(9) Å, is longer than the sum of the van der Waals radii, indicating no particular O–O interaction. One of the effects of this hydrogen bonding is to twist both of the phenyl rings to angles of 34.63(29)° (the ring to which O1 and O2 are

attached) and 32.79(36)^o (the ring to which O3 and O4 are attached) with respect to the nitrogen-containing ring, so that one oxygen atom is below the proton and one above. In the solution ¹H NMR spectrum this proton is very deshielded (δ =12.77). The positions of the two OR chains that are hydrogen bonded to this proton are locked in the solid state and remain locked in solution, as shown by the unusual proton resonances for these chains (for instance, the terminal methyl groups of these chains appear at δ =0.69 rather than at the more normal value of δ = 0.95 for the other chains).

The solution ^1H NMR spectrum of **3** shows no unusual features (in particular, the resonances for the two different OR chains are identical), indicating that there are no unexpected steric restrictions on the conformations. Indeed, our own preliminary studies show that pyridine **3** exhibits a perfectly normal coordination chemistry.^[14] On mixing **3** with $\text{K}_2[\text{PtCl}_4]$ in solution, one would expect that **3** would initially coordinate to the platinum center through the nitrogen atom. Such a coordinated species then has C-H bonds in close proximity that can be activated in an intramolecular fashion, giving rise to a cyclometalated species. All else being equal, the relative reactivity of intramolecular activation, compared with intermolecular activation, based upon the effective concentration, has been estimated at a factor of 10.^[3] Thus the exclusive formation of the carbene species that we observe implies that this formation must be a very favorable process, which is presumably assisted by the stabilization offered by

the hydrogen-bonded proton. One other feature of complex **4** is its remarkable stability: it melts in air at 246°C with no decomposition.

Experimental Section

2: 2,6-bis(4-*n*-hexyloxyphenyl)pyridine (**1**; 103 mg, 0.239 mmol) was added to a solution of $K_2[PtCl_4]$ (99 mg, 0.239 mmol) in acetic acid (400 mL). The mixture was stirred at 70 °C for 60 h. The solvent was removed, and the product washed with water. The product was dissolved in chloroform, filtered, washed with hexane, and crystallized from ethyl acetate. Yield: 100 mg (63 %, 0.075 mmol). 1H NMR (400 MHz, $CDCl_3$, 25 °C): δ = 7.71 (4H, AA'XX'), 7.70 (2H, t, 3J = 7.6 Hz, pyridine), 7.36 (2H, dd, 3J = 8.5 Hz, cycloplatinated ring), 7.21 (2H, d, 3J = 8.5 Hz, cycloplatinated ring), 6.91 (4H, AA'XX'), δ = 2.3 Hz, cycloplatinated ring), 6.46 (2H, d, 3J = 8.5 Hz, cycloplatinated ring), 3.97 (6H, t, 3J = 6.7 Hz, OCH_2), 3.86 (6H, t, 3J = 6.7 Hz, OCH_2), 1.44 (24H, m, CH_2), 0.95 (6H, t, 3J = 7.0 Hz, CH_3), 0.95 (6H, t, 3J = 7.0 Hz, CH_3); elemental analysis: found 55.5 (5.5), N 2.2 (2.1).

4: 2,6-bis(2,4-di-n-hexyloxyphenyl)pyridine (3; 159 mg, 0.260 mmol) was added to a solution of $K_2[PtCl_4]$ (108 mg, 0.260 mmol) in acetic acid (400 mL). The mixture was stirred at 70 °C for 60 h. The solvent was removed, and the product washed with water. The product was dissolved in chloroform, filtered, washed with hexane, and crystallized from acetone. Yield: 84 mg (36 %, 0.047 mmol). 1H NMR (400 MHz, $CDCl_3$, 25 °C): δ = 12.77 (2H, t, 4J = 2.1 Hz, NH), 8.03 (4H, d, 4J = 2.1 Hz, pyridine ring), 7.78 (4H, d, 3J = 8.9 Hz), 6.64 (4H, dd, 3J = 8.9, 4J = 2.4 Hz), 6.52 (4H, d, 4J = 2.4 Hz), 4.00 (8H, t, 3J = 6.4 Hz, C4-OCH₂), 3.99 (8H, t, 3J = 5.8 Hz, C2-OCH₂), 1.80 (8H, m), 1.58 (8H, m), 1.44 (8H, m), 1.34 (24H, m), 1.15 (8H, m), 0.95 (20H, m, CH₂, CH₃ of the non-hydrogen-bonded chain), 0.69 (12H, t, CH₃ of the hydrogen-bonded chain); ^{13}C NMR (100.5 MHz, $CDCl_3$, 25 °C): δ = 324.3 (C attached to Pt).

Crystal data for 4: $C_{42}H_{122}Cl_4N_2O_8Pt_2 \cdot Me_2CO$, $M_r = 1853.93$, monoclinic, space group $C2/c$, $a = 32.261(2)$, $b = 15.7989(7)$, $c = 20.0825(9)$ Å, $\beta = 119.867(1)^\circ$, $V = 8876.4(7)$ Å³, 180(2) K; final $R1$, $wR2$, and S values are 0.052, 0.084, and 1.013 for 454 parameters. Data were collected with a Siemens SMART CCD area-detector diffractometer. Refinement was by full-matrix least squares on F^2 for all data with SHELXL-96.^[15] Crystallographic data (excluding structure factors) for the structure reported in this paper have been deposited with the Cambridge Crystallographic Data Centre as supplementary publication no. CCDC-101757. Copies of the data can be obtained free of charge on application to CCDC, 12 Union Road, Cambridge CB2 1EZ, UK (fax: (+44) 1223-336-033; e-mail: deposit@ccdc.cam.ac.uk).

Received: June 2, 1998 [Z119281E]
German version: *Angew. Chem.* 1998, 110, 3466–3468

Keywords: carbene complexes • C–H activation • metalations • N ligands • platinum

- [1] A. D. Ryabov, *Synthesis* 1985, 233–252.
- [2] M. Pfeffer, *Pure Appl. Chem.* 1992, 64, 335–342.
- [3] A. D. Ryabov, *Chem. Rev.* 1990, 90, 403–424.
- [4] P. Steenwinkel, R. A. Gossage, G. van Koten, *Chem. Eur. J.* 1998, 4, 759–762.
- [5] R. M. Ceder, J. Sales, *J. Organomet. Chem.* 1985, 294, 389–396.
- [6] A. J. Arduengo, S. F. Gamper, J. C. Calabrese, F. Davidson, *J. Am. Chem. Soc.* 1994, 116, 4391–4394.
- [7] R. Walker, K. W. Muir, *J. Chem. Soc. Dalton Trans.* 1975, 272–276.
- [8] A. B. Goel, S. Goel, D. Vanderveer, *Inorg. Chim. Acta* 1981, 54, L267–L269.
- [9] L. W. Conzelman, J. D. Koola, U. Kunze, J. Strähle, *Inorg. Chim. Acta* 1984, 89, 147–149.
- [10] L. Chassot, E. Muller, A. von Zelewsky, *Inorg. Chem.* 1984, 23, 429–434.
- [11] Y. T. Struchkov, G. G. Aleksandrov, V. B. Pukhnarevich, S. P. Sushchinskaya, M. G. Voronkov, *J. Organomet. Chem.* 1979, 172, 269–272.
- [12] J. Terheijden, G. van Koten, F. Muller, D. M. Grove, K. Vrieze, E. Nielsen, C. H. Stam, *J. Organomet. Chem.* 1986, 315, 401–417.
- [13] A. Bondi, *J. Phys. Chem.* 1964, 68, 441–445.
- [14] G. W. V. Cave, J. P. Rourke, unpublished results.
- [15] G. M. Sheldrick, Universität Göttingen, Germany 1996.

Solid-Phase Synthesis and Encoding Strategies for Olefin Polymerization Catalyst Libraries **

Thomas R. Boussie, Carla Coutard, Howard Turner, Vince Murphy,* and Timothy S. Powers*

Although the application of combinatorial methods in the pharmaceutical industry is fast becoming an industrial standard for the discovery and optimization of novel drug-based molecules,^[1] similar methods aimed towards the identification of new materials and catalysts remain in their infancy.^[2]

Recent reports have appeared describing the synthesis and screening of libraries of organometallic catalysts for examining a number of transformations.^[3] The application of combinatorial methods aimed toward the discovery and optimization of olefin polymerization catalysts is an area that promises to be of major importance especially to the chemical industry, which produces approximately 46 million metric tons of polyolefins annually.^[4]

Since most commercial-scale polyolefin processes employ supports with high surface areas for immobilizing olefin polymerization catalysts, it is somewhat surprising that few reports have appeared examining the use of polystyrene as a catalyst support.^[5] Fréchet and co-workers have recently shown that suitably modified cross-linked polystyrene can function as an efficient activator for catalysts based on Group 4 metallocenes.^[6] Polystyrene with low cross-linking not only acts as a more chemically compatible support relative to silica, but also provides a “solutionlike” environment that more closely resembles the environment in which homogeneous metallocene catalysts function. In addition, a plethora of solid-phase synthetic methodologies have appeared in recent years, providing a broad knowledge base which should facilitate efforts in the field of olefin polymerization catalysis.^[7]

Recent reports have shown that certain catalysts based on complexes of late transition metals with diimines exhibit olefin polymerization activities comparable to those found for early transition metal single-site metallocene-based systems.^[8] These systems offer advantages over their early transition metal counterparts in that they are easily synthesized and provide a broader range of functional-group compatibilities.^[9] Herein we report the first example of a combinatorial approach to the parallel synthesis of a 1,2-diimine library complexed with Ni^{II} and Pd^{II} as olefin polymerization catalysts using 1% cross-linked polystyrene as a solid support. Specifically, a general synthetic methodology has been developed that allows for the parallel synthesis and screening of ethylene polymerization catalyst libraries in a spatially addressable format.^[10] Furthermore, we have discovered that it is possible to apply chemical encoding techniques to these catalysts and distinguish catalyst performance trends. Since steric bulk on the aryl rings has been shown to play a dramatic role on polymer yield and molecular weight (M_w) for these catalytic systems, we chose to synthesize aryl-substituted 1,2-diimine complexes of Ni^{II} and Pd^{II} on 1% cross-linked polystyrene. In addition, we sought to examine how electronic perturbations may affect catalyst performance.

Our synthetic approach began with a regioselective alkylation of the unsymmetrical 1,2-diimine **1** with bromomethyl polystyrene (1.05 equiv of lithium diisopropylamide (LDA), 0°C, THF) to give the polystyrene-grafted 1,2-diimine ligand **2** (Scheme 1).^[11] To incorporate a variety of functionalized aryl-substituted 1,2-diimines, a divergent approach was explored starting from diketone resin **3**, which was obtained in high yield (>95% based on recovered 2,4,6-trimethylaniline) from the hydrolysis of 1,2-diimine resin **2** with oxalic acid in THF/H₂O (5/1 v/v) at 70°C for 12 h. This transformation was monitored by single-bead FT-IR spectroscopy ($\bar{\nu}$ = 1635 (C=N), 1712 cm⁻¹ (C=O)).

* V. Murphy, T. S. Powers, T. R. Boussie, C. Coutard, H. Turner
Symyx Technologies
3100 Central Expressway, Santa Clara, CA 95051 (USA)
Fax: (+1) 408-748-0175
E-mail: vmurphy@symyx.com
tpowers@symyx.com

** Financial support from Hoechst Research and Technology is acknowledged.

High-Yield Synthesis of a C \wedge N \wedge C Tridentate Platinum Complex

Gareth W. V. Cave, Nathaniel W. Alcock, and Jonathan P. Rourke*

Department of Chemistry, Warwick University, Coventry, U.K. CV4 7AL

Received December 10, 1998

Summary: 2,6-Diphenylpyridine is metalated twice by potassium tetrachloroplatinate in acetic acid to give in high yield a complex with a tridentate ligand bound to the metal via a C \wedge N \wedge C donor set. This complex and three derivatives have been characterized, including the single-crystal X-ray analysis of one derivative.

Introduction

Cyclometalation is a reaction that has been both widely used^{1,2} and widely studied.^{3,4} Typically, a ligating species coordinates to a metal center and a proximal C–H bond is activated, generating a five- or six-membered chelate ring.³ Our own use of the reaction has been to generate novel cyclopalladated metallocenes^{5–7} and some unusual platinum complexes.⁸ Tridentate cyclometalated species where two coordinating groups hold a C–H bond close to the metal and this bond becomes activated are relatively common; thus, N \wedge C \wedge N⁹ donor sets,¹⁰ P \wedge C \wedge P donor sets,^{11–14} or S \wedge C \wedge S donor sets¹⁵ are well-known. Indeed, some groups have used two ligating groups to induce C–C activation¹⁶ or C–Si activation.¹⁷ In addition, the use of a chelating N \wedge N donor set to yield N \wedge N \wedge C tridentate cyclometalated species has been reported.¹⁸ The double cyclo-

metalation of two ligands by one metal center is also known.^{19–22} What is not common are tridentate C \wedge N \wedge C or C \wedge P \wedge C donor sets where two cyclometalated rings have been formed via two C–H activations. One paper reports the isolation, in low yield, of the dicyclopalladated platinum complex of 2,6-diphenylpyridine.²³ The subject of this paper is the high-yield synthesis of such tridentate C \wedge N \wedge C compounds of platinum.

Results and Discussion

The reaction of potassium tetrachloroplatinate with diphenylpyridine in acetic acid to give a complex we tentatively formulate as **2** is essentially quantitative (Scheme 1). While we could get no solution data on **2**, as it either is insoluble or reacts with solvent, solid-state characterization is consistent with this formulation. Thus, elemental analysis and mass spectrometry (both positive and negative ion) confirm our hypothesis. On dissolution in dimethyl sulfoxide (dmsO) **2** gives complex **3**, which has been fully characterized (NMR, elemental analysis, single-crystal X-ray diffraction). Characterization of **3** provides additional support for our formulation of **2**.

The synthesis of **2** is simplicity itself and has been used for monocycloplatination before.²⁴ Complex **2** is a robust yellow powder stable to air and water, which decomposes without melting at 320–370 °C (TGA analysis shows this decomposition process to be complete, leaving only platinum). Our major use of **2** is in the synthesis of complexes **3** and **4**. Complex **3** was isolated in essentially quantitative yield by the simple act of dissolution in dmsO. Thus, the isolated yield of **3**, starting from our platinum source, is 98%. The NMR spectrum of **3** is unexceptional, and crystals suitable for X-ray analysis were grown. The X-ray structure itself is as expected (Figure 1): three molecules are found within the asymmetric unit, with little to distinguish among them. The diphenylpyridine and the Pt are essentially flat, though the dmsO is bent out of plane with the N–Pt–S angles being 170.9(2), 173.3(2), and 173.8(2)° in the three molecules in the asymmetric unit. The C1–Pt–S–O torsion angles also differ, being –14.1, 13.2, and 6.6° in the three molecules. Quite why the

* To whom correspondence should be addressed. E-mail: j.rourke@warwick.ac.uk.

- (1) Ryabov, A. D. *Synthesis* **1985**, 233.
- (2) Pfeffer, M. *Pure Appl. Chem.* **1992**, 64, 335.
- (3) Ryabov, A. D. *Chem. Rev.* **1990**, 90, 403.
- (4) Steenwinkel, P.; Gossage, R. A.; van Koten, G. *Chem. Eur. J.* **1998**, 4, 759.
- (5) Lydon, D. P.; Cave, G. W. V.; Rourke, J. P. *J. Mater. Chem.* **1997**, 7, 403.
- (6) Lydon, D. P.; Rourke, J. P. *Chem. Commun.* **1997**, 1741.
- (7) Cave, G. W. V.; Lydon, D. P.; Rourke, J. P. *J. Organomet. Chem.* **1998**, 555, 81.
- (8) Cave, G. W. V.; Hallett, A. J.; Errington, W.; Rourke, J. P. *Angew. Chem.* **1998**, 37, 3466; *Angew. Chem., Int. Ed. Engl.* **1998**, 37, 3270.
- (9) The abbreviation N \wedge C \wedge N refers to a tridentate ligand bonding through two N donors and one C donor, with the ligand connectivity being N linked to C linked to N. Thus, N \wedge N \wedge C also represents a tridentate ligand bonding through two N donors and one C donor, but this time the ligand connectivity is N linked to N linked to C.
- (10) Terheijden, J.; van Koten, G.; Muller, F.; Grove, D. M.; Vrieze, K.; Nielsen, E.; Stam, C. H. *J. Organomet. Chem.* **1986**, 315, 401.
- (11) Moulton, C. J.; Shaw, B. L. *J. Chem. Soc., Dalton Trans.* **1976**, 1020.
- (12) Rimml, H.; Venanzi, L. M. *J. Organomet. Chem.* **1983**, 259, C6.
- (13) Bennett, M. A.; Jin, H.; Willis, A. C. *J. Organomet. Chem.* **1993**, 451, 249.
- (14) Weisman, A.; Gozin, M.; Kraatz, H.-B.; Milstein, D. *Inorg. Chem.* **1996**, 35, 1792.
- (15) Dupont, J.; Beydon, N.; Pfeffer, M. *J. Chem. Soc., Dalton Trans.* **1989**, 1715.
- (16) Rybtchinski, R.; Vigalok, A.; Ben-David, Y.; Milstein, D. *J. Am. Chem. Soc.* **1996**, 118, 12406.
- (17) Steenwinkel, P.; Gossage, R. A.; Maunula, T.; Grove, D. M.; van Koten, G. *Chem. Eur. J.* **1998**, 4, 763.
- (18) Constable, E. C.; Henney, R. P. G.; Leese, R. A.; Tocher, D. A. *J. Chem. Soc., Chem. Commun.* **1990**, 513.

- (19) Cheney, A. J.; McDonald, W. S.; O'Flynn, K.; Shaw, B. L.; Turtle, B. L. *J. Chem. Soc., Chem. Commun.* **1973**, 128.
- (20) Chassot, L.; Muller, E.; von Zelewsky, A. *Inorg. Chem.* **1984**, 23, 4249.
- (21) van der Boom, M. E.; Liou, S.-Y.; Shimon, L. J.; Ben-David, Y.; Milstein, D. *Organometallics* **1996**, 15, 2562.
- (22) Thorn, D. L. *Organometallics* **1998**, 17, 348.
- (23) Cornioley-Deuschel, C.; Ward, T.; von Zelewsky, A. *Helv. Chim. Acta* **1988**, 71, 130.
- (24) Ceder, R. M.; Sales, J. J. *J. Organomet. Chem.* **1985**, 294, 389.

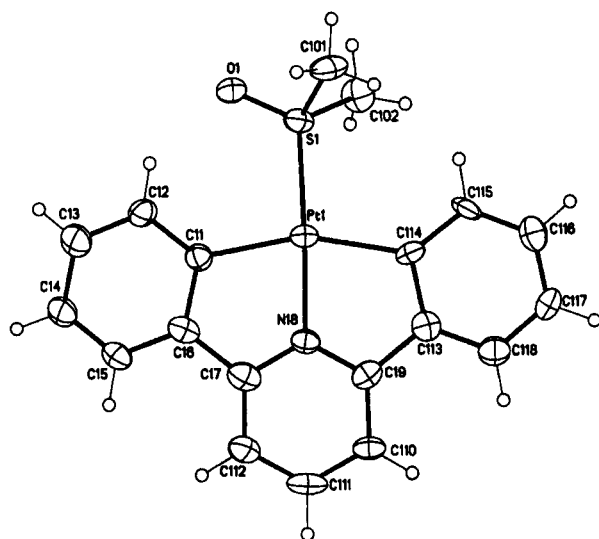
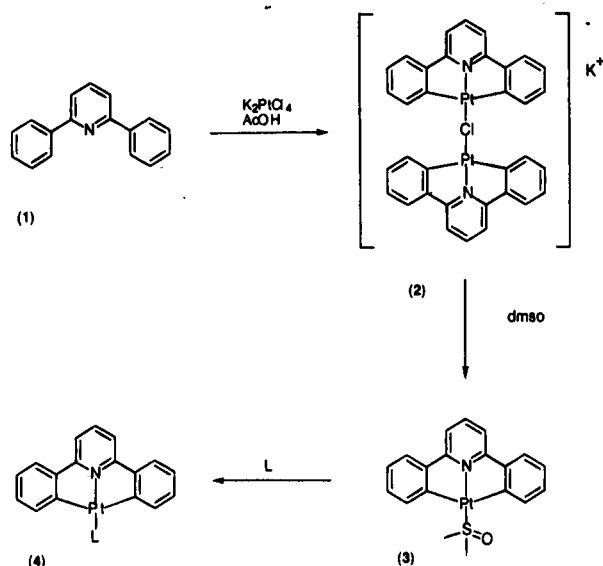


Figure 1. Crystal structure of **3** (50% thermal ellipsoids).

Scheme 1



4a, L = PMe₃

4b, L = stilbazole =

dmsol is not in plane is unclear: presumably it arises through packing constraints, constraints which cannot be equal for all three molecules, given the 3° variation in the N–Pt–S angle. All other bond lengths and angles are normal. Selected bond lengths and angles are listed in Table 1.

Complex **3** may be reacted with other ligating species to give complexes **4** (Scheme 1). A sample of **3** in an NMR tube was treated with 1 equiv of trimethylphosphine, whereupon an instantaneous reaction took place to give **4a** in quantitative yield. The complex may be isolated by the simple expedient of solvent removal. Likewise, the pyridine-based stilbazole ligand reacts to give **4b**. Hence, **3** is a very convenient source of the C[∧]N[∧]C–Pt moiety.

Table 1. Selected Bond Lengths (Å) and Angles (deg) in the Crystal Structure of **3**

	<i>n</i> = 1	<i>n</i> = 2	<i>n</i> = 3
Pt(<i>n</i>)–N(<i>n</i> 8)	2.004(7)	2.014(7)	2.016(7)
Pt(<i>n</i>)–C(<i>n</i> 1)	2.068(9)	2.069(9)	2.074(9)
Pt(<i>n</i>)–C(<i>n</i> 14)	2.082(9)	2.106(9)	2.085(9)
Pt(<i>n</i>)–S(<i>n</i>)	2.201(2)	2.190(2)	2.197(2)
S(<i>n</i>)–O(<i>n</i>)	1.469(6)	1.474(6)	1.485(6)
S(<i>n</i>)–C(<i>n</i> 01)	1.772(9)	1.766(9)	1.772(9)
S(<i>n</i>)–C(<i>n</i> 02)	1.773(9)	1.777(9)	1.775(10)
N(<i>n</i> 8)–Pt(<i>n</i>)–C(<i>n</i> 1)	79.8(3)	80.3(3)	80.0(3)
N(<i>n</i> 8)–Pt(<i>n</i>)–C(<i>n</i> 14)	80.6(3)	80.6(3)	79.8(3)
C(<i>n</i> 1)–Pt(<i>n</i>)–C(<i>n</i> 14)	159.8(3)	160.4(3)	159.2(3)
N(<i>n</i> 8)–Pt(<i>n</i>)–S(<i>n</i>)	170.9(2)	173.8(2)	173.3(2)
C(<i>n</i> 1)–Pt(<i>n</i>)–S(<i>n</i>)	98.4(2)	98.6(3)	100.3(2)
C(<i>n</i> 14)–Pt(<i>n</i>)–S(<i>n</i>)	101.7(2)	100.9(2)	100.3(3)
O(<i>n</i>)–S(<i>n</i>)–Pt(<i>n</i>)	117.7(3)	119.3(3)	119.3(3)
C(<i>n</i> 01)–S(<i>n</i>)–Pt(<i>n</i>)	114.6(3)	112.2(3)	112.7(3)
C(<i>n</i> 02)–S(<i>n</i>)–Pt(<i>n</i>)	110.1(3)	109.9(3)	109.8(3)
C(<i>n</i> 6)–C(<i>n</i> 1)–Pt(<i>n</i>)	112.8(6)	111.5(6)	111.9(6)
C(<i>n</i> 9)–N(<i>n</i> 8)–Pt(<i>n</i>)	118.7(6)	118.1(6)	118.5(6)
C(<i>n</i> 7)–N(<i>n</i> 8)–Pt(<i>n</i>)	118.6(6)	118.5(6)	117.7(6)
C(<i>n</i> 13)–C(<i>n</i> 14)–Pt(<i>n</i>)	110.8(6)	110.5(6)	111.6(7)

The dicyclopalladated platinum complex of 2,6-diphenylpyridine has been reported previously: a synthetic procedure involving the double lithiation of diphenylpyridine followed by reaction with PtCl₂(SEt₂)₂ gave **4** (L = SEt₂) in 10% yield;²³ the same paper reports the analogous palladium complex in 1.4% yield. Other than this report there are only three structurally characterized species containing a C[∧]N[∧]C or a C[∧]P[∧]C donor set. The first reported example was a platinum phosphine complex, though this C[∧]P[∧]C,P complex is unstable with respect to the (P[∧]C)₂ isomer;¹⁹ the other examples are palladium species metalated to a pyridine with pendant β-dicarbonyls, where the reaction is with a fairly acidic hydrogen.^{25,26}

We are at present investigating the reactivity of both **2** and **3** and seeking to broaden the scope of this reaction to other metals (for instance, preliminary studies indicate that the palladium analogue of **2** may be isolated in a yield of around 20%).

Experimental Section

General Considerations. All chemicals were used as supplied; unless noted otherwise, the stilbazole was synthesized via the published route.²⁷ All elemental analyses were performed by Warwick Analytical Service.

Synthesis of K⁺[(2,6-diphenylpyridine)PtCl₂][−] (2**).** Potassium tetrachloroplatinate (374 mg, 0.900 mmol) was added to a solution of 2,6-diphenylpyridine (233 mg, 1.00 mmol) in glacial acetic acid (250 mL). The reaction mixture was stirred at 80 °C until the red platinum salt was no longer visible (3 days). The reaction mixture was filtered, yielding the product as an insoluble yellow powder which was washed with water, acetone, and ether. Yield: 407 mg (98%, 0.441 mmol). Anal. Found (calcd): C, 43.7 (44.2); H, 2.6 (2.4); N, 3.0 (3.0). MALDI MS (2,5-dihydroxybenzoic acid matrix): negative ion peaks at *m/z* 35 and 37 indicating Cl[−]; positive ion peaks at *m/z* 39 and 425 corresponding to K⁺ and (diphenyl)Pt.

(25) Newkome, G. R.; Kawato, T.; Kohli, D. K.; Puckett, W. E.; Oliver, B. D.; Chiari, G.; Fronczek, F. R.; Deutsch, W. A. *J. Am. Chem. Soc.* **1981**, *103*, 3423.

(26) Newkome, G. R.; Kohli, D. K.; Fronczek, F. R. *J. Am. Chem. Soc.* **1982**, *104*, 994.

(27) Bruce, D. W.; Dunmur, D. A.; Lalinde, E.; Matulis, P. M.; Styring, P. *Liq. Cryst.* **1988**, *3*, 385.

Synthesis of [(2,6-diphenyl)Pt(dmsO)] (3). The yellow $K^+[(2,6\text{-diphenylPt})_2\text{Cl}]^-$ produced above was dissolved in hot dmsO (1 mL), the solution was cooled, and precipitation was induced with water (1 mL) to give a yellow crystalline product. Yield: 443 mg (98%, 0.882 mmol). Anal. Found (calc): C, 45.0 (45.4); H, 3.4 (3.4); N, 2.8 (2.8). NMR data: δ_{H} (250 MHz, CDCl_3) 7.80 (2H, dd, $^3J = 7.6$, $^4J = 1.2$, $^3J(\text{Pt-H}) = 24$ Hz, phenyl ortho to Pt), 7.62 (1H, t, $^3J = 7.3$ Hz, central pyridine), 7.47 (2H, dd, $^3J = 7.6$, $^4J = 1.2$ Hz, phenyl ortho to pyridine, meta to Pt), 7.30 (2H, d, $^3J = 7.3$ Hz, pyridine), 7.28 (2H, td, $^3J = 7.6$, $^4J = 1.2$ Hz, phenyl), 7.21 (2H, td, $^3J = 7.6$, $^4J = 1.2$ Hz, phenyl), 3.68 (6H, s, $^3J(\text{Pt-H}) = 26.8$ Hz, dmsO).

X-ray Crystallographic Study of 3. Crystals suitable for structural analysis were grown from dmsO. A golden yellow prism (dimensions $0.2 \times 0.06 \times 0.06$ mm) was mounted with oil on a thin glass fiber. Data were collected at 180(2) K using a Siemens SMART CCD area-detector diffractometer. Crystal data for 3: $\text{C}_{19}\text{H}_{17}\text{NOSPt}$, $M_r = 502.49$, monoclinic, space group $P2_1/c$, $a = 17.9050(10)$ Å, $b = 9.9528(5)$ Å, $c = 27.658(2)$ Å, $\beta = 97.885(5)^\circ$, $V = 4882.2(5)$ Å³, $Z = 12$, $D(\text{calcd}) = 2.051$ Mg/m³. Refinement was by full-matrix least squares on F^2 for 7378 reflection positions using SHELXL-96²⁸ with additional light atoms found by Fourier methods. Hydrogen atoms were added at calculated positions and refined using a riding model with freely rotating methyl groups. Anisotropic displacement parameters were used for all non-H atoms; H atoms were given isotropic displacement parameters equal to 1.2 (or 1.5 for methyl hydrogen atoms) times the equivalent isotropic displacement parameter of the atom to which the H atom is attached. The weighting scheme was calculated using $w = 1/[\sigma^2(F_o^2) + (0.0520P)^2]$, where $P = (F_o^2 + 2F_c^2)/3$. The goodness of fit on F^2 was 0.914, $R1$ (for 7378 reflections with $I > 2\sigma(I)$) = 0.0481, $wR2 = 0.1076$. The data/parameter ratio was 11 487/628. The largest difference Fourier peak and hole were 1.912 and -1.431 e Å⁻³; the only large peaks are near the Pt atoms. The asymmetric unit contains three essentially identical molecules. Selected bond lengths and angles are listed in Table 1.

(28) Sheldrick, G. M. SHELXL-96, Program for Crystal Structure Refinement; University of Göttingen, Göttingen, Germany, 1996.

Synthesis of [(2,6-diphenyl)Pt(PMe₃)] (4a). Trimethylphosphine (9 mg, 0.12 mmol) was added to a solution of [(2,6-diphenyl)Pt(dmsO)] (56 mg, 0.108 mmol) in chloroform (1 mL). All solvents were removed in vacuo to give a yellow product. Yield: 54 mg (99%, 0.107 mmol). Anal. Found (calcd): C, 48.2 (48.0); H, 4.0 (4.0); N, 3.0 (2.8). NMR data: δ_{P} (161.9 MHz, CDCl_3) -20.98 (s, $^1J(\text{Pt-P}) = 1606$ Hz); δ_{H} (250 MHz, CDCl_3) 8.38 (1H, t, $^3J = 8.5$ Hz, central pyridine), 8.11 (2H, d, $^3J = 8.5$ Hz, pyridine), 7.93 (2H, dd, $^3J = 7.6$, $^4J = 1.2$ Hz, phenyl ortho to pyridine, meta to Pt), 7.80 (2H, dd, $^3J = 7.6$, $^4J = 1.2$, $^3J(\text{Pt-H}) = 16$ Hz, phenyl ortho to Pt), 7.41 (2H, td, $^3J = 7.6$, $^4J = 1.2$ Hz, phenyl), 7.34 (2H, td, $^3J = 7.6$, $^4J = 1.2$ Hz, phenyl), 3.68 (6H, d, $^3J(\text{P-H}) = 1.8$, $^3J(\text{Pt-H}) = 64.5$ Hz, PMe_3).

Synthesis of [(2,6-diphenyl)Pt(stilbazole)] (4b). Octyloxystilbazole (33 mg, 0.119 mmol) was added to a solution of [(2,6-diphenyl)Pt(dmsO)] (56 mg, 0.108 mmol) in chloroform (1 mL). The mixture was stirred (30 min), solvents were removed in vacuo, and the residue was washed with ether to give a yellow product. Yield: 76 mg (99%, 0.108 mmol). Anal. Found (calcd): C, 61.0 (61.3); H, 4.8 (4.9); N, 4.0 (4.0). NMR data: δ_{H} (400 MHz, CDCl_3) 8.92 (2H, AA'XX', $^3J(\text{Pt-H}) = 43.5$ Hz, stilbazole pyridine, ortho to N), 7.53 (2H, AA'XX', stilbazole phenyl ring), 7.51 (1H, t, $^3J = 8$ Hz, central pyridine), 7.46 (2H, m, phenyl ortho to Pt), 7.44 (2H, AA'XX', stilbazole pyridine), 7.41 (1H, d, $^3J = 16.6$ Hz, stilbazole double bond), 7.23 (2H, d, $^3J = 8$ Hz, pyridine), 7.20 (2H, dt, $^3J = 7.5$, $^4J = 1.3$ Hz, phenyl), 7.05 (2H, dt, $^3J = 7.5$, $^4J = 1.3$ Hz, phenyl), 7.00 (2H, dd, $^3J = 7.5$, $^4J = 1.3$ Hz, phenyl ortho to pyridine), 6.93 (2H, AA'XX', stilbazole), 6.91 (1H, d, $^3J = 16.6$ Hz, stilbazole double bond), 3.99 (2H, t, $^3J = 6.5$ Hz, OCH_2), 1.80 (2H, m), 1.46 (2H, m), 1.31 (8H, m), 0.89 (3H, t, $^3J = 6.5$ Hz).

Acknowledgment. We thank the EPSRC for a studentship (G.W.V.C.) and Johnson-Matthey for a loan of precious metal salts.

Supporting Information Available: Tables of positional parameters, bond distances, bond angles, and anisotropic parameters for the structural analysis of 3. This material is available free of charge via the Internet at <http://pubs.acs.org>.

OM981006O